Surface Modification with Polymers using Living Radical Polymerisation and Click Chemistry

by

CHEN, Gaojian

A thesis submitted in partial fulfilment of the requirements for the degree of
Doctor of Philosophy in Chemistry

Department of Chemistry
University of Warwick

September 2007

Table of Contents

List of Figures

List of Tables

Acknowledgements

I would like to thank all the people who contributed in some way to the work described in this thesis. First and foremost, I thank my supervisor, Professor David M. Haddleton, for the support and guidance that was necessary for the completion of this work. I have been fortunate to have you as my supervisor and I consider it an honour to be your student.

Dr Giussepe Mantovani, thank you for your continuous help during these three years. Although my Ping Pong may be slightly better than you, I greatly benefited from your keen scientific insight, without your effort my job would have undoubtedly been more difficult.

I would also like to express the pleasure of working with a great group of individuals in the polymer lab. I will not forget the warm smile from Emma Melia when she brought me to her house from Pool Meadow 1 a.m. in the morning the first day I arrived England. Benjamin MacCreath generously gave me any help I need, not to mention the wonderful organisations of basketball, badminton and beers. And without the help and support of fellow lab-mates and collaborators, many results described in this thesis would not be accomplished. Lei Tao and I worked together on dendron modified carbon nanotubes. Jin Geng helped me for sugar related synthesis. Daniel Nystrom taught me how to cast isoporous films when we synthesised the polystyrene modified carbon nanotubes. Helen Middleton and I made an antibiotic metronidazole-containing polymer onto cotton surface. Peter Wright showed me his expertise in dispersant and we made thermo-responsive water dispersible carbon nanotubes.

Claire Sayers helped me for HPLC characterisation. Solene Cauet often gave me helpful comments on my work. And Dr Josefina Lindqvist helped reviewing my thesis. I would like to thank all the members of the polymer group past and present. You provided a friendly and cooperative atmosphere at work. All the happy things happened during my PhD study in Warwick with you guys are my treasures.

Further special thanks should go to Dr Julie Macpherson and Dr Paul Taylor for evaluating the progress of my PhD study, Dr. Adam Clarke for assistance with NMR experiments, Dr Steve York for SEM and TEM characterisation, Miss Sara Dale for assistance with Confocal Microscopy.

I am grateful for the funding sources that allowed me to pursue my PhD studies: the Overseas Research Students Award Scheme (ORSAS) and Warwick Postgraduate Research Fellowship Scheme (WPRFS).

Finally, I would like to thank my parents for their encouragements and support, and especially my wife Yan, your love and support drive me to do my best. Everything I do I only hope brings you and our daughter joy and happiness for the rest of our lives.

Declaration

Experimental work contained in this thesis is original research carried out by the author, unless otherwise stated, in the Department of Chemistry at the University of Warwick, between October 2004 and September 2007. No material contained herein has been submitted for any other degree, or at any other institution.

Results from other authors are referenced in the usual manner throughout the text.

_____ Date: _____

Gaojian CHEN

Abstract

Thin organic and polymer layers on solid substrates play a key role in many processes aimed at modifying surface properties. Both "grafting to" and "grafting from" methods have been used in this project to modify a variety of surfaces including cellulose, resins and carbon nanotubes (CNT) with functional polymers. Living radical polymerisation and Huisgen [2+3] cycloaddition (often termed “click” reaction) were used to carry out these modifications.

Living radical polymerisation was first used to synthesize different α-functional polymers and used for surface modification. For example, Living radical polymerisations of methyl methacrylate and a fluorescent comonomer with 2-bromo-2-methyl-propionic acid 3-azido-propyl ester and 2-bromo-2-methyl-hept-6-yn-3-one as initiators have been successfully employed for the synthesis of fluorescently tagged azide and alkyne terminated PMMA with molecular weight (Mn) close to that predicted and polydispersity index (PDi) less than 1.20 and good first order kinetics that would be expected for living radical polymerisation. Cotton and organic resin surfaces have been functionalised with alkyne groups using simple condensation with 4-chlorocarbonyl-butyric acid prop-2-ynyl ester. The surfaces have been further modifies using a Huisgen [2+3] cycloaddition (click) reaction of both polymeric and small molecule azides. Different functional azides, namely mono azido-PEG and a new fluorescent hostasol derivative have also been prepared and tested as model substrates for cotton surface modification. This approach is shown to be very general allowing soft and hard surfaces with different geometries to be modified. In particular it is an excellent method to alter the nature of organic resins allowing the incorporation of many different functionalities.

The covalent immobilization of a range of carbohydrate derivatives onto resin beads was then carried out. Copper-catalysed Huisgen [2+3] cycloaddition was used to graft mannose-containing azides to complementarily functionalised alkyne surfaces, namely: a) Wang resin or b) "Rasta" particles consisting of a "clickable" alkyne polymer loose outer shell and a Wang resin inner core. For the second approach, Wang resin beads were first converted into immobilized ATRP initiators, and then polymerisation of trimethylsilanyl-protected propargyl methacrylate followed by deprotection with TBAF·$3H_2O$ afforded the desired polyalkyne clickable scaffold. An appropriated α-mannopyranoside azide was then clicked onto it, to give a mannose functionalized "Rasta" resin. The binding abilities of these D-mannose-modified particles were then tested using fluorescein labelled Concanavalin A (Con A), a lectin known for its ability of binding certain mannose-containing molecules. Our preliminary results indicated that the novel glycohybrid materials presented in this work are able to efficiently recognize mannose-binding model lectins such as Con A, opening the way for their potential application in affinity chromatography, sensors and other protein recognition/separation fields.

Other functional polymers with antibiotic or chiral properties were also grafted from surfaces. Living radical polymerisation of poly(ethylene glycol) methyl ether methacrylate (PEGMA) and a metronidazole monomer (MTD-MA) has been successfully employed for the synthesis of antibiotic metronidazole containing polymers with Mn close to that predicted, narrow polydispersity and good first order kinetics that would be expected for living radical polymerisation. Using the monomers PEGMA and MTD-MA, with preformed immobilized initiator on cotton, surface initiated LRP was carried out to give cotton bearing antibiotic polymers.

Surface initiated living radical polymerisation of GMA was then successfully carried out for the synthesis of PGMA containing bead base on Aquagel resin. The hydroxyl groups of the PGMA moiety were then reacted with a single enantiomer (*R*)-(+)-1-phenylethyl isocyanate (EtPhNCO). This demonstrates a convenient way of immobilise enantiomer moiety onto resin surface and the resulting solid support may be used as chiral stationary phases (CSP) for HPLC chromatography.

To modify CNTs with functional polymers not only increase the dispersability of the CNTs, it has also enlarged the application areas of CNT's due to the polymers' own functional properties. MWCNTs were first converted to a solid support LRP initiator by an esterification reaction and styrene was grafted from MWCNTs through surface-initiated LRP, the PSt modified CNTs were then used to form isoporous membranes. Similarly, Poly(amidoamine) (PAMAM) dendrons were covalently attached to MWCNTs and dendron-MWCNT-Ag(0) hybrid materials were made afterwards which occurred via Ag(I) coordination to the PAMAM dendron nitrogen donors, followed by reduction with formaldehyde. Finally, noncovalent method was used to make a thermo-sensitive water soluble CNTs. The homopolymerisations and copolymerisation of poly(ethylene glycol) methyl ether methacrylate (PEGMA) and di(ethylene glycol) methyl ether methacrylate (DEGMA) using a pyrene-containing initiator and a Cu(0)/Me_6-Tren catalyst system was investigated. The pyrene-functionalised polymers synthesised were then used to modify CNTs and thus thermo-sensitive water-dispersible CNTs were made.

Abbreviations

AFM	atomic force microscopy
AGET	activators generated by electron transfer
APS	(γ-aminopropyl) triethoxysilane
ARGET	activator regenerated by electron transfer
ATRP	atom transfer radical polymerisation
Au-NPs	gold nanoparticles
CCl_4	carbon tetrachloride
CL	caprolactone
CNTs	carbon nanotubes
COD	cyclooctadiene
Con A	Concanavalin A
Conv.	conversion
CuBr	copper(I)bromide
DCC	*N, N'*-dicyclohexylcarbodiimide
DCM	dichloromethane
DEGMA	di(ethylene glycol) methyl ether methacrylate
DIAD	di-isopropyl azodicarboxylate
DIPEA	diisopropylethylamine
DMAEMA	2-(dimethylamino)ethyl methacrylate
DMAP	4-dimethylamino pyridine
DMF	dimethyl formamide
DMSO	dimethyl sulfoxide
DNA	deoxyribose nucleic acid

DP	degree of polymerisation/kinetic chain length
d-PDMS	deuterated poly(dimethylsiloxane)
DPE	diphenylethylene
DVB	divinylbenzene
EDS	energy-dispersive spectroscopy
EGDMA	ethylene glycol dimethacrylate
EtPhNCO	(R)-(+)-1-phenylethyl isocyanate
f	initiator efficiency
FE-SEM	field-emission scanning electron microscopy
FITC-Con A	fluorescein isothiocyanate-labelled Concanavalin-A
GMA	Glycerol methacrylate
GPC	gel permeation chromatography
GR	grafting ratio
HEA	2-hydroxyethyl acrylate
HEMA	2-hydroxyethyl methacrylate
HMA	hostasol monomer
Hostasol-azide	5-[1,3-dioxo-1H-benzo[3,4]isothiochromeno[7,8,1-def] isoquinolin-2(3H)-yl]pentyl
HPMA	*N*-(2-hydroxy-propyl)-2-methyl-acrylamide
I	initiator
IR	infrared
k_d	rate constant of deactivation
k_p	rate constant of polymerisation
k_t	rate constant of termination
k_{tc}	rate constant of termination by combination

k_{td}	rate constant of termination by disproportionation
k_{tr}	rate constant of chain transfer
L-LA	L-lactide
LRP	living radical polymerisation
M	monomer
MA	methyl acrylate
MADIX	macromolecular design via interchange of xanthates
MAEDAPS-DMA	poly(3-[2-(*N*-methylacrylamido)-ethyldimethyl ammonio]propane sulfonate-b-*N,N*-dimethylacrylamide)
METAC	2-(methacryloyloxy)ethyl trimethylammonium chloride
MMA	methyl methacrylate
M_n	number average molecular weight
$M_{n,NMR}$	Mn by nuclear magnetic resonance
$M_{n,SEC}$	Mn by size exclusion chromatography
$M_{n,th}$	Theoretical number average molecular weight
MTD-MA	metronidazole monomer
M_w	weight average molecular weight
MWCNT	multiwalled carbon nanotube
MWD	molecular weight distribution
NaPSS	poly(sodium 4-styrenesulfonate)
NCA	*N*-carboxyanhydrides
NHS	*N*-hydroxy succinimide
NIPAAm	*N*-isopropyl-2-methyl-acrylamide
NMP	nitroxide-mediated polymerisation
NMR	nuclear magnetic resonance

PAMAM	poly(amidoamine)
PAmPV	poly{(5-alkoxy-*m*-phenylenevinylene)-*co*-[(2,5-dioctyloxy-*p*-phenylene)-vinylene]}
PB	poly(butadiene)
PBLG	poly-γ- benzyl-*L*-glutamate
PCL	poly(ε-caprolactone)
PDi	polydispersity index
PDMA	poly(*N,N*-dimethylacrylamide)
PDMAEMA	poly(dimethylamino)ethyl methacrylate
PDMS	polydimethylsiloxane
PEG	poly(ethylene glycol)
PEGMA	poly(ethylene glycol) methyl ether methacrylate
PEO	poly(ethylene oxide)
PGMA	poly(glycerol methacrylate)
PMEMA	poly(2-(*N*-morpholino)-ethyl methacrylate)
PMMA	poly(methyl methacrylate)
PmPv	poly(*m*-phenylenevinylene)
PNIPAM	poly(*N*-isopropylacrylamide)
POEGMA	poly(oligo(ethylene glycol) methacrylate)
PPEI	poly(*N*-propionyl ethyleneimine)
ppm	parts per million
PSt	polystyrene
PVA	poly(vinyl alcohol)
PVBTAC	poly((ar-vinylbenzyl) trimethylammonium chloride)
PVP	poly(vinyl pyridine)

RAFT	reversible addition fragmentation chain transfer
RH	hydrodynamic radius
ROMP	ring opening metathesis polymerisation
ROP	ring-opening polymerisation
R_p	rate of polymerisation
R_t	rate of termination
SAM	self-assembled monolayer
SEC	size exclusion chromatography
SEM	scanning electron microscopy
SET	single-electron transfer
SI-VDP	surface-initiated vapour deposition polymerisation
SKMA	solketal methacrylate
St	styrene
SWCNTs	single-walled carbon nanotubes
TEM	transmission electron microscopy
TGA	thermal gravimetric analysis
THF	tetrahydrofuran
TMM-LRP	transition metal mediated living radical polymerisation
UV	ultra violet
λ	wave length (nm)
ν	frequency (Hz)

Chapter 1. Polymers at Solid Surfaces

1.1 Introduction

Thin organic and polymer layers on solid substrates play a key role in many processes aimed at modifying surface properties. These organic/polymer modified surfaces can be applied in many fields, including adhesion and wetting, [1-3] microfluidics, [4] microfabrication, [3,5,6] chemical sensing [5] and organic synthesis. [6-8] In addition, many examples of bio-related applications, such as tissue engineering, [9] drug delivery, [10-12] implants and cell adhesion [13,14] and protein recognition [1] have also been reported.

With the development of polymer and surface science, new grafting technologies promise to offer unprecedented control of the polymer architecture with micrometer and nanometer resolutions. A brief introduction of current technologies used in (polymer) surface modification will be given below.

1.2 Self-assembled monolayers (SAMs)

A very fashionable method for the preparation of well-controlled surface layers is the use of molecules with a reactive head-groups to form a covalent bond with a complementary chemical site on the surface of a target substrate to be modified. This can lead to the formation of a so-called self-assembled monolayer (SAM).[15] This technology has been extended and widely used in the area of surface modification with polymers, especially for the attachment of initiators or chain transfer agents onto a surface for subsequent polymerisation. In general, SAMs are surfaces consisting of a single layer of molecules on a substrate. Rather than having to use a technique such as chemical vapor deposition[16] or molecular beam epitaxy[17] to add molecules to a

surface (often with poor control over the thickness of the molecular layer), self assembled monolayers can be prepared simply by adding a solution of the desired molecule onto the substrate surface and washing off the excess, Figure 1.

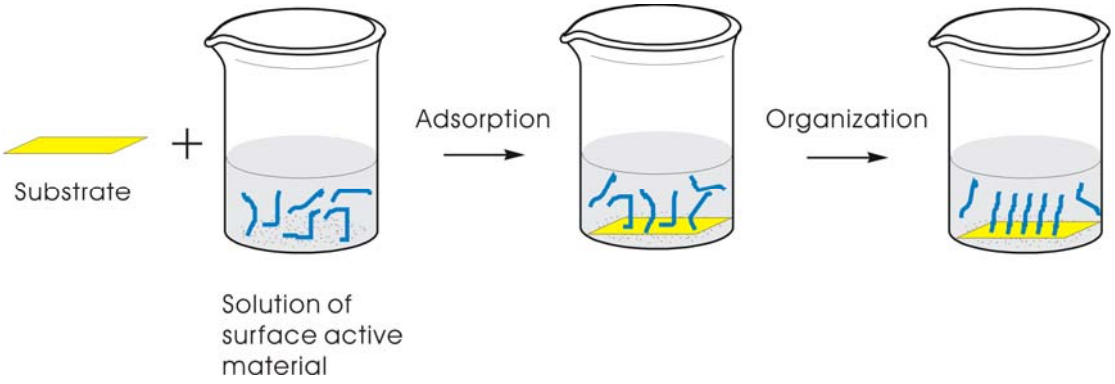

Figure 1. Schematic representation of a self-assembled monolayer (SAM).

The most common example is probably an alkane thiol assembled on a gold surface. Sulfur has a high affinity for gold, with a binding energy in the range of 20–35 kcal/mol (85–145 kJ/mol). An alkane with a thiol head group will stick to the gold surface and form an ordered assembly with the alkyl chains packing together due to van der Waals forces. Although the majority of papers describing SAMs in recent years have described thiols on gold [18,19], this is by no means the only system to consider. As shown in Figure 2, there are in general three types of SAMs: (1) monolayers of fatty acids: the spontaneous adsorption of *n*-alkanoic acids ($C_nH_{2n+1}COOH$) onto aluminium oxide or silver is a good example.[20-22] This is an acid-base reaction, and the driving force is the formation of a surface metal cation. (2) Monolayers of organosilicon derivatives: SAMs of alkylchlorosilanes, alkylalkoxysilanes, and alkylaminosilanes can be formed on hydroxylated surfaces. The driving force for this self-assembly is the *in situ* formation of a polysiloxane, which is connected to surface silanol groups (-SiOH) via Si-O-Si bonds. Substrates on which these monolayers have been successfully prepared include silicon oxide, [23-26] aluminium oxide, [27,28] quartz, [29-31] glass, [26] mica, [32,33] zinc elenide, [26,27] germanium

oxide, [26] and gold. [18,19] (3) Organosulfur adsorbates on metal and semiconductor surfaces: Sulfur and selenium compounds have a strong affinity to transition metal surfaces. [34,35] This is probably due to the possibility of forming multiple bonds with surface metal clusters. Until now, the most studied, and probably most understood SAM is that of alkane thiolates on Au surfaces. [36-39] Organosulfur compounds coordinate very strongly also to silver, [40,41] copper, [41,42] platinum, [43] mercury, [44] iron, [45] nanosized γ-Fe_2O_3 particles, [46] GaAs, [47] and InP surfaces. [48]

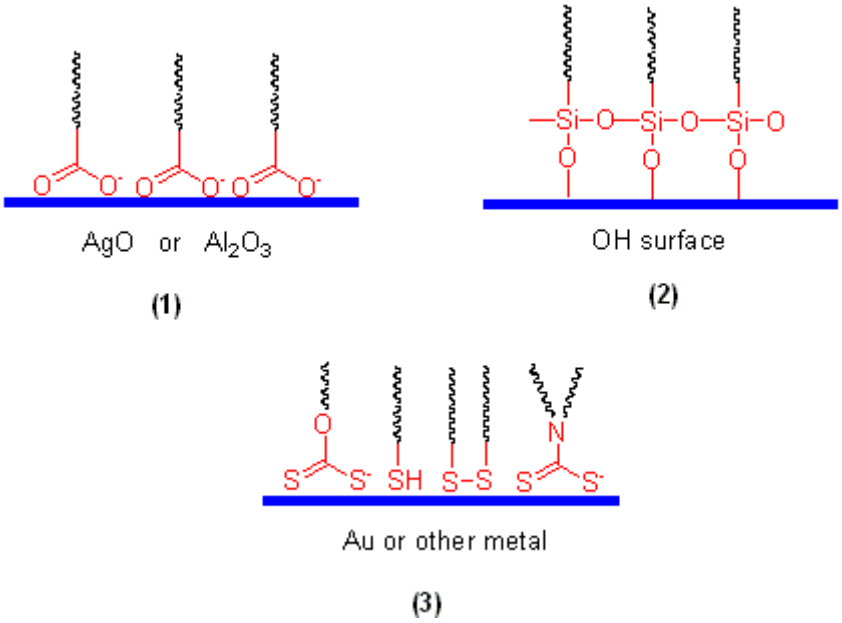

Figure 2. Schematic representation of different types of SAMs.

1.3 Surface modification with polymers

For the modification of planar surfaces with polymer or organic materials, there are in general three methods, Figure 3. The simplest method is spin casting or dip coating techniques, in this way, the "physisorbed" material is formed on the surface. A typical method for spin casting is the following. A solution of the substrate material is prepared with a volatile solvent. Cleaned glass microscope slides are mounted on a

centrifuge rotor head, which holds the slides in a horizontal position during centrifugation. A drop of solution is deposited on the slide. The centrifuge is then operated at moderate speed and under slightly evacuated conditions until all the solvent has evaporated, leaving a thin smooth film on the glass slide. Although easy and simple, the polymers coated onto the surface using these techniques may become detached under certain conditions. Therefore other approaches have been researched and investigated. One strategy commonly employed for solving this problem is to form a covalent chemical bond between the substrate and the polymer molecules.

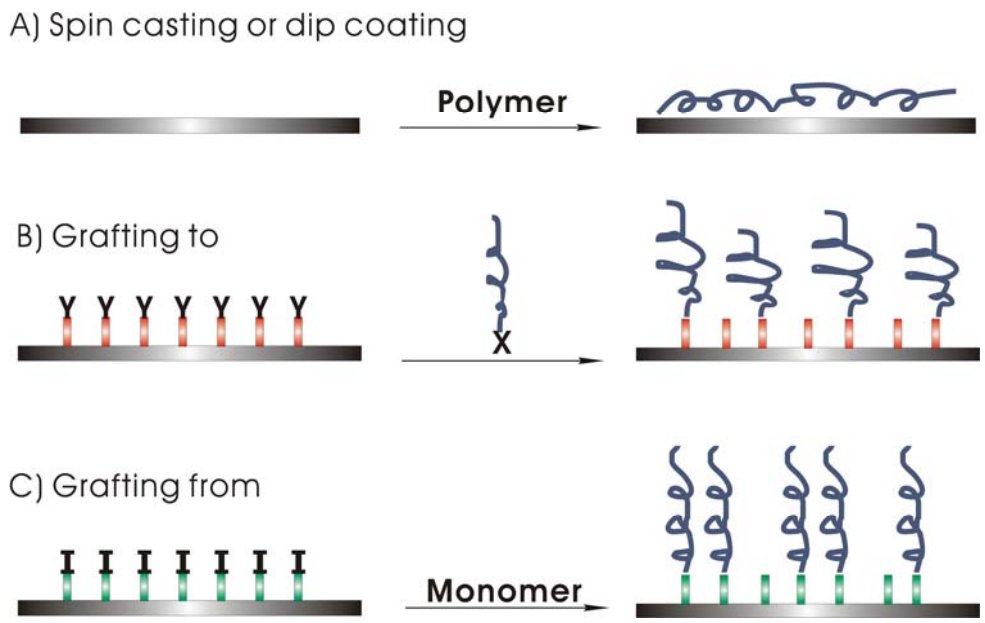

Figure 3. Approaches for modifying surfaces with organic polymers.

There may be two different types, according to where the functionality of the polymer is used to form a bond with the surface, either on the side chain or end group. Surfaces modified with functional polymers with reactive end-groups are known as polymer brushes. [49-52] There are two general techniques for obtaining polymer brushes: firstly the "grafting to" method [53-55], where polymers carrying an "anchor" end-group are used to react with appropriate sites at the substrate surface. Another approach

widely employed to make polymer brushes is to generate polymers directly at the surface of the substrate using surface-attached initiators, ("grafting from" method or sometimes called surface-initiated polymerisation[52]). Examples of these two techniques for surface modification are given below.

1.4 Typical surface modification using "grafting from" method

The "grafting from" method is by far the most widely employed synthetic strategy for the production of high density polymer brushes since the emergence of living radical polymerization [50,56]. Many examples of the "grafting from" method using anionic, cationic, ring-opening, nitroxide-mediated polymerisation (NMP), reversible addition–fragmentation chain transfer (RAFT) polymerisation and in particular transition metal mediated living radical polymerisation (TMM-LRP) have been reported. [57-60] The latter technique, often termed atom transfer radical polymerisation (ATRP), provides polymers with controlled molecular weight and low polydispersities and gives better control of the properties of the surface [56,61-63]. Here some example of the methods used in surface modification through "grafting from" approach will be given:

1.4.1 Ring opening polymerisation

In ring-opening polymerisation (ROP), the monomer is a cyclic compound. The chain typically propagates through cationic or anionic propagation. The simplified schematic representation of ROP is shown in Figure 4, where Z is normally a non-

carbon atom, such as O and N atoms. Typical examples of surface-initiated ROP are given below.

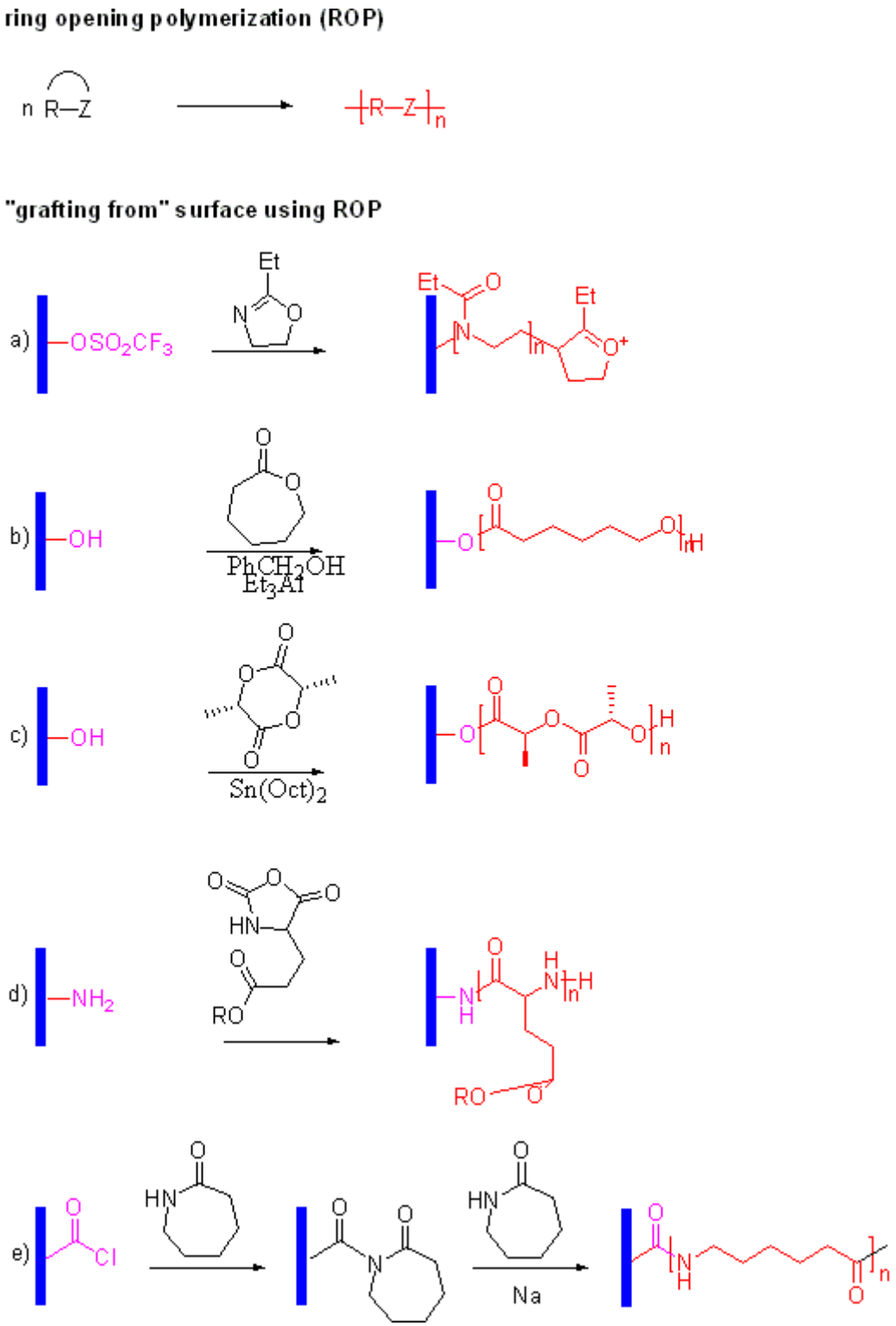

Figure 4. Scheme of ring opening polymerisation (ROP) and typical example of polymer brushes grown by ROP. (a) Poly(*N*-propionylethyleneimine), (b) poly(ε-caprolactone), (c) poly(lactic acid), (d) poly(glutamate), (e) poly(ε-carprolactam).

Jordan *et al.* firstly reported the living cationic ROP of 2-ethyl-2-oxazoline to produce linear poly(*N*-propionyl ethyleneimine) (PPEI).[64] Self-assembled monolayer (SAM) technology was used to attach trifluoromethane sulfonate groups on a gold coated glass slide by the adsorption of 11-hydroxyundecanethiol and subsequent vapor-phase functionalization. A thick layer of PPEI was produced by reaction with 2-ethyl-2-oxazoline in refluxing chloroform for seven days. Amphiphilic brushes were obtained after adding *N, N*-dioctylamine to terminate this polymerisation. (Figure 4a)

Aluminium alkoxide catalysed ROP was used by Husseman *et al.* to grow brushes of poly(e-caprolactone) (PCL) on gold surfaces.[65] A SAM with di(ethylene glycol) terminating moieties was used to present -*OH* groups for initiation. Organometallic catalysis with diethylaluminium alkoxides, which were prepared from triethylaluminium, allowed the formation of thick PCL brushes at ambient temperature within a few hours. (Figure 4b) Similarly, Choi and Langer explored the use of the tin(II) octanoate catalyst to produce chiral poly(lactic acid) (PLA) brushes on gold and silicon substrates by ROP of L-lactide.[66] (Figure 4c) In a more recent example of this type reported by Lattuada *et al*., surface-initiated ROP of L-lactide was used for the preparation of monodisperse, water-soluble magnetic nanoparticles. [67] Also, ROP of ε-caprolactone (ε-CL) and L-lactide (L-LA) have been performed from cellulose fibres. The hydroxyl groups on cellulose act as initiators in the polymerisation.[68] In another example of nanotube modification using ROP method, Chen *et al.* reported that MWCNTs were modified to possess hydroxyl groups and were used as co-initiators to polymerise L-lactide. [69]

Schouten and co-workers grew poly(L-glutamate) brushes from amine-functionalized silicon wafers and glass slides. The ROP of *N*-carboxyanhydrides (NCA) of γ-benzyl L-glutamate and γ-methyl L-glutamate from (γ-aminopropyl)triethoxysilane (APS)

pretreated substrates such as silicon wafers and quartz slides was investigated,[70] (Figure 4d). In addition, the electromechanical properties of a poly-γ-benzyl-L-glutamate (PBLG) film grafted at the carboxyl-terminal end to a flat aluminum surface were measured by Jaworek *et al.*[71]

More recently, the functionalization of carbon nanotubes with nylon-6 was accomplished through surface-initiated ROP strategy in a two-step process. ε-Caprolactam molecules were first covalently attached to nanotubes, followed by the ROP of these bound ε-caprolactam species with the same monomers in bulk, Figure 4e.[72]

1.4.2 Ring opening metathesis polymerisation (ROMP)

Ring opening metathesis polymerisation (ROMP) is a polymerisation method where which cyclic olefins (*e.g.* norbornene or cyclopentene) are polymerized with a metathesis catalyst, Figure 5. For the application of ROMP on surface modification, Whitesides and co-workers used an immobilized ruthenium catalyst to grow brushes from norbornene-derived monomers onto silicon wafer surfaces.[73] The active surface-bound catalytic sites were produced by exposing the preformed trichlorosilane norbornene-containing SAMs to a solution of Grubbs-type ROMP catalyst. Polymer brushes from norbornene-based monomers were then obtained. Exposure of these brushes to a solution of a second monomer allowed the growth of diblock copolymer brushes. Similarly, Grubbs and co-workers use a surface-bound ruthenium catalyst with a norbornene monomer as a route to very well defined insulating layers on silicon, with applications in electrical device construction.[74] More recently, Moon and Swager used ROMP to grow brushes with poly(*p*-phenylene ethynylene) "molecular wire" side chains for applications in chemical sensing.[75] Surface-initiated ROMP of

cyclooctadiene (COD) carried out in the vapor phase was also reported by Feng *et al.* This is advantageous compared to conventional solution methods in terms of minimizing chain transfer by reducing polymer chain mobility at the vapor/solid interface. [76]

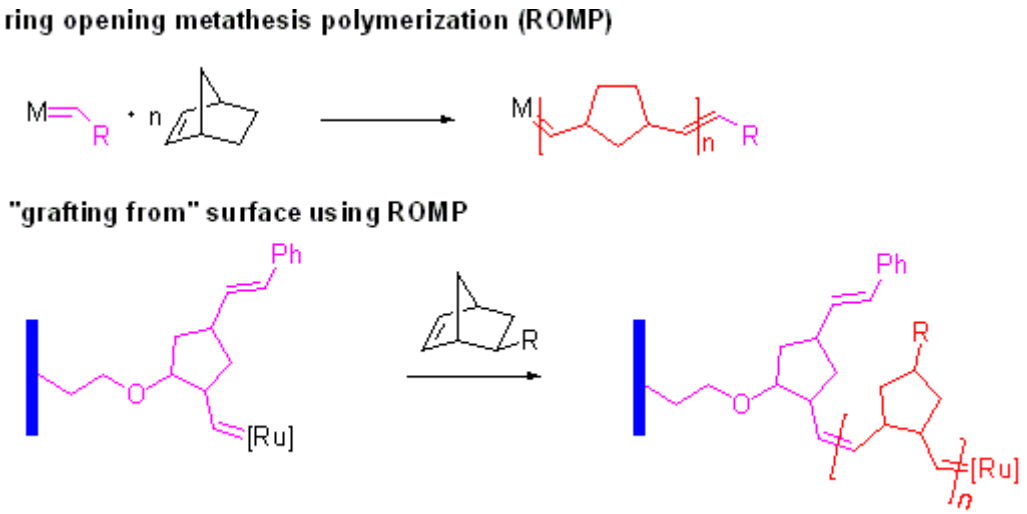

Figure 5. Scheme of ROMP and example of polymer brushes grown by ring opening metathesis polymerisation (ROMP) of norbornene-derived monomers.

1.4.3 Living ionic (anionic/cationic) polymerisation

Anionic addition polymerisation of vinyl monomers is normally initiated by a strong base and anion, such as an alkali amide, or an organometallic compound, such as *n*-butyllithium. Conversely, in cationic polymerisation, the carbocation acts as the active center for monomer to add on the growing chain. The highly living nature of anionic/cationic polymerisation has made it an attractive choice for the synthesis of well-defined polymer brushes. Examples of polymer brushes made by these two living ionic polymerisation techniques are given below, Figure 6.

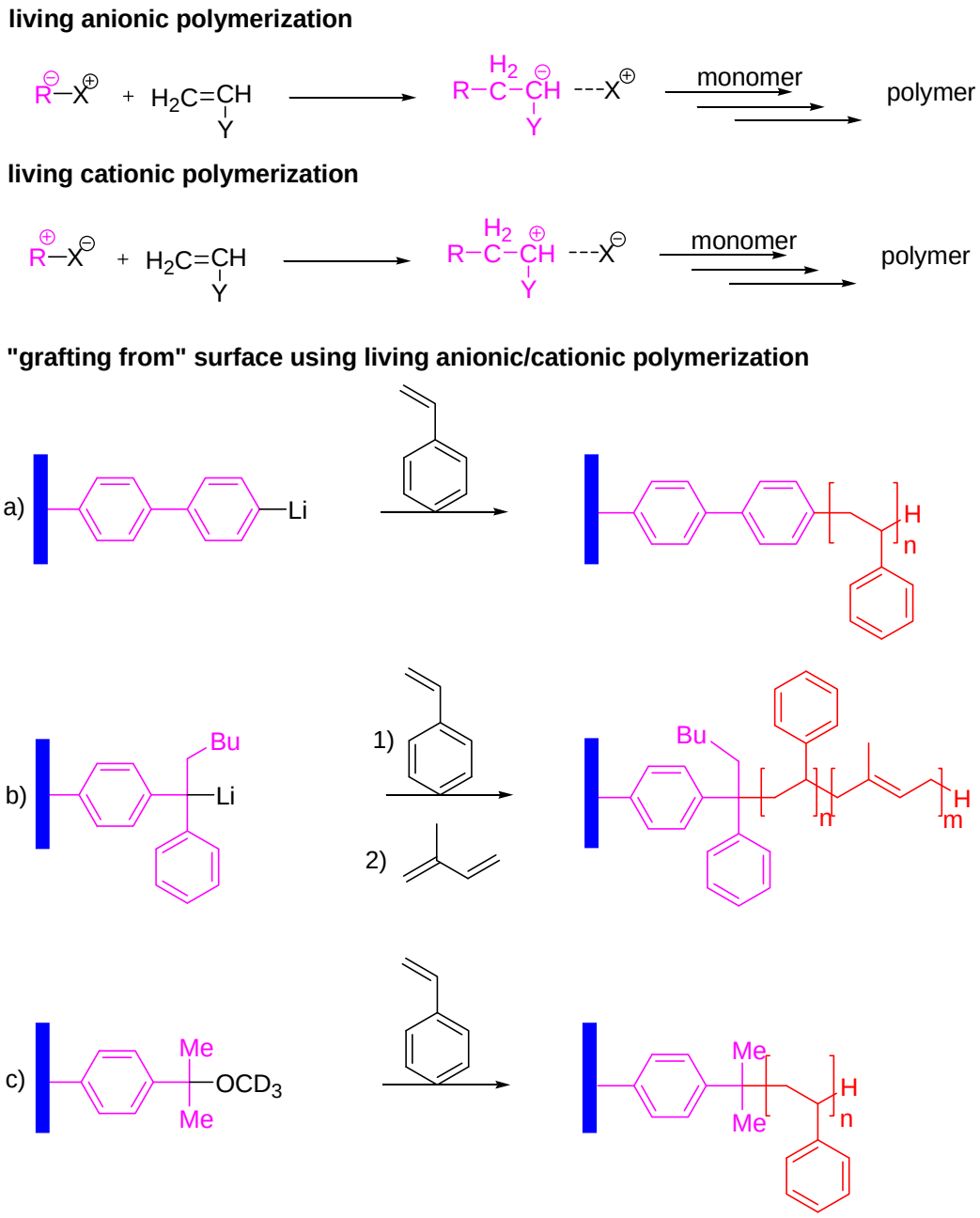

Figure 6. Scheme of living anionic/cationic polymerisation and typical examples of polymer brushes grown by [(a) polystyrene, (b) polystyrene-*b*-polyisoprene] living anionic polymerisation and [(c) polystyrene] living cationic polymerisation.

Jordan and Ulman used SAMs containing biphenyllithium groups to initiate the anionic polymerisation of styrene from gold surfaces. SAMs containing bromobiphenyl groups were formed, and converted to the initiating species by reaction with sec-butyl lithium. Very uniform styrene films with a thickness of 18 nm were obtained, although the polymerisation is slow, taking three days to reach this thickness.[77] (Figure 6a) Advincula *et al.* used SAMs containing diphenylethylene

(DPE) groups, activated with n-butyl lithium, to initiate the anionic polymerisation of styrene.[78], Figure 6b. Similarly, in another example using DPE groups as the immobilized precursor initiator for living anionic surface-initiated polymerisation, after activated with *n*-BuLi, different monomers (styrene, isoprene, ethylene oxide, and methyl methacrylate) have been polymerized from flat gold substrates.[79] More recently, Chen et al reported soluble carbon nanotubes were prepared by treating SWNTs with sec-butyl lithium and subsequently using the generated carbanions as the initiator to graft PtBA and PtBA-*b*-PMMA onto the surface of SWNTs. [80]

For the application of cationic polymerisation to the synthesis of polymer brushes, Brittain and coworkers reported that SAMs terminating in cumyl methyl ether moieties were deposited on silicon wafer surfaces, activation with $TiCl_4$ in the presence of styrene and a proton scavenger (di-tert-butyl pyridine) leads to the growth of brushes at -78°C,[81] Figure 6c. A very low temperature was needed in this case to suppress chain transfer reactions.

1.4.4 Nitroxide-mediated polymerisation (NMP)

Also called stable free radical mediated polymerisation, NMP was discovered while using a radical scavenger called TEMPO when investigating the rate of initiation during free radical polymerisation.[82] The coupling of the stable free radical with the polymeric radical is sufficiently reversible, therefore termination is reversible, and the propagating radical concentration can be limited to levels that allow controlled polymerisation. The equilibrium between dormant chains (those reversibly terminated with the stable free radical) and active chains (those with a radical capable of adding to monomer) is designed to heavily favor the dormant state. A schematic representation of NMP is shown in Figure 7.

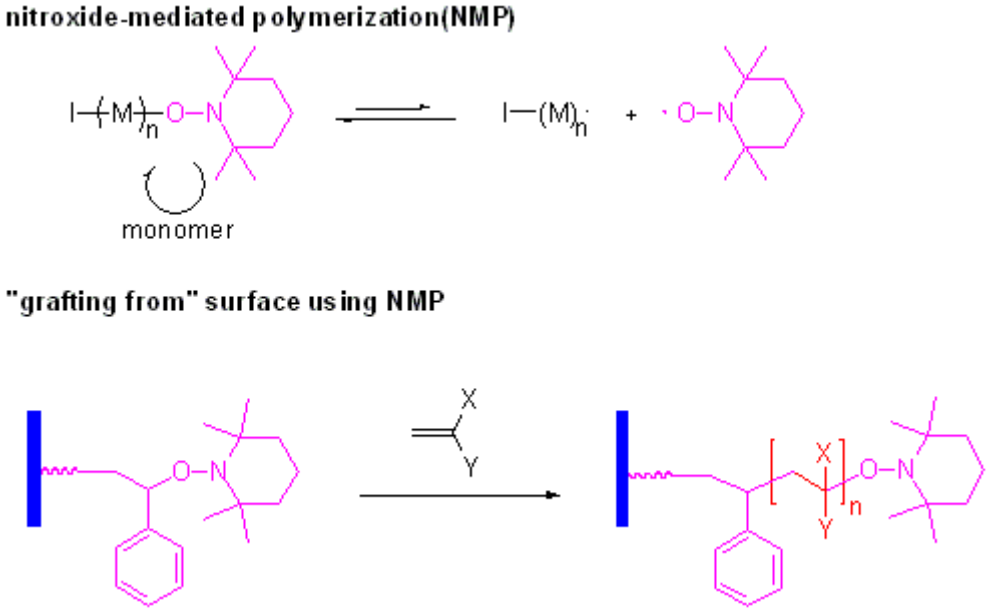

Figure 7. Schematic representation of nitroxide-mediated polymerisation (NMP) and polymer brushes grown by NMP.

When applying this concept to surface modification, the attachment of TEMPO-containing initiator to surface will be the key issue. Depending on the surface used, different surface-bound TEMPO initiators with different functionality and spacers have been made to polymerise different monomers, although the most widely used is styrene, where X = H, Y = C_6H_5 in Figure 7. Examples of surface-initiated NMP are given below.

Husseman *et al.* reported the synthesis of polystyrene brushes on silicon wafers using surface-bound alkoxyamine initiator molecules.[83] Polymerisation of styrene from this surface was carried out, upon heating the initiator-functionalized wafer to 120°C, when the alkoxyamine moiety is cleaved off to give an alkyl radical and the stable nitroxide radical, TEMPO. However, using surface-bound initiators alone did not give a controlled polymerisation, as the very small amount of growing polymer chains, compared to the monomer concentration, gives a very low overall concentration of free TEMPO and so inefficient capping of chain ends. The addition of "free" alkoxyamine initiator to the polymerisation solution solves this problem, but leads to

the formation of free polymer, which must be removed from the brushes by excessive washing with solvents. In another example, Hawker and co-workers applied surface-initiated NMP to the formation of crosslinked, hollow nanoparticles, which may be of interest for applications such as drug delivery and as building blocks for nanotechnology.[84] In a further report, a gas-phase polymerisation approach was used to create end-grafted vinyl based polymer films on silicon oxide based surface.[85] The "surface-initiated vapor deposition polymerisation" (SI-VDP) of vaporized vinyl monomers, via NMP mechanism, was developed to fabricate various homo- and block copolymer brushes from surface-bound TEMPO initiators. Different monomers like styrene, acrylic acid (AAc), *N*-(2-hydroxy-propyl)-2-methyl-acrylamide (HPMA) and *N*-isopropyl-2-methyl-acrylamide(NIPAAm) were used. More recently, polystyrene (PS)-grafted-titanium oxide (TiO_2) nanoparticles with a diameter of 15 nm were prepared by surface-initiated NMP. [86]

1.4.5 Reversible addition–fragmentation chain transfer (RAFT) polymerisation

Reversible Addition Fragmentation chain Transfer polymerisation (RAFT) was presented by Rizzardo *et al.* from CSIRO,[87,88] and a mechanistically identical process termed Macromolecular Design via Interchange of Xanthates (MADIX) from Zard *et al.* at Rhodia [89,90] were both first reported in 1998/early 1999. RAFT is a degenerative chain transfer process and is free radical in nature. Most RAFT agents contain thiocarbonyl-thio groups, and it is the reaction of polymeric and other radicals with the C=S that leads to the formation of stabilized radical intermediates. In an ideal system, these stabilized radical intermediates do not undergo termination reactions, but instead reintroduce a radical capable of re-initiation or propagation with monomer,

while they themselves reform their C=S bond. The cycle of addition to the C=S bond, followed by fragmentation of a radical, continues until all monomer is consumed. Termination is limited in this system by the low concentration of active radicals. (Figure 8)

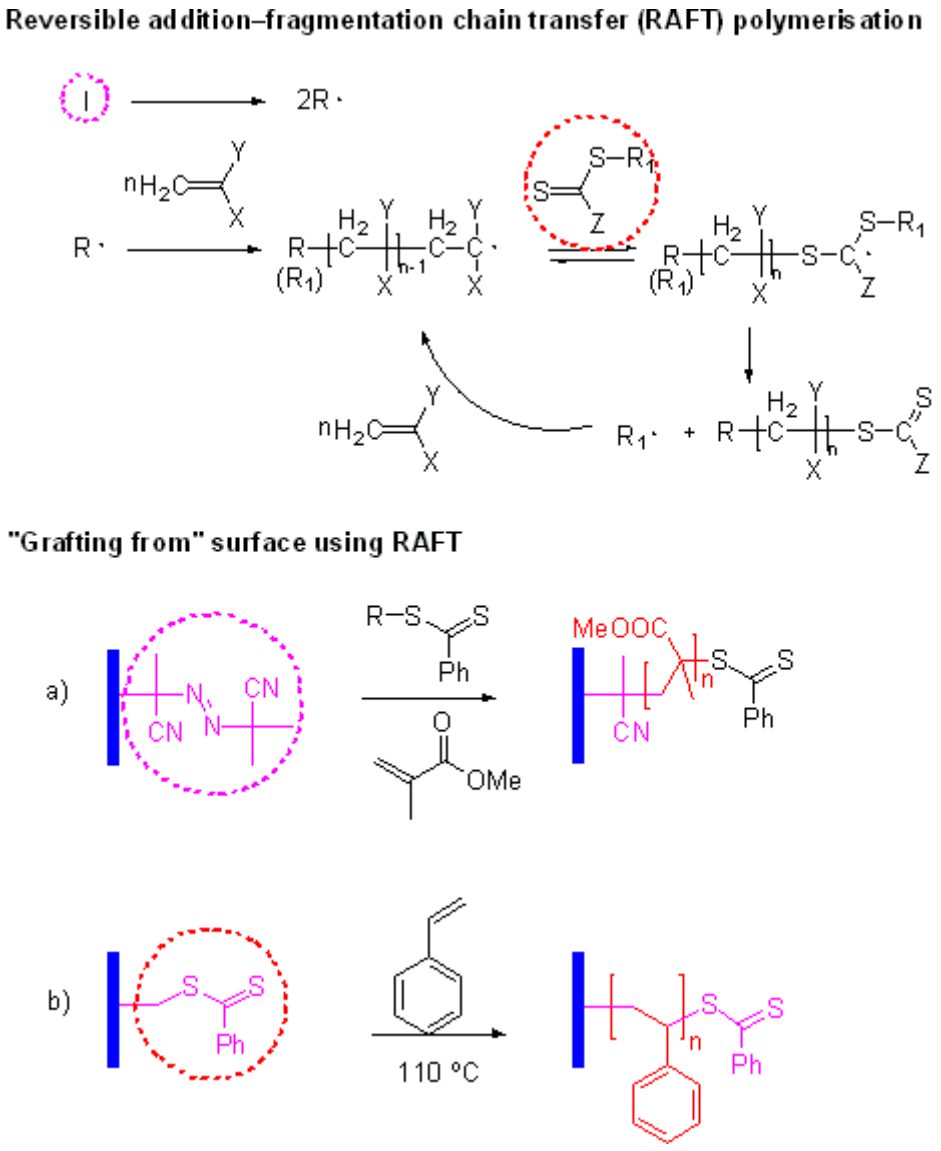

Figure 8. Scheme of Reversible Addition Fragmentation chain Transfer polymerisation (RAFT) and typical example of polymer brushes grown by RAFT. (a) Poly(methyl methacrylate), (b) polystyrene.

For surface modification using RAFT there are generally two approaches, firstly the attachment of initiating groups onto a surface, in this way, the chain transfer agent need to be added and therefore radical transfer between growing chains takes place in

solution. The other approach is the immobilization of a chain transfer agent directly on a surface, here radical transfer between growing chains takes place on the surface. In the first approach, Brittain and coworkers reported the usage of a SAM containing an azo initiator group to grow polymer brushes from silicon surfaces in the presence of a dithiobenzoate chain transfer agent. [91] It was found that a small amount of untethered radical initiator (AIBN) was required in solution for brush growth. Similarly as mentioned earlier, extensive washing with solvent (DCM in this case) was needed to rinse out the free polymers formed in solution.

In the second approach, Tsujii *et al.* reported the RAFT-mediated graft polymerisation of styrene initiated from a silica particle. In order to obtain a surface with a dithiobenzyl chain transfer agent, oligomeric polystyrene (PSt) was grafted onto a silica particle by the surface-initiated atom transfer radical polymerisation (ATRP) technique, [92] and then the terminal halogen atoms of the graft polymer were converted to dithiobenzoyl groups by the reaction with 1-phenylethyl dithiobenzoate in the presence of CuBr/dHBipy complex in toluene. A free RAFT agent was used in order to have a well-controlled polymerisation. The RAFT-mediated graft polymerisation of styrene was then carried out by heating at 110 °C. In a more recent example, RAFT agents were attached to multi-walled carbon nanotubes (MWCNTs) by treating MWCNT-Br with phenylmagnesium bromide; subsequently, different kinds of water soluble ionic polymer chains, such as cationic polymer (poly(2-(dimethylamino) ethyl methacrylate)), anionic polymer (poly(acrylic acid)) and zwitterionic polymer (poly(3-[*N*-(3- methacrylamidopropyl)-*N*,*N*-dimethyl] ammoniopropane sulfonate)) were easily grafted onto the surface of MWCNTs directly by surface RAFT polymerisation technique.[93]

1.4.6 Transition metal medicated living radical polymerisation (TMM-LRP)

Transition metal mediated living radical polymerisation (TMM-LRP) is one of the most promising methods to prepare well-defined polymers[94,95]: it can be carried out under mild reaction temperatures, and is suitable for most vinyl monomers and tolerant to some impurities such as water and alcohol. The most widely used recipe includes a halide initiator, copper(I) salt and a nitrogen containing ligand as catalyst system. It is normally termed as atom transfer radical polymerisation (ATRP). However robust, the mechanism of ATRP is still under debate. The most widely accepted mechanism believe that the polymerisation proceeds by an inner-sphere electron-transfer mechanism in which a low oxidation state metal complex acts as the catalyst, mediating a fast exchange between radicals and their dormant alkyl halide species. (Figure 9)

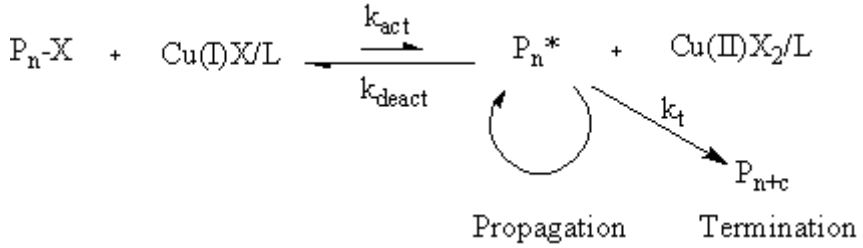

Figure 9. Inner-sphere electron-transfer mechanism of Copper Mediated Living Radical Polymerisation.

More recently, in order to diminish catalyst concentration, AGET (activators generated by electron transfer) ATRP was reported by Matyjaszewski *et al.* They used tin(II) 2-ethylhexanoate ($Sn(EH)_2$)[96] or ascorbic acid[97] to reduce Cu(II) to Cu(I), which could then catalyze ATRP under appropriate polymerisation conditions. The concentration of catalyst relative to initiator can be significantly decreased when the reducing agent in this system (which cannot initiate new chains) is present in excess relative to the catalyst. Cu(II) that accumulates as a persistent radical is then

continuously reduced to Cu(I) as the activator is regenerated by electron transfer (ARGET). [98,99] This should also follow an inner-sphere mechanism.

Although the inner-sphere mechanism is widely quoted by researchers, an outer-sphere mechanism is favored under certain conditions, especially in polar solvents in the presence of *N*-ligands. Single-electron transfer (SET)-LRP, based on this mechanism, has been reported by Percec and co-workers.[100] In this mechanism, copper(I) disproportionates into Cu(II) and Cu(0), where after Cu(0) acts as an electron donor and the initiator and dormant propagating species act as electron acceptors.(Figure 10) This polymerisation can be carried out under very mild reaction conditions, at room temperature, using a small amount of catalyst and generates polymers with high molecular weight with fast rate.

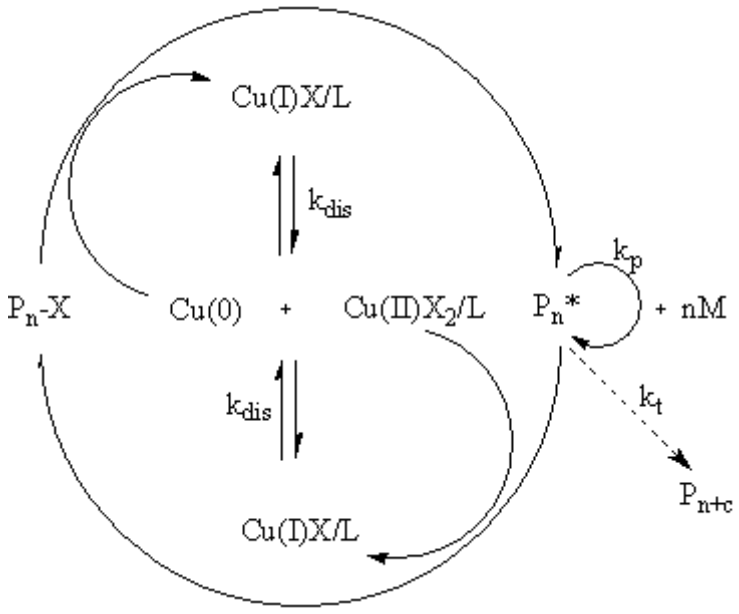

Figure 10. Out-sphere electron-transfer mechanism of Copper Mediated Living Radical Polymerisation according to Percec.

In the field of surface modification, many applications have used "grafting-from" processes from various surfaces such as gold,[56,101] silicon, [60,102] Wang resin, [103,104] glass,[103,104] and cellulose.[61,105,106] The earliest example is the polymerisation of MMA from silicon via surface-initiated ATRP by Fukuda and coworkers,[60] as shown in

Figure 11a. Similarly, Matyjaszewski and coworkers reported that controlled polymerisations of MA onto silicon and polystyrene (PSt) brushes were re-initiated to form PSt-b-PMA block copolymer films.[107]

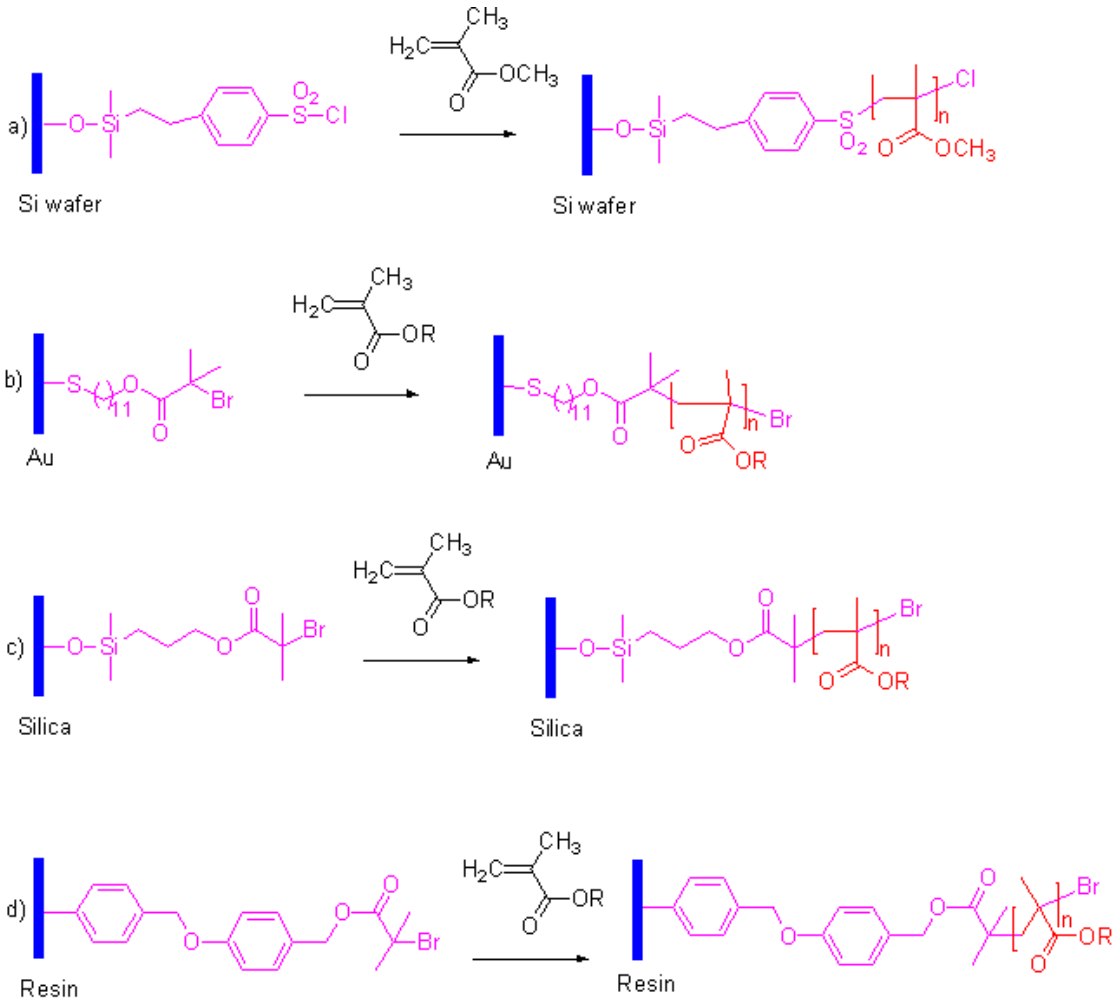

Figure 11. Typical examples of polymer brushes grown by ATRP.

Later on, it was found that surface-initiated polymerizations in aqueous media give faster polymerisation rates even at low temperatures. Huang *et al.* reported that water-accelerated ATRP is an efficient procedure for growth of thick PHEMA films on gold.[108] This method yields polymer films with controlled thicknesses up to 700 nm within a 12 h period, and the living character of the grafting polymerisation allows the growth of a second polymer block. Moreover, the grafted PHEMA films can be further functionalized in high yield via reaction of their hydroxyl groups. This

provides opportunities for tailoring the surface properties of polymer brushes for possible applications in separation and controlled release. Other examples of gold surface-initiated ATRP carried out in aqueous media include PMMA, PGMA, and PHEMA brushes.[108,109] PDMAEMA,[110] cross-linked films of ethylene glycol dimethacrylate (EGDMA),[111] and poly(*N*-isopropylacrylamide) (PNIPAM),[112] Figure 11b. Most of them attribute the relatively fast rate to 'the accelerating effect of water' on surface initiated ATRP. Considering the recently arising discussion concerning inner/outer-sphere mechanism of copper mediated LRP, the reason of this accelerating effect may need further investigation.

Surface-initiated polyelectrolyte brushes have been made via ATRP as polyelectrolytes have the interesting property of changing their conformation in solution depending pH. This unique responsive property makes polyelectrolytes attractive as they might be used in various nanotechnologies. There are generally two approaches to modify surface with polyelectrolyte brushes, either using charged monomers [113] (Figure 12a) or using normal acrylates followed by hydrolysis [114]. (Figure 12b)

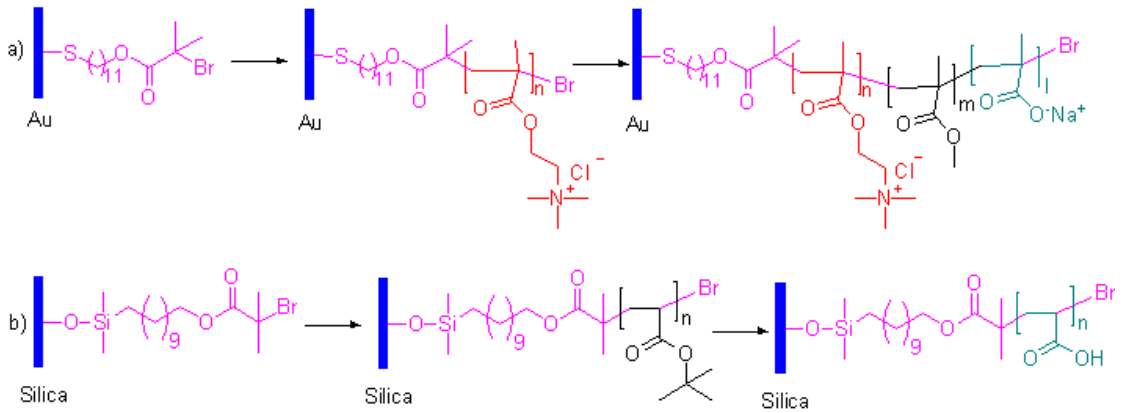

Figure 12. Examples of polyelectrolyte brushes grown by ATRP.

Surface-initiated ATRP has also been carried out on colloidal substrates and polymeric substrates. Huang *et al.* reported that polyacrylamide was grown from

porous silica gel.[115] Perruchot *et al*. made poly(oligo(ethylene glycol) methacrylate) (POEGMA) and poly(2-(*N*-morpholino)-ethyl methacrylate) (PMEMA) onto silica supports. [116] Polyelectrolyte brushes include poly(sodium 4-styrenesulfonate), poly(sodium 4-vinylbenzoate) , PDMAEMA and poly(2-(diethylamino)ethyl methacrylate) have also been grafted to silica.[117] (Figure 11c) Examples of polymer brushes on polymeric substrates include Polyacrylamide brush on a cross-linked polydimethylsiloxane (PDMS) surface. [118] PNIPAM, PHEMA and poly(poly(ethylene glycol)-1100 monomethacrylate) on polystyrene microspheres.[119]. PMA, PMMA, PHEMA and PDMAEMA on divinylbenzene/hydroxyethyl methacrylate copolymer microspheres[120] , 2-hydroxyethyl acrylate (HEA) and 2-(methacryloyloxy)ethyl trimethylammonium chloride (METAC) onto poly[styrene-co-2-(2-bromopropionyloxy)] latex particles. [121], poly(*N,N*-dimethylacrylamide) from polystyrene latex, [122] and poly(methyl methacrylate), PMMA, homopolymer, and poly(methyl methacrylate)-block-poly(benzyl methacrylate-co-methyl methacrylate), P(MMA)-block-P(BzMA-co-MMA), block copolymers onto Wang resin.[103] (Figure 11d)

1.5 Typical surface modification using "grafting to" method

As mentioned earlier, in the "*grafting to*" method, pre-made polymers carrying an "anchor" group, either as an end-group or in a side chain, are attached to appropriate sites at the surface of the substrate. Therefore, the "*grafting to*" method offers the possibility to design and control of the properties of the polymers to be grafted to the surface relatively easily. A range of polymerisation methods have been used to make functional polymers for grafting to surfaces. The moieties (functional groups) in the polymer used to attach the chains to the surface are either obtained directly from the

initiator or by post-functionalization of the polymer. Different moieties will be needed depending on the type of surfaces. In general, moieties used for the attachment of the side chain or chain ends to a solid surface can be summarized as the following:

1.5.1 Highly polar groups

Functional groups such as mercapto (-*SH*) and cyano (-*CN*) are known to have a high affinity for Au, as it is widely used for making SAMs, polymers with mercapto or cyano groups either as side-chain or end group can be used to modify gold surfaces using the "grafting to" approach. Protective polymers having cyano or mercapto groups were synthesized by Teranishi *et al.*, the polymers were directly obtained by normal free radical polymerisation or by a one step treatment, and were used to form linear polymers protected metal (Pt,Pd and Au) nanoparticles [123-125] Also using a gold surface, the attachment of derivatized poly(methyl methacrylate) (PMMA) copolymers containing both side chain anchor (sulfide) and backbone spacer (methyl methacrylate) groups was reported by Lenk *et al.*.[126] (Figure 13)

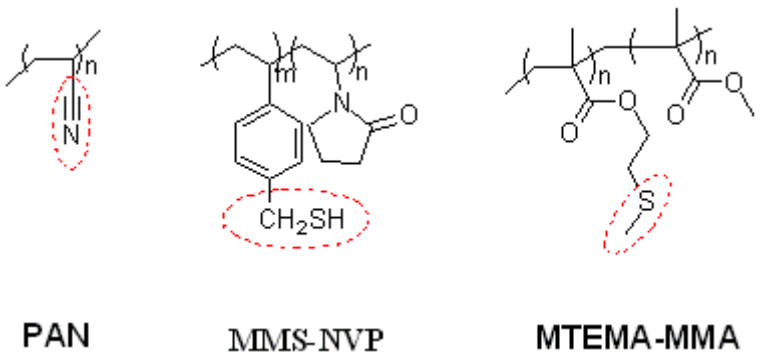

Figure 13. Chemical structures of the protective polymers poly(acrylonitrile) (PAN), poly(mercaptomethylstyrene-co-N-vinyl-2-pyrrolidone) (MMS-NVP) and poly(2-(methylthio)ethyl methacrylate-co-methyl methacrylate) (MTEMA-MMA).

Besides the side-chain functional polymers mentioned above, thiol-terminated polymers have also been used to graft onto gold surfaces. El Sayed reported polystyrene thin films containing terminal thiol were spin-coated and adsorbed from

0.1 to 0.001 wt% of polymer solution in toluene onto an evaporated gold film supported on a Si-wafer substrate.[127] In another similar example using mercapto functionality to modify gold surfaces, thiol-terminated polystyrene (PSt-SH) was prepared by anionic polymerisation. The polystyryl anions were titrated with propylene sulfide and subsequently protonated with acidic methanol to obtain the thiol-terminated polystyrene.[128,129] Other examples of modifying surface by "grafting to" method using mercapto functionality as end group include thio-end-capped PSt prepared by anionic polymerisation to Gold Nanoparticles (Au-NPs), [130] and synthesis of thio terminal NIPAM to make thermo-sensitive Au-NPs [131,132]

As mentioned earlier, reversible addition-fragmentation chain transfer (RAFT) is a versatile, controlled free radical polymerisation technique that operates via a degenerative transfer mechanism in which a thiocarbonylthio compound acts as a chain transfer agent. The subsequent reduction of the dithioester end groups to thiols allows the preparation of (co)polymer-modified gold surfaces. Examples of making a variety of thiol-terminal polymers are given below. Immobilization of poly(sodium 4-styrenesulfonate) (NaPSS), poly((ar-vinylbenzyl) trimethylammonium chloride) (PVBTAC), poly(*N*,*N*-dimethylacrylamide) (PDMA), and poly(3-[2-(*N*-methylacrylamido)-ethyldimethyl ammonio]propane sulfonate-*b*-*N*,*N*-dimethylacrylamide) (MAEDAPS-DMA) onto gold films has been reported. [133,134] (Figure 14)

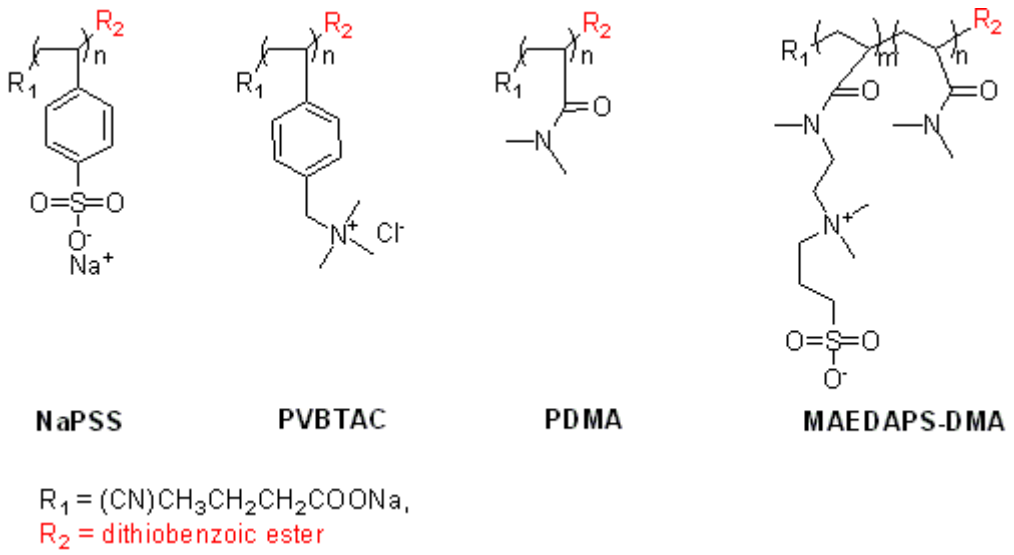

Figure 14. Chemical structures of the functional polymers with dithiobenzoic ester as end group synthesised by RAFT, poly(sodium 4-styrenesulfonate) (NaPSS), poly((ar-vinylbenzyl) trimethylammonium chloride) (PVBTAC), poly(*N,N*-dimethylacrylamide) (PDMA), and poly(3-[2-(*N*-methylacrylamido)-ethyldimethyl ammonio]propane sulfonate-b-*N,N*-dimethylacrylamide) (MAEDAPS-DMA).

In addition to the widely used thiol-functionality, other highly polar groups such as carboxylic acid and amine groups have also been reported. Carboxylic acid-terminated polystyrene (PSt) absorbed on silicon oxide from deuterated cyclohexane has reported and results showed that because of the affinity of the acid group for the silicon oxide surface, the PSt adsorbed amount is 4 times larger than the unfunctionalized PSt at 23°C.[135] In similar work, polymerizations were initiated with sec-butyl lithium, and therefore the polymers were terminated on one end with a secondary butyl group. The other chain end was capped with a carboxylic acid for surface modification. [136] In another paper, amine end-functionalized PSt made by living anionic polymerisation was used to graft to silicate glass beads, [137]

1.5.2 Charged groups and Blocks of segmentally adsorbing polymer different from the rest of the chain

It is well known that polymer brushes can be self-assembled onto a solid surface using a solvent that is good for one block but poor for the other.[138-142] Earlier studies of

forces between solid surfaces bearing polymeric or oligomeric surfactants, which have been interpreted in terms of an adsorbing moiety and non-adsorbing tail, have been reported in a number of cases. It is now well established that under suitable solvent conditions, ABA type "telechelic" polymers, “monochelic" AB-type block copolymers as well as end-functionalized polymers are capable of terminal attachment to a substrate. (Figure 15)

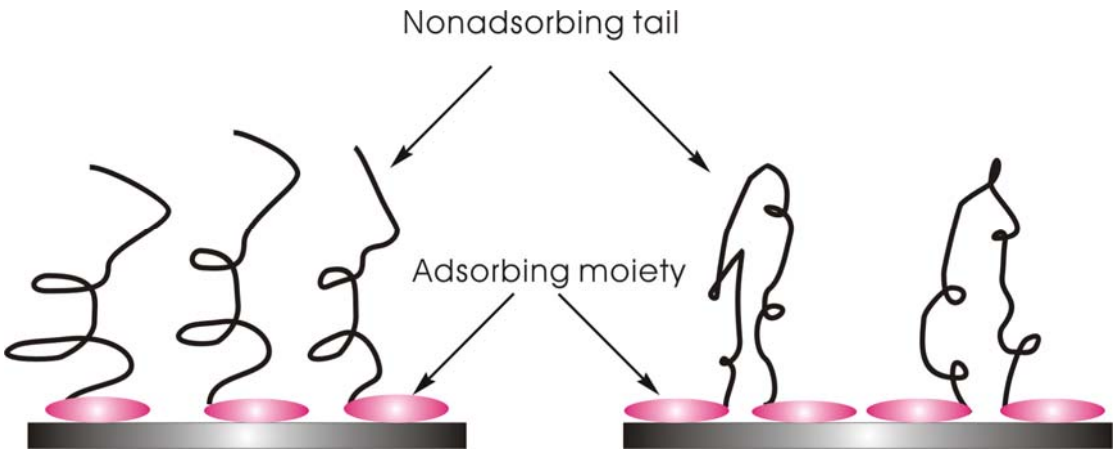

Figure 15. Schematic representation of polymers capable of terminal attachment to a substrate.

Charged groups are often used as the adsorbing moiety to attach polymers to mica surfaces. Fetters and co-workers synthesized an anionically polymerized polystyrene (PSt) chains terminated with the zwitterionic group $-N^{+}(CH_3)_2(CH_2)_3SO_3^{-}$. They determined the structure of polymer brushes formed onto mica, from dilute solutions of this zwitterion-terminated polystyrene chains in toluene.[143,144]

Furthermore, Fetters *et al.* reported the adsorption of end-functionalized polymers on colloidal spheres.[145] Anionically polymerised poly(ethylenepropy1ene) (PEP) terminated with a tertiary amino group and with a zwitterionic group was used for attachment onto a colloidal particle consisting of a calcium carbonate ($CaCO_3$) core with an adsorbed monolayer of a randomly branched calcium alkyl benzene sulfonate (CaSA) surfactant. It is found that the adsorption of the end-functionalized polymers on the colloid has to occur through the functional end groups interacting favorably

with the polar cores of the colloidal particles. The adsorption energy between the functional group and the colloidal surface is estimated to be $4k_BT$. Fetters *et al.* also reported the use of AB-type block copolymers to attach to mica surface. Polystyrene-poly(ethylene oxide) diblock copolymers (PSt-PEO) with a short PEO block was used.[146]

Other examples of AB-type block copolymers include poly(butadiene-*co*-vinylpyridine) (PB-PVP) [147] and poly(styrene-*co*-vinylpyridine) (PSt-PVP) [148,149]. They can successfully self-assemble onto mica from tetradecane or toluene, where tetradecane and toluene are good solvents for poly(butadiene) and poly(styrene) respectively, while poly(vinyl pyridine) acts as a solvophobic "anchor" in both of these solvents.

Similarly, ABA-type telechelic polymers are also capable of terminal attachment to a substrate, and normally adsorb in a loop conformation.[150] Anastassopoulos *et al.* reported a neutron reflectivity study of brushes formed at the toluene/quartz interface by end-functionalized polystyrene X-PSt-X, where X is a zwitterionic end group described previously, as well as poly(ethylene oxide)-polystyrene-poly(ethylene oxide) triblock copolymer, PEO-PSt-PEO. It is well established that both types of polymer exhibit a terminal mode of attachment in toluene (which is a good solvent for PSt), while the PSt block remains non-adsorbing and dangles in solution.

1.5.3 Chemically reactive groups

Depending on the nature and functionality of different surfaces, different functional polymers have been used to graft to surfaces through chemical reactions. Fetters *et al.* reported that end-grafted polystyrene chains are prepared in cyclohexane where the chains are chemically attached to the silicon wafers surface utilizing a trichlorosilane

end-group. [151] Jones *et al.* reported deuterated and protonated end-functionalized polystyrenes of low and high molecular weight were grafted onto silicon substrates by solution-spin casting, followed by annealing and removal of un-grafted chains.[152] Luzinov *et al.* reported that carboxylic acid- and anhydride-terminated polystyrenes of different molecular weights from 4500 to 672 000 were grafted from melt onto silicon substrates modified with epoxysilane monolayer.[153] Similarly, carboxylic acid terminated polystyrene and polybutylacrylate were grafted from melt onto a silicon substrate modified with the epoxysilane monolayer.[154] Furthermore, end-grafted deuterated poly(dimethylsiloxane) (d-PDMS) brushes have been grafted onto SiO_x wafers.[155] In another example, PSt-N_3 with targeted molecular weight and narrow molecular weight distribution was synthesized by ATRP of styrene (St) followed by end group transformation and then added to SWNT.[156]

More recently, "click Chemistry", a term introduced by Sharpless[157,158], is a topic that has been attracting many researchers. [157] Among these reactions, the Huisgen 1,3-dipolar cycloaddition[159] has been receiving increasing interest following the emergence of enormous improvement in regioselectivity and yields in the presence of copper(I)-based catalysts. More details about click chemistry and its applications will be given in the next chapter.

1.6 "*Grafting to*" versus "*grafting from*" and aim of this project

The different methods to modify surfaces with polymers have tremendously expanded the range of applications. It is now possible to graft any polymers with any functionality on virtually any surface through either the "grafting to" or "grafting from" method. These two methods of making polymer brushes, both have advantages

and disadvantages. The main disadvantage of the "grafting to" method is the limitation of approaching high grafting density. This is due to steric crowding of reactive surface sites by already adsorbed polymers, and film thickness is also limited by the molecular weights of the polymer in solution. However, the "grafting to" method is experimentally simple, and the polymer can be fully characterized before attaching to surface. Using a controlled polymerisation technique, it is possible to predetermine the molecular weight and polydispersity of the polymer about to be grafted to the substrate. Thus, it is also possible to control the end-groups of the attached polymer. Conversely, using the "grafting from" method, it is not difficult to get a high grafting density of polymers from the surface, although not as simple as "grafting to". But the disadvantage associated with most “grafting from” approaches is imprecise control of the molecular weight of the brush and also poorly controlled polydispersity. Another feature, if not disadvantage, for “grafting from” is that the addition of “free” initiator to the polymerisation solution is often needed for better control, but leads to the formation of free polymer, which must be removed from the brushes before analysis. Finally, most “grafting from” approaches require moisture-free or oxygen-free conditions, while the “grafting to” approach can be conducted under ambient conditions, although making the polymer may still need oxygen free conditions. It is clear that both methods have advantages and disadvantages, and it is not easy to judge which is better or easier. The development of polymer science has made both approaches better and more robust than years ago. Whether to choose "grafting to" or "grafting from" will mainly depend on the purpose of the modification and whether the “density” of the grafted polymer chains matters or not. A simplified comparison table of these two approaches is summarized below. (Table 1)

Table 1. Comparison of the two surface modification approaches of "grafting to" and "grafting from".

"Grafting to" approach	"Grafting from" approach
Polymers made first	Polymers made in-situ
Polymers can be precisely controlled	Polymers can be controlled, although may be not so precise
Can be conducted under ambient condition and mostly tolerate to moisture and oxygen	Mostly require moisture-free and oxygen-free
Normally produce low grafting density	Produce high grafting density
No need for free initiator, polymers designed first.	Often need free initiator for better control

Considering the above attributes of these two approaches this project can be summarized in the following two categories: (I) exploring better "grafting to" methods: emphasis will be put on "click" chemistry for surface modification and the combination of click and TMM-LRP technology; (II) using a "grafting from" approach to make polymer brushes from different surfaces: emphasis will be on surface-initiated TMM-LRP of functional polymers and the potential application aspects of the modified materials.

Chapter 2. Cellulose surface modification through click chemistry and Living Radical Polymerisation

2.1 Introduction

2.1.1 Click chemistry and Huisgen 1,3-dipolar cycloaddition

"Click Chemistry", a term introduced by Sharpless[157,158] which identifies a class of chemical transformations with a number of attractive features including excellent functional-group tolerance, high yields and good selectivity under mild experimental conditions, is a topic that has been attracting many researchers especially in the last few years. [157] There are some criteria required for a process to be considered a click transformation:

- Modular, wide in scope,
- Give very high yields,
- Generate only inoffensive by-products that can be removed by non-chromatographic methods,
- Simple reaction conditions,
- Readily available starting materials and reagents, use of no solvent or a solvent that is benign or easily removed,
- Simple product isolation.
- Normally have high thermodynamic driving force (>20 kcal/mol).

Classes of chemical transformations that have been used includes cycloadditions of unsaturated species, nucleophilic substitution chemistry, carbonyl chemistry of the

"non-aldol" type, additions to carbon-carbon multiple bonds. Among these reactions, the Huisgen 1,3-dipolar cycloaddition has been receiving increasing interest following the emergence of enormous improvements in regioselectivity and yields in the presence of copper(I)-based catalysts. The overall reaction is a cycloaddition of a terminal alkyne and an organic azide to give a five-membered 1,2,3-triazole. (Figure 16) This discovery has led to its application in many processes including the synthesis of therapeutics,[160,161] protein-based biohybrids,[162-165] sugar arrays,[166] dendrimers[167,168] and functional polymers.[169-172]

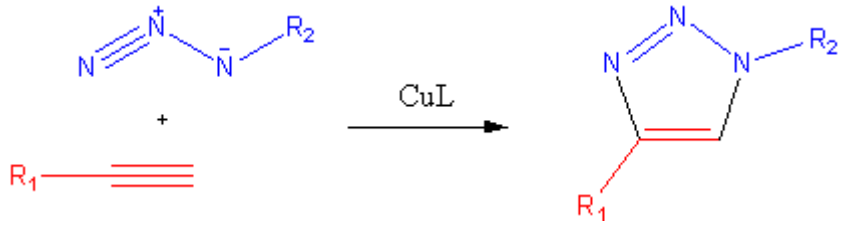

Figure 16. Cu(I)-catalysed Huisgen 1,3-dipolar cycloaddition.

2.1.2 Proposed mechanism of Cu(I)-catalysed Huisgen 1,3-dipolar cycloaddition

The Huisgen 1,3-dipolar cycloaddition,[159,173] in which a terminal alkyne is "clicked" to an organic azide to give an 1,2,3-triazole, was first reported in 1961. It has not received much attention until 2002. Two research groups discovered that this reaction could be efficiently catalysed by copper(I)-based catalysts, leading to an increase in the rate of reaction of approximately seven orders of magnitude, being totally regioselective towards the formation of 1,4-disubsituted 1,2,3-triazoles and the reaction tolerates a wide range of functional groups.[174,175]

The mechanistic proposal by Fokin and Sharpless for the catalytic cycle of the copper(I)-catalysed version of Huisgen 1,3-dipolar cycloaddition is shown in Figure 17. It begins with formation of the copper (I) acetylide **I**, then, instead of the concerted [2+3] cycloaddition (B-direct), a stepwise, annealing sequence (B-1 → B-2 → B-3, hence the term "ligation"), which proceeds via the intriguing six-membered copper-containing intermediate III. A ring contraction with the liberation of the triazole product follow. [176]

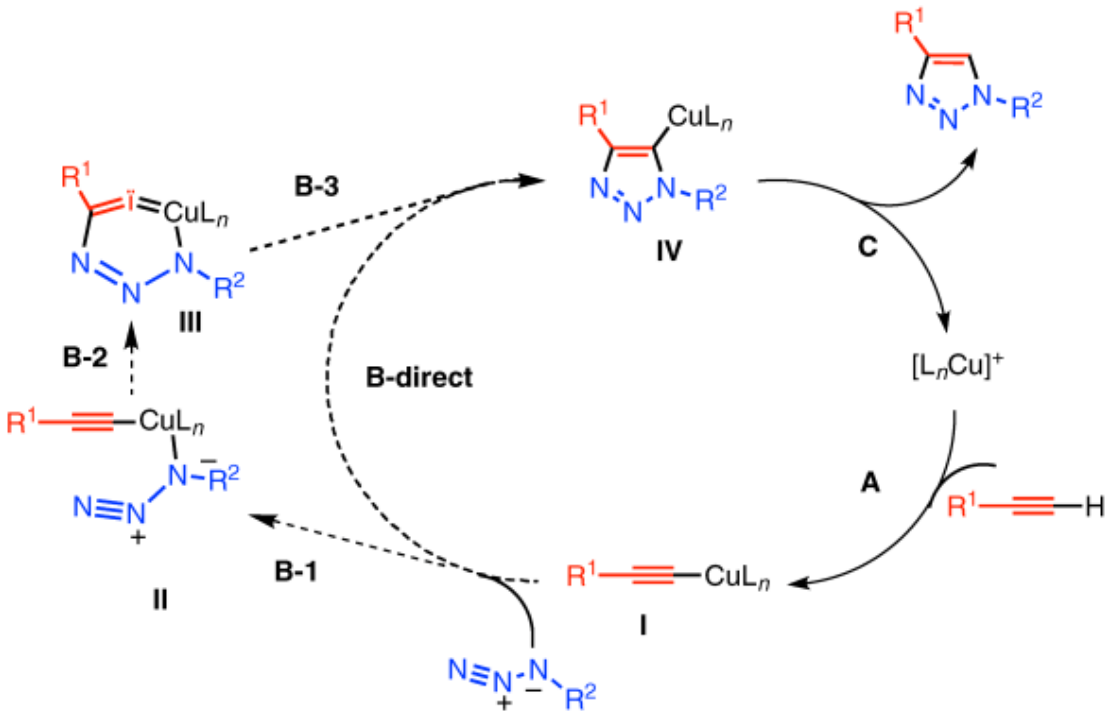

Figure 17. Proposed catalytic cycle for the Cu(I)-catalysed ligation by Fokin and Sharpless.

2.1.3 TMM-LRP and click chemistry

Transition metal medicated living radical polymerisation (TMM-LRP), often called atom transfer radical polymerisation (ATRP) has emerged as an excellent method to prepare polymers with complex architecture, predetermined molecular weights, and low polydispersities. [94,177] Many applications using ATRP for surface modification have been reported, mainly using the "*grafting-from*" approach from various surfaces

including gold,[56,101] silicon[60,102] and other materials. [103,104, 61,105,106] However, although "*grafting from*" will always give a much thicker polymer coating than the "*grafting-to*" approach in many surface property modifications the depth of coverage is not always the major concern but rather extent of coverage; this of course depends upon the final application. The "*grafting-to*" approach is versatile in that once a library of polymers have been prepared they can each be reacted independently with different surfaces under appropriate conditions whereas grafting-from requires separate polymerisation reactions in each case.

Both TMM-LRP and click chemistry share a number of important features including robustness, versatility and excellent tolerance towards many functional-groups, including water. Therefore, combining these two technologies to prepare new functonal polymers has attracted increasing interest. [178-183] We envisaged the possibility of combining TMM-LRP and click chemistry, and applying it for surface modification. One advantage of using TMM-LRP is that both azide- and alkyne- terminated polymers can be synthesized directly, using appropriate azide or alkyne initiators, depending on the convenience of making either alkyne or azide modified surfaces.

Due to the features of click chemistry, high yield and mild reaction conditions, we envisaged the possibility of applying it for surface modification using the "grafting to" method. (Figure 18) There are many advantages to combine "click" and "grafting to". For example, for the gold surface modification via S-Au bond, relatively low temperatures are necessary, as the S-Au bond is fairly weak (~30-40 kcal mol^{-1}), [56] which limits its further grafting of polymers either "to" or "from". Click chemistry would be advantageous in this case, due to its mild reaction conditions and high yield, which will also very possibly give higher grafting density.

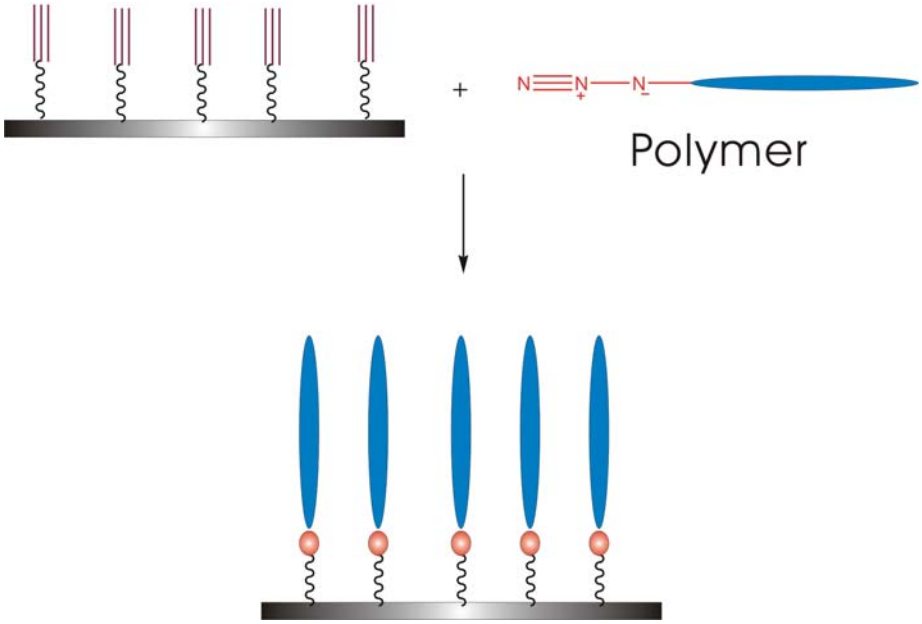

Figure 18. Click chemistry (Huisgen 1,3-dipolar cycloaddition) on surface modification.

Cellulose is one of the most common organic polymer, representing about 1.5×10^{12} tons of the total annual biomass production, and is considered an almost inexhaustible source of raw material for the increasing demand for environmentally friendly and biocompatible products.[184-186] Cellulose (cotton) surface modifications through both "*grafting to*" and "*grafting from*" methods have been carried out and will be discussed in this chapter. In the first part of this chapter, different α-functional (including azide/alkyne terminal) polymers have been synthesized using copper(I) mediated LRP, and their polymerisation behaviours have been investigated. For the azide-terminal case, it has been used to graft to an alkyne-modified cotton surface through Huisgen 1,3-dipolar cycloaddition, click reaction. In the second part, an antibiotic monomer containing metronidazole moiety has been synthesized and used to copolymerise with PEG-MA. A "*grafting from*" approach was used to grow this metronidazole-containing monomer from a bromo-modified cotton surface.

2.2. Synthesis of α-functional polymers through TMM-LRP

Synthesis of α-functional polymers is the key issue for making polymer brushes through the "grafting to" approach. The TMM-LRP technique is used to make polymers with different α-functionalities. These polymers may further be used for surface modification.

2.2.1 Synthesis of initiators for TMM-LRP

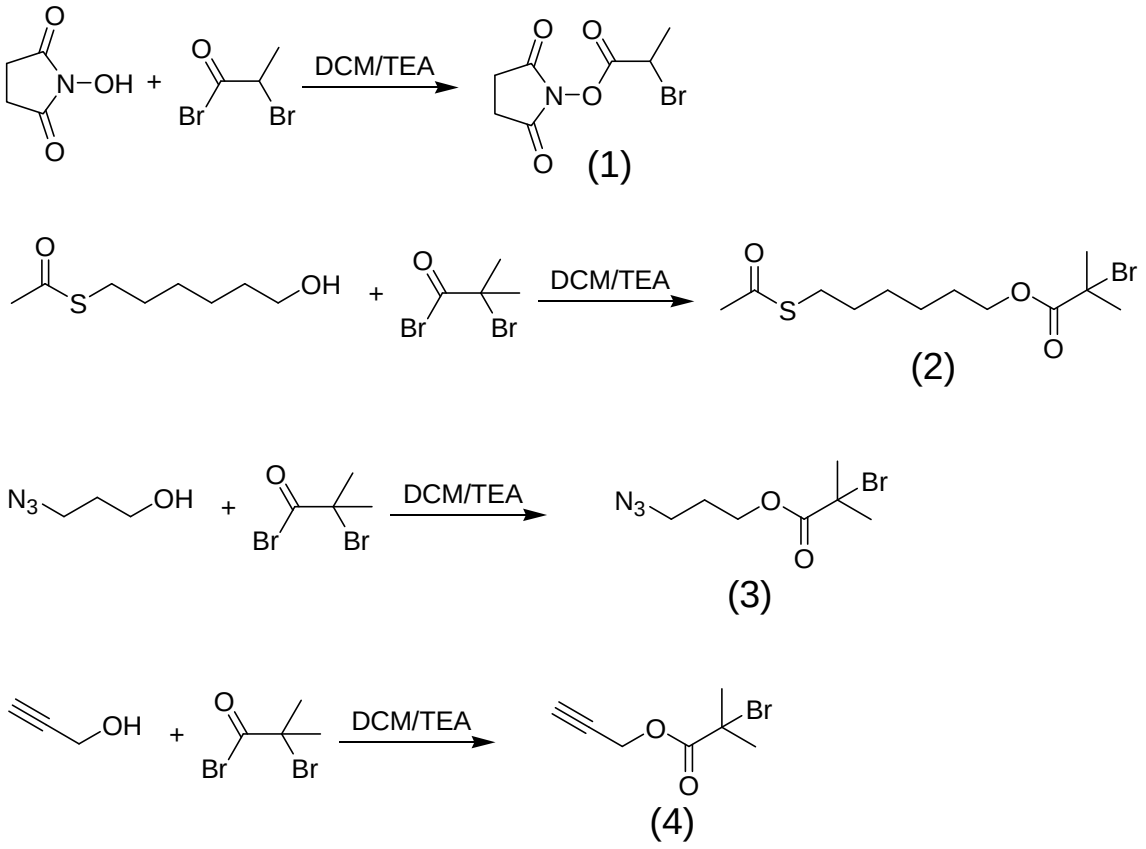

Figure 19. Synthesis of initiators bearing different functional groups.

_N_-Hydroxy succinimide 2-bromopropionate (1)

N-Hydroxy succinimide 2-bromopropionate, **1**, (Figure 19) was chosen as a succinimide initiator due to its high reactivity towards amine. A polymer with an *N*-

hydroxy succinimide (NHS) ester at chain end can be prepared by TMM-LRP, and this polymer could be used to modify amine-functionalized surfaces. The synthesis proceeded via coupling of *N*-hydroxysuccinimide and 2-bromopropionic bromide in dichloromethane. The initiator was obtained in good yield and satisfactory purity after column chromatography.

2-Bromo-2-methyl propionic acid 6-acetylsulfanyl-hexyl ester (2)

For gold surface modification, a thiol-functional molecule/polymer is often used. Here an acetylsulfanyl-terminal polymer was synthesised using 2-bromo-2-methyl propionic acid 6-acetylsulfanyl-hexyl ester **2** (Figure 19) as the initiator. This polymer was easily transformed into the thiol by treatment with hydrazine hydrate in acetonitrile, and the polymer then used to modify gold surfaces. The synthesis proceeded via coupling of thioacetic acid *s*-(6-hydroxy-hexyl) ester and 2-bromopropionic bromide in dichloromethane.

2-Bromo-2-methyl-propionic acid 3-azido-propyl ester (3)

2-Bromo-2-methyl-propionic acid 3-azido-propyl ester **3** was prepared as shown in Figure 19. The azido-alcohol intermediate 3-azido-propan-1-ol was obtained by treatment of bromo alcohol with NaN_3 in refluxing acetone/water solution. Subsequent acylation of the azido-alcohol with 2-bromopropionic bromide and triethylamine gave the desired azido-ester initiator 3 in good yields. Polymers made using this initiator could be used to modify alkyne-functionalized surface through Huisgen 1,3-dipolar cycloaddition (click chemistry).

2-Bromo-2-methyl-hept-6-yn-3-one (4)

An alkyne terminal initiator 2-bromo-2-methyl-hept-6-yn-3-one **4** (Figure 19) was also synthesized. The synthesis proceeded via coupling of prop-2-yn-1-ol and 2-

bromopropionic bromide in dichloromethane. The initiator was obtained in good yield and satisfactory purity after column chromatography. Polymers synthesized using this initiator could be used to modify azide-functionalized surface through Huisgen 1,3-dipolar cycloaddition.

2.2.2 TMM-LRP of DMAEMA with N-hydroxy succinimide 2-bromopropionate (1)

Figure 20 shows the scheme of the polymerisation of DMAEMA initiated with initiator **1**.

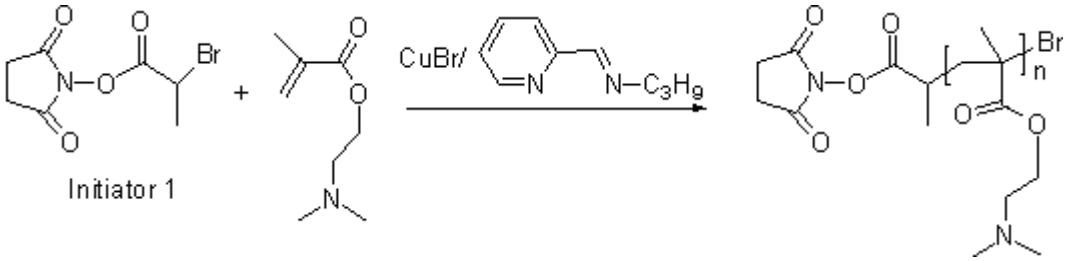

Figure 20. Synthesis of succinimide-terminal PDMAEMA.

DMAEMA was chosen as a monomer with 2-bromo-2-methyl propionic acid 6-acetylsulfanyl-hexyl ester (**1**) as initiator and copper (I) bromide (CuBr)/*N*-(*n*-propyl)-2-pyridyl methanimine as the catalytic system. Polymerisation was carried out at 75˚C. The results are shown in Figure 21 and Table 2, the first order kinetic plot is almost linear, however, the molecular weight of the polymer is not well controlled, and the PDi is not very narrow. The possible reason for this is that oxygen is not totally removed from the reaction system, as an induction period can be seen in the kinetics and the molecular weight is quite high at the beginning, similar to free radical polymerisation. The difference of PDMAEMA and the PMMA standard used in GPC

may also contribute to the relatively high molecular weight of the polymer samples, compared to theoretical values.

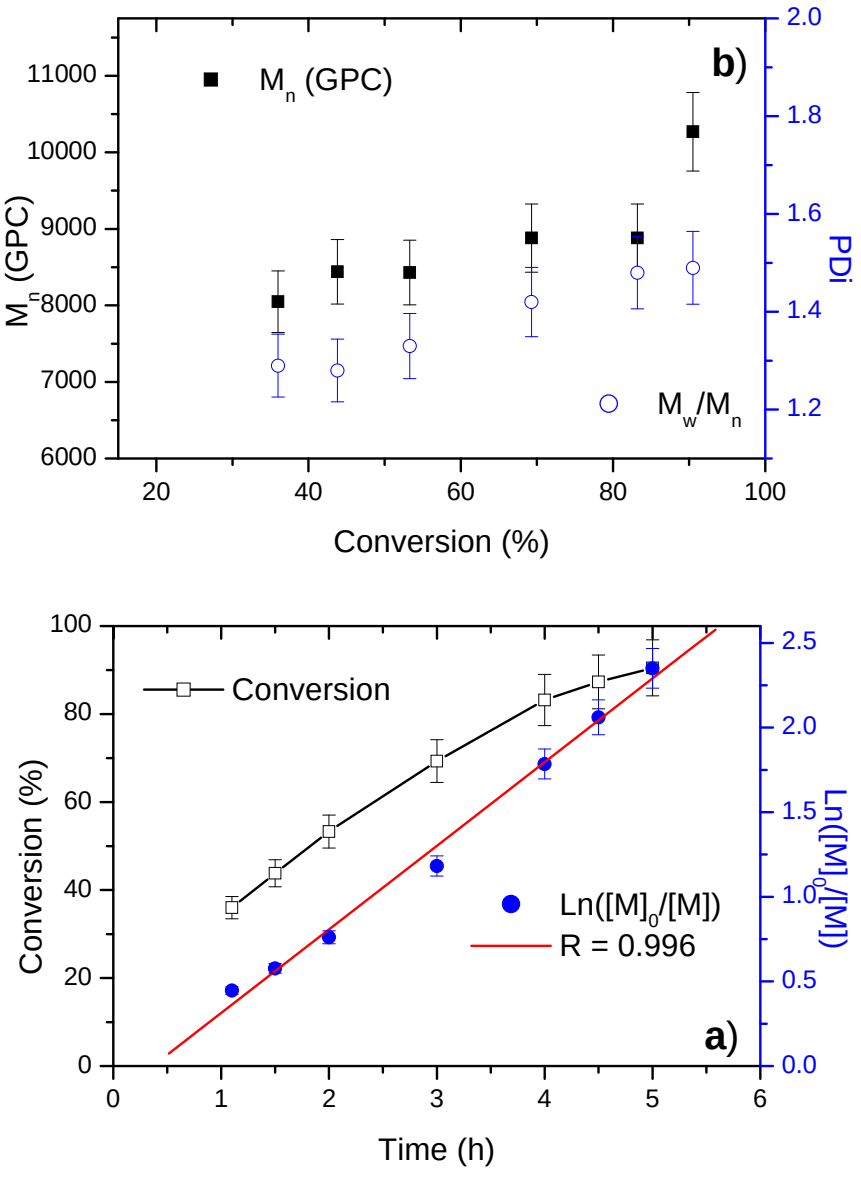

Figure 21. a) Conversion vs. time and semilogarithmic kinetic curves and b) Mn, Mw/Mn vs. conversion curves for the TMM-LRP of DMAEMA with 1. $[M]_0/[I]_0/[CuBr]_0/[L]_0$ = 50: 1: 1: 2

Table 2 Results and conditions of TMMLRP for DMAEMA by initiator 1.[a]

No.	Time (h)	Conv. (%)	M_n(SEC)	M_n(th) [b]	M_w/M_n
1	1.1	36	8050	3320	1.29
2	1.5	43.8	8440	3940	1.28
3	2	53.3	8430	4680	1.33
4	3	69.3	8880	5960	1.42
5	4	83.2	8880	7040	1.48
6	4.5	87.3	10440	7360	1.41
7	5	90.5	10270	7620	1.49

a. The polymerisation was performed at 75˚C with toluene as solvent, $[M]_0$ = 4.67 M. $[M]_0$:$[I]_0$:[CuBr]:[L] = 50:1:1:2;
b. Theoretical molecular weight calculated according to: $M_n(th) = ([M]_0/[I]_0) \times Conv. \times 157.2 + 250$, where 157.2 and 250 are the molecular weights of monomer and initiator 2 respectively.

The typical ^{1}H NMR of the poly(DMAEMA) with *N*-succinimidyl ester as chain-end is shown in (Figure 22).

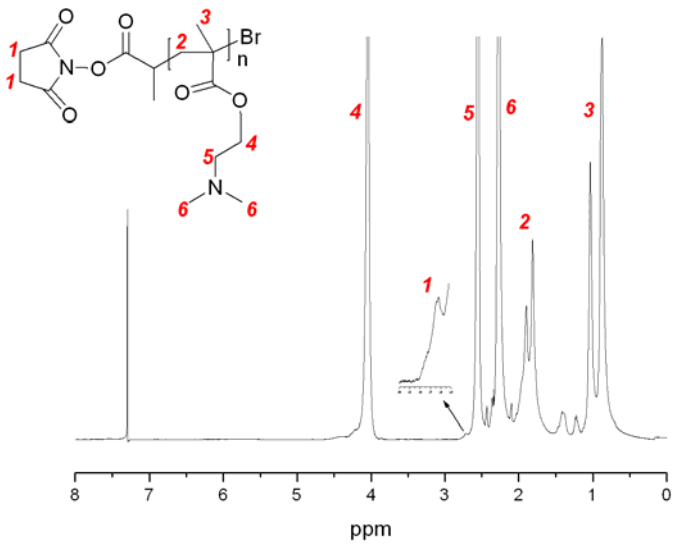

Figure 22. ^{1}H NMR of PDMAEMA with succinimide ester as alpha terminal group.

The peak at 2.8 ppm (peak 1) corresponds to the proton on the succinimide ring, the peak at 4.0 ppm (peak 4) is the -OCH_2 of the PDMAEMA chain, with the ratio of the integrations, $(4 \times I_{4.0}) / (2 \times I_{2.8})$, **n**, the number of the repeat unit on the main chain can be obtained. Thus the average molecular weight can be calculated by equation (1), and to compare to the theoretical value calculated by equation (2).

$$M_n(\text{NMR}) = \mathbf{n} \times MW_{\text{monomer}} + MW_{\text{initiator}} \quad (1)$$

$$M_n(\text{th}) = ([M]_0/[I]_0) \times \text{Conv.} \times MW_{\text{monomer}} + MW_{\text{initiator}} \quad (2)$$

Where the 157.2 and 250 are the molecular weights of the monomer (MW_{monomer}) and the initiator ($MW_{\text{initiator}}$) respectively. The M_n (NMR) (8,600 g mol^{-1}) is very close to the theoretical molecular weight M_n(th) (8,110 g mol^{-1}), where Conv. = 100%. This indicates that the efficiency of initiator is high and the polymerisation has a good controllable nature.

*2.2.3 TMM-LRP of MMA with N-hydroxy succinimide 2-bromopropionate (**1**)*

Figure 23 shows the scheme of the polymerisation of MMA initiated with initiator **1**.

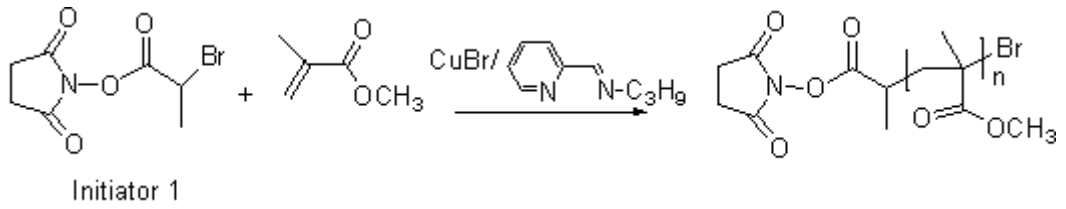

Figure 23. Synthesis of succinimide-terminal PMMA.

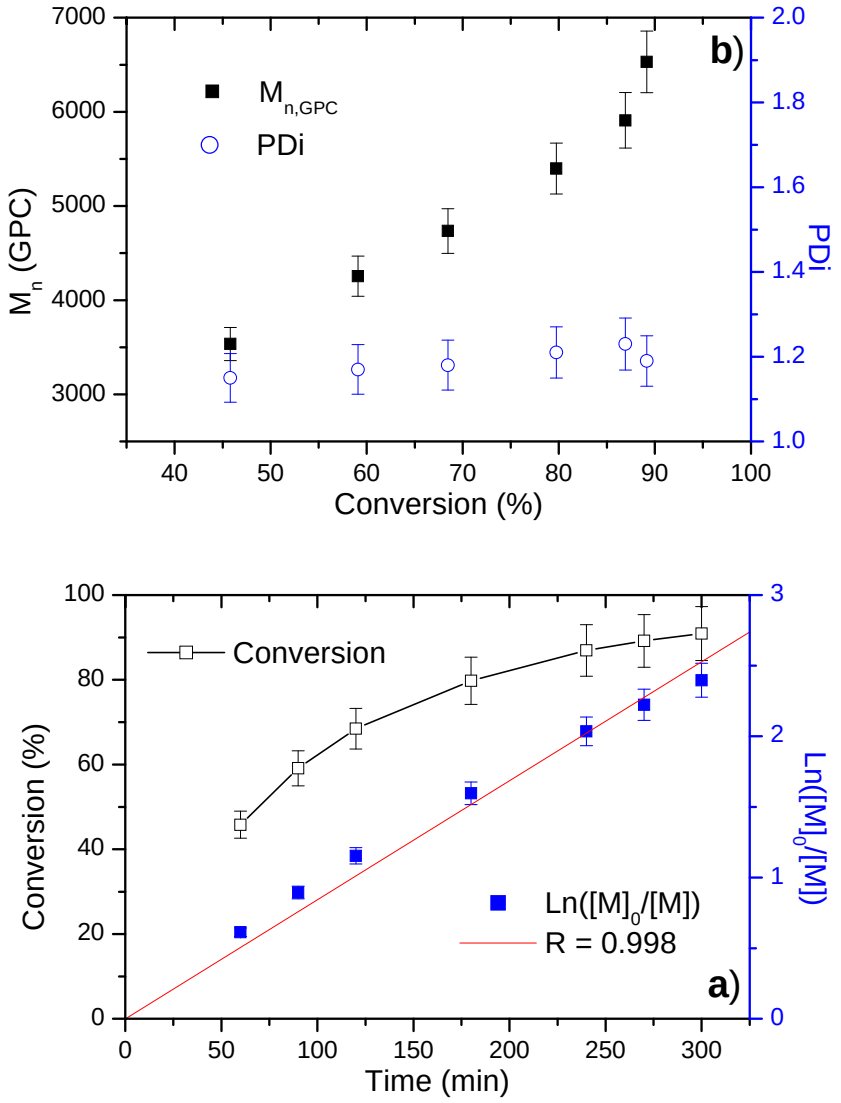

Figure 24. a) Conversion vs. time and semilogarithmic kinetic curves and b) Mn, Mw/Mn vs. conversion curves for the TMM-LRP of MMA with 1.

2-Bromo-2-methyl propionic acid 6-acetylsulfanyl-hexyl ester, **1**, was used with MMA as monomer and copper(I)bromide (CuBr) / *N*-(*n*-propyl)-2-pyridyl methanimine as catalyst at 90˚C. Figure 24, Table 3. The kinetic results show a linear dependence of $\ln[M]_0/[M]$ versus time, Figure 24a, indicating that the chain radical concentration remains constant during the polymerisation. The M_n(SEC) increases linearly with conversion, therefore, the molecular weight can be controlled by the

molar ratio of monomer consumed to initiator added, Figure 24b. As the molecular weight increase, the PDi remains narrow (≤1.3), suggesting that the polymerisation of MMA using initiator **1** has a living character.

Table 3 Results and conditions of TMMLRP for MMA by initiator 1.[a]

No.	Time (min)	Conv. (%)	M_n(SEC)	M_n(th) [b]	M_w/M_n
1	60	45.8	3530	2540	1.15
2	90	59.1	4250	3205	1.17
3	120	68.5	4730	3673	1.18
4	180	79.7	5400	4237	1.21
5	240	86.9	5910	4596	1.23
6	270	89.2	6530	4708	1.19

a. The polymerisation was performed at 90˚C with toluene as solvent, $[M]_0$ = 4.67 M. $[M]_0$:$[I]_0$:[CuBr]:[L] = 50:1:1:2
b. Theoretical molecular weight calculated according to: $M_n(th) = ([M]_0/[I]_0) \times Conv. \times 100 + 250$, where 157.2 and 250 are the molecular weights of monomer and **2** respectively.

A typical ^{1}H NMR of PMMA with *N*-succinimidyl ester as chain-end is shown in Figure 25. The peak at 2.8 ppm (peak 1) corresponds to the proton on the succinimidyl ring, the peak at 3.6 ppm (peak 2) is from the methyl group of the PMMA chain. Based on the ratio of the integrations, $(4 \times I_{3.6}) / (3 \times I_{2.8})$, **n**, the number of the repeat unit on the main chain can be obtained. The average molecular weight can be calculated by eq (1). Where the 100 and 250 are the molecular weights of the monomer ($MW_{monomer}$) and the initiator ($MW_{initiator}$) respectively. The M_n (NMR) (5,600 g mol^{-1}) is very close to the theoretical molecular weight M_n(th) (5,250 g mol^{-}

[1]), where conversion = 100%. This indicates that the efficiency of initiator is high and polymerisation shows good control.

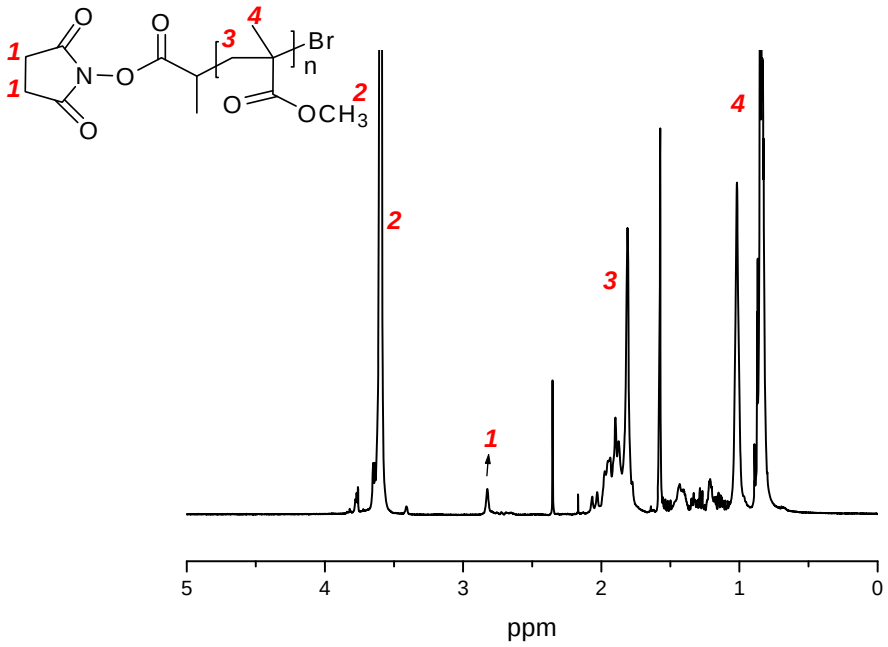

Figure 25. ^{1}H NMR of PMMA with succinimide ester as alpha terminal group.

*2.2.4 TMM-LRP of MMA with 2-bromo-2-methyl propionic acid 6-acetylsulfanyl-hexyl ester (**2**)*

Figure 26 shows the scheme of the polymerisation of MMA initiated with initiator **2**.

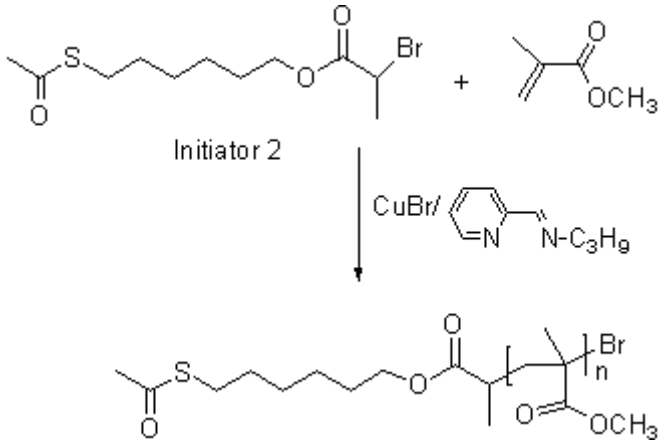

Figure 26. Synthesis of acetylsulfanyl-terminal PMMA.

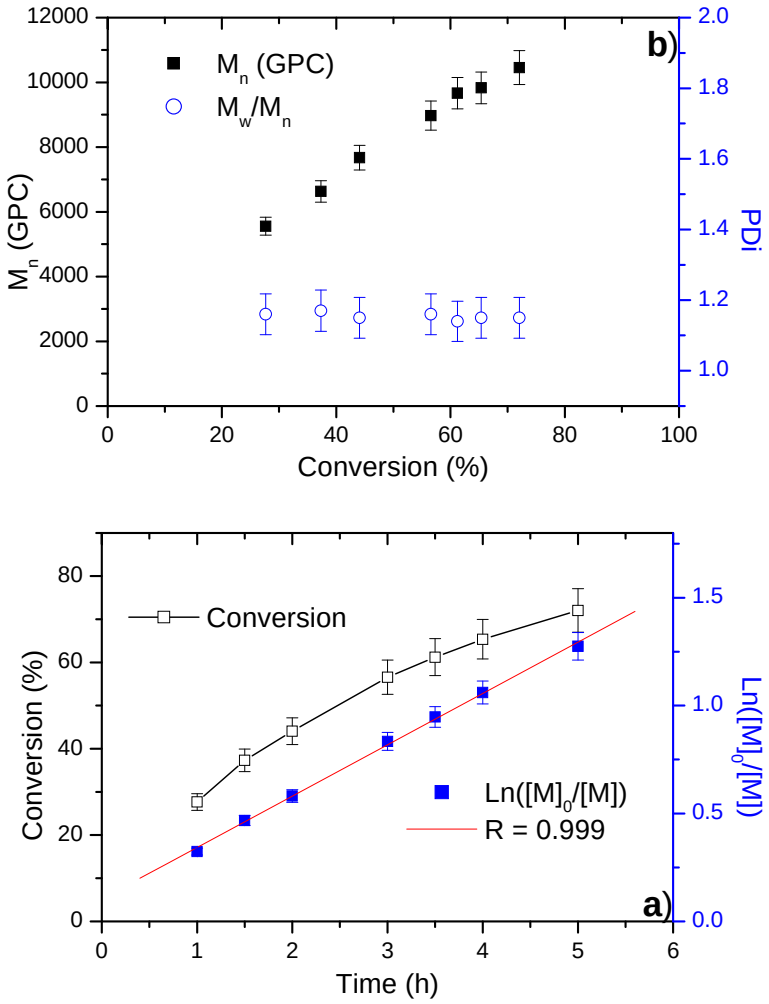

Figure 27. a) Conversion vs. time and semilogarithmic kinetic curves and b) Mn, Mw/Mn vs. conversion curves for the TMM-LRP of MMA with 2.

MMA was used with 2-bromo-2-methyl propionic acid 6-acetylsulfanyl-hexyl ester (**2**) as initiator and copper (I) bromide (CuBr)/*N*-(*n*-propyl)-2-pyridyl methanimine as catalyst ($[M]_0/[I]_0/[CuBr]_0/[L]_0$ = 100: 1: 1: 2). The kinetic results show a linear dependence of $\ln[M]_0/[M]$ versus the polymerisation time, and the M_n(SEC) increases linearly with increasing conversion, therefore, the molecular weight can be controlled by the molar ratio of monomer consumed to initiator added. As the molecular weight increases, the PDi remains narrow (<1.20), Figure 27, Table 4:

Table 4 Results and conditions of TMMLRP for MMA by initiator 2.[a]

No.	Time (h)	Conv. (%)	M_n(SEC)	M_n(th) [b]	M_w/M_n
1	1	27.7	5550	3090	1.16
2	1.5	37.3	6630	4060	1.17
3	2	44.1	7670	4730	1.15
4	3	56.6	8970	5980	1.16
5	3.5	61.2	9670	6450	1.14
6	4	65.4	9830	6860	1.15
7	5	72	10500	7530	1.15

a. The polymerisation was performed at 50˚C with toluene as solvent, $[M]_0$ = 4.67 M. $[M]_0$:$[I]_0$:[CuBr]:[L] = 100:1:1:2;
b. Theoretical molecular weight calculated according to: $M_n(th) = ([M]_0/[I]_0) \times Conv. \times 100 + 325$. Where 100 and 325 are the molecular weights of monomer and initiator 2 respectively.

A typical ^{1}H NMR of the PMMA with acetylsulfanyl-hexyl ester as chain-end is shown in Figure 28.

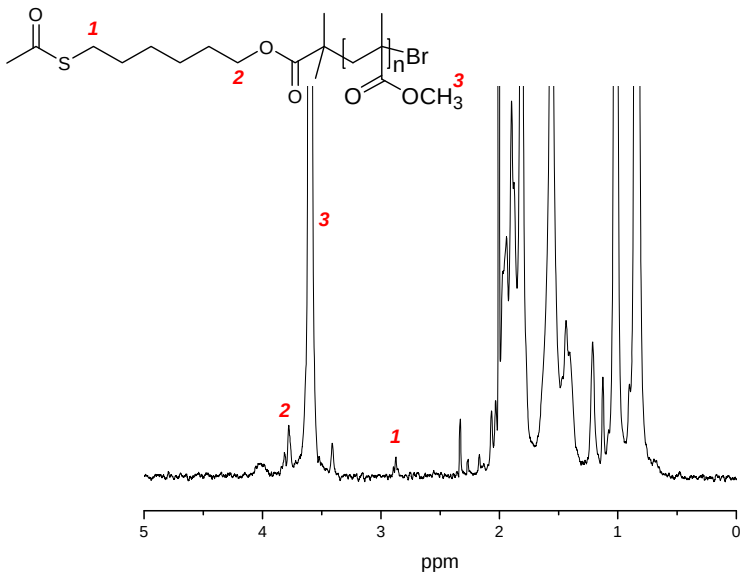

Figure 28. ^{1}H NMR of PMMA with acetylsulfanylhexyl ester as alpha terminal group.

The peak at 2.9 ppm (peak 1) corresponds to the proton of CH_2 adjacent to the sulfanyl group, the peak at 3.6 ppm (peak 2) is from the methyl group on the PMMA chain. Based on the ratio of the integrations, $(2 \times I_{3.6}) / (3 \times I_{2.9})$, **n**, the number of the repeat unit on the main chain can be obtained. Where the 100 and 250 are the molecular weights of the monomer ($MW_{monomer}$) and the initiator ($MW_{initiator}$) used in equation (1) and (2). The M_n (NMR) (13,990 g mol^{-1}) is slightly higher the theoretical molecular weight M_n (th) (10,325 g mol^{-1}), where conversion = 100%. The efficiency of initiator f = 0.74, based on eq (3).

$$f = M_n \text{ (th)} / M_n \text{ (NMR)} \qquad (3)$$

*2.2.3 TMM-LRP of MMA and hostasol monomer (HMA) with 2-bromo-2-methyl-propionic acid 3-azido-propyl ester (**3**)*

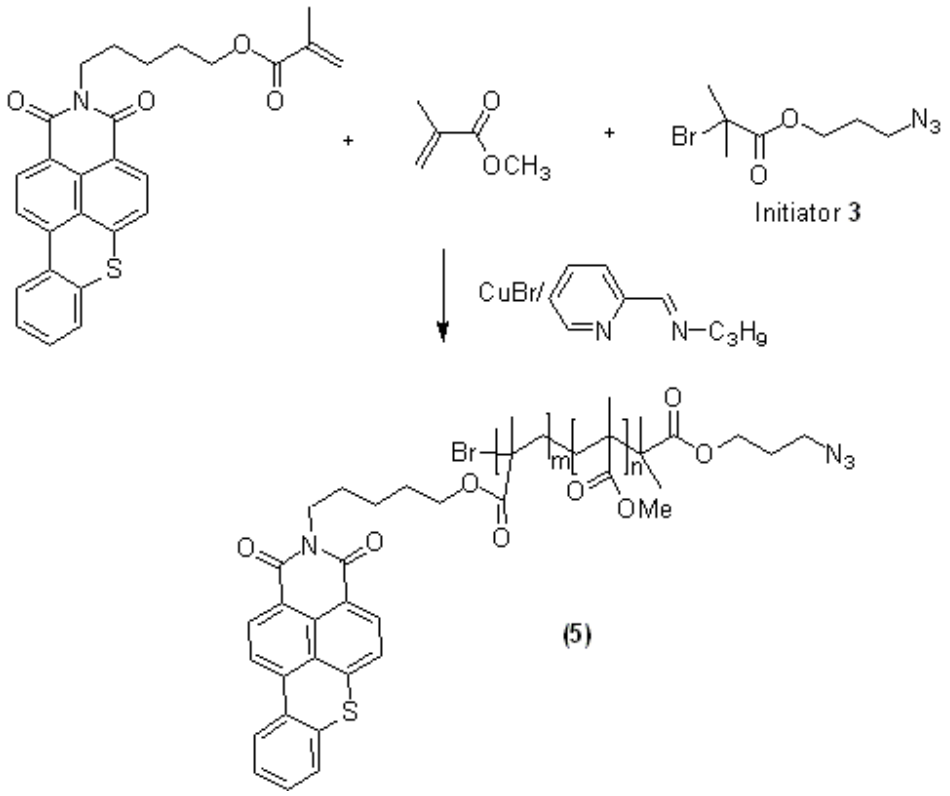

Figure 29. Synthesis of azido-terminal Poly(MMA-*co*-HMA).

Figure 29 shows the scheme of the polymerisation of MMA and HMA initiated with **3**. Copolymerisation of MMA and hostasol monomer (HMA) in the presence of 2-bromo-2-methyl-propionic acid 3-azido-propyl ester (**3**) and CuBr/*N*-(n-propyl)-2-pyridyl methanimine[187] in toluene was carried out at 90˚C ($[MMA]_0$:$[hostasol]_0$:$[I]_0$:$[CuBr]_0$:$[L]_0$ = 40: 0.2 : 1: 1: 2).

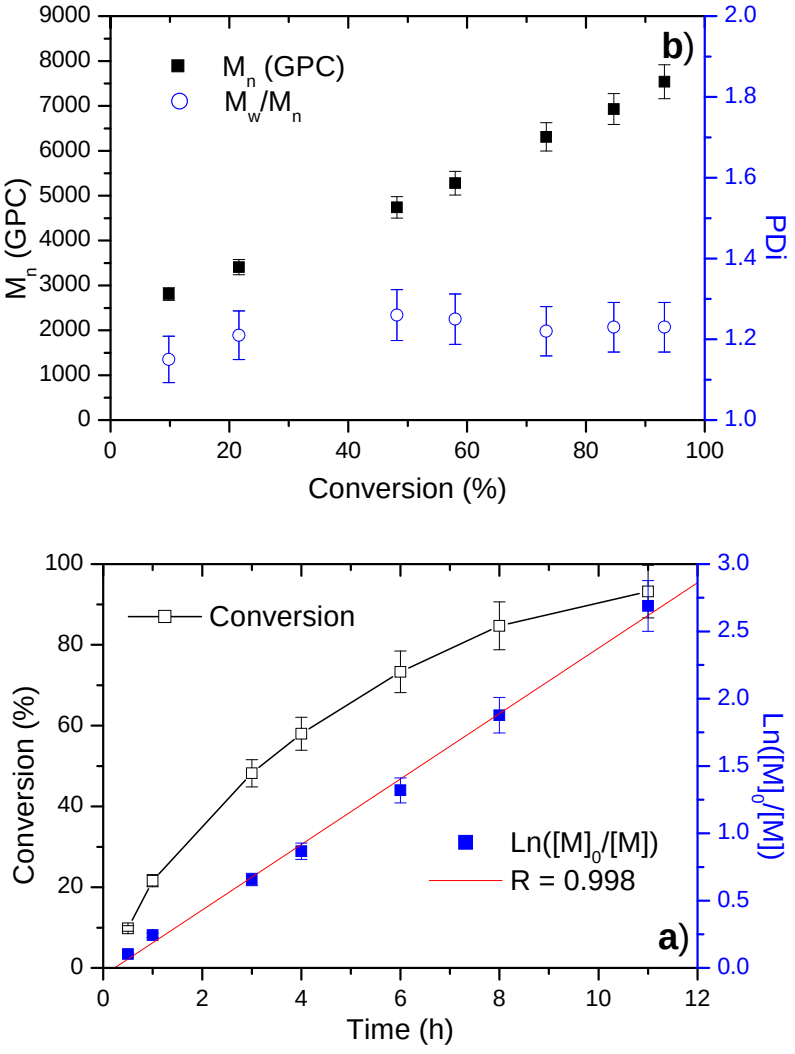

Figure 30. a) Conversion vs. time and semilogarithmic kinetic curves and b) Mn, Mw/Mn vs. conversion curves for the TMM-LRP of MMA and HMA with 3.

The kinetic results show a linear dependence of $\ln[M]_0/[M]$ vs. time, Figure 30a with M_n(SEC) increasing linearly with conversion, Figure 30b. As the molecular weight increases, the PDi remains narrow (<1.30), suggesting that the TMM-LRP of MMA has living character, Table 5. The aim of making this azido-terminated polymer is to graft this polymer to an alkyne modified surface using click chemistry. Another important feature of this polymer is the hostasol content, which is fluorescent and makes it possible to view using confocal microscopy.

Table 5 Results and conditions for TMMLRP of MMA and HMA by initiator 3.[a]

No.	Time (h)	Conv. (%)	M_n(SEC)	M_n(th) [b]	M_w/M_n
1	0.5	9.8	2810	640	1.15
2	1	21.6	3410	1120	1.21
3	3	48.2	4740	2180	1.26
4	4	58.0	5280	2570	1.25
5	6	73.3	6310	3180	1.22
6	8	84.7	6930	3640	1.23
7	11	93.2	7540	3980	1.23

a. The polymerisation was performed at 90˚C with toluene as solvent, $[MMA]_0/[HMA]_0/[I]_0/[CuBr]_0/[L]_0 = 40: 0.2 : 1: 1: 2$;
b. Theoretical molecular weight calculated according to: $M_n(th) = ([M]_0/[I]_0) \times Conv. \times 100 + 250$. Where 100 and 250 are the molecular weights of monomer and initiator respectively.

A typical ^{1}H NMR of the PMMA with azido-propyl ester as chain-end is shown in Figure 31. The peaks between 7.4 and 8.9 ppm (peak 1) correspond to the proton of hostasol group in HMA, the peaks at 4.1 ppm (peak 2) and 3.4 ppm (peak 3) are from the $-OCH_2$ and $-CH_2N_3$ groups of the initiator. The peak at 3.6 ppm (peak 4) is from the methyl group of main chain PMMA

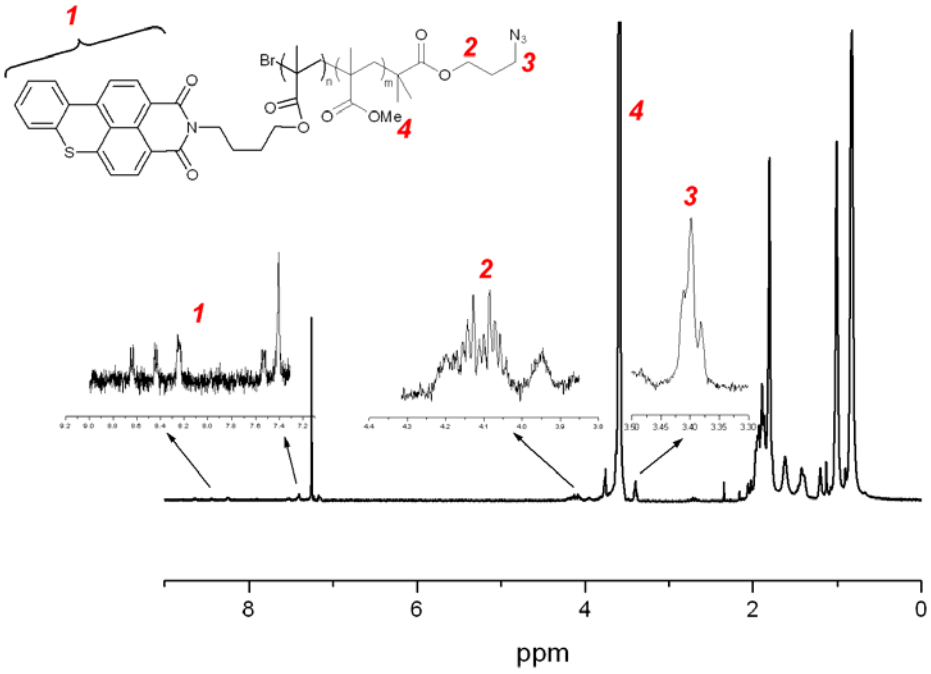

Figure 31. ^{1}H NMR of Poly(MMA-co-HMA) with azido-propyl ester as alpha terminal group.

Based on the ratio of the integrations, $(8 \times I_{3.6}) / (3 \times I_{7.4\text{-}8.9})$, **m**, the number of the repeat unit of HMA and $(2 \times I_{3.6}) / (3 \times I_{3.4})$, **n**, the number of the repeat unit of MMA on the main chain can be obtained. The average molecular weight can be calculated by eq (4).

$$M_n(\text{NMR}) = m \times 457.5 + n \times 100 + 250.1 \quad (4)$$

$$M_n(\text{th}) = ([\text{HMA}]_0/[\text{I}]_0) \times \text{Conv.} \times 457.5 + ([\text{MMA}]_0/[\text{I}]_0) \times \text{Conv.} \times 100 + 250.1 \quad (5)$$

457.5, 100 and 250.1 in equation (4) and (5) are the molecular weights of the monomer HMA, MMA and the initiator respectively. The repeating unit number of HMA, m = 0.19, and n = 47. The M_n (NMR) (5,040 g mol^{-1}) is slightly higher than the

theoretical molecular weight M_n (th) (4,342 g mol^{-1}), where conversion = 100%. The efficiency of initiator f = 0.86, based on eq (3).

*2.2.4 TMM-LRP of PEG-MA with 2-bromo-2-methyl-hept-6-yn-3-one (**4**)*

Figure 32 shows the scheme of the polymerisation of PEG-MA initiated with **4**.

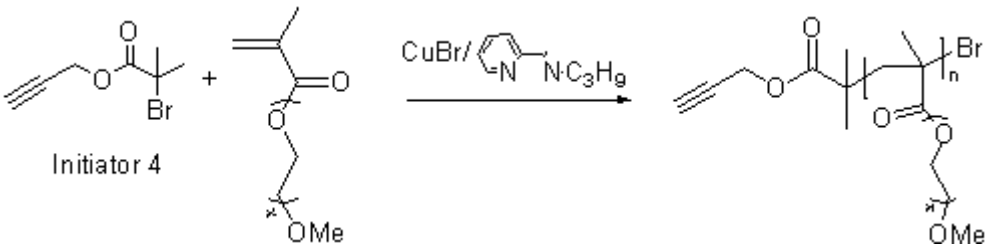

Figure 32. Synthesis of alkyne-terminal PEG-MA.

Table 6 Results and conditions for TMMLRP of PEG-MA by initiator 4.[a]

No.	Time (h)	Conv. (%)	M_n(SEC)	M_n(th) [b]	M_w/M_n
1	1	19.1	3810	2500	1.15
2	3	52	6170	6120	1.14
3	4	62.5	6280	7280	1.14
4	5	71.6	7050	8280	1.14
5	6	79.9	7590	9200	1.15
6	7	85.8	8210	9860	1.15

a. The polymerisation was performed at 50˚C with toluene as solvent, $[PEG\text{-}MA]_0 : [I]_0 : [CuBr]_0 : [L]_0$ = 10: 1 : 1: 1: 2;
b. Theoretical molecular weight calculated according to: $M_{n(th)} = ([M]_0/[I]_0) \times Conv. \times 1100 + 205$. Where 1100 and 205 are the molecular weights of monomer and initiator respectively.

Polymerisation of PEG-MA in the presence of 2-bromo-2-methyl-hept-6-yn-3-one (Initiator **4**) and CuBr/*N*-(n-propyl)-2-pyridyl methanimine in toluene was carried out at 50˚C. ($[PEG\text{-}MA]_0:[I]_0:[CuBr]_0:[L]_0$ = 10:1:1:2) The kinetic results show the linear dependence of $\ln[M]_0/[M]$ versus time, Figure 33a, with M_n(SEC) increasing linearly with increasing conversion, Figure 33b. As the molecular weight increases, the PDi remains narrow (<1.20), Table 6. The aim of making this alkyne-terminated polymer was to graft to an azide-modified surface using click chemistry.

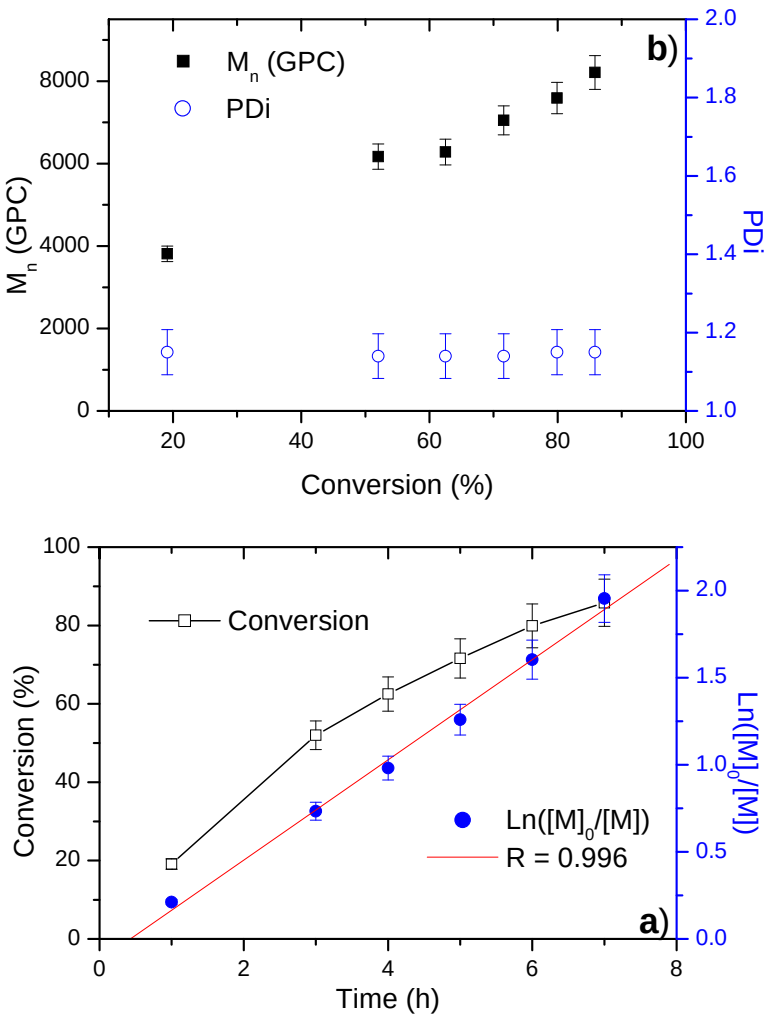

Figure 33. a) Conversion vs. time and semilogarithmic kinetic curves and b) Mn, Mw/Mn vs. conversion curves for the TMM-LRP of PEG-MA in toluene.

A typical ^{1}H NMR of the alkyne-terminal Poly(PEG-MA) is shown in Figure 34. The peak at 4.6 ppm (peak 2) corresponds to the proton of -CH_2 near alkyne group, the peak at 4.1 ppm (peak 5) is from the -OCH_2 group of the PEG-MA chain. Based on the ratio of the integrations, $I_{4.1}$ / $I_{4.6}$, **n**, the number of the repeat unit on the main chain can be obtained. M_n (NMR) and M_n(th) can be calculated using equation (1) and (2), where 1100 and 205 are the molecular weights of the monomer and the initiator respectively. The M_n (NMR) (20,000 g mol^{-1}) is higher than the theoretical molecular weight M_n (th) (11,205 g mol^{-1}), where Conv. = 100%. The efficiency of initiator f = 0.56, based on eq (3).

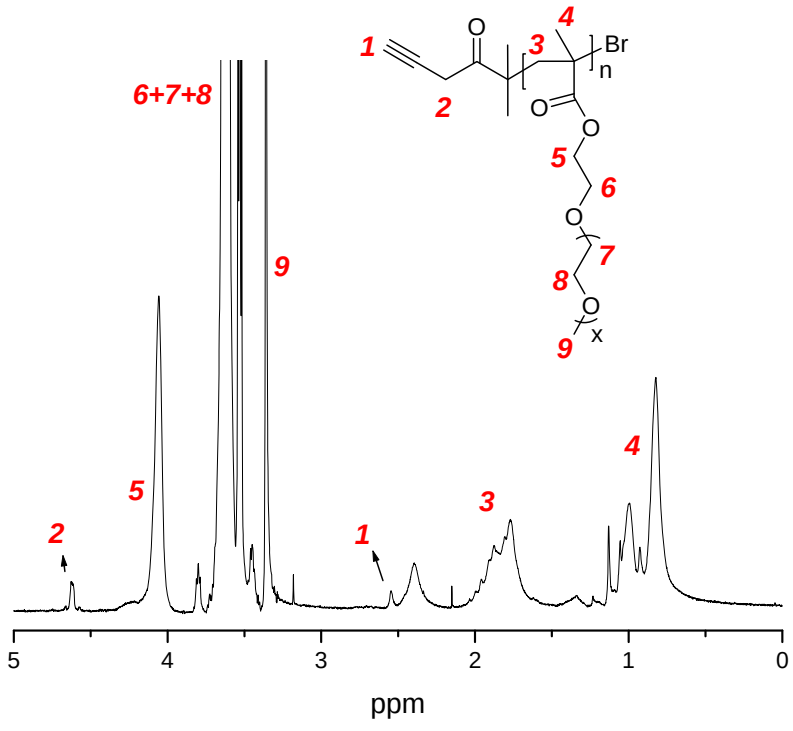

Figure 34. ^{1}H NMR of Poly(PEG-MA) with alkyne terminal group.

2.3 Cellulose surface modification using click chemistry and LRP[188]

The synthetic strategy here involved the synthesis of appropriate azide-terminal materials, followed by a subsequent click reaction to a pre-functionalised cotton surface bearing terminal alkyne groups. The azido-materials employed for cotton functionalization are shown in Figure 35. The synthesis of polymer **5** using initiator **3** has been described earlier. The synthetic route for the other two (**6** and **7**) will be given below.

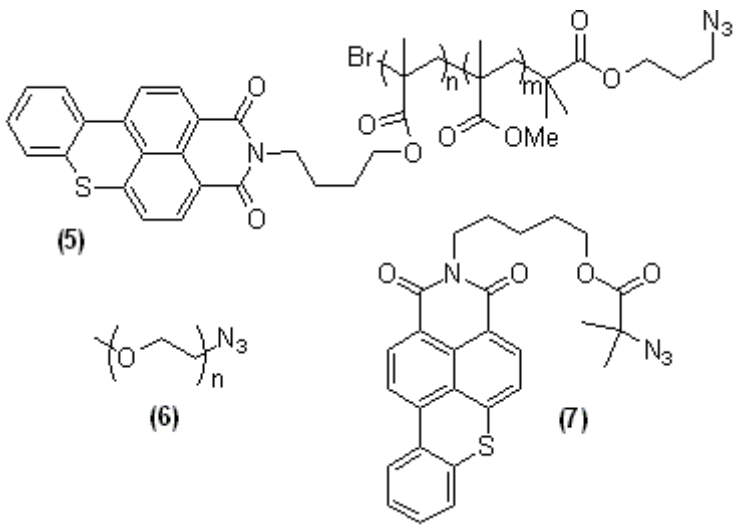

Figure 35. Materials employed for cotton functionalization.

*2.3.1 Synthesis of Monomethoxy-PEG$_{5000}$-N$_3$ (**6**).*

Monomethoxy-PEG$_{5000}$ was first treated with methanesulfonyl chloride and triethylamine in toluene, Figure 36. After removing the ammonium salts by filtration and removing solvents, the residue were redissolved in ethyl acetate, passed through a short silica column and precipitated into Et_2O to give the intermediate. The

intermediate was then treated with sodium azide in DMF and the final product was purified by dialysis and freeze-drying to give a white solid.

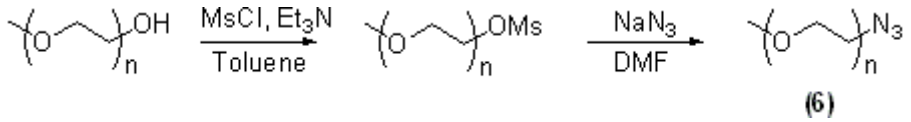

Figure 36. Synthesis of azide-terminal Monomethoxy-PEG$_{5000}$.

*2.3.2 Synthesis of 5-[1,3-dioxo-1H-benzo[3,4]isothiochromeno[7,8,1-def]isoquinolin-2(3H)-yl]pentyl, (Hostasol-azide), (**7**)*

Hostasol-bromide, 2-(8-(2-bromodimethyl)-3,6-dioxa-octyl)-thioxantheno[2,1,9-dej]isoquinoline-1,3-dione[189] was treated with sodium azide in a mixture of acetone and water and the resulting solution refluxed overnight at 60˚C, Figure 37. The acetone and other volatiles were removed under reduced pressure, water was added and the mixture extracted with dichloromethane. The organic layers were collected together and dried over $MgSO_4$. Removal of volatiles under reduced pressure gave the product, **(7)**, as an orange solid.

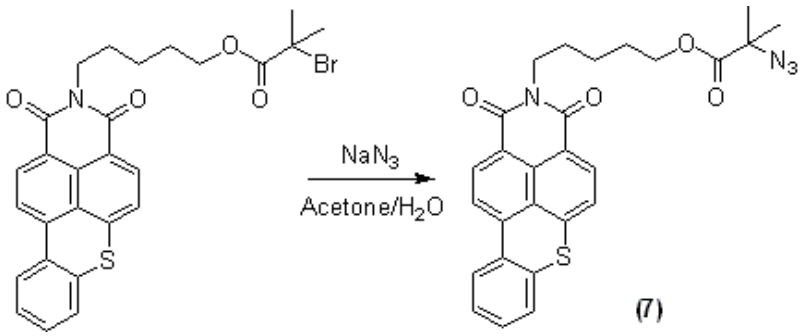

Figure 37. Synthesis of Hostasol-azide.

2.3.3 Click reaction to cotton surfaces

Figure 38 shows the schematic representation of the cotton surface modification. *4-Chlorocarbonyl-butyric acid prop-2-ynyl ester* **(8)** was obtained by treatment of glutaric anhydride with propargyl alcohol and DMAP in refluxing dichloromethane, and subsequent conversion of the resulting carboxylic acid to the acid chloride **(8)** with oxalyl chloride. Treatment of cotton fibres with **(8)** and DMAP in anhydrous pyridine resulted in the desired alkyne modified cotton fibres (cotton-alkyne). The azide-containing derivatives **(5)**, **(6)**, **(7)** were then successfully attached via a click reaction to the alkyne-modified cotton surface in the presence of *N*-(*n*-propyl)-2-pyridyl methanimine/Cu(I)Br as catalyst, at 70°C.

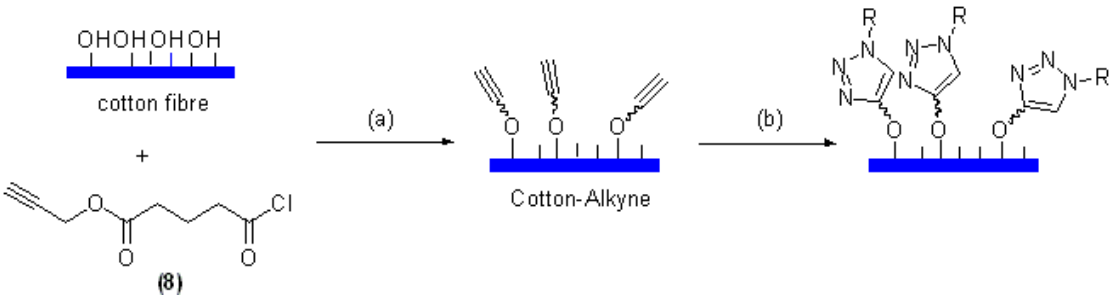

Figure 38. Reagents and conditions for cotton modification: a) anhydrous pyridine, DMAP, b) *N*-(n-propyl)-2-pyridyl methanimine/Cu(I)Br, R-N_3, 70°C, (R = Poly(MMA-co-HMA), methoxy-PEG, Hostasol).

FTIR was used to characterise the cotton before and after modification (Figure 39). Significant differences can be seen between native cotton and cotton-alkyne with a new peak at 1730 cm^{-1} corresponding to the C=O stretching band from the ester seen after the cotton is treated with **(8)**. After conducting the click reaction in the presence of **(7)** at least three new peaks attributed to the hostasol azide moiety can be observed at 1685, 1640 and 1580 cm^{-1}. FTIR characterisation of the cotton-**(5)** conjugate

proved to be more difficult, as the C=O bands from the attached PMMA are superimposed on those from the cotton-alkyne starting material. However, after "clicking", the cotton clearly fluoresced in the visible, confirming that the cycloaddition reaction was successful.

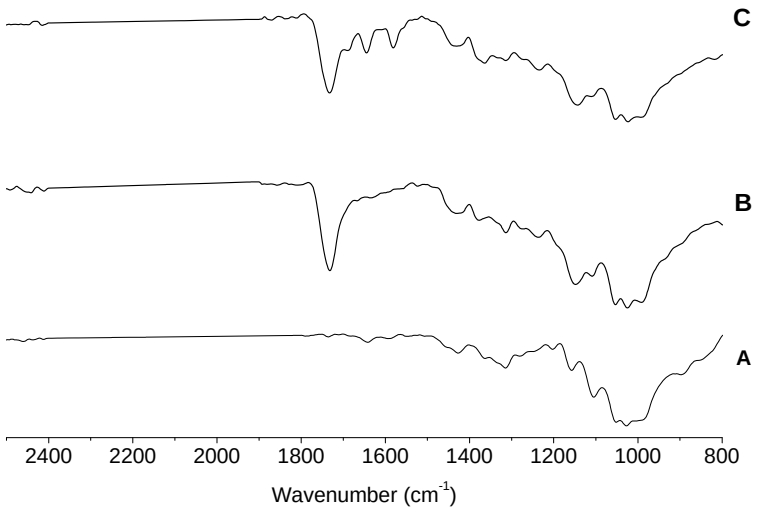

Figure 39. FTIR spectra of cotton fibre before and after modification. A: cotton; B: cotton-alkyne; C: cotton-(7).

Wettability tests were carried out in order to both further verify the success of clicking to the cotton surface, and to have a preliminary assessment of the physical properties of the hybrid materials, Figure 40. Individual yarns were taken from the fabric and cut into short segments (1 cm in length) for testing. The cotton yarn was attached to a wire and hung on the balance in a vertical orientation to determine the force during the testing. A beaker containing water was slowly levelled at a constant speed to make the yarn immersed in the water surface. The force reading was automatically zeroed at the beginning of the test. It was observed that whilst for unmodified cotton yarn, the force rises sharply after touching the water surface; for the alkyne-cotton derivative,

an opposite behaviour was observed, indicating an increase in the hydrophobicity of this surface. No significant differences were observed after the clicking of the hydrophobic azides **(5)** and **(7)** to the cotton surface, while for the PEG azide **(6)**, the hybrid material appeared to be hydrophilic, suggesting that grafting of the PEG azide had indeed occurred.

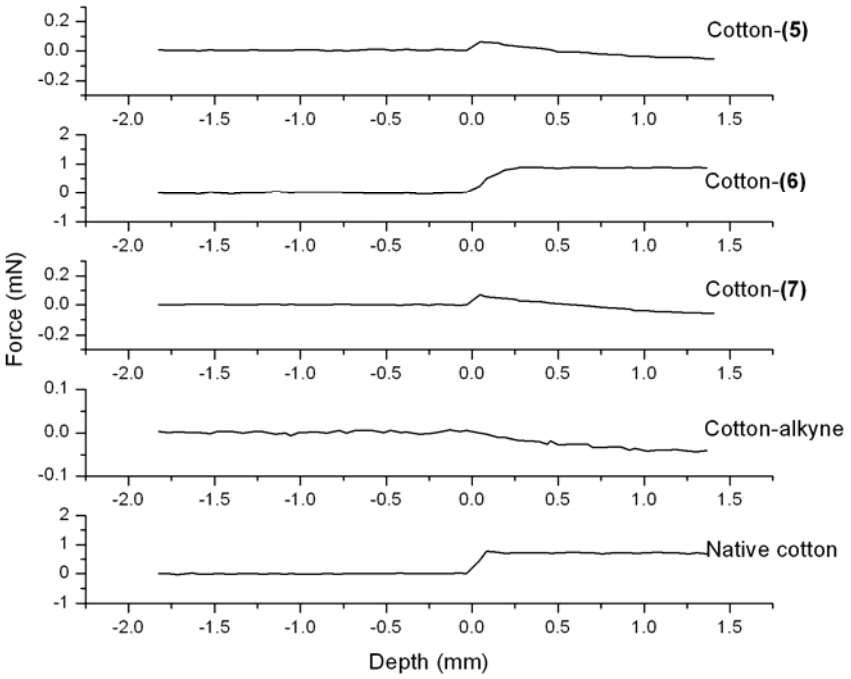

Figure 40. Microbalance curves of the cotton before and after modification.

Field-Emission Scanning Electron Microscopy (FE-SEM) provided further insights on the hybrid conjugates features, highlighting the differences between cotton before and after modification, Figure 41. The appearance of the surface changed significantly after the grafting, and a loss of fine features could be observed. The surface looks smoother after covered with polymers.

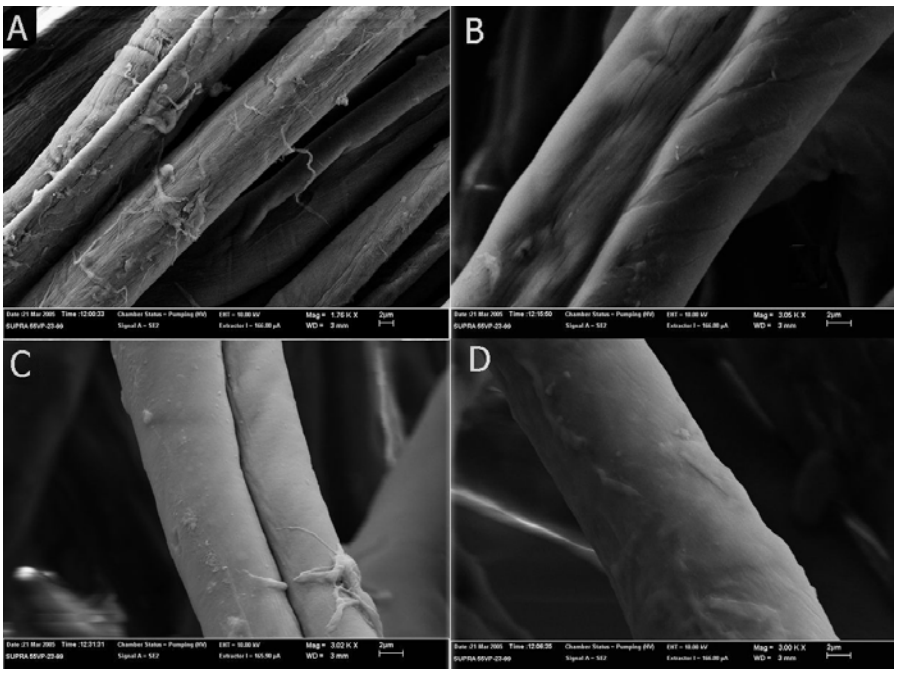

Figure 41. FE-SEM images of cotton before and after modification. A: Native cotton; B: Cotton-(7); C: Cotton-(5); D: Cotton-(6).

Figure 42 shows confocal microscope images of the cotton fibre modified with fluorescent groups (B and C), and the control cotton fibre sample (A), which was subjected to the conditions identical to the click reaction but without the use of the catalyst (copper(I) bromide and ligand). As can be seen, it is hard to see fluorescence on the surface of the control cotton fibre, whilst bright fluorescence is observed in the modified cotton fibre. The cotton-hostasol **(7)** appeared brighter than the polymer modified cotton-**(5)** due to the higher surface density with the small molecule, in theory, by using a low molecular weight azide such as **(7)** rather than the polymeric azide **(5)**.

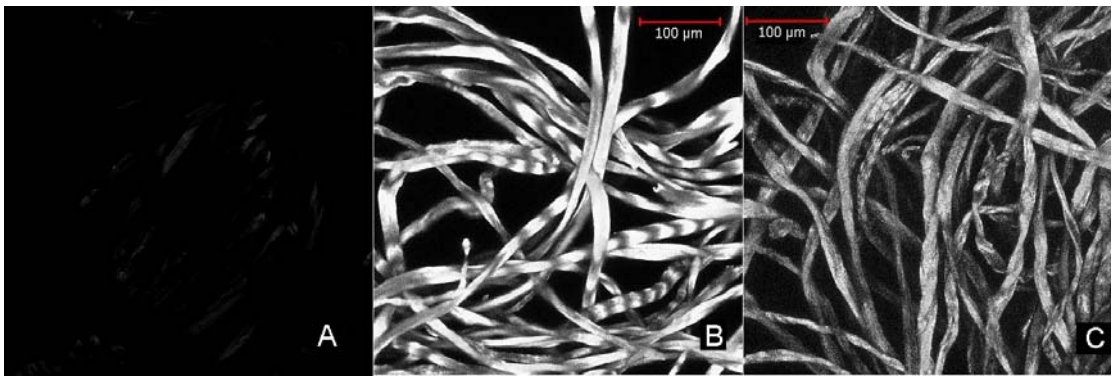

Figure 42. Confocal images of fluorescently modified cotton. A: Cotton-control, B: Cotton-(7), C: Cotton-(5).

2.3.3 Conclusions

In summary, living radical polymerisation of MMA and a fluorescent comonomer using 2-bromo-2-methyl-propionic acid 3-azido-propyl ester as initiator has been successfully employed for the synthesis of fluorescently tagged azide-terminated PMMA. These polymers have been subsequently grafted onto cotton using Huisgen [2+3] cycloaddition ("click"). Different functional azides, namely mono azido-PEG and a new fluorescent hostasol derivative have also been prepared and tested as model substrates for cotton surface modification. This approach constitutes a useful tool for the synthesis of new materials and for surface modification.

2.4 Polymerisation of Metronidazole monomer (MTD-MA) onto cellulose surface

Since its development in 1959, metronidazole (MTD, Figure 43) has grown in popularity as the drug of choice for the treatment of a wide range of infections caused by anaerobic and microaerophilic bacteria and protozoan parasites. [190,191]

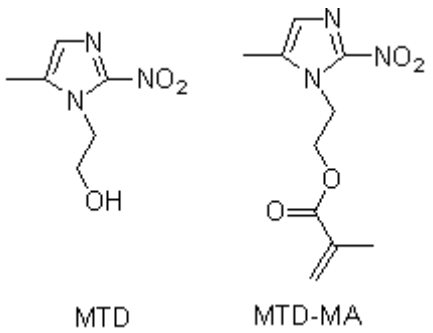

Figure 43. Structure of metronidazole and metronidazole monomer (MTD-MA).

Over the last half century, metronidazole therapy has proven effective against parasitic infections such as *Entamoeba histolytica*[192], which causes amebic dysentery and liver abscess, *Giardia lamblia*[193], which is responsible for causing malabsorption and epigastric pain and *Trichomonas vaginalis*[194], which causes vaginal itching. Metronidazole sensitive bacteria include many *Clostridium, Fusobacterium, Prevotella, Porphyromonas* and *Peptostreptococcusi* species, *Campylobacter jejuni, Gardnerella vaginalis* and *Helicobacter pylori*[195-197]. The aforementioned are all responsible for causing a wide range of serious anaerobic bacterial infections including acute dental infections, tetanus, blood poisoning, endocarditis, intraperitoneal infections, infections of the bones and joints, gastritis, acute peptic ulcer disease and anaerobic brain abscesses and cerebritis[198-202]. The cytotoxicity of metronidazole against anaerobes comes from the reduction of its nitro group by low redox potential electron transport proteins (such as ferredoxin and flavodoxin), which gives rise to a metabolite that reacts with guanine and cytosine to disrupt cellular DNA[203].

Metronidazole exhibits very low solubility in water (<10 mg/ml at 25°C), renal clearance of 10 mL $min^{-1}/1.73m^2$ 20% of which is unmetabolised, and can cause

unfavourable side effects including nausea, anxiety, fatigue, loss of appetite, depression, panic attacks and loss of coordination. The incorporation of metronidazole into polymers may offer several improvements for its role in chemotherapy. Specifically; increased retention times in the body due to increased bulk and a consequential reduction in hepatic and renal filtration, which in turn could lead to lower doses being prescribed and could allow for longer intervals between doses. There is also scope for making metronidazole polymers water soluble, which would offer improved delivery. Using PEG-based polymers for example, which is FDA approved and already used in many polymer-drug conjugates presently on the market[204-206], may also offer benefits such as decreased immunogenicity, higher stability against enzymatic degradation and lower antigenicity[207-215].

Living radical polymerisation allows for polymers to be prepared with targeted molecular weights, narrow polydispersities and targeted compositions. The presence of the primary hydroxyl group of metronidazole, which is not directly linked to its biological activity, lends itself to simple transformation into a monomer suitable for polymerisation.

Thus, copolymers of $PEG_{300}MA$ and MTD monomer (MTD-MA, Figure 43) were prepared to yield water-soluble metronidazole containing polymers, as an alternative to polymer-metronidazole conjugates. Therefore, the copolymer containing PEG and Metronidazole has been made, in addition, metronidazole modified cotton has been made through surface-initiated polymerisation.

2.4.1 Polymerisation of metronidazole-containing monomer (MTD-MA) and poly(ethylene glycol) methacrylate (PEG-MA).

Figure 44 shows the scheme of the polymerisation of MTD-MA and PEG-MA initiated with 2-bromo-2-methyl-propionic acid benzyl ester.

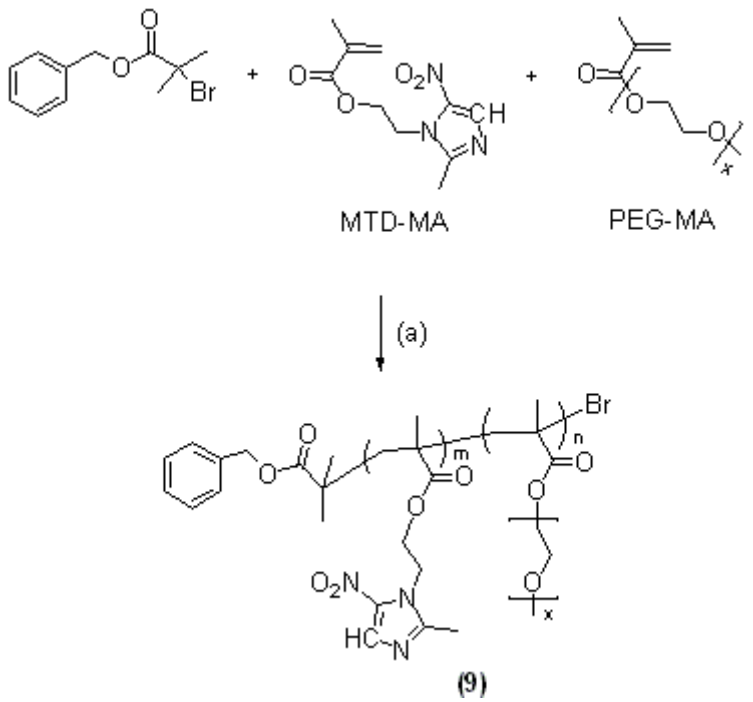

Figure 44. Polymerisation of metronidazole-containing monomer (MTD-MA) and PEG-MA. a) CuBr/bpy, 25 ˚C.

Polymerisation of MTD-MA and PEG-MA in the presence of 2-bromo-2-methyl-propionic acid benzyl ester and CuBr/bpy in toluene was carried out at 25˚C. ([MTD-MA]$_0$:[PEG-MA]$_0$:[I]$_0$:[CuBr]$_0$:[L]$_0$ = 31.5: 3.5 : 1: 1: 2) The kinetic results are shown in Figure 45a with the polymerisation rate of MTD-MA slightly higher than PEG-MA. The kinetic plot of the total copolymerisation is close to that of PEG-MA, as more PEG-MA was used for this polymerisation. The overall M_n(SEC) increases linearly with increasing conversion, Figure 45b with PDi remaining narrow (<1.20), Table 7.

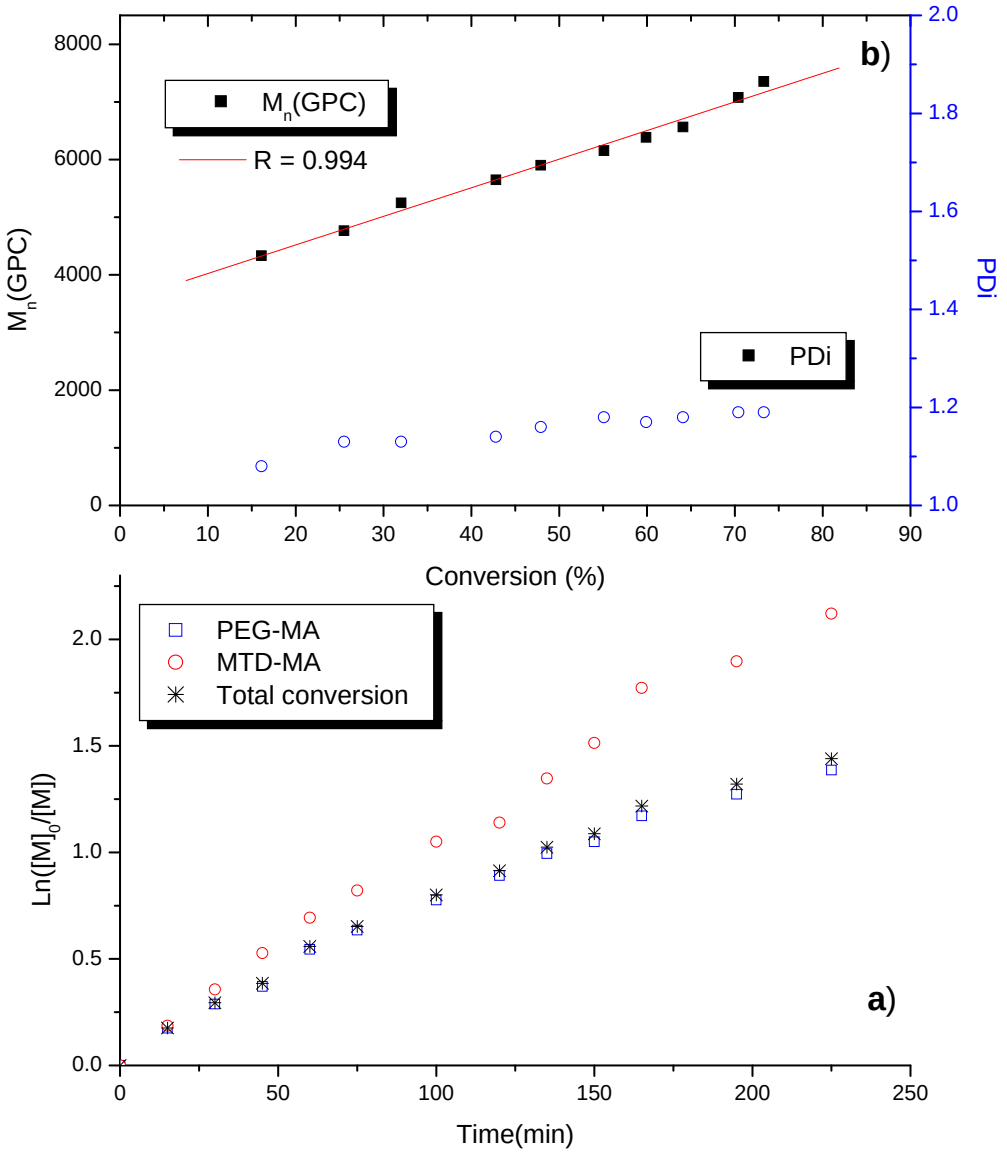

Figure 45. a) Semilogarithmic kinetic curves and b) Mn, Mw/Mn vs. conversion curves for the polymerisation of MTD-MA and PEG-MA in toluene.

Table 7 Results and conditions of TMMLRP for MTD-MA and PEG-MA.[a]

No.	Time (min)	Conv. (%)	M_n(SEC)	M_n(th) [b]	M_w/M_n
1	15	16.1	4330	1914	1.08
2	30	25.5	4770	2881	1.13
3	45	32	5250	3550	1.13
4	60	42.8	5650	4661	1.14
5	75	47.9	5900	5186	1.16
6	100	55.1	6150	5927	1.18
7	120	59.9	6380	6421	1.17
8	135	64.1	6560	6853	1.18
9	150	66.3	6620	7079	1.19
10	165	70.4	7080	7501	1.19
11	195	73.3	7350	7800	1.19
12	225	76.3	8030	8108	1.18

a. Polymerisation at 25˚C with methanol as solvent, $[PEG\text{-}MA]_0 : [MTD\text{-}MA]_0 : [I]_0 : [CuBr]_0 : [L]_0 = 31.5 : 3.5 : 1 : 1 : 2$;
b. Theoretical molecular weight calculated according to: $M_{n(th)} = ([M]_0/[I]_0) \times Conv. \times 294 + 257$. Where 294 and 257 are the average molecular weight of monomers ($239 \times 10\% + 300 \times 90\% = 294$, $M_{w,MTD\text{-}MA} = 239$; $M_{w,PEG\text{-}MA} = 300$) and initiator respectively.

A typical ^{1}H NMR of the polymer **(9)** is shown in Figure 46. The peak at 8.0 ppm (peak 7) corresponds to the proton of -*CH* group in MTD-MA, the peaks at 7.4 ppm (peak 1) and 5.0 ppm (peak 2) are from the -C_6H_5 and –OCH_2 groups of the initiator. The peak at 4.0 ppm (peak 5) is from the –OCH_2 groups of MTD-MA and PEG-MA. Based on the ratio of the integrations, $(5 \times I_{8.0}) / I_{7.4}$, the number of the repeat unit (**m**) of MTD-MA and ($5 \times I_{4.0} / 2 \times I_{7.4} - \mathbf{m}$), the number of the repeat unit (**n**) of PEG-MA on the main chain can be obtained.

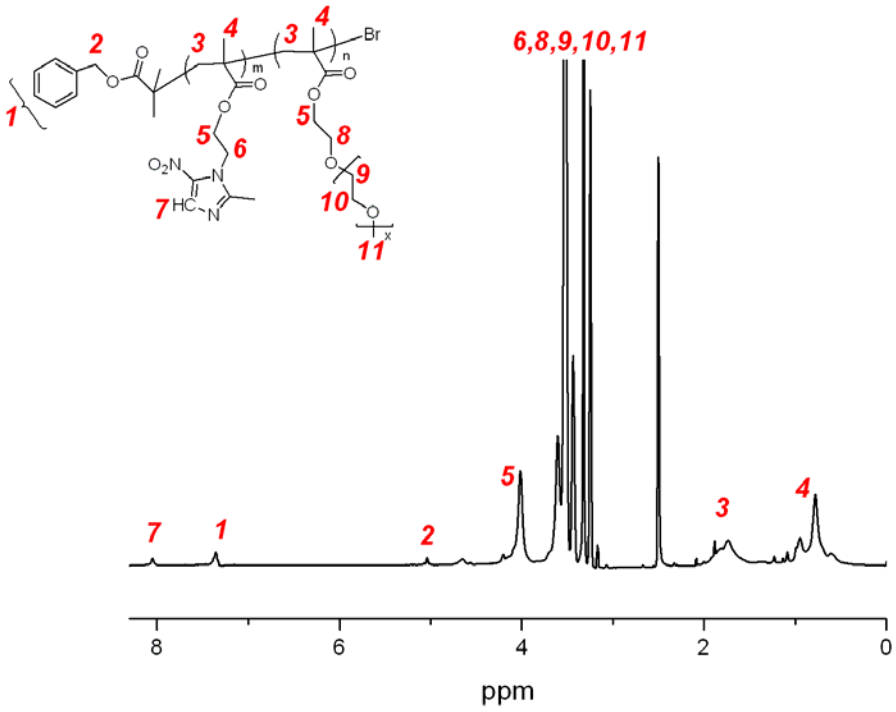

Figure 46. ^{1}H NMR of Poly(MTD-MA-co-PEG-MA).

The average molecular weight can be calculated by eq (6).

$$M_n(\text{NMR}) = m \times 239 + n \times 300 + 257 \quad (6)$$

$$M_n(\text{th}) = ([\text{MTD-MA}]_0/[\text{I}]_0) \times \text{Conv.} \times 239 + ([\text{PEG-MA}]_0/[\text{I}]_0) \times \text{Conv.} \times 300 + 257 \quad (7)$$

Where the 239, 300 and 257 are the molecular weights of the monomer MTD-MA, PEG-MA and the initiator respectively. The repeating unit number of MTD-MA, m, is calculated to be 2.3, and n calculated to be 29.7. The M_n (NMR) (9,717 g mol^{-1}) is slightly smaller than the theoretical molecular weight M_n (th) (10,543 g mol^{-1}), where conversion = 100%. This may due to the conversion of polymerisation not reaching 100%.

2.4.2 Graft of metronidazole-containing monomer from cellulose surface

Figure 47 shows the synthetic route for making metronidazole-modified cotton. Cotton fibres were first treated with 2-bromo-2-methyl-propionyl bromide to yield surface initiating moieties covalently bound to the surface. Subsequently, polymerisation of MTD-MA and PEG-MA was carried out at ambient temperature for 48 hours. The cotton fibre was then taken out and washed extensively with anisole, dichloromethane, and methanol, then dried under vacuum. It was thereafter characterised by FT-IR, tensiometer and FE-SEM.

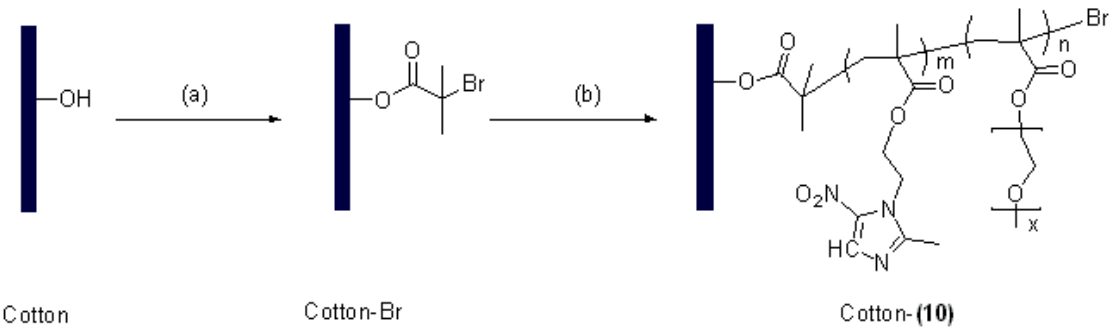

Figure 47. Reagents and conditions for cotton modification: a) anhydrous pyridine, DMAP, 2-bromo-2-methyl-propionyl bromide, b) Cu(I)Br/bpy, MTD-MA, PEG-MA, RT, anisole).

The conversion of cotton fibre into cotton-Br was confirmed by the appearance of an ester *C=O* at ca. 1730 cm^{-1} and the disappearance of -*OH* stretching (ca. 3300 cm^{-1}) in the FT-IR spectrum, Figure 48. Subsequent polymerisation of MTD-MA and PEG-MA led to the immobilized metronidazole Cotton-(10), for which the FT-IR spectrum showed small sharp peaks at ca 1530 cm^{-1} and 1370 cm^{-1}, attributed to the asymmetric and symmetric stretch of -NO_2 group. In addition, broad peaks at around 2900 cm^{-1} from methyl groups of both MTD-MA and PEG-MA are clearly observed, further verifying the successful grafting of the copolymer from the cotton surface.

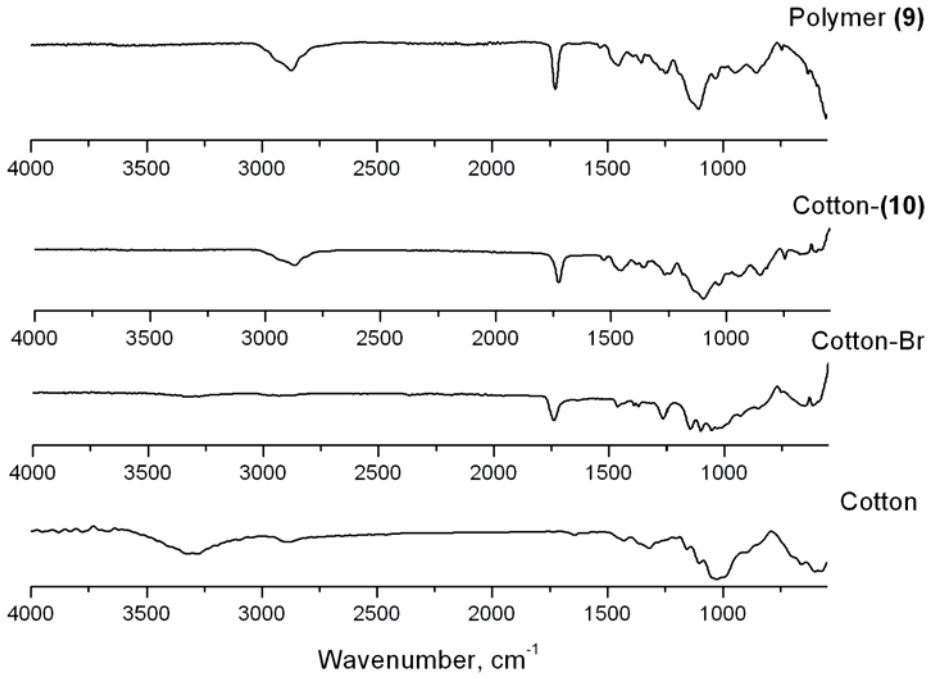

Figure 48. FTIR spectra of Polymer (9), the cotton fibre and the cotton fibres after modification.

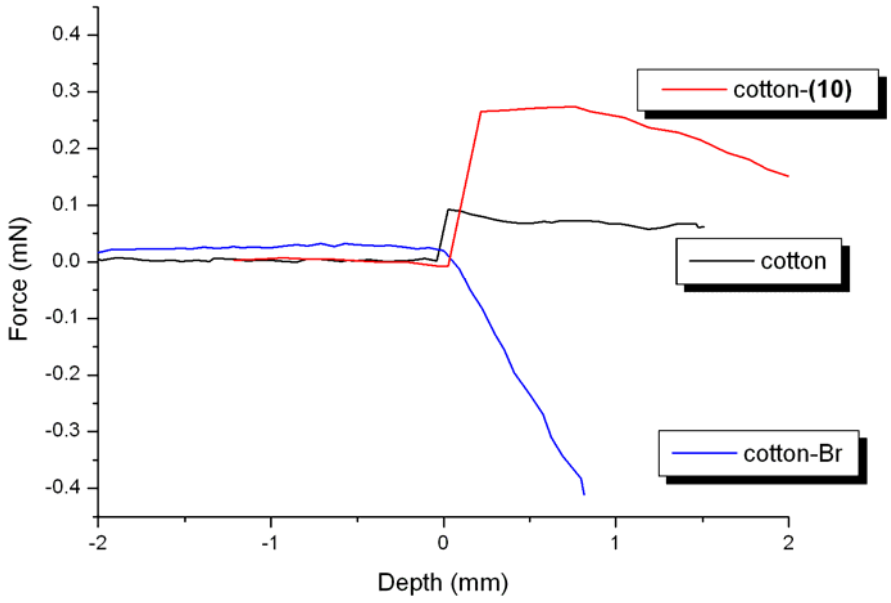

Figure 49. Microbalance curves of the cotton fibres before and after modification.

Figure 49 shows the result of the wettability tests. It was observed that for unmodified cotton yarn the force increases after contact with the water surface, indicating a hydrophilic material. For cotton-Br, an opposite behaviour was observed indicating an increase in the hydrophobicity of the surface is formed. While for the cotton-(10), the hybrid material appeared to be hydrophilic again and with higher reading, suggesting that grafting of the copolymers of MDT-MA and PEG-MA had indeed occurred. These tests further verify the success of cotton surface modification and give a preliminary assessment of the physical properties of the hybrid materials.

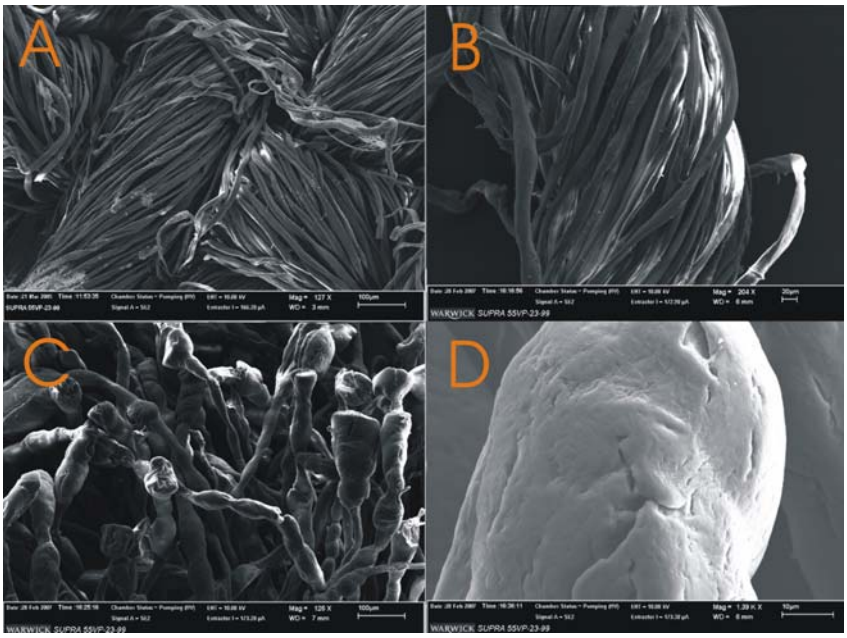

Figure 50. FE-SEM images of cotton before and after modification. A: Native cotton; B: Cotton-Br; C &D: Cotton-(10).

Field-Emission Scanning Electron Microscope (FE-SEM) images of the cotton fibres, Figure 50, provide further insights on the hybrid conjugates features, highlighting the differences between cotton before and after modification, especially between Cotton

and Cotton-**(10)**. The nature of the surface changed significantly when the metronidazole-containing polymer were grafted and the diameter of the cotton fibre increased, especially in the end of the fibre, where more functionality sites are available with larger surface areas, leading to denser polymer growth.

2.4.3 Conclusion

Living radical polymerisation of MTD-MA and PEG-MA using 2-bromo-2-methyl-propionic acid benzyl ester as initiator has been successfully employed for the synthesis of metronidazole containing polymer. This approach would greatly improve the poor solubility of metronidazole in water and a better antibiotic property to certain bacteria would be expected. Similarly, surface-initiated ATRP has also been used to grow copolymers of MTD-MA and PEG-MA onto cotton fibre surface. This shows a convenient way of making polymers containing antibiotic materials and relevant surface modifications.

Chapter 3 Resin surface modification and its potential application in chromatography

3.1 Introduction

In general, there are two types of polymer particles: magnetic polymer particles and non-magnetic polymer particles. Magnetic beads/particles are normally generated by coating finely divided magnetic iron oxides with polymers of natural or synthetic origin. For synthetic polymers, colloidal iron oxide particles are mixed with monomer before formation of monomer droplets and polymerisation. In other methods magnetic particles are formed in situ from ferrous and ferric chlorides. [216-220] Non-magnetic polymer particles are produced from a wide spectrum of monomers and mixtures of monomers, with a particle size in the range of 1-100 μm. They can be widely used as chromatographic supports and catalytic supports in a variety of areas such as ion exchange, biological separation, size exclusion chromatography (SEC), chiral separation, etc.[221]

This chapter focuses on the preparation of functional polymer particles and their potential application in chromatography. Chromatographic methods have been developing at high speed during the last 30 years in response to an ever-increasing demand for high quality products. The need for increased sample throughput has stimulated rapid development of column materials, which can be operated at high flow rate and high pressures. The demands on today's packing materials for high

performance liquid chromatography are: rigidity, chemical stability towards solvents and pH-changes, high load capacities, low non-specific interactions, and no hindrance of solute diffusion. Most columns available for HPLC use stationary phases based on porous beads made of either silica or synthetic polymers. Highly crosslinked packing materials prepared from synthetic polymers, which are mechanically and chemically stable, have been developed to meet the demand for packing materials that are able to withstand high pressures and high flow rates. Compared to silica particles, which are the most commonly used packing material in chromatography (In general, colloidal silica can be stable in the range of pH 10–11, however, the gel time of it is short in the range of pH 3–8.), the advantage of the synthetic polymers is a much-increased chemical stability. For example, highly crosslinked styrene-divinylbenzene copolymers are very rigid and may be operated over a wide pH range, 1-14. Polymeric supports displaying a broad range of functionalities are often prepared in a single step by copolymerisation of appropriate functional monomers. For example, solid supports based on cross-linked functionalised polystyrene beads can be prepared by suspension copolymerisation of monomers, such as styrene and divinylbenzene (DVB), with a functional monomer.[222,223] Although simple, this approach requires re-optimisation of the entire preparation process to control the ultimate properties of the beads each time a new monomer is used. Another strategy involves the functionalization of silica- or polymer-based preformed beads, either through modification with small functional molecules[224-227] or through grafting functional polymers from surface active site of the solid support to increase the density of the binding groups.[228-231] This is particularly attractive as it enables the formation of numerous stationary phases starting from a single type of material with optimised size and porous properties.

In this chapter, polymer-based preformed beads have been functionalised using different methods. Click chemistry has been used to graft fluorescent polymers onto Wang and Merrifield resins, further proving the robust and convenience of modifying polymer beads. In the second part, supports bearing covalently immobilized carbohydrates starting from preformed Wang-resin beads have been synthesized, and these hybrid materials have been used in a preliminary lectin-glycopolymer recognition study for affinity chromatography. In the third part, a chiral polymer based resin has been made for application in chiral separation as a stationary phase of HPLC. Glycerol methacrylate (GMA) was first grafted to Aquagel resin surface through surface-initiated LRP, and then single enantiomers were further immobilised by reacting with the hydroxyl groups of GMA, giving a chiral polymer based resin.

3.2 Click reactions to the surfaces of Wang and Merrifield resins with fluorescent polymers

The synthetic strategy involved the synthesis of appropriate azide/alkyne initiators, polymerisation of alkyl methacrylates in the presence of a Cu(I)/iminopyridine catalyst followed by a subsequent click reaction to a pre-functionalised surface bearing terminal alkyne or azide groups. Both azido-terminated poly(methacrylates) and an alkyne terminated poly(methacrylate), more convenient for the modification of Merrifield resin, have been investigated.

3.2.1 Copolymerisation of MMA and hostasol methacrylate (HMA).

The scheme of the synthesis of azide/alkyne terminal polymers is shown in Figure 51.

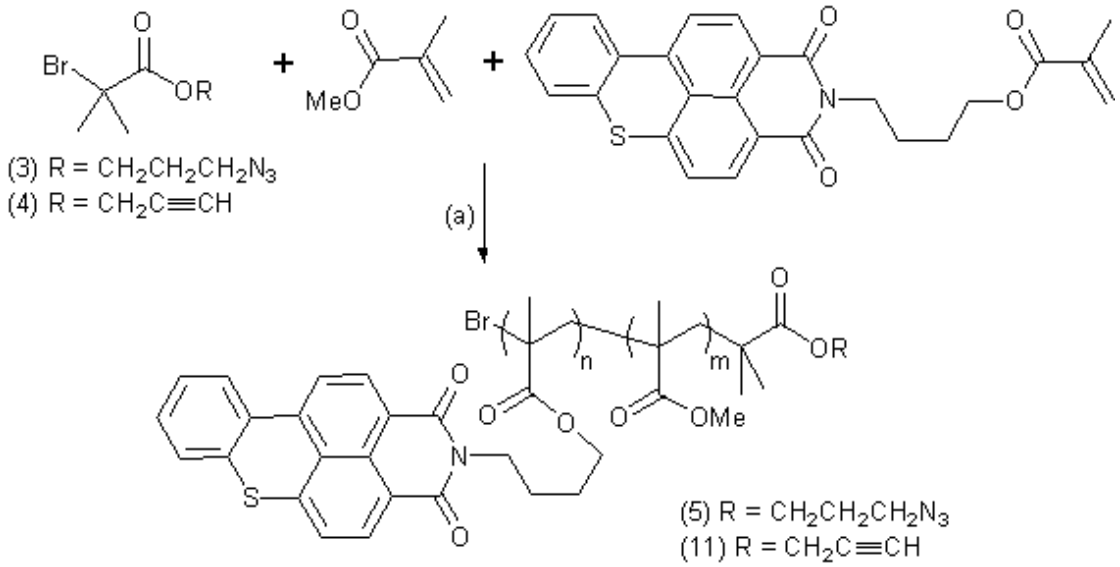

Figure 51. Copolymerisation of MMA and HMA. Reagents and conditions: a) CuBr, *N*-(n-propyl)-2-pyridyl methanimine, 90°C.

The synthesis of azide-terminal Poly(MMA-co-HMA) (**5**) initiated by **3** has been described in Chapter 2. The synthesis of alkyne-terminal polymer was from copolymerisation of MMA and HMA initiated by **4** at 90°C, Figure 51. We observed good first order kinetics with the molecular weights increasing fairly linearly with conversion and PDi remaining narrow throughout the polymerisation, Figure 52. This resulted in alkyne terminated polymer **(11)**, supported by the observation of a singlet at 2.50 ppm in the ^{1}H NMR spectrum of the final polymer confirming the presence of the -*C*≡*CH* group in **(4)**. According to NMR, the **m** and **n** value (DP of MMA and HMA) of the final polymers has been calculated, **m** = 118; **n** = 0.19, Figure 53.

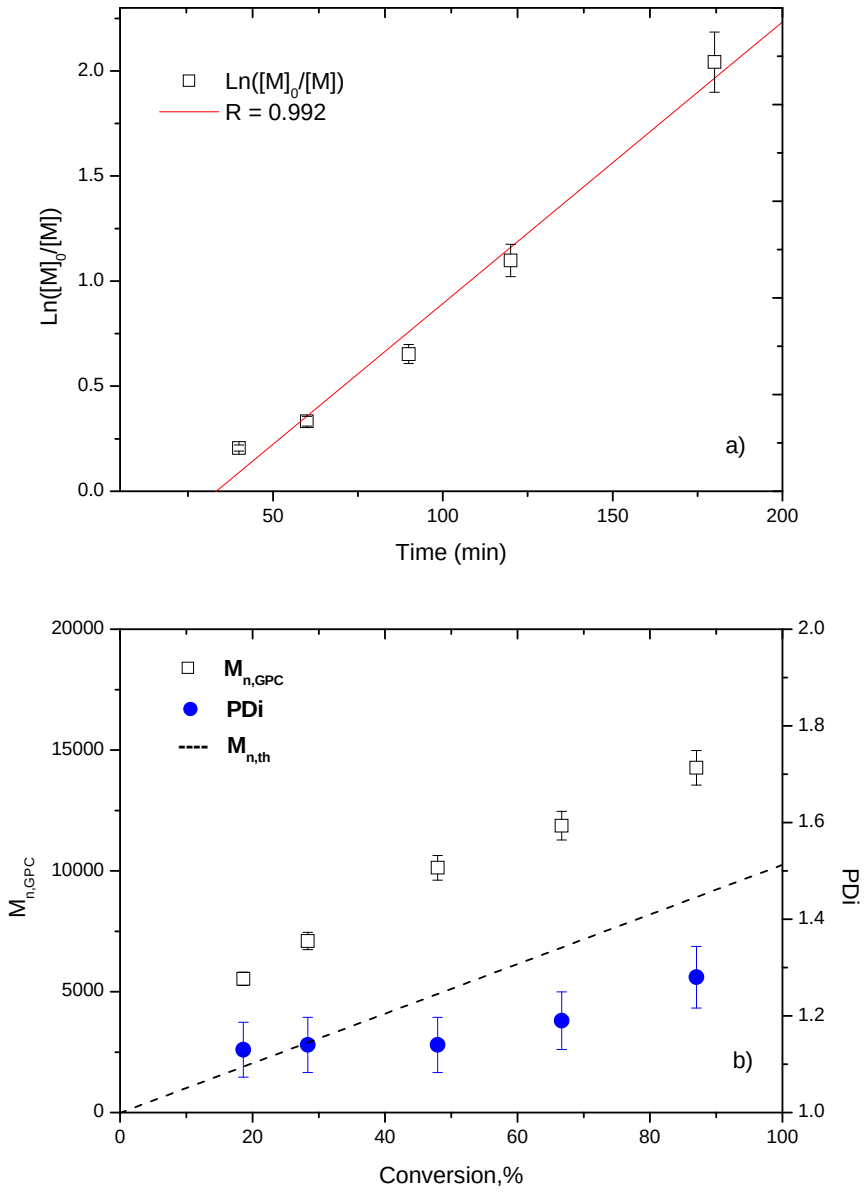

Figure 52. a) Semilogarithmic kinetic curve and b) Mn, PDi vs. conversion curves for the copolymerisation of MMA and HMA. Reaction conditions:$[MMA]_0/[HMA]_0/[I]_0/[CuBr]_0/[L]_0$ = 100: 0.2 : 1: 1: 2, 90˚C, I = (4).

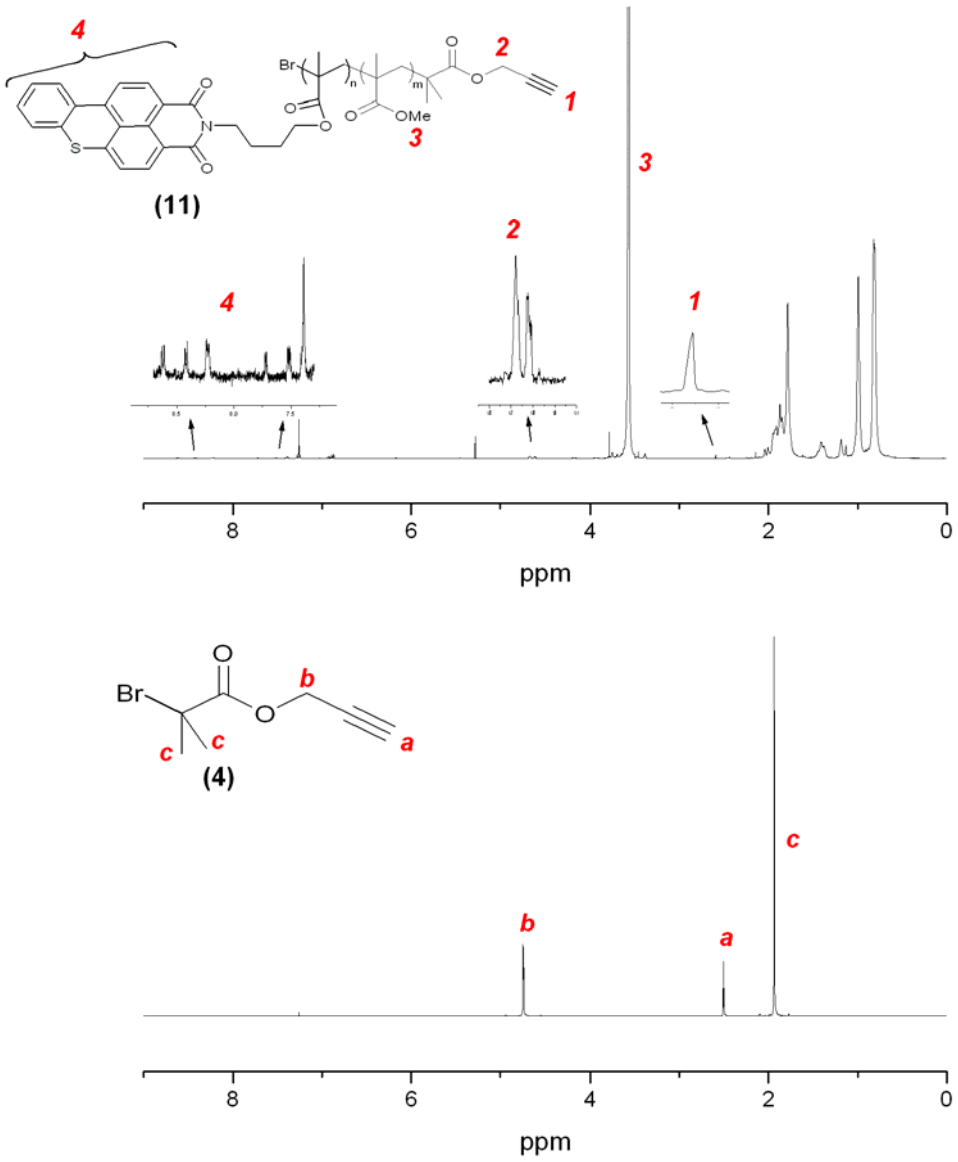

Figure 53. ^{1}H NMR spectra of polymer (11) and initiator (4).

3.2.2 Wang and Merrifield resins: surface modification.

The reaction scheme for the resins surface modification is shown in Figure 54.

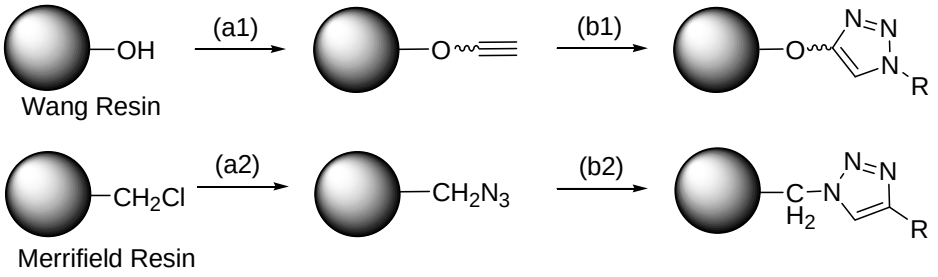

Figure 54. Reagents and conditions for resin modification: a1) Anhydrous pyridine, (7), DMAP; b1) $(PPh_3)_3Cu(I)Br$, R-N_3 , 70˚C, (R = (5)); a2) NaN_3, DMSO/H_2O, b2) $(PPh_3)_3Cu(I)Br$, R-C≡CH, 70 ˚C, (R = (11)).

A similar procedure to the method used for cotton surface modification described in Chapter 2 was used to click onto the surface of Wang resin with (**7**) and DMAP in anhydrous pyridine resulting in the desired alkyne modified Wang resin. Azide functional poly(MMA-co-hostasol) was then successfully clicked to the surface of alkyne-modified cotton in the presence of $(PPh_3)_3Cu(I)Br$ catalyst, at 70°C. Merrifield resin was transformed to azide by treatment with sodium azide. Thus this required alkyne terminal PMMA which was synthesized using the alkyne initiator 2-bromo-2-methyl-hept-6-yn-3-one prior to the polymer being clicked to the azide modified Merrifield resin.

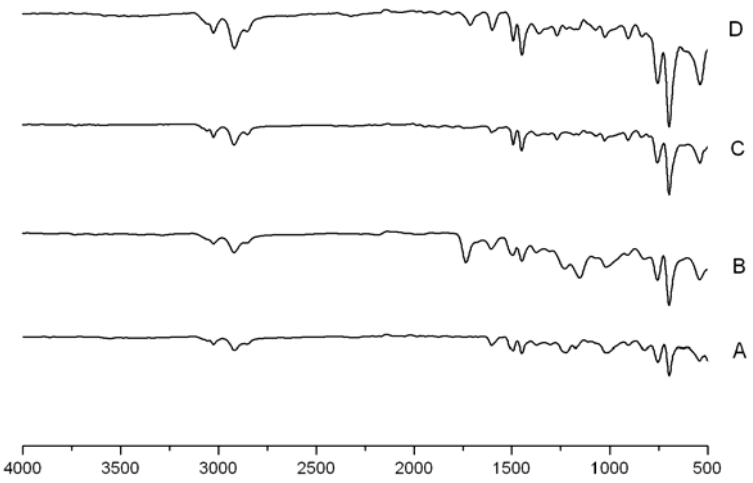

Figure 55. FTIR spectra of Wang and Merrifield resins before and after modification. A: Wang Resin; B: Wang Resin-(5); C: Merrifield Resin; D: Merrifield Resin-(11).

FTIR was used to confirm the successful click reaction, Figure 55. Differences can be seen between the native Wang and Merrifield resins and the PMMA functionalised resins with new peaks at 1730 cm^{-1}, $\nu_{(C=O)}$ after the click reaction in the presence of **(5)/(11).**

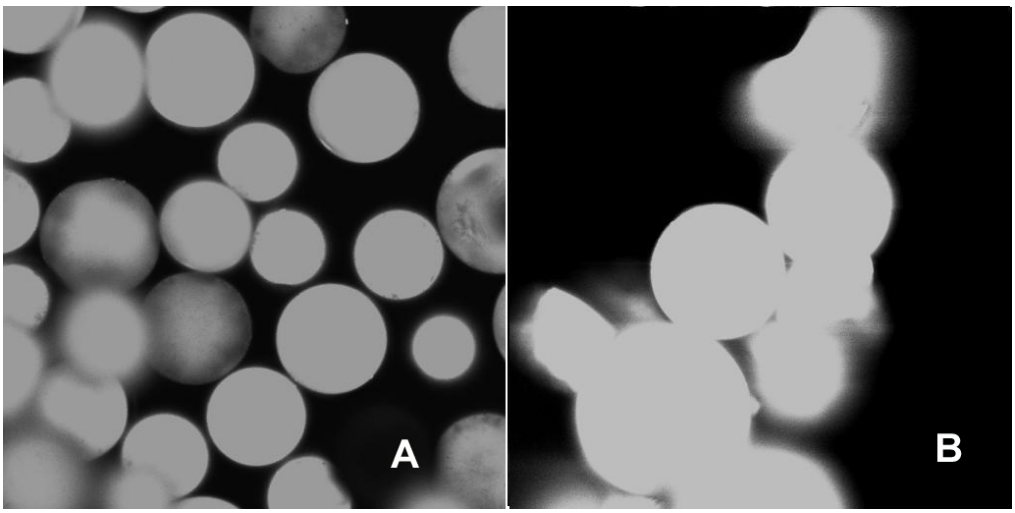

Figure 56. Images of modified Merrifield and Wang resins obtained by confocal microscopy. A: Merrifield resin-(11), B: Wang resin-(5).

Confocal microscope images of poly(MMA-co-HMA) modified Wang and Merrifield resins, Figure 56, are a further indication of the successful reaction. No fluorescence was observed in the control experiment in which unmodified resins were used.

Field-Emission Scanning Electron Microscopy (FE-SEM) provided further insights highlighting the differences between the resin before and after modification. The surface of polymer modified Wang resin lost many of the fine features indicating the grafting of polymers onto Wang resin, Figure 57.

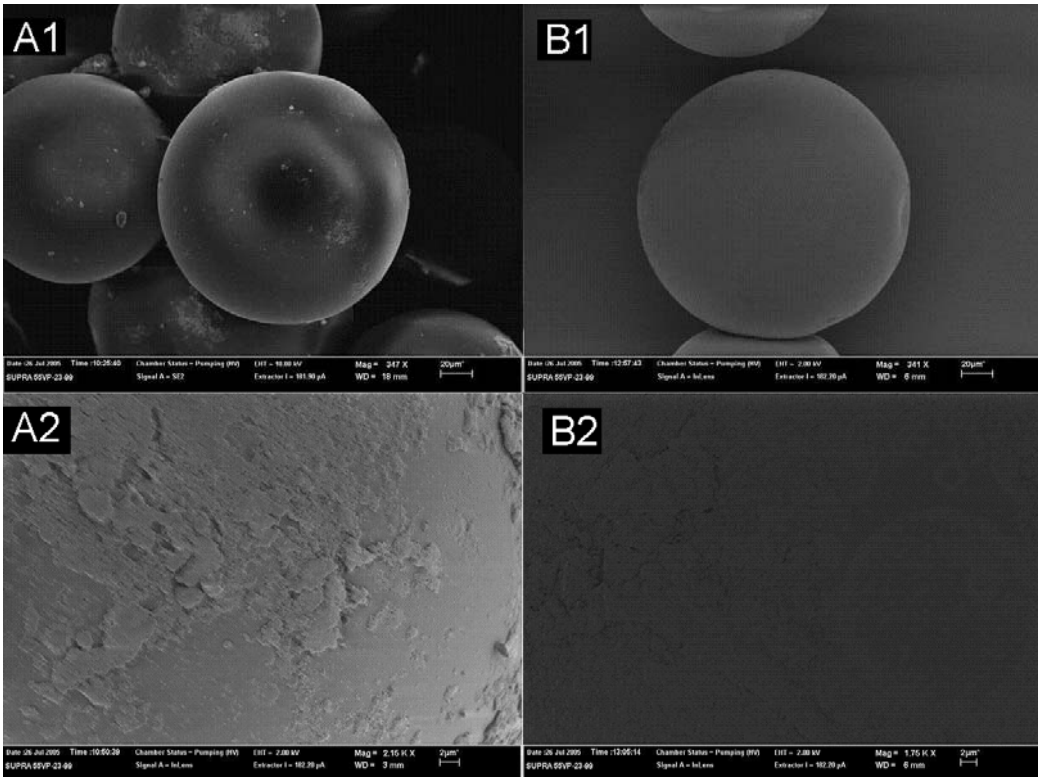

Figure 57. FE-SEM images of Wang resin before and after modification. A1, A2: native Wang resin; B1, B2: Wang resin-(5)

In conclusion, Huisgen 1,3-dipolar cycloaddition has been demonstrated to be very convenient and robust for bead surface modification. In addition, TMM-LRP with either azido or alkyne terminal initiators produce the desired functional polymers relatively easily for the modification of different resin surfaces. These results give a better understanding and enlighten the following Wang resin surface modification for affinity chromatography.

3.3 "Click" Modular Approach to Glycosylated Resins[232]

Thin organic and polymer films on solid substrates play a key role in many natural and non-natural processes. Based on the immobilization of molecular probes onto a variety of solid supports that exploits specific donor/receptor interactions in the presence of appropriate substrates (such as between antibodies and antigens, enzymes and inhibitors and carbohydrates and lectins), affinity chromatography has evolved as one of the most powerful and effective fractionation techniques for proteins purification. In Nature, sugars are often employed as information-rich molecules and an increasingly large number of known lectins are able to recognize subtle variations of oligosaccharide structure, acting as decoders for this carbohydrate-encoded information.[233] The considerable scientific effort spent in preparing immobilized sugar probes onto different surfaces led to the use of these functional materials in a number of different applications which include microarrays, microbeads, and biosensor chips.[234,235] Carbohydrate groups were bound to the substrate either non-covalently[236-238] or covalently.[239-241] Important examples of immobilized synthetic neoglycopolymers include controlled radical polymerisation of sugar monomers from silica[242] (ATRP) and silicon wavers[243] (RAFT), grafting of biotin- terminated polymers to (strept)avidin surfaces,[244-247] attachment of thiol-terminated materials prepared by RAFT to gold nanoparticles,[248,249] and functionalization of polypropylene microporous membranes.[250-252] Despite these advances, however, the use of immobilizes sugar as ligands in lectin-recognition studies has been less extensively investigated,[248,253,254] probably due to the difficulties in the synthesis of suitable carbohydrate probes.

In chapter 2, we developed a novel synthetic strategy that combined copper-catalysed ATRP and Huisgen 1,3-dipolar cycloaddition and was used in cellulose surface

modification. Previous efforts of modifying resins with fluorescent polymers also demonstrate that the "click" process constitutes an extremely valuable tool for surface modification. In addition, the click reaction has also been successfully used in the synthesis of carbohydrate-based materials. In one approach done by our group, appropriate sugar azides are clicked onto preformed well-defined polyalkyne methacrylic scaffolds. One of the main advantages in using this protocol is the possibility of preparing libraries of different copolymers that only differ for the relative proportion of carbohydrate epitopes by simply employing appropriate mixtures of sugar azides in the reaction feed, starting from one single polyalkyne precursor (we termed this process co-clicking). This is of importance, as it allows for the study of the influence of one specific epitope density on the biological behaviour of the neoglycopolymers, with all the other macromolecular features remaining unchanged. Another advantage is the avoidance of preparing and handling sugar methacrylic monomers that often tend to spontaneously self-polymerise.

Alkyne-azide cycloaddition has also been employed for the preparation of cross-linked polymer[255] and silica-based[254] stationary phase supports for chromatography. The present work is focused on the synthesis of supports bearing covalently immobilized carbohydrates starting from preformed Wang-resin beads, and the use of these hybrid materials in a preliminary lectin-glycopolymer recognition study. Our synthetic approaches involved a combination of Cu-catalysed LRP and Huisgen 1,3 dipolar cycloaddition. Recently, we and others reported that these two powerful synthetic tool can be successfully combined for preparing α-functional polymers[169,256], glycopolymers[257] and functional surfaces.[188]

Two distinct classes of immobilized carbohydrate displays were prepared. In the first one mannose monosaccharide moieties were clicked onto alkyne-modified Wang

resin, in the second case polyalkyne polymers were grown from immobilized LRP initiators, and then mannose-azide units were clicked onto this macromolecular scaffold to give the desired glycopolymers-bead hybrid material, Figure 58. The latter materials will be also referred here as "rasta" resins: a general term indicating polymer chains grafted to crosslinked polymeric bead cores.[258]

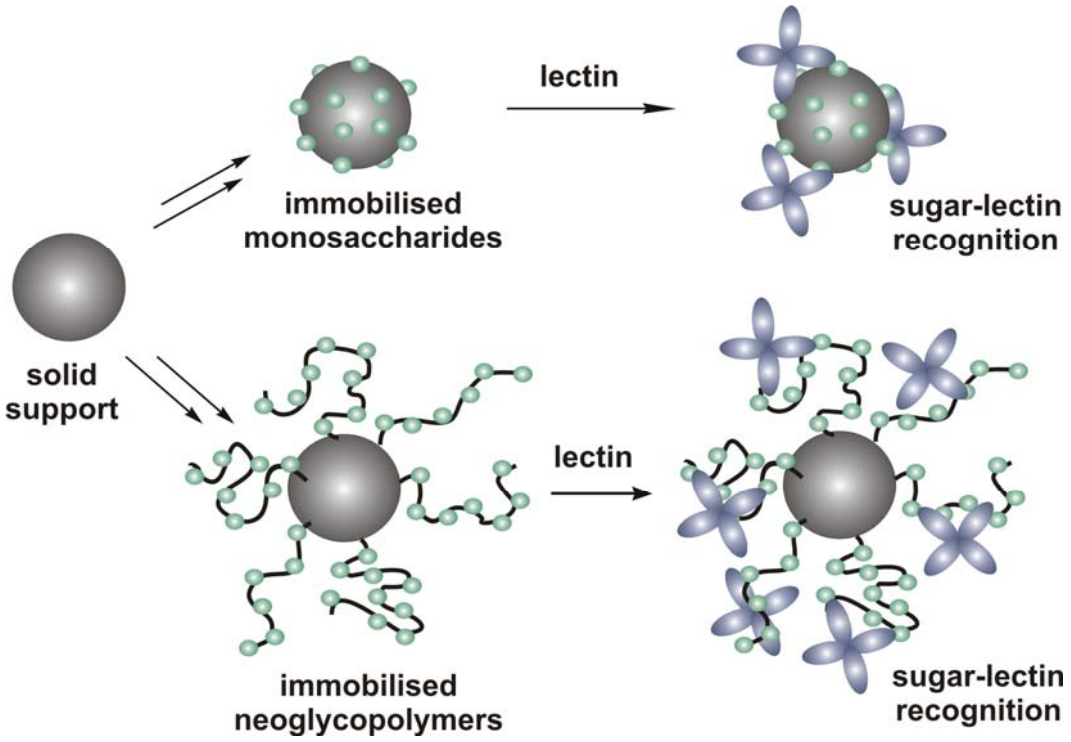

Figure 58. Immobilized sugar supports: two general approaches employed in this work.

3.3.1 Synthesis of the sugar supports

Commercially available Wang resin (1 mmol g^{-1} OH groups loading) was chosen as the solid support starting material for the present study. The polymerisation of methyl methacrylate[103,259] and *N,N*-dimethylacrylamide from LRP initiators immobilized to Wang resin via living radical polymerisation using Cu(I)Br/iminopyridine ligand catalysts were reported. More recently, grafted copolymers, such as poly(*tert*-butyl acrylate-*b*-styrene)[260] and azlactone-functionalized copolymers,[261] have been

synthesized following similar strategies and the resulting materials employed for a number of different applications.

Our general strategy here involved the click of appropriate azide sugar" to preformed resin surfaces bearing terminal alkyne groups, affording either *immobilized monosaccharides* or *immobilized neoglycopolymers* , Figure 59.

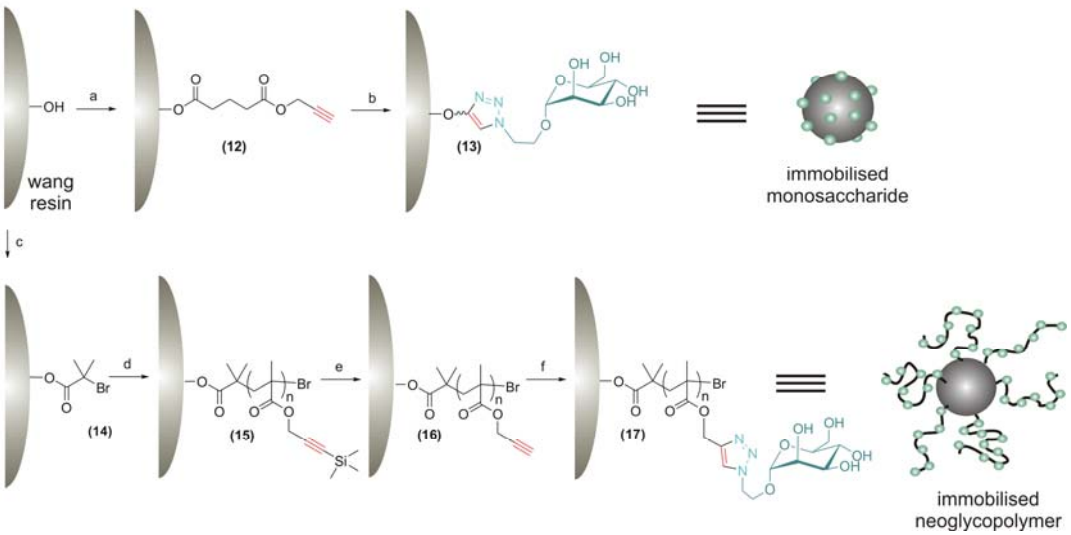

Figure 59. Synthesis of mannose modified Wang Resins by 'click' reaction. Reagents and conditions: a) 4-Chlorocarbonyl-butyric acid prop-2-ynyl ester, DMAP, pyridine, 60˚C; b) $(PPh_3)_3Cu(I)Br$, α-2-azidoethyl mannopyranoside, DMSO, 60˚C; c) 2-bromoisobutyryl bromide, triethylamine, DMAP, dichloromethane; d) trimethylsilyl-propargyl methacrylate, *N*-(ethyl)-2-pyridylmethanimine/Cu(I)Br, toluene, 70˚C; e) TBAF·$3H_2O$, acetic acid, THF; f) $(PPh_3)_3Cu(I)Br$, a-2-azidoethyl mannopyranoside, DIPEA, DMSO, 60˚C.

In the former case each OH present at the beads surface (1 mmol g^{-1} loading) was first converted into a monoalkyne handle in the presence of 4-chlorocarbonyl-butyric acid prop-2-ynyl ester, following a protocol that we have recently developed.[188] α-2-azidoethyl mannopyranoside, prepared in two steps from unprotected D-mannose, was then clicked to this alkyne-functional support **(12)**, to give the desired immobilized monosaccharide resin **(13)**.

In the second approach, Wang resin was first converted into the immobilized LRP initiator **(14)** in the presence of 2-bromoisobutyryl bromide. Polymerisation of

trimethylsilyl-propargylmethacrylate[257] at 70ºC using Cu(I)Br/*N*-(ethyl)-2-pyridylmethanimine as the catalyst in 51:1:1:2 (monomer : **(14)** : CuBr : ligand) molar ratio afforded the "rasta" intermediate **(15)**. Removal of the trimethylsilyl protecting groups with TBAF gave the polyalkyne scaffold **(16)** that was then "clicked" with α-2-azidoethyl mannopyranoside using $[(PPh_3)_3Cu(I)Br]$ as the catalyst to give the desired immobilized neoglycopolymer **(17)**.

3.3.2 Characterization of the sugar hybrid supports

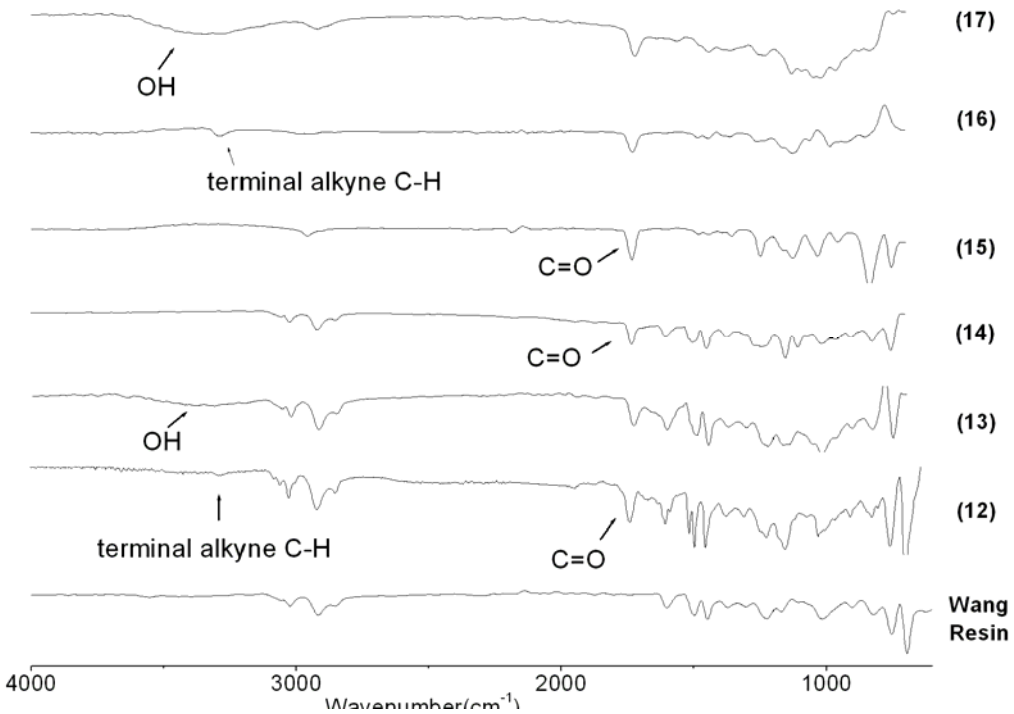

Figure 60. FTIR spectra of Wang resin, Wang-initiator and Wang-mannose.

The carbohydrate-based supports **(13)** and **(17),** as well as all the resin intermediates were characterized by FTIR, gel-phase NMR and CHN elemental analysis.

The conversion of 1 g/mmol Wang resin into the alkyne support **(12)** was confirmed by the appearance of an ester C=O and a weak alkyne C-H stretching in the IR spectrum, at ca. 1730 and 3300 cm^{-1} respectively, Figure 60. Subsequent clicking of α-2-azidoethyl mannopyranoside led to the immobilized monosaccharide resin **(13)**, in which a broad OH band centred at ca 3400 cm^{-1}.

For the synthesis of the immobilized glycopolymer **(17)**, the same Wang resin starting material was first converted into the polyvalent initiator **(14)** which gave the typical ester C=O stretching band at 1730 cm^{-1}, which increased substantially after the subsequent polymerisation of trimethylsilyl propargylmethacrylate to give the intermediate **(15)**. Removal of the protective groups gave the polyalkyne scaffold **(16),** which showed a characteristic 1-alkyne C-H stretching band in the IR spectrum at ca. 3300 cm^{-1}. After clicking the latter band disappeared, while a broad signal at ca. 3400 cm^{-1} corresponding to the sugar hydroxyl groups of **(17)** became evident.

The "rasta" materials were also characterized by gel-phase ^{1}H NMR analysis. The spectrum of a suspension of **(15)** in $CDCl_3$ showed the presence of all the expected major signals, including the ester OCH_2 (ca 4.5 ppm) and the $Si(CH_3)_3$ (ca. 0 ppm) peaks, Figure 61. The latter signal was absent in the spectrum of **(16)** in the same solvent confirmed the complete removal of the silylated protecting group, with the C≡CH signal clearly visible at ca. 2.5 ppm. Analysis of mannose neoglycopolymer **(17)** was slightly more problematic, probably due to less efficient swelling of the beads in the very polar solvents required for solvating the pendant sugar polymer chains. However, analysis of a suspension of **(17)** in DMSO-d_6 allowed detection of both the OCH_2 signal at ca. 5.2 ppm and the 1,2,3-triazole proton at 8.2 ppm.

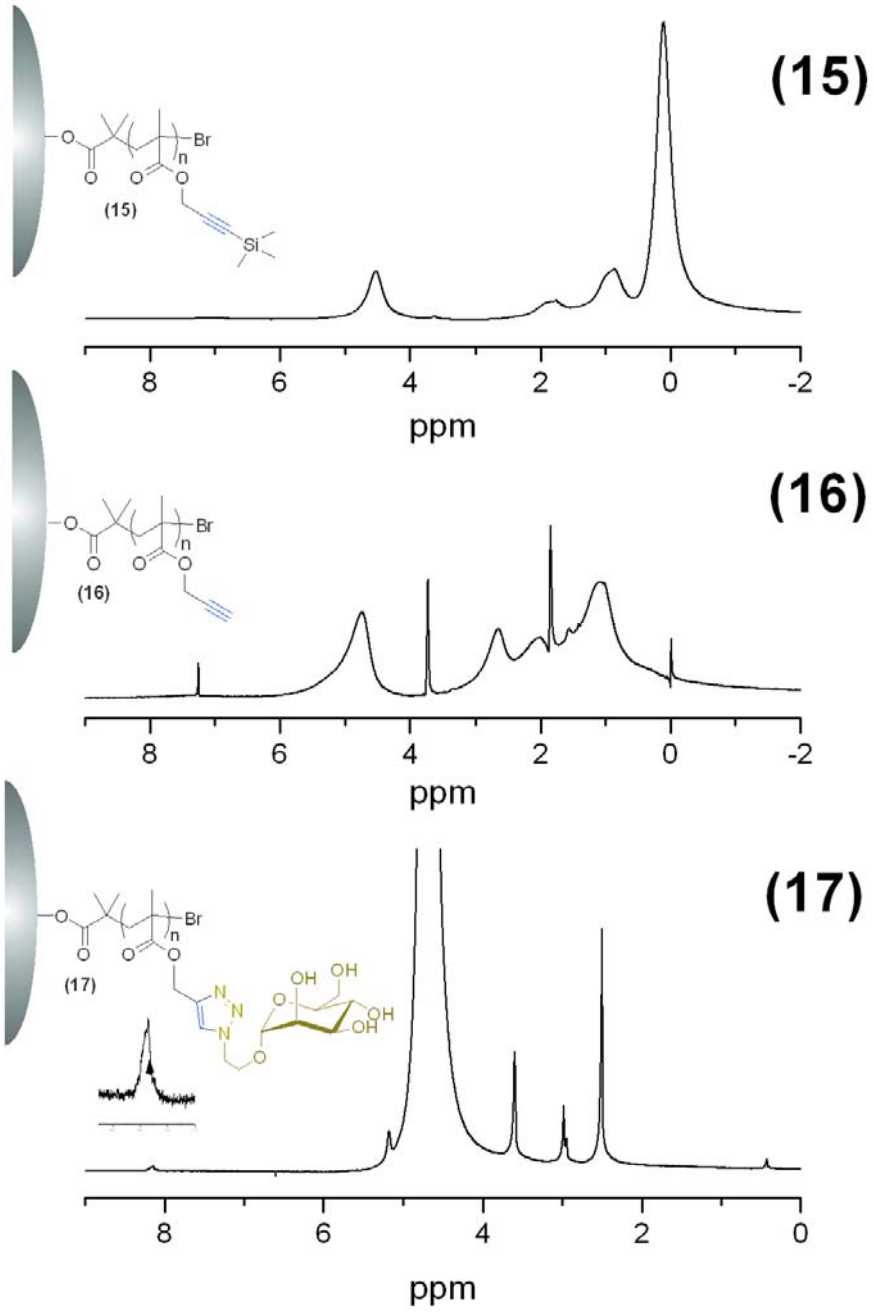

Figure 61. Gel-phase ^{1}H NMR spectra of "rasta" polymers presented in this study. Beads were suspended either in $CDCl_3$ ((4) and (5)) or DMSO-d6.((6)).

CHN analysis of the sugar beads and intermediates prepared in this work was carried out in an attempt to estimate their elemental composition, Table 8. Nitrogen content analysis of the immobilized monosaccharide beads **(13)** showed that approximately

75% of the Wang resin hydroxyl groups have been converted into clicked mannose units.

All of the rasta intermediates showed compositions very close to the theoretical values, calculated considering the alkyne monomer vs. initiator **(14)** weight ratio of 10:1 employed for the synthesis of the rasta intermediate **(15)** and monomer conversion very close to 100 %. The loading in 1-alkyne in the resin **(16)** was therefore calculated to be approximately 7.3 mmol g^{-1}. The elemental analysis of the clicked immobilized neoglycopolymer **(17)** indicated the amount of nitrogen after grafting being 6.6 per cent, which corresponds to efficiency in the cycloaddition step of ca. 65 %.

Table 8 Elemental analysis of some of the functionalized Wang resins prepared in this work.

Product	value	C (%)	H (%)	N (%)
Wang resin	Theoretical[a]	89.03	7.68	-
	Obtained	89.16	7.56	-
(13)	Theoretical[a]	77.9	7.21	3.10
	Obtained	79.21	7.17	2.31
(15)	Theoretical[b]	63.07	8.10	-
	Obtained	63.41	7.99	-
(16)	Theoretical[c]	69.03	6.55	-
	Obtained	69.98	6.82	-
(17)	Theoretical[d]	51.32	6.29	10.23
	Obtained	51.64	6.32	6.57

[a] assuming a styrene/[4-(4-Vinyl-benzyloxy)-phenyl]-methanol molar ratio of 7/1; [b] the weight ratio between monomer and initiator **(14)** was 10:1 and the final monomer conversion was approximately 100%: C (%) = 82.01 × 1/11 + 61.18 ×10/11, H (%) = 7.04 ×1/11 + 8.21 ×10/11; [c] C (%) = 82.01 × 1/11 + 67.73 ×10/11, H (%) = 7.04 ×1/11 + 6.50 ×10/11; [d] C (%) = 82.01 × 1/11 + 48.25 ×10/11, H (%) = 7.04 ×1/11 + 6.21 ×10/11, N (%) = 11.25 ×10/11.

In addition, FE-SEM was used to investigate the difference between the beads before and after modification, Figure 62 shows the general and cross-section images of Wang resin and sample **(15)**. The size of **(15)** is much larger than the starting Wang resin and the structures of the beads also show clear difference, which are mainly due to the high loading of the polymers being grafted.

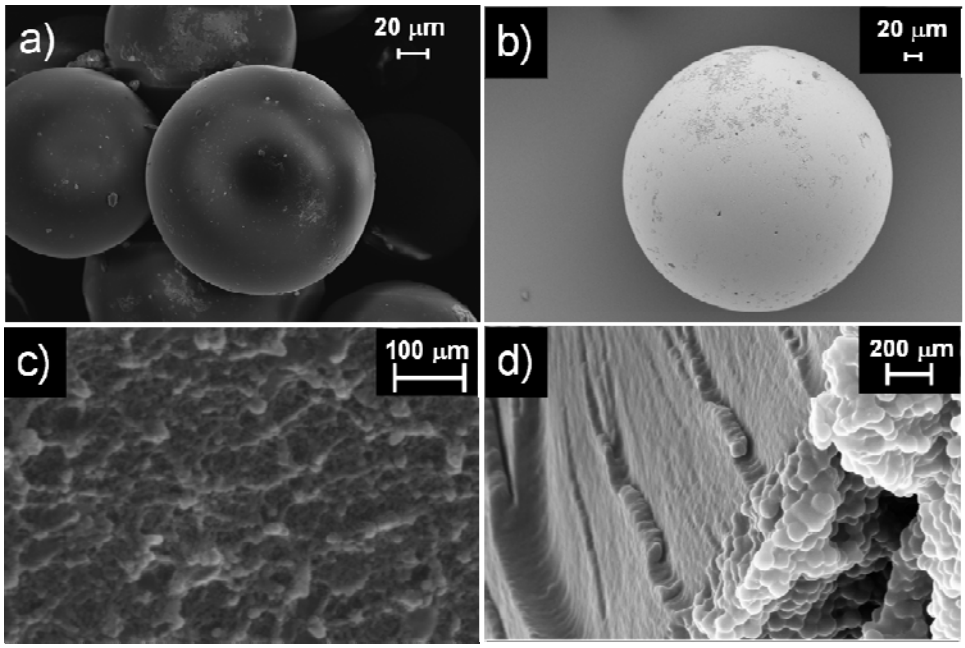

Figure 62. FE-SEM images of Wang resin (a&c) and Resin (15) (b&d).

3.3.3 Preliminary lectin recognition experiments

The ability of the immobilized sugar displays to selectively recognize specific lectins was investigated qualitatively. Commercially available Concanavalin A (Con A) was chosen as the model D-mannose-binding lectin, due the bulk of literature focusing on both its chemical and biological behavior.[262-265] Fluorescently labelled Con A (Fluorescein isothiocyanate-labelled Concanavalin-A, FITC-Con A) was used in order to facilitate the detection and qualitative characterization of the sugar-lectin clusters

by SEC-HPLC (system equipped with a fluorescence detector) and confocal microscopy.

Firstly, slurry suspensions of 100 mg of sugar beads **(13)** and **(17)** in PBS buffer (pH 7.4, 50 mM) were packed into small cartridges. 1.0 mL of a 1.0 mg mL^{-1} ($9.6 \cdot 10^{-3}$ μmol Con A tetramer mL^{-1}) solution of FITC-Con A solution was loaded onto the columns and allowed to elute by gravity. Approximately three minutes were required for the solution to pass through the cartridge. The residual solution still present in the column was eluted by applying a slight pressure at the top of the column. 50 μL aliquots of the starting FITC-Con A solution and of the sample collected after the column were then analysed by SEC-HPLC.

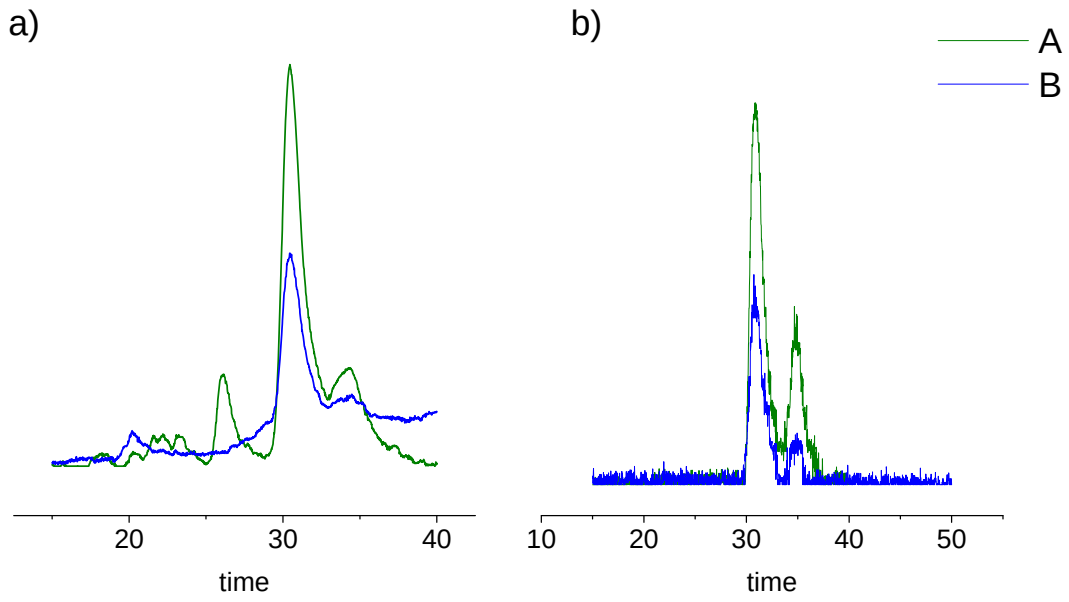

Figure 63. SEC-HPLC analysis of the FITC-Con A solution before (A, greed solid line) and after (B, blue solid line) elution through the immobilized monosaccharide (13) cartridge: a) UV detection, λ = 280 nm, b) fluorescence detection (λ_{ex} = 495 nm, λ_{em} = 525 nm).

Figure 63 shows typical chromatograms obtained by SEC-HPLC, using both UV (λ = 280 nm) and fluorescence (λ_{ex} = 495 nm, λ_{em} = 525 nm) detection, for the case the

immobilized monosaccharide resin **(13)**. Con A, existing mainly as tetramer aggregates of 26 kDa monomer units at pH 7.4, tend to form dimers in more acidic environments.[266] The presence of two main peaks in the SEC-HPLC traces seems to indicate that two distinct aggregation states may coexist under the conditions employed for the analysis (mobile phase: water/acetonitrile/TFA 35:65:0.1 volume ratio). SEC-HPLC data allowed us to estimate that around 50 % of the FITC-Con A had been retained by the immobilized monosaccharide **(13)** cartridge, under the experimental conditions employed for this preliminary study.

An analogous protocol was followed using "rasta" polymannose beads **(17)** instead of the immobilized monosaccharide resin **(13)**. **(17)** was expected to interact with lectins much more efficiently than **(13)** for a number of reasons that include higher loading in mannose epitopes per bead mass unit and the presence of flexible neoglycopolymer chains able to span over multiple lectin actives sites, which is known for improving the binding ability of sugar multivalent ligands. A previous report indicated that for the case of silica-based supports a substantial increase in Con A binding ability was observed even by passing from immobilized monosaccharide to analogous tripodal ones.[254]

In our experiments resin precursors with no sugar binding epitopes were employed as controls. As expected, only the resin **(17)** was able to specifically recognize Con A, with virtually no lectin eluted from the cartridge, Figure 64. The beads were then washed with 1 mL of 50 mM pH 7.4 PBS in order to remove physically absorbed Con A and all the fractions were separately analysed by SEC-HPLC.

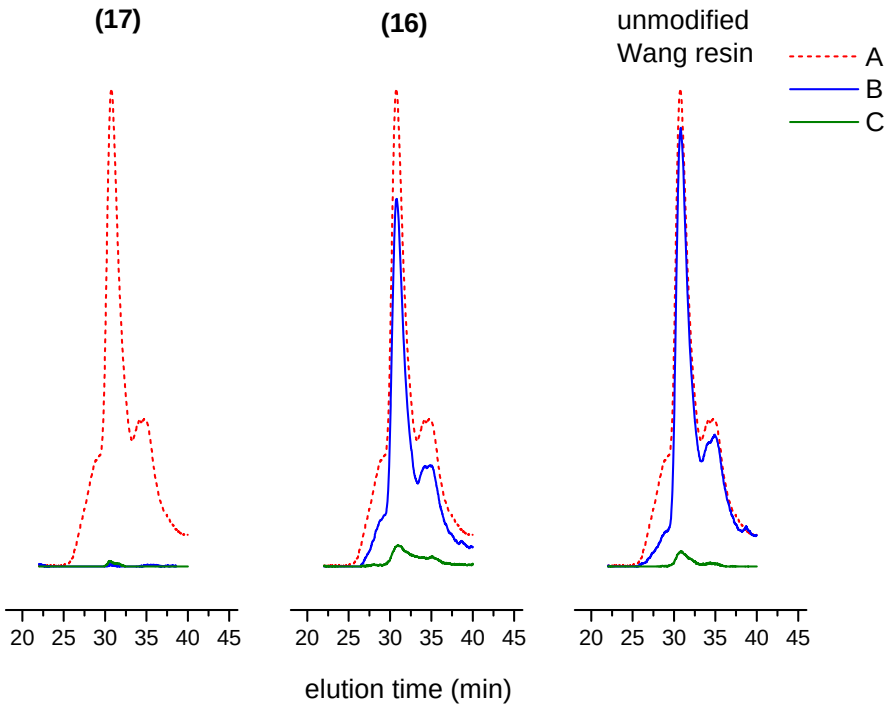

Figure 64. SEC-HPLC analysis (UV detection, l = 280 nm) of the FITC-Con A solution before (A, red dot line line) and after (B, blue solid line) elution through the immobilized "rasta" neoglycopolymer resin (17) cartridge. Analogous mini-columns packed with non-sugar-functionalized supports (16) and Wang resin were used as controls and the solutions eluted from them were analysed by SEC-HPLC under the same conditions employed for (17). The resin cartridges were then washed with 1 mL of 50 mM pH 7.4 PBS and the eluted solution was analysed by SEC HPLC (C, green solid line).

From these simple experiments, it appeared that non-specific interactions between the FITC-Con A and the control resins, **(16)** and Wang resin starting material, were negligible. It should be noted here, for comparison, that the non-specific interactions between silica (another solid support commonly employed as stationary phase in affinity chromatography) and lectins can be in some cases relatively significant,[254,267] possibly due to the negatively charged nature of the silica surface and the effect of electrostatic repulsions.

Rinsed Wang, **(16)** and **(17)** supports were then analysed by confocal microscopy. As expected, only **(17)** was highly fluorescent, in agreement with the HPLC results

obtained previously, that indicated that only the resin **(17)** presenting pendant polymers with multiple copies of α-mannopyranoside epitopes could bind the fluorescently tagged Con A lectin, Figure 65.

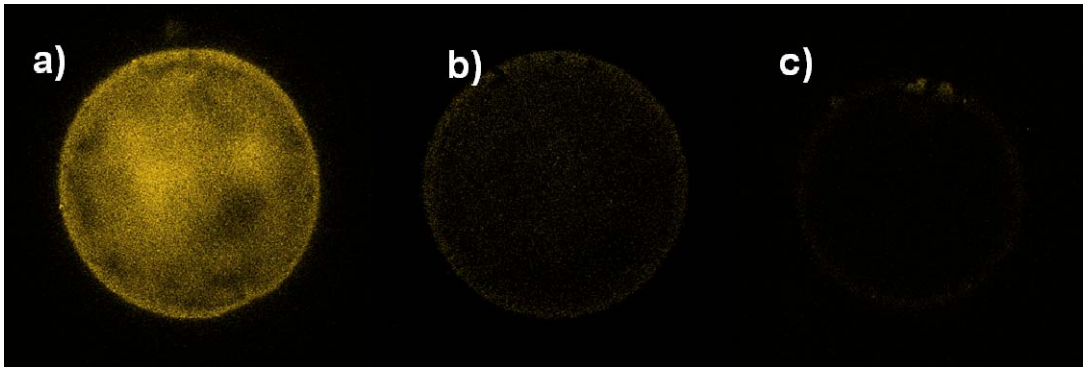

Figure 65. Confocal microscopy images of the (17) (a), (16) (b) and Wang resin (c) beads obtained after passing 1 mL of a 1 mg mL^{-1} FTIC-Con A solution in 50 mM pH 7.4 PBS through micro-column cartridges packed with the aforementioned resins. The resins were rinsed with 50 mM pH 7.4 PBS before confocal microscopy analysis.

In protein purification chromatography, the elution of the substrates can be promoted in various ways, i.e. by increasing the ionic strength of the mobile phase, by changing its pH, or by adding a competitive ligand for the protein analyte to the elution buffer.[221] In the present work, FITC-Con A was easily removed from the resin **(17)**-FITC clusters (still packed in the cartridge described previously) by adding a large excess (4.0 M) of α-methyl-D-mannopyranoside, a competitive monovalent ligand for Con A, to the mobile phase, Figure 66. Confocal microscopy analysis on the resulting beads revealed that the previously bound fluorescent lectin was successfully removed from the supported mannose glycoplymer **(17)**, confirming the sugar epitope-lectin nature of the interactions in the **(17)**-Con A clusters.

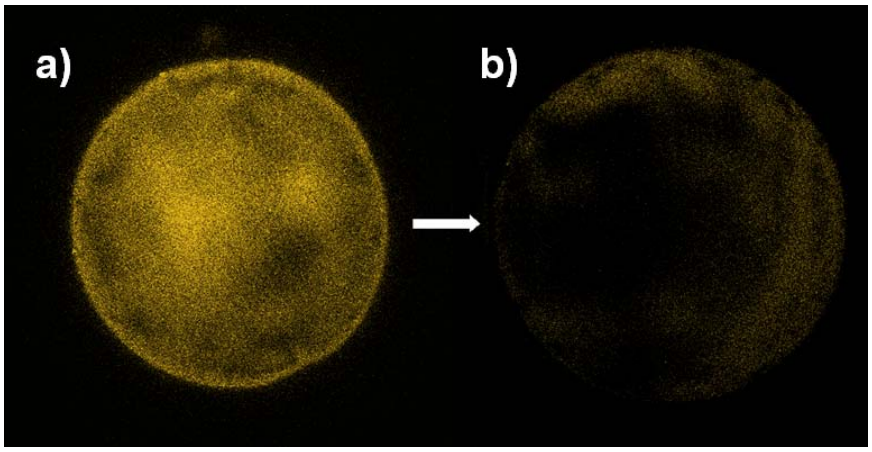

Figure 66. Confocal microscopy images of the resin (17)-FITC Con A cluster beads before (a) and after washing with a 4.0 M solution of α-methyl-D-mannopyranoside, a competitive monovalent ligand for Con A, in 50 mM pH 7.4 PBS.

3.3.4 Conclusion

Design and synthesis of two structurally distinct sugar supports is described. Both the synthetic protocols involve a key step in which an α-mannopyranose azide is clicked into immobilized alkyne moieties by Cu(I)-catalysed Huisgen [2+3] cycloaddition.

Immobilized monosaccharide resins were prepared by converting Wang resin hydroxyl groups into alkyne handles, followed by Cu(I)-catalysed clicking of α-2-azidoethyl mannopyranoside moieties.

The second class of materials, termed rasta "immobilized glycopolymers", consist of macromolecular chains displaying multiple copies of carbohydrate epitopes, grafted onto a crosslinked polystyrene core. This time, Wang resin hydroxyl groups were converted into ATRP initiators, then Cu-catalysed polymerisation in the presence of trimethylsilyl-protected propargyl methacrylate followed by TBAF-mediated deprotection afforded clickable beads consisting of a crosslinked polystyrene core and a loose polyalkyne outer shell.

The hybrid materials prepared in this work have shown the ability of recognizing Con A, a well-known mannose binding lectin, and their use in the purification of complex mixtures of mannose-binding biologically relevant lectins is under investigation.

We also believe that the strategy developed for mannose-functional beads is very general and future research will focus on the synthesis and use of immobilized ligands bearing a plethora of different sugar epitopes, potentially opening the way for an application of these materials in a number of fields which include chemical sensing, responsive surfaces and affinity chromatography.

3.4 TMM-LRP of Glycerol Methacrylate (GMA) onto resin surface and their modification for chiral separation

The separation of chiral compounds has been of great interest because the majority of bioorganic molecules are chiral. Living organisms, for example, are composed of chiral biomolecules such as amino acids, sugars, proteins and nucleic acids. In nature these biomolecules exist in only one of the two possible enantiomeric forms, e.g., amino acids in the L-form and sugars in the D-form. Because of chirality, living organisms show different biological responses to one of a pair of enantiomers in drugs, pesticides, or waste compounds, etc.[268] Therefore, chirality is a major concern in the modern pharmaceutical industry, largely due to the fact that enantiomers of a racemic drug may have different pharmacological activities, as well as different pharmacokinetic and pharmacodynamic effects.[269,270] An extreme example is the tragic case of the racemic drug of n-phthalyl-glutamic acid imide that was marketed in the 1960's as the sedative Thalidomide. Its therapeutic activity resided exclusively in

the R-(+)-enantiomer. It was discovered only after several hundred births of malformed infants that the S-(+)-enantiomer was teratogenic.[271]

Together with the importance of chiral compounds in other applications like asymmetric synthesis[272-274], agrochemicals and fragrances [275], there is a great need to develop technology for analysis and separation of racemic compounds. Although a large number of approaches have been used to isolate single enantiomers [276], enantioselective chromatography using high performance liquid chromatography (HPLC) and super- and sub-critical fluid chromatography (SFC) on chiral stationary phases (CSPs) has become the most widely utilized technique in the context of obtaining pure enantiomers quickly, particularly in drug discovery[277]. For chiral HPLC, columns are made by immobilising single enantiomers onto the stationary phase. Resolution relies on the formation of transient diastereoisomers on the surface of the column packing. The compound which forms the most stable diastereoisomer will be most retained, whereas the opposite enantiomer will form a less stable diastereoisomer and will elute first. To achieve discrimination between enantiomers there needs to be a minimum of three points of interaction to achieve chiral recognition. Consequently, various efforts have been devoted to the development of effective CSPs. [278,279] The different chiral separation principles in HPLC could be summarised as the following: phases based on multiple hydrogen bonding,[280,281] chiral π-donor and π-acceptor phases,[282,283] cyclodextrin phases,[284] polysaccharides phases,[285-289] macrocyclic antibiotics,[290] synthetic chiral macrocycles,[291] chiral synthetic polymers,[292] chiral imprinted polymers,[293-295] protein-based phases,[296] ligand-exchanging phases[297,298] and ion-pairing phases[299]. Among them, direct chromatographic resolution using CSPs is preferred to indirect approaches, such as

derivatization[300] or use of chiral additives in the mobile phase, because much less sample manipulation is required, and more rapid solute recovery is possible after the preparative chromatography.

3.4.1 Synthesis of chiral polymer based CSP

In this section, chiral polymer based CSP are made using TMM-LRP technology by grafting glyco-monomers onto certain beads through surface-initiated LRP. Subsequently, single enantiomers are immobilised onto the glyco-modified bead by reacting with the multiple hydroxyl groups of carbohydrate moieties. Glycerol methacrylate was used as a model to modify Aquagel beads, which is further modified with enantiomer (R)-(+)-1-phenylethyl isocyanate (EtPhNCO), Figure 67.

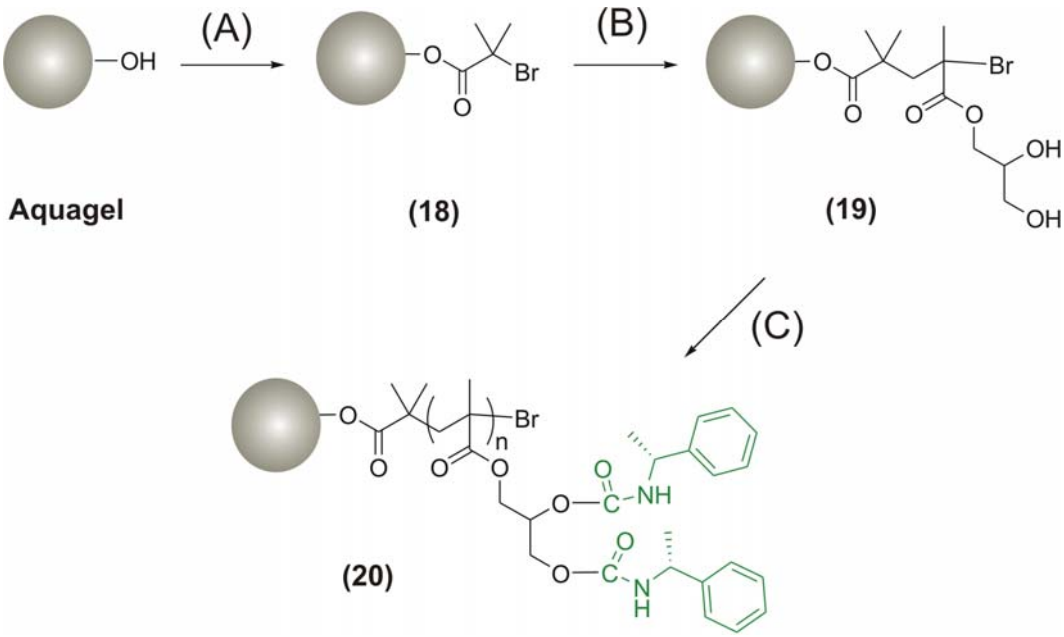

Figure 67. Synthesis of enantiomer-immobilised resins by surface-initiated polymerisation. Reagents and conditions: A) 2-bromoisobutyryl bromide, anhydrous pyridine, ambient temperature; B) GMA, Cu(I)Br/bpy, methanol, 25˚C; C) EtPhNCO, anhydrous pyridine, 50 ˚C.

Aquagel resin was first converted into the immobilized ATRP initiator **(18)** in the presence of 2-bromoisobutyryl bromide in pyridine, Figure 67. Polymerisation of

GMA at 25ºC using Cu(I)Br/HETEA as the catalytic system 15:1:5:5 (monomer : **(18)** : CuBr : ligand) molar ratio afforded the poly(glycerol methacrylate) (PGMA) modified resin **(19)**, which then was treated with EtPhNCO to afford **(20)**, a chiral polymer based resin with potential as a CSP for HPLC.

3.4.2 Characterisation of the hybrid supports

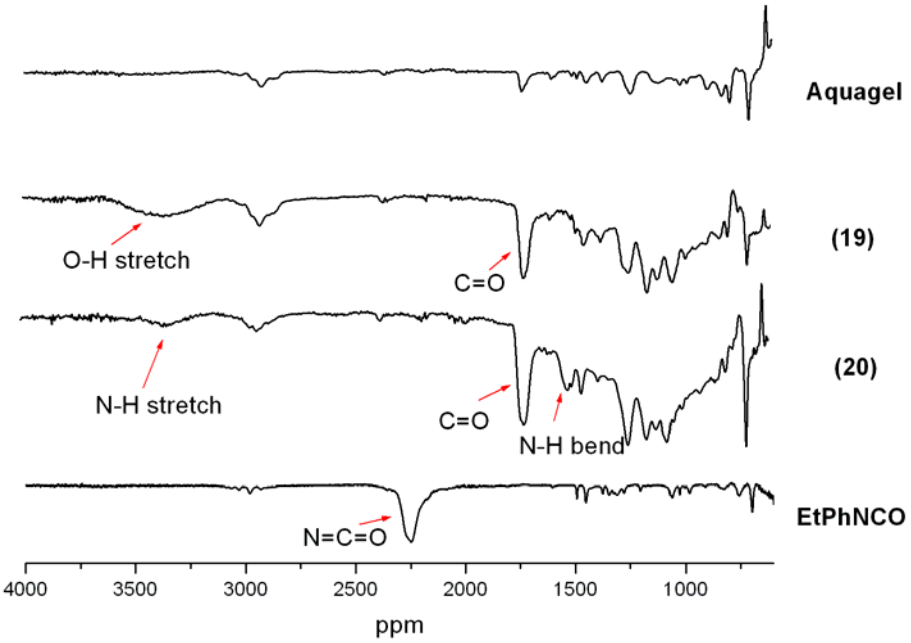

Figure 68. FTIR spectra of Aquagel resins before and after modification.

The PGMA-based supports **(19)** and **(20)** were characterized by FTIR, gel-phase NMR, FE-SEM, and CHN elemental analysis. The synthesis of Aquagel-PGMA **(19)** was confirmed by the appearance of an O-H stretching in the IR spectrum, at ca. 3370 cm^{-1}, in addition, the peak at ca. 1720 cm^{-1} become larger, attribute to the C=O of GMA, Figure 68. Subsequent reaction with EtPhNCO led to the immobilized chiral resin **(20)**, in which a N-H stretch centred at ca 3350 cm^{-1} and a N-H bend at ca. 1520

cm^{-1}. There is no obvious peak at 2250 cm^{-1}, where an intense peak in the starting material EtPhNCO, from N=C=O group, is observed. This indicates there is no free EtPhNCO in the final resin **(20)**.

The final EtPhNCO modified Aquagel resin was also characterized by gel-phase ^1H NMR analysis. The spectrum of a suspension of **(20)** in $CDCl_3$ showed the presence of all the expected major signals, including the ester OCH_2 (ca 4.5 ppm, peak c in Figure 69) and phenyl (ca 7.2 ppm, peak a in Figure 69) peaks.

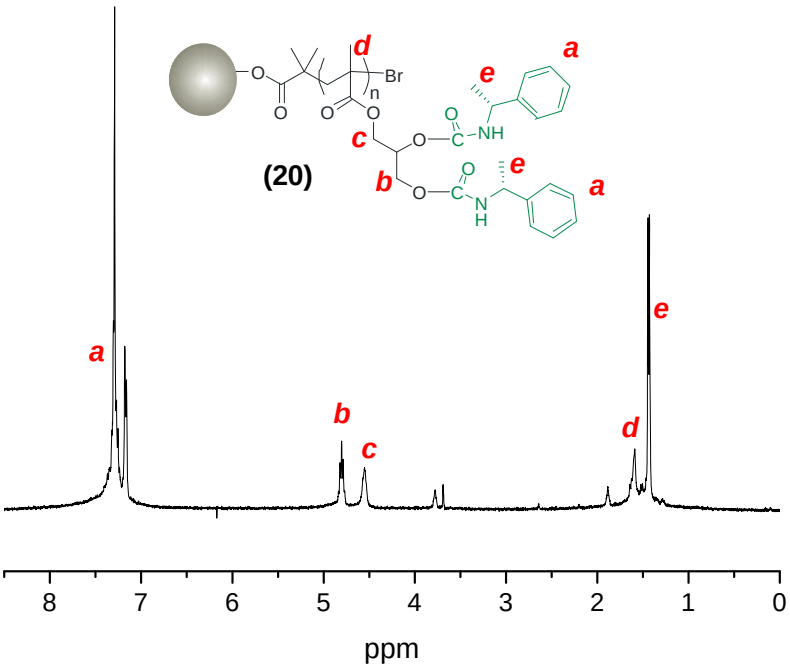

Figure 69. Gel-phase ^1H NMR spectra of EtPhNCO modified Aquagel resin (20) suspended in $CDCl_3$.

CHN analysis of the EtPhNCO modified beads and intermediates prepared in this work were carried out in an attempt to estimate their elemental composition, Table 9.

The intermediate resin showed compositions close to the theoretical values, calculated based on the weight increase (~45%) of monomer GMA for the synthesis of the rasta intermediate **(19)**. The loading in hydroxy groups in the resin **(19)** was therefore calculated to be approximately 5.6 mmol/g. The elemental analysis of the final EtPhNCO modified beads **(20)** indicated the amount of nitrogen after grafting being 2.68 per cent, which correspond to a 1.9 mmol g^{-1} loading of chiral functionality EtPhNCO.

Table 9. Elemental analysis of some of the functionalized Aquagel resins prepared in this work.

Product	value	C (%)	H (%)	N (%)
Aquagel Resin	Obtained	83.65	8.07	-
(18)	Obtained	78.95	7.79	
(19)	Theoretical[a]	67.04	7.68	-
	Obtained	67.22	7.68	-
(20)	Theoretical[b]	73.15	7.28	2.77
	Obtained	69.46	7.15	2.68

[a] %: C (%) = 78.95 × 0.55 + 52.49 × 0.45, H (%) = 7.79 × 0.55 + 7.55 × 0.45; [b] C (%) = 78.95 × 0.55 + 66.06 × 0.45, H (%) = 7.79 ×0.55 + 6.65 × 0.45, N (%) = 6.16 × 0.45.

In addition, FE-SEM was used to see the difference of the beads before and after modification. Figure 70 shows the general and cross-section images of starting Aquagel resin and sample **(19) (20)**. Although the size difference between resins is not obvious, the surface and inner structures of the beads show clear differences, which mainly due to the grafting of polymers onto the starting resin.

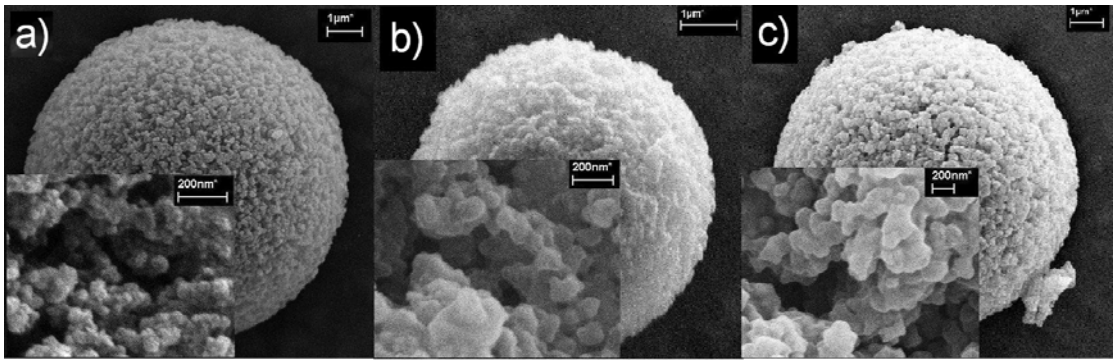

Figure 70. FE-SEM images of Aquagel (a), resin (19) (b) and resin (20) (c).

3.4.3 Conclusion

Aquagel resin has been transformed into a resin initiator, surface initiated living radical polymerisation of GMA was then successfully carried out for the synthesis of PGMA containing bead. The hydroxyl groups of the PGMA moiety were then reacted with a single enantiomer EtPhNCO. The resins before and after modification have been characterized by FTIR, gel-phase NMR FE-SEM, and CHN elemental analysis. This demonstrates a convenient way to immobilise an enantiomer moiety onto a resin surface and the resulting solid support may be used as a CSP for HPLC chromatography. The beads have now been sent to a UK chromatography company (Chromotide) for chiral separation tests.

Chapter 4 Multiwalled Carbon Nanotube (MWCNT) Surface Modification

4.1 Introduction

The discovery of carbon nanotubes (CNTs) in 1991[301] has stimulated intensive research to characterize their structure, to determine their properties and to explore their applications. The walls of these tubes are made up of a hexagonal lattice of carbon atoms analogous to the atomic planes of graphite. They are capped at their ends by one half of a fullerene-like molecule. In the most general case, a CNT is composed of a concentric arrangement of many cylinders, termed as multi-walled carbon nanotubes (MWCNTs). Single-walled carbon nanotubes (SWCNTs) possess the simplest geometry, consisting of a single graphite sheet seamlessly wrapped into a cylindrical tube. These nanoscale tubes not only exhibit appealing electronic properties, but also remarkable thermal and mechanical characters. Much pioneering work has been carried out to apply CNT's in different fields. For example, by combining CNT's with nanoparticles[302-305] and protein/gene[306,307], the complexes could be used as chemical sensors, catalyst and protein/gene transporters. However, the poor solubility of CNT's has hindered their application. Therefore, dispersion of the tubes is particular import. (Note: Researchers also use the term 'soluble carbon nanotubes', although 'dispersible' may be better. Bearing this in mind, the term 'soluble' is also used in this chapter.) The surface modification of CNT's with polymers was one of the routes to make soluble CNTs. There are two main

approaches for the surface modification of CNTs: non-covalent and covalent attachments. Obviously, the advantage of non-covalent attachment is that the perfect structure of the nanotubes is not altered, thus its mechanical properties should not change. The main disadvantage is the relatively weak force between the wrapping molecule and the nanotube. For covalent attachment, although functional groups might introduce defects on the walls of the nanotubes, it is still an attractive target. Functional polymers bonding to CNTs increase the dispersability of the CNTs, at the same time, they have also enlarged the application areas of CNTs due to their own functional properties. Examples of the typical methods for nanotube surface modification will be given below.

4.1.1 CNT surface modification by non-covalent attachment

This type of solubilization is particularly attractive for not destroying the π structure of the CNT. It was first found that CNTs could be solubilized in aqueous media in the presence of amphiphilic molecules. [308,309] It is believed that the hydrophobic part attaches on the surface of the CNT, whereas the hydrophilic part interacts with the solvent molecules. Smalley and co-workers reported that SWCNTs could be solubilized in water by associating them with a variety of linear polymers such as polyvinyl pyrrolidone and polystyrene sulfonate.[310] They propose that the wrapping of the SWNTs by water-soluble polymers is a general phenomenon, driven largely by a thermodynamic force to eliminate the hydrophobic interface between the tubes and their aqueous medium.

Another method widely used is the use of polymers bearing aromatic moiety to either wrap (backbone or side chain functionality) or attach (end terminal functionality) CNTs. It is presumed to be mainly due to π- π stacking and van der Waals interactions

between the polymers and CNTs. Conjugated polymers are widely used to solubilize CNTs, Heath and co-workers reported that a substituted poly(metaphenylenevinylene) (PmPv) provided a useful route toward "functionalising" the SWNT without destroying their electrical character. [311,312] Similarly, poly{(5-alkoxy-m-phenylenevinylene)-co-[(2,5-dioctyloxy-p-phenylene)-vinylene]} (PAmPV) derivatives have been prepared and used to solubilize SWNT in organic solvents by wrapping themselves around the nanotube bundles.[313] Tang *et al.* reported that carbon nanotube-containing poly(phenylacetylenes) (NT/PPAs) are prepared by in situ polymerisations of phenylacetylene catalysed by WCl_{6e}-PK_4Sn and [Rh(2,5-norbornadiene)Cl]$_2$ in the presence of the nanotubes.[314] The short nanotubes thickly wrapped in the PPA chains are soluble in common organic solvents including tetrahydrofuran, toluene, chloroform, and 1,4-dioxane. Recently, molecules containing pyrene moieties have been used for noncovalent anchoring to the side-walls of CNTs. Substituents of pyrene have been selected to link, for example, proteins[315] or initiators of ring-opening metathesis polymerisation[316] to CNTs. In addition, pyrene-containing polymers has also been made to wrap CNTs. [317,318]

DNA molecules is another type of material researchers have attached to CNTs, the DNA molecules may be encapsulated inside or warped around CNTs due to the van der Waals attraction between DNA and CNT. A review about the recent advances in this area has been written by Gao *et al.*.[319]

CNTs have also been encapsulated by polymers[320] or encased by cross-linked, amphiphilic copolymer micelles[321].

4.1.2 CNT surface modification by covalent attachment

The most widely used method for the chemical modification of CNTs uses the introduction of carboxyl groups to the CNTs. This oxidation process of CNTs involved treatment in strong acid either under sonication[322] or not[323]. This treatment leads to the opening of the tube caps as well as the formation of holes in the sidewalls, followed by an oxidative etching along the walls with the concomitant release of carbon dioxide. Thus, the CNTs' ends and sidewalls are decorated with various oxygen containing groups, mainly carboxylic acid groups. These carboxyl groups could then be easily turned into other functionalities. The introduction of carboxyl groups to CNTs enables the covalent coupling of molecules through the creation of amide and ester bonds, Figure 71.

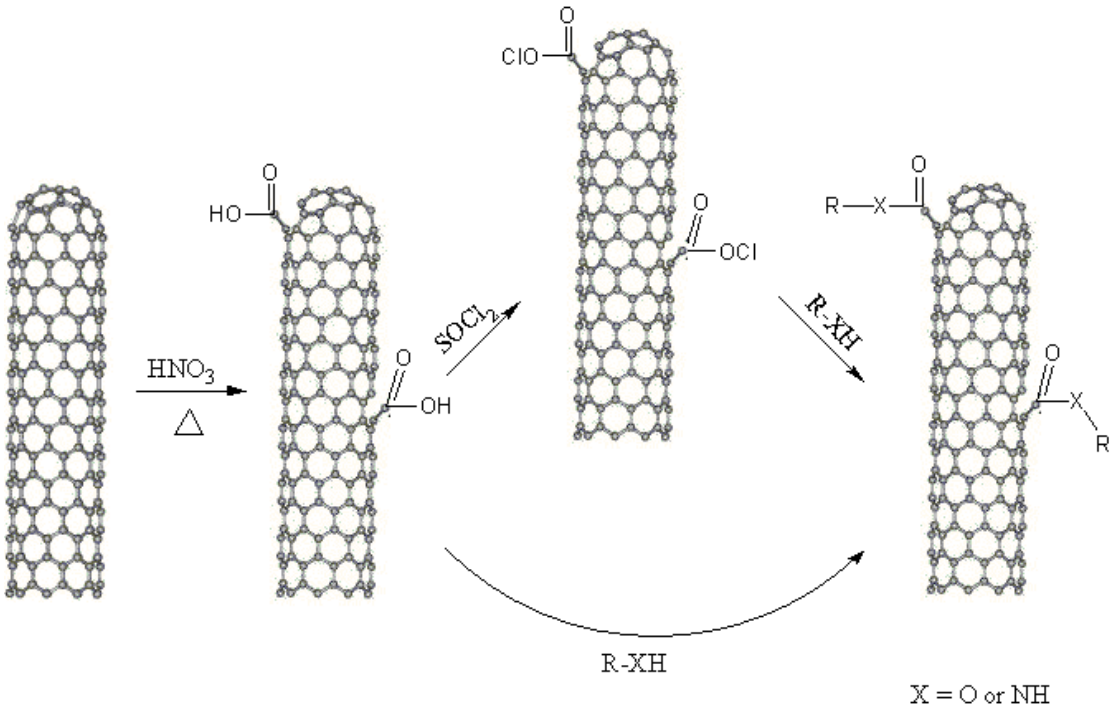

Figure 71. Chemical modification of CNTs through thermal oxidation, and the subsequent esterification or amidization reactions.

By this method the CNTs can be provided with a wide range of functional moieties. For example, to increase the solubility in different solvents, a variety of polymers were attached to CNTs including poly (propionyl-ethylenimine)-*co*-ethylenimine(PPEI-EI)[324], polystyrene (PS)[156,325,326], poly (sodium 4-styrenesulfonate)[327], multi-hydroxy polymers[328], poly (methyl methacrylate) (PMMA)[329-331], poly (vinyl alcohol) (PVA) and poly (vinyl acetate-co-vinyl alcohol) (PVA-VA)[332]. Recently, some polymers with complex structures, such as hyperbranched polymers, have also been connected onto CNTs effectively[333,334], the poly(amidoamine) dendrimer (PAMAM) with amine as peripheral group was also used as cross-linking reagent to prepare star-shaped CNTs[335].

Another approach is the direct coupling of functional groups onto the π-conjugated carbon framework of CNTs using addition reactions. Burghard *et al.* summarised the possible addition reactions for the functionalisation of CNTs in their review[336], as shown in Figure 72.

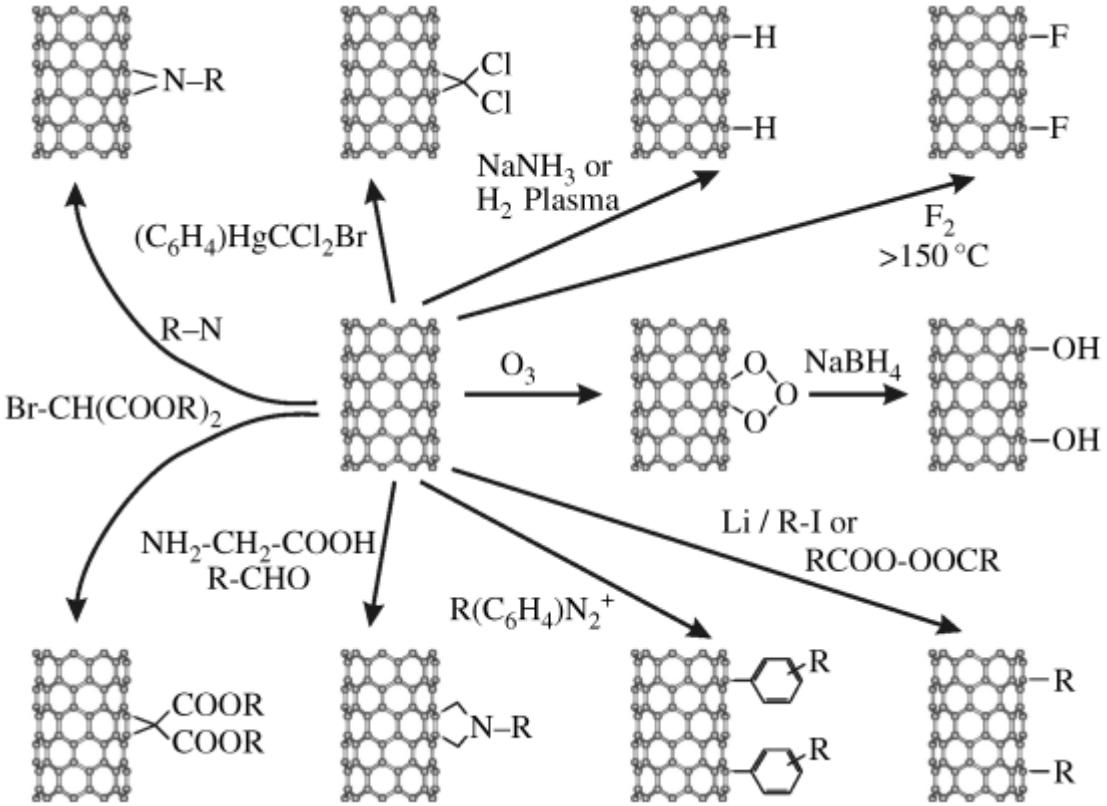

Figure 72. Overview of possible addition reactions for the functionalization of the CNTs. (copied from Balasubramanian, K.; Burghard, M. Small 2005, 1, 180-192).

Reactive species (atoms, radicals, carbenes or nitrenes) are required for this approach. For the examples of polymer modified CNTs, the 'living' polystyrene, poly(3-caprolactone) or their block copolymers end-capped by a 2,2,6,6-tetramethylpiperidine-1-oxyle (TEMPO) group reacted with MWCNTs by addition reaction of the alkoxyamine-terminated precursors according to a radical mechanism.[337] PSt–N_3 with designed molecular weight and narrow molecular weight distribution was synthesized by atom transfer radical polymerisation (ATRP) of styrene (St) followed by end group transformation and then added to SWNT via a cycloaddition reaction.[156] Liu reported a novel method for the polymer or copolymer grafted SWNTs.[326] The chain radical of polystyrene and poly[(*tert*-butyl acrylate)-*b*-styrene] with well-defined molecular weights and polydispersities, prepared by nitroxide-mediated free-radical polymerisation, were successfully used for the

functionalization of the SWNTs through a radical coupling reaction involving polymer-centred radicals generated at 125 °C via loss of the stable free-radical nitroxide capping agent. In another example, SWNTs were functionalized along their sidewalls with phenol groups using the 1,3-dipolar cycloaddition reaction.[330] These phenols could be further derivatized with 2-bromoisobutyryl bromide, resulting in the attachment of ATRP initiators to the sidewalls of the nanotubes. These initiators were found to be active in the polymerisation of MMA and *tert*-butyl acrylate (*t*-BA) from the surface of the nanotubes.

4.1.3 Summary of CNT surface modification in this project

In this chapter, covalent and non-covalent methods have both been used to modify CNTs. MWCNTs was first converted to a solid support LRP initiator by esterification reaction and styrene was grafted from MWCNTs through surface-initiated ATRP, the PSt modified CNTs were then used to form isoporous membranes. Similarly, Poly(amidoamine) (PAMAM) dendrons were covalently attached to MWCNTs and dendron-MWCNT-Ag(0) hybrid materials were made afterwards which occurred via Ag(I) coordination to the PAMAM dendron nitrogen donors, followed by reduction with formaldehyde. Finally, non-covalent method was used to make thermo-sensitive water soluble CNTs. The homo(co)polymerisation of poly(ethylene glycol) methyl ether methacrylate (PEGMA) and di(ethylene glycol) methyl ether methacrylate (DEGMA) using a pyrene-containing initiator and a Cu(0)/Me_6-Tren catalyst system was investigated. The pyrene-functionalised polymers synthesised were then used to modify CNTs and thus thermo-sensitive water-dispersible CNTs were made.

4.2 Synthesis of PSt modified CNT and the formation of isoporous membranes

Isoporous films have attracted increasing attention as functional materials in various fields such as biotechnology[338,339] and photonics.[340] François *et al.*[341] discovered that highly-regular porous films were obtained, without the use of a template, when a solution of CS_2 and poly(p-phenylene)-block-polystyrene or polystyrene stars were cast under humid conditions. The proposed mechanism is shown in Figure 73. The evaporation of solvent leads to a decrease in solution temperature, and water droplets start to condense onto the solution surface. The stabilized water droplets will self-organize into a hexagonal array before the polymer precipitates around them. The precipitation of the polymer at the solution-water interface prevents droplet coagulation. When the solvent and water have evaporated, an ordered hexagonally packed polymeric structure will remain. The water droplets act as a sacrificial template for the ordered film.[342,343] The pore size can be tailored by changing the rate of the applied air flow, concentration of the cast solution, and humidity.[344-346] It has also been discovered that changes on the molecular level (molecular weight, polymeric compositions, and end-groups) will affect the characteristics of the film.[347] The range of polymers that are known to self-organize into macroporous membranes, has been extended from simple block copolymers to more complicated architectures such as comb and star-block copolymers.[348] Also, there is a report describing the formation of isoporous films by incorporation of nanoparticles into a polymeric matrix.[349]

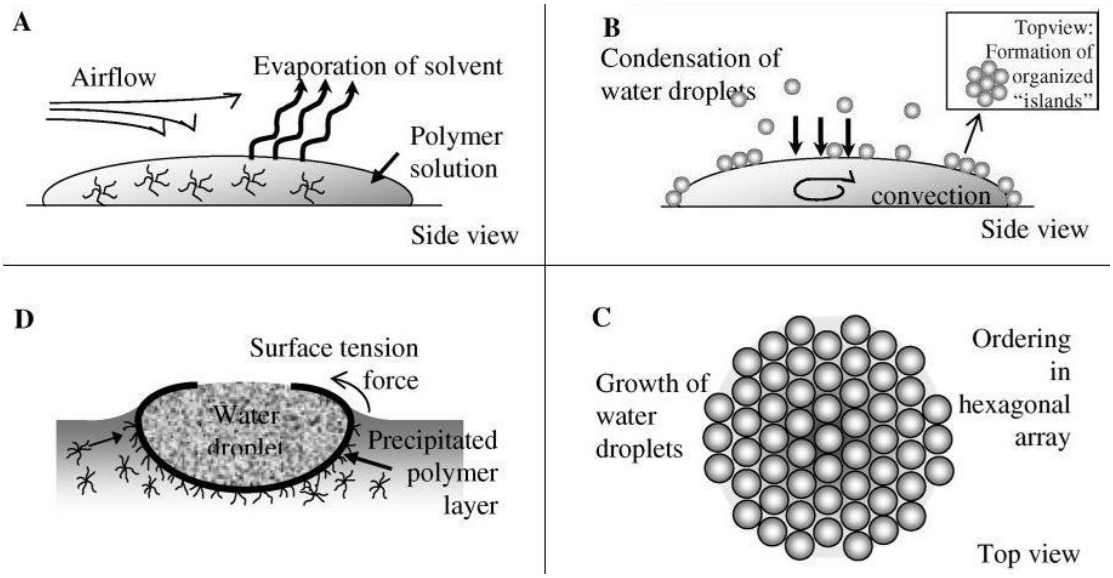

Figure 73. Proposed mechanism (Stenzel, M. H.; Barner-Kowollik, C.; Davis, T. P. J. Polym. Sci., Polym. Chem. 2006, 44, 2363-2375.) for the formation of honeycomb-structured porous films: (A) evaporation of the solvent of the polymer solution, (B) condensation of water droplets cause by the cold surface temperature of the solution, (C) formation of a hexagonal closest packing of water droplets on the solution surface, (D) precipitation of the polymer on the interface and prevention of coagulation.

The resulting organic-inorganic hybrid material, or nanocomposite, represents a new class of material that has attracted both industrial and academic interest. It is important that the nanoparticles are well dispersed, i.e., no aggregates, in the matrix to obtain optimum properties. One way to avoid particle aggregation is to modify the surfaces of the particles with polymers. Polymer chains, covalently attached to the particles, will separate the particles from one another and stabilize the dispersion. Silica particles, modified via grafting, have been used in nanocomposites and resulted in materials with better thermal stability and improved mechanical properties.[350-352] In addition, Nyström *et al.* successfully used the silica-polymer hybrid materials to form isoporous films.[353,354]

Here we focused on the fabrication of isoporous membranes based on polymer modified Carbon nanotube (CNT). This work describes fabrication of highly-ordered isoporous membranes based on polymer modified CNTs. Modification of the CNTs were performed via TMM-LRP, since well-defined polymer chains have proven to

facilitate the fabrication of membranes with monodisperse pore size.[348] The paper describes both the grafting of polymers from CNTs using TMM-LRP and the subsequent use of these hybrids to make highly ordered isoporous membranes. Optical characterization revealed that the membranes consisted of hexagonally ordered pores of uniform size. The combination of an open pore structure and high surface area makes isoporous membranes into materials of high interest in fields as biotechnology and photonics.

4.2.1 Synthesis of CNT-g-PSt through surface-initiated LRP

Commercially available multiwalled CNTs (MWCNTs) were treated initially with nitric acid to form carboxyl group at the CNTs surface, **(21)** then with thionyl chloride to give the corresponding acid chlorides **(22)**. The latter were then efficiently reacted with previously prepared 2-bromo-2-methyl-propionic acid 6-hydroxy-hexyl ester via ester linkages to give the expected MWCNTs supported initiator **(23)**. Grafting of styrene, from the functionalised CNTs, was then catalysed by Cu(I)Br and Bipy, and conducted at 110 °C to give **(24)**, Figure 74.

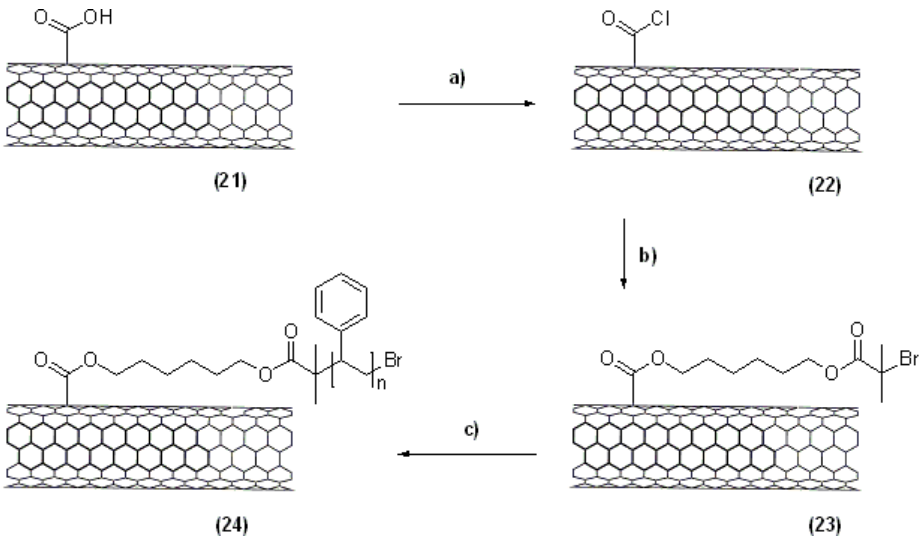

Figure 74. Synthesis of PSt modified CNTs. (a) $SOCl_2$; (b) 2-bromo-2-methyl-propionic acid 6-hydroxy-hexyl ester, toluene; (c) Styrene, Cu(I)Br/ Bipy, 110 °C.

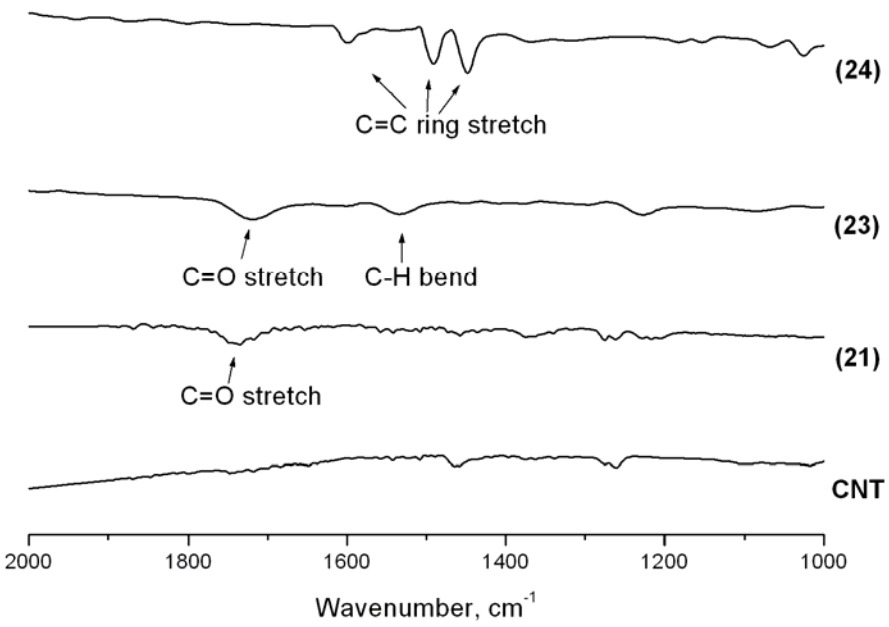

Figure 75. IR spectra of CNTs before and after modification.

The IR data of the native and functionalised CNTs are shown in Figure 75. Compared with the native CNT, a new peak assigned to the carboxyl group of **(21)** appeared at ~1736 cm^{-1} after reaction with HNO_3 acid indicating the surface of the CNT had been functionalised with a carboxyl group. According to the IR curve of the solid support initiator **(23)**, a shift of carbonyl stretch was observed at ~1720 cm^{-1} (C=O) and a peak at ~1530 cm^{-1} corresponding to the C-H bend was also observed, indicating a successful immobilisation of initiating groups. After the styrene was grafted from the CNT, peaks at ~1600 cm^{-1}, 1490 cm^{-1} and 1450 cm^{-1} from C=C ring stretch were observed in the IR curve of **(24)**.

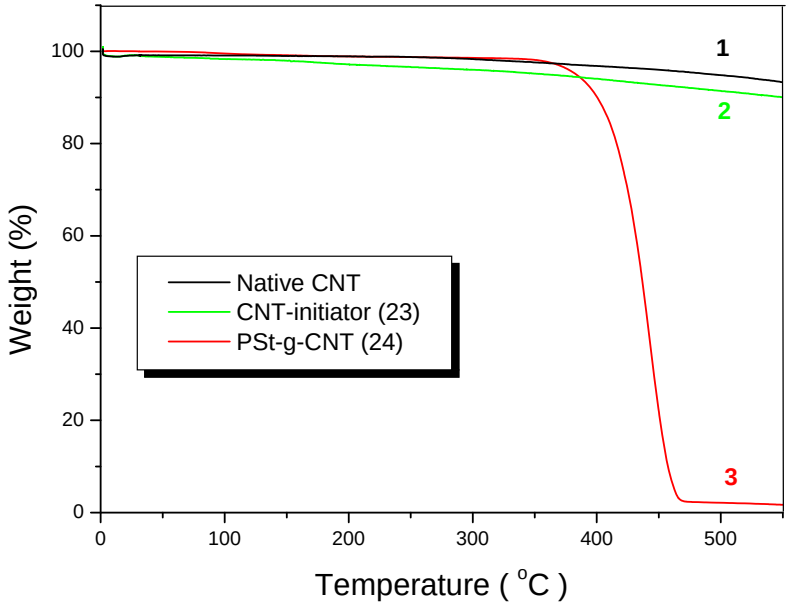

Figure 76. TGA traces of native and functionalised CNTs.

Thermal gravimetric analysis (TGA) of starting material CNT (curve 1) and modified CNTs has been carried out to better understand the composition. CNT-initiator **(23)** (curve 2) gave very similar results to CNT, with a weight loss of ~5% up to ca. 450 ºC. At the same temperature the PSt-g-CNT conjugate **(24)** (curve 3) showed ~98 % weight loss, which can be ascribed to the presence of the PSt grafted onto the nanotubes surface, Figure 76.

Transmission electron microscopy (TEM) images of the CNTs before and after the modification with PSt are shown in Figure 77. Grey layers around CNTs, attributing to polystyrene grafted from the nanotubes, were observed for **(24)**, further proves the successful modification of polymers onto CNTs through surface-initiated LRP.

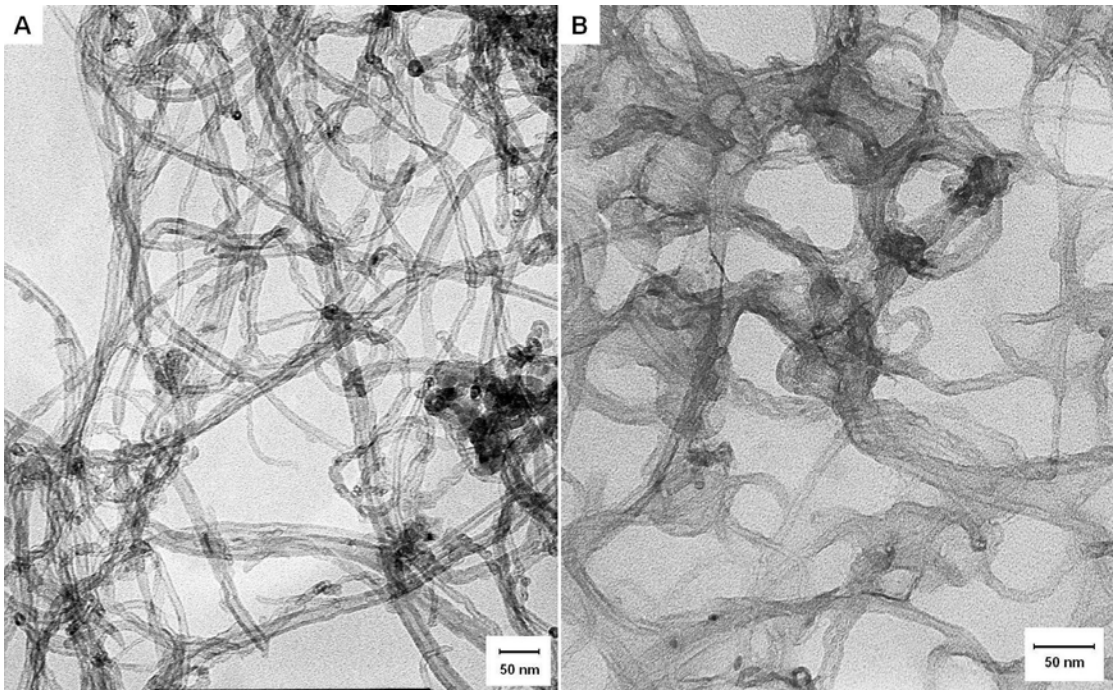

Figure 77. TEM of MWCNTs before and after modification. A: CNT-COOH, (21); B: PSt-g-CNT, (24).

The PSt-g-CNT (24) was dissolved in THF and the grafted PSt-chains were further cleaved from the MWCNTs with KOH/ethanol in THF under reflux for three days. The cleaved chains were precipitated in MeOH and then analysed with SEC, Figure 78. The molecular weight of the cleaved polymer is 117000 with a PDi value of 1.71, indicating that the surface initiated ATRP was carried out in a controlled manner.

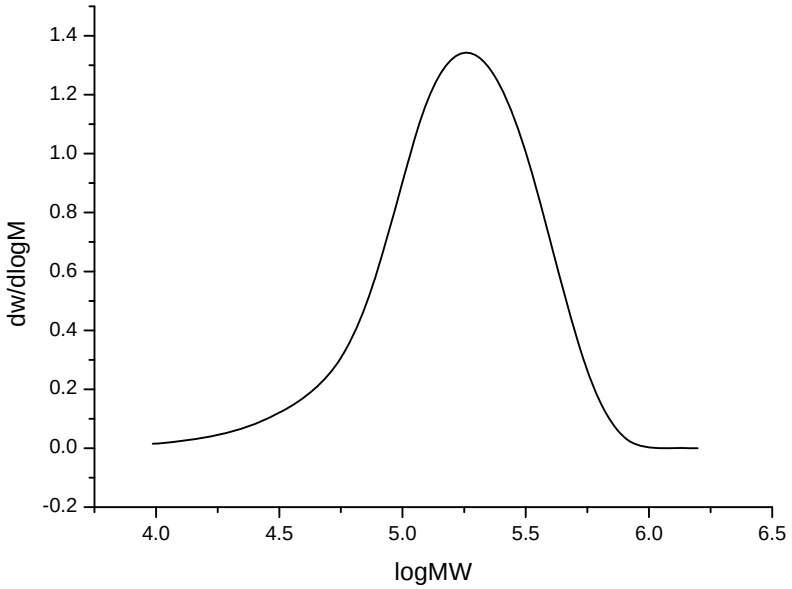

Figure 78. SEC trace of the PSt chains cleaved from the CNTs.

4.2.2 Isoporous Membranes

The PSt-modified CNT was cast from $CHCl_3$ to yield isoporous membranes. Once the film was cast, the volatile solvent started to evaporate immediately causing the temperature at the film surface to decrease. This causes water droplets from the humid environment to condense onto the film surface. The PSt-modified CNT starts to precipitate at the water/solvent interface resulting in stabilized water droplets. When the solvent had evaporated an opaque/grey film was obtained. An image obtained from optical microscope clearly reveals the arrangement of the close-packed pores into a hexagonal array, so-called honeycomb structure with a pore size of approximately 7 microns, Figure 79.

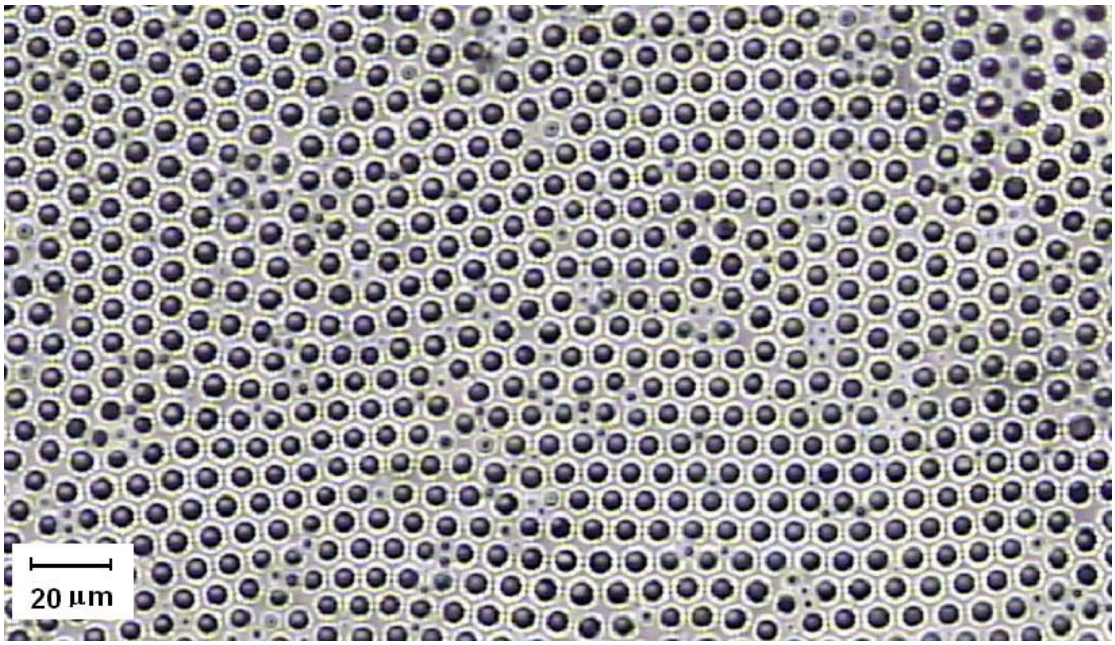

Figure 79. Image from optical microscope of hybrid nanoparticle membrane of PSt-g-CNT.

A SEM image of the cross-section revealed that only one layer of pores is formed when $CHCl_3$ is used for casting, this is indeed in agreement with the literature, Figure 80. The solvent is an important parameter for the fabrication of porous films of high quality. Attempts were made to cast films using CS_2 as solvent, however the resulting films consisted of non-close packed pores with low ordering.

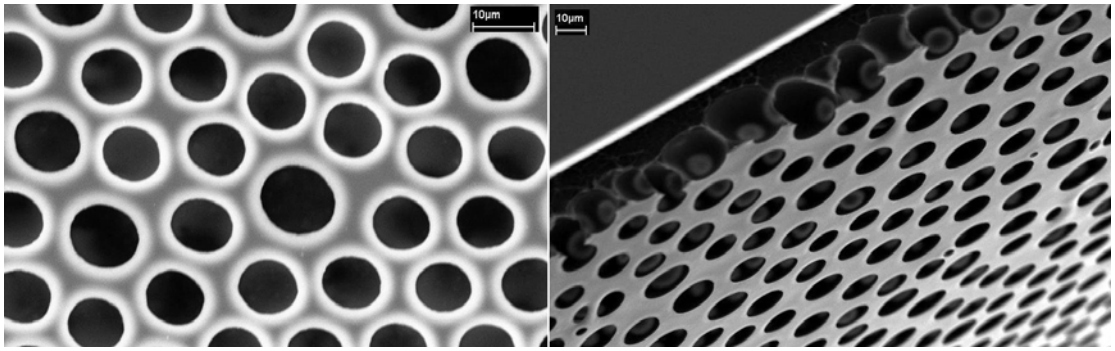

Figure 80. FE-SEM images of the hybrid nanoparticle membrane of PSt-g-CNT.

The porous membrane was further analysed with AFM. The characterization revealed the 3-D structure of the pores, Figure 81. The depths of the pores is ~6.8 μm. The combination of an open pore structure and isoporous nature (high surface area), makes honeycomb film into materials of high interest in applications such as membranes.

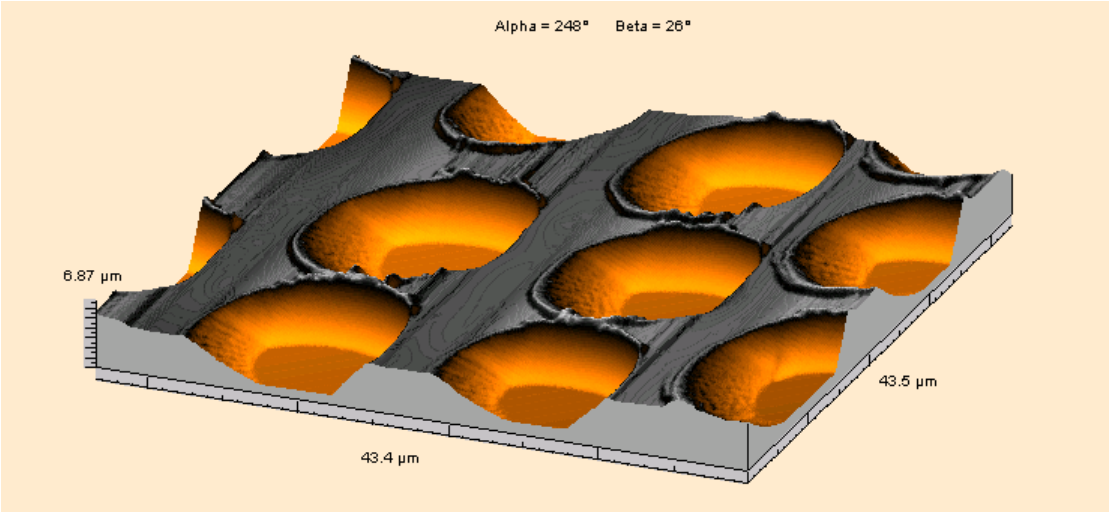

Figure 81. AFM image of the hybrid nanoparticle membrane of CNT-g-PSt.

In conclusion, this work has demonstrated that new systems based on polymer modified CNT hybrid materials can be used for the formation of isoporous films. A single layer of pores with a pore size of approximately 7 microns was formed, consisting of CNTs modified with PSt chains via surface-initiated LRP.

4.3 Synthesis of Poly(amidoamine) (PAMAM) dendron modified CNT and its metal templating[355]

The PAMAM dendrimers, the first synthesized dendrimer in the dendrimer family, have been utilized in different fields since it was synthesized by Tomalia *et al.* in 1985[356,357]. As a cationic polymer, the PAMAM dendrimer is compatible well with anionic materials such as DNA, thus they have been employed in pharmaceutical field as gene delivery reagents[358-362]. Using the PAMAM dendrimer as template, various dendrimer-coated nanoparticles with small size, narrow distributives have been prepared, such as Au[363-365], Pd[366-368], Pt[369-371], Pt/Pd[372], Pd/Au[373,374] and iron oxide[375]. Due to their structures are similar to natural proteins, PAMAM dendrimers are also employed as protein/enzyme mimic[376,377]. In this part, a hydroxyl terminal PAMAM dendron (A dendrimer that radiates from fewer than all of its branch points at the core, often half a dendrimer, Figure 82) was synthesised, the effort to modify the surface of CNTs with this PAMAM dendron will be discussed.

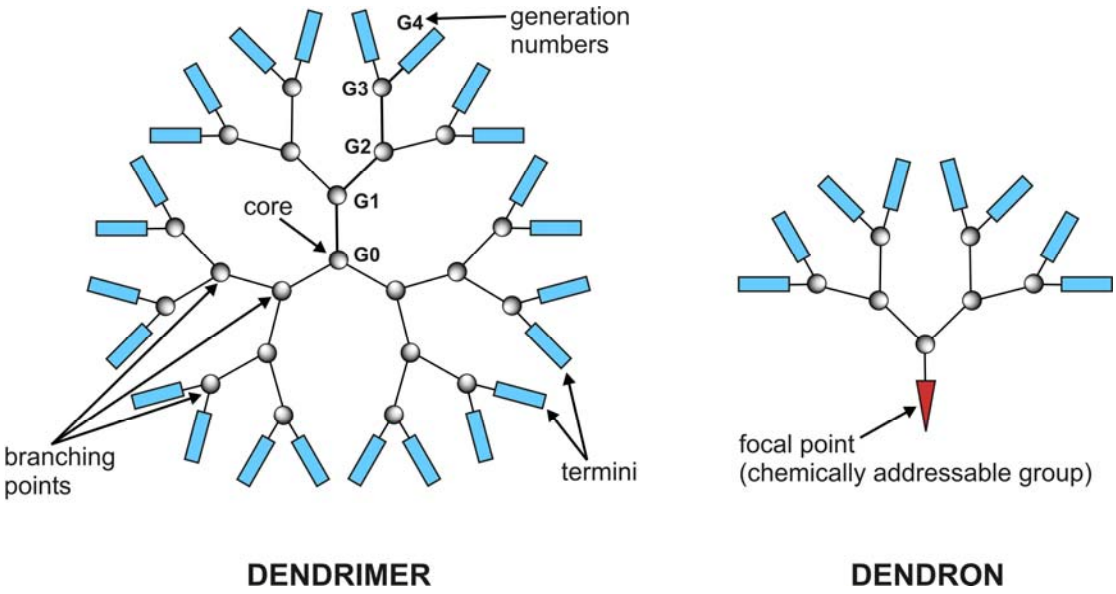

Figure 82. Scheme (copied from http://en.wikipedia.org/wiki/Dendrimer) of dendrimer and dendron.

4.3.1 Synthesis of hydroxyl terminal PAMAM G3.5 dendron

The hydroxyl α-functionalized PAMAM dendron was designed and prepared, the synthesis routes are shown in Figure 83.

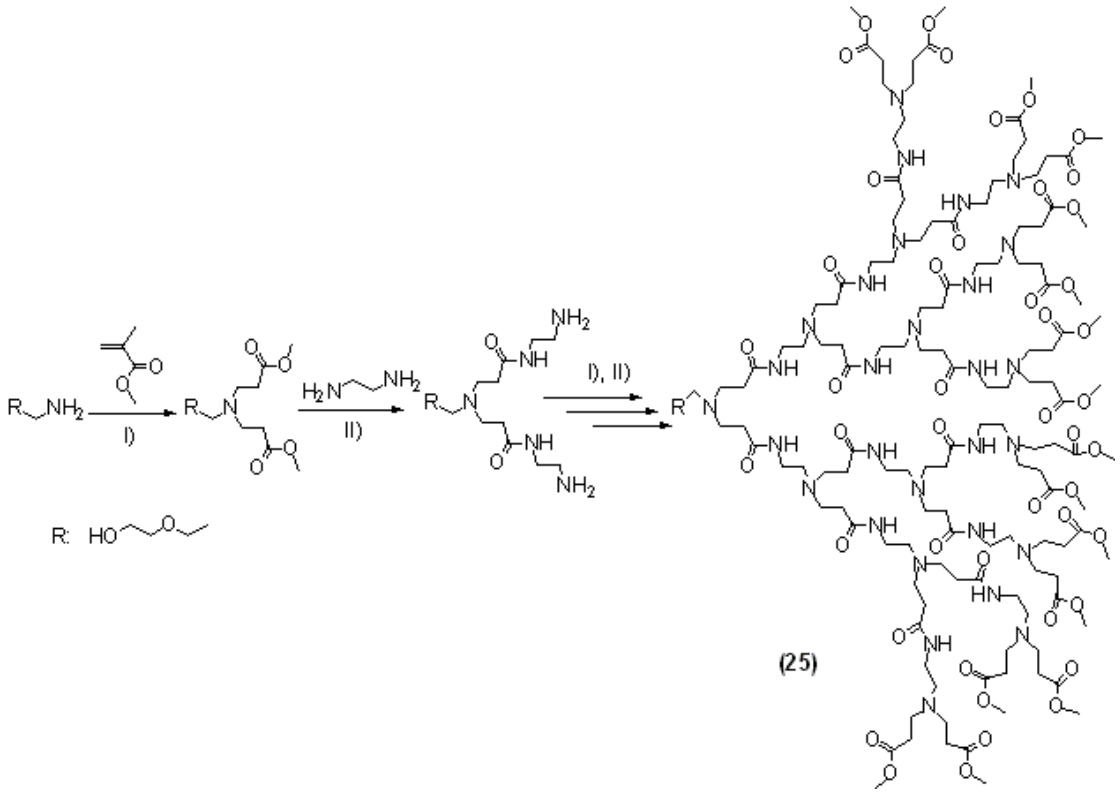

Figure 83. Synthesis of α-functional PAMAM dendron.

2-(2-Amino-ethoxy)-ethanol was employed as initiator to prepared PAMAM dendron. The Michael addition reaction occurred when the amines reacted with methyl acrylate (MA) to form branched ester, the ester bond was replaced when the amination reaction was carried out with large excess of ethylene diamine. The reactions were repeated and the target α-functional PAMAM dendron was obtained. The hydroxyl-terminated dendron was then utilized to modify the surface of multi-wall carbon nanotubes.

The ^{1}H NMR spectrum of the hydroxyl terminally functional PAMAM dendron is shown in Figure 84.

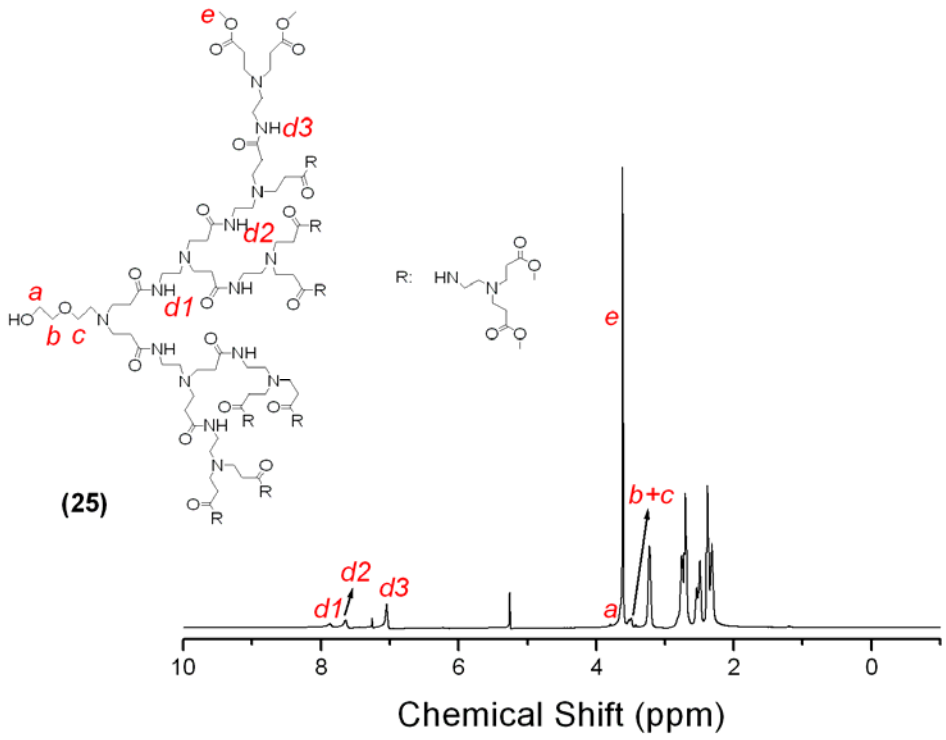

Figure 84. ^{1}H NMR spectrum of hydroxyl terminal PAMAM G 3.5 dendron.

The peaks of two methylene group by the ether oxygen mixed together and appeared as peak b and c in Figure 84, with the peripheral ester methyl groups appearing as a single peak (peak e in Figure 84) at 3.62 ppm. The integration ratio of (b+c)/e gives 4/48, in agreement with the theoretical value, which indicates that the alcohol terminated PAMAM dendron has been synthesized.

4.3.2 Modification of MWCNT surface with PAMAM dendron and metal templating

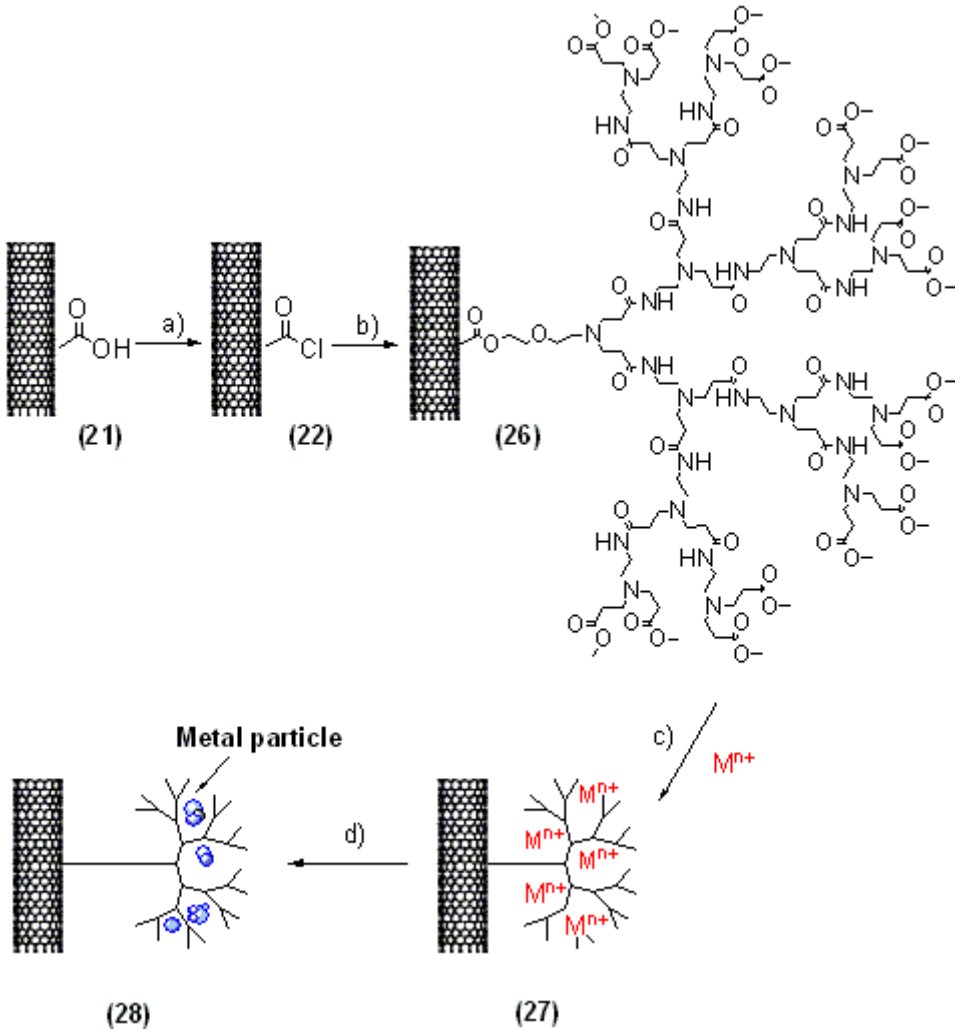

Figure 85. Synthesis of PAMAM dendron modified MWCNT and dendron-MWCNT-Ag(0) hybrid materials. Reagents and conditions: a) thionyl chloride, toluene; b) (25), toluene; c) $AgNO_3$ aqueous solution; d) formaldehyde solution.

MWCNT modified with carboxyl groups, **(21)**, was easily transferred to be the highly reactive carboxyl chloride by reacting with thionyl chloride. The HO-PAMAM dendron **(25)** was then mixed with **(22)**, a PAMAM dendron modified CNT **(26)** was thus formed through the ester-bond that linked the PAMAM dendron on the surface of MWCNT. The process was outlined in Figure 85.

Direct detection of the dendrons grafted at the MWCNT's surface using TEM microscopy had proven to be problematic, probably due to the relatively small

dendron size. We reasoned that the deposition of appropriate metal particles onto the CNTs surface using dendron molecules as template could have furnished a direct observable proof of the presence of dendron at the nanotubes surface, and at the same time highlighted the potential of these hybrid materials to act as starting materials for the preparation of more complex nano-materials. Addition of a reducing agent such as formaldehyde to a PAMAM dendron **(25)** /$AgNO_3$ solution led to the precipitation of Ag(0) particles in less than three seconds. The test was then repeated using the PAMAM-MWCNT's conjugate **(26)** instead of the unmodified dendron, Figure 85.

Thermal gravimetric analysis (TGA) of MWCNT starting material (curve 1) and MWCNT-COOH **(21)** (curve 2) gave very similar results, with no significant weight loss up to ca. 400 ºC. At the same temperature the MWCNT-PAMAM conjugate **(26)** (curve 3) showed 39 % weight loss, which can be ascribed to the presence of the dendron grafted onto the nanotubes surface, Figure 86. As expected the Ag(0)-containing material **(28)** (curve 4) showed a profile analogous to that of the unmodified conjugate **(26)**, with lower weight loss percentage, consistent with the lower dendron content of this material, due to the presence of an estimate 23 % weight content of Ag(0).

The IR dates of the native and functionalised MWCNTs are shown in Figure 87. Compared with the native MWCNT, a new peak attributed to the carboxyl group appeared at ~1736 cm^{-1} after reaction with HNO_3 acid indicating the surface of the MWCNT had been functionalised with a carboxyl group. According to the IR curve of the MWCNT-dendron **(26)**, the peak at ~1740 cm^{-1} became more intense and the peak at ~1640 cm^{-1}, from the amido band of the dendron was observed.

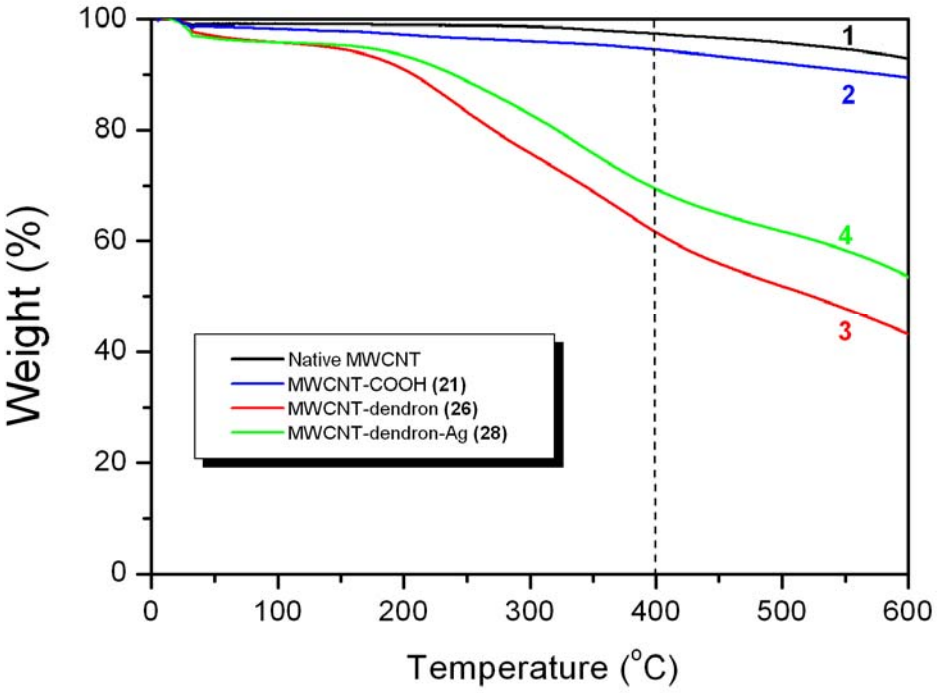

Figure 86. TGA curves of native and functionalised MWCNT.

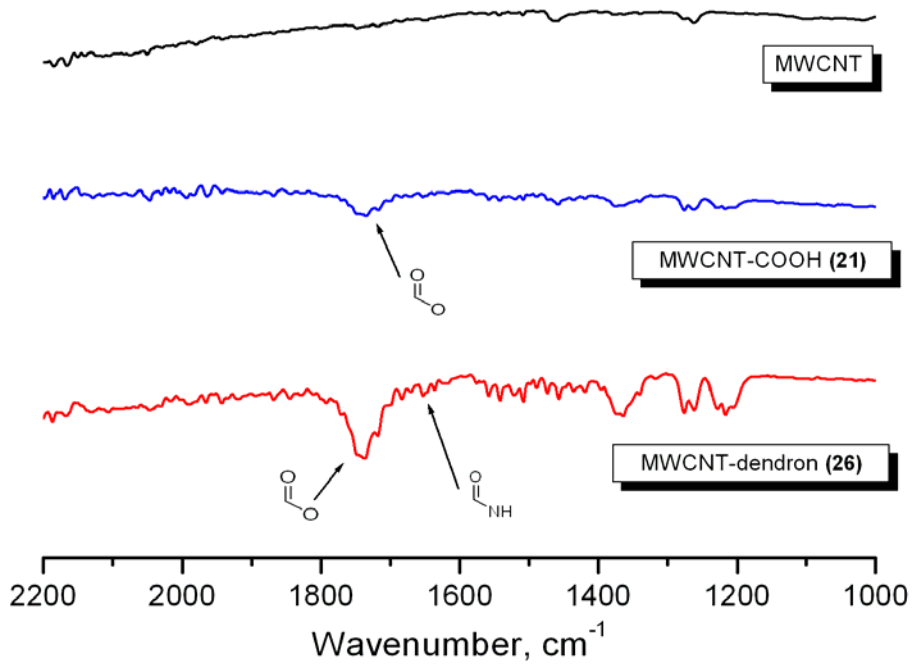

Figure 87. FTIR of native and functionalised MWCNTs.

Field-Emission Scanning Electron Microscopy (FE-SEM) provided further insights on the hybrid conjugates features, highlighting the differences between native and functionalised MWCNTs, Figure 88. Ag(0) can be observed at the surface of MWCNT-dendron conjugate, indicating the formation of nanoparticles via Ag(I) coordination to the PAMAM dendron nitrogen donors, followed by reduction with formaldehyde.

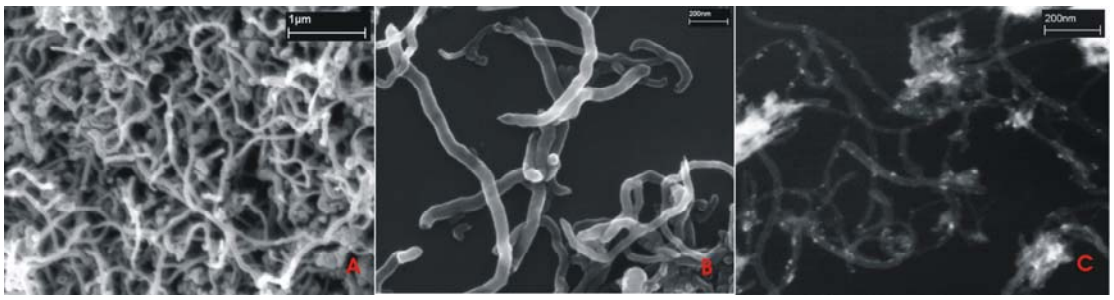

Figure 88. FE-SEM images of native and functionalised MWCNTs. A. native MWCNTs; B. MWCNT-dendron (26); C. MWCNT-dendron-Ag (28).

Transmission electron microscopy (TEM) images of the MWCNTs before and after the modification with the hydroxyl-terminated PAMAM are shown in Figure 89. Ag(0) could only be detected at the surface of MWCNT-dendron conjugate, Figure 89D. No silver deposition was observed either in the background, Figure 89D, or when MWCNT-COOH **(21)** was employed, Figure 89C, which is in agreement with the proposed mechanism that the formation of nanoparticles via Ag(I) coordination to the PAMAM dendron nitrogen donors. The nature of the observed particles was confirmed by energy-dispersive spectroscopy (EDS), peak at 3.0 KeV in Figure 89E.

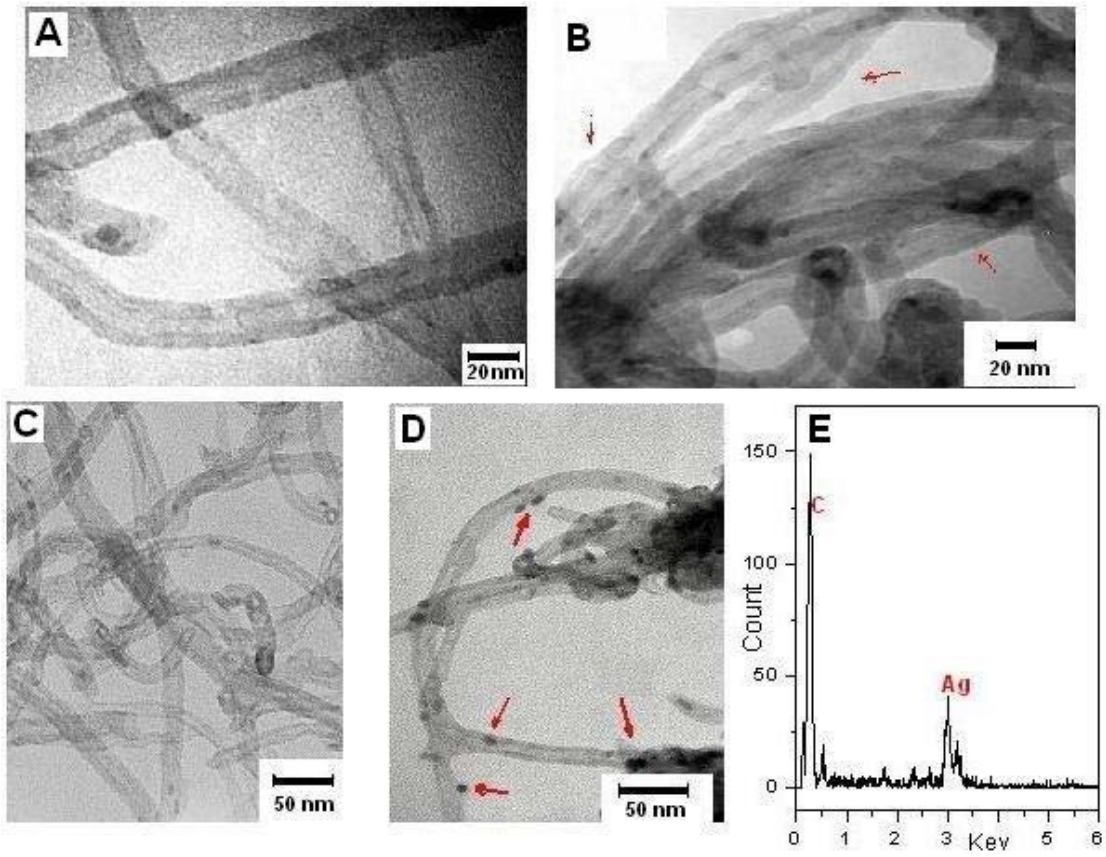

Figure 89. TEM of MWCNTs and EDS dates: A) native MWCNTs; B) MWCNT-dendron (26); C) Control: MWCNT-COOH (21) + $AgNO_3$ + CH_2O; D) MWCNT-dendron-Ag (28); E) the EDS spectrum of (28).

In conclusion, the hydroxyl-terminated dendrons have been successfully linked to MWCNTs via ester linkages. The corresponding MWCNT-dendron conjugates have been characterized by FT-IR, TGA, FE-SEM and TEM. In addition these hybrid materials have been employed as templates for the deposition of Ag(0) nanoparticles, via dendron coordination of Ag(I) ions, followed by reduction with formaldehyde. Silver particles were clearly visible on the nanotubes surface by FE-SEM and TEM analysis.

4.4 Thermo-responsive water-dispersible CNTs.

The design of materials that exhibit 'bio-like' behaviour, such as a response to a stimulus or environment has attracted increasing interests, due to its potential applications, especially in the biological field. Responsive polymers are one of the materials that have been investigated intensively with different types of switching properties, such as responsive to light, pH, heat and biochemical stimuli. [114,378-389] Among them, thermo-responsive polymer is one of the hit subjects being investigated in nano-technology and biotech applications. [380,385,390] Poly(N-isopropylacrylamide) (PNiPAM), exhibiting a lower critical solution temperature (LCST), is the most common polymer used as a responsive water-soluble polymer and has potential applications in different biomedical fields. [28,384,391-393] Poly(ethylene glycol) (PEG) is a cheap, neutral, water-soluble, biocompatible, FDA-approved polymer and one of the most applied synthetic polymer in the biomedical field, and recently interest has been raised on PEG in terms of thermo-responsive water-soluble property. [204-206] Lutz and co-workers reported that copolymers of tuneable LCST (26-90˚C) could be obtained by changing the ratio of the long chain-length Oligo(ethylene glycol) Methacrylate and shorter chain-length 2-(2-Methoxyethoxy)ethyl Methacrylate.[204,206] This is rather attractive in applications with variable temperature requirements.

Transition metal medicated living radical polymerisation (TMM-LRP, often termed ATRP) is one of the most promising methods to prepare well-defined polymers.[94,95] The most widely used recipe includes a halides initiator, copper(I) salt and a ligand. AGET (activators generated by electron transfer) ATRP was then reported by Matyjaszewski *et al*., using tin(II) 2-ethylhexanoate ($Sn(EH)_2$)[96] or ascorbic acid[97] to reduce Cu(II) to Cu(I), which could then catalyse ATRP under appropriate

polymerisation conditions. However robust, the mechanism of TMM-LRP is still under debate. The most widely accepted mechanism believe that the polymerisation proceeds by an inner-sphere electron-transfer mechanism in which a low oxidation state metal complex acts as the catalyst, mediating a fast exchange between radicals and their dormant alkyl halide species. However, out-sphere mechanism in which copper(I) disproportionate into Cu(II) and Cu(0), and then Cu(0) act as electron donors and the initiator and dormant propagating species act as electron acceptors is favoured under certain conditions, especially in polar solvents in the presence of N-ligands. Recently, Single-electron transfer (SET)-LRP has raised more interest, after being reported by Percec and co-workers.[100,394] This polymerisation normally uses zero valent copper power/wire as the catalyst, in polar solvents and in the presence of N-ligands, and can be carried out under very mild reaction conditions, at room temperature, using a small amount of catalyst and generates polymers with high molecular weight with ultra-fast rates.

PEG or MEO are widely used monomers in ATRP and are polar in nature. Therefore the polymerisation of PEG-MA is supposed to favour SET-LRP without even adding additional polar solvent. Will PEG-MA facilitates the SET-LRP and will the polymerisation still be controllable? We investigate the behaviour of the homo(co)polymerisation of poly(ethylene glycol) methyl ether methacrylate (PEGMA) and di(ethylene glycol) methyl ether methacrylate (DEGMA) using a pyrene-containing initiator and a Cu(0)/Me_6-Tren catalyst system. As pyrene containing polymers (materials) are often used to non-covalently modify carbon nanotubes as a non-destructive strategy, [315-318,395] we could then make a water-dispersible carbon nanotube, which is of great interest for their possible bio-applications by modification with different materials including natural products, water-soluble polymers and

dendrimers.[310,355,396-400] Through this non-covalent side-wall functionalization strategy, the pyrene-functionalised polymers synthesised were used to modify carbon nanotube and thus thermo-sensitive water-dispersible carbon nanotubes were made, Figure 90.

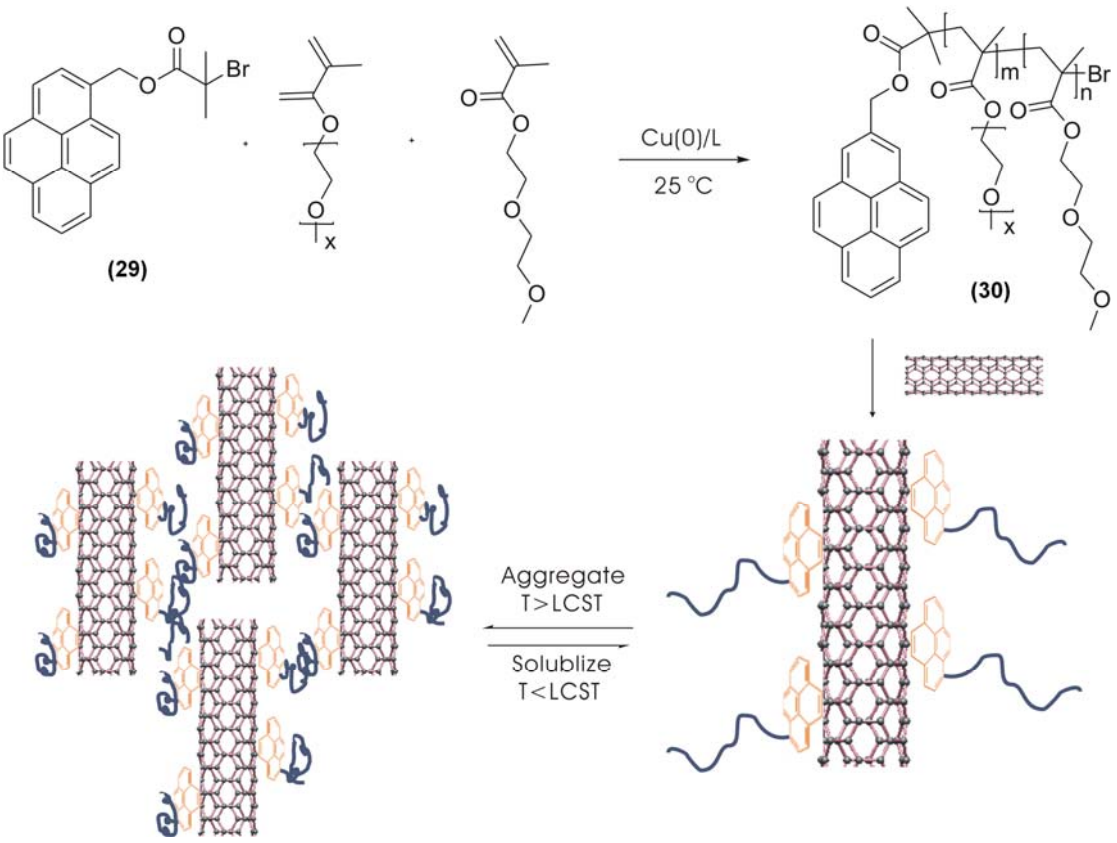

Figure 90. Synthesis of pyrene-terminal copolymer by SET-LRP and preparation of thermo-sensitive water-soluble CNTs.

4.4.1 Synthesis of pyrene-terminal copolymer by SET-LRP.

4.4.1.1 Synthesis of pyrene initiator (29)

In order to make pyrene containing polymers for non-covalent modification of CNTs through π-π stacking, a pyrene initiator has been synthesised. The synthesis proceeded

via coupling of 1-pyrenemethanol and 2-bromopropionic bromide in dichloromethane. The final product was further purified by recrystallization in methanol, Figure 91.

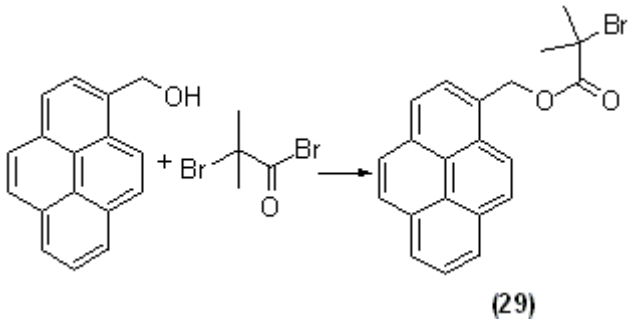

Figure 91. Synthesis of the pyrene initiator.

4.4.1.2 (Co)Polymerisation of PEGMA and DEGMA

Homopolymers and copolymers of PEGMA475 and DEGMA with pyrene-terminal functionality have been obtained using SET-LRP technique, where a copper(0) powder/Me_6Tren catalyst system has been used to carry out the polymerisation at 25°C. Table 10 lists the (co)polymers synthesized with different compositions and molecular weights, together with their variable LCSTs.

Table 10. Summary of molecular characteristics of the SET-LRP synthesized (co)polymers employed as stabilizing species.

polymer	Composition [a] (PEGMA:DEGMA)	$M_{n,SEC}$ [b]	$M_{n,NMR}$ [c]	$M_{n,th}$ [d]	PDi [b]	LCST [e]
30	0:1	32,300	20,700	19,200	1.21	29
31	1:9	32,600	21,500	22,100	1.53	45
32	1:0	60,100	49,100	47,900	1.75	91

[a] Initial ratio of monomer. [b] Measured by SEC in THF, with MMA standards. [c] Determined by ^{1}H NMR in $CDCl_3$. [d] Calculated using equation $M_{n,th} = DP \times MW_m + MW_i$, where DP is 100, MW_m is the (average) molecular weight of (co)momomer and MW_i is the molecular weight of initiator. [e] Measured by Varian Cary 100 UV-Vis spectrophotometer with temperature controller.

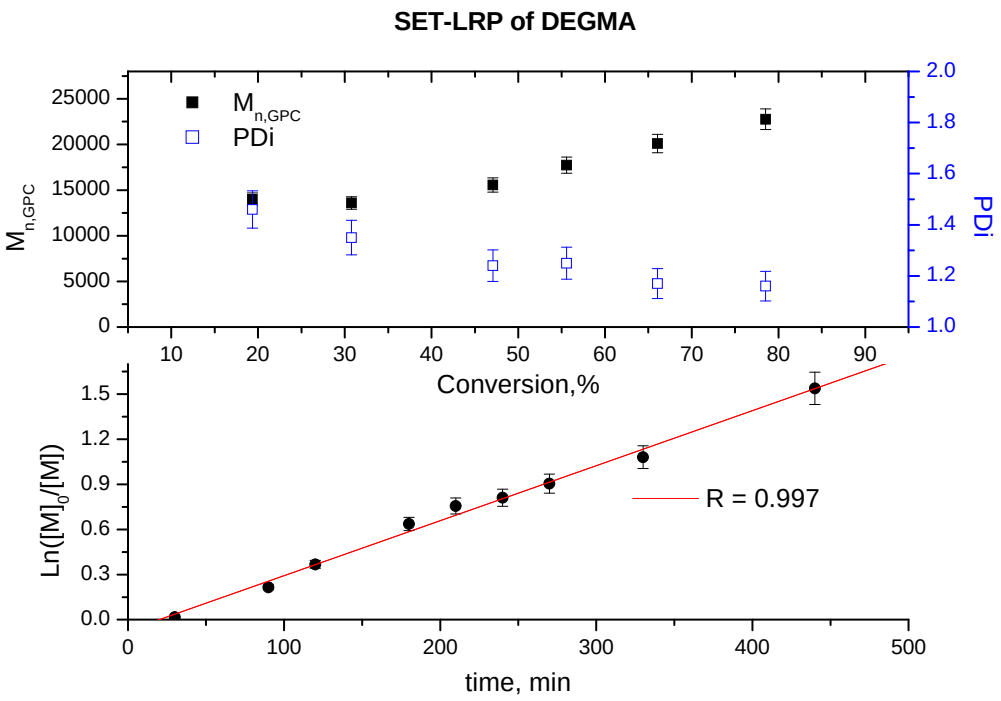

Figure 92. Semilogarithmic kinetic curves and Mn, PDi vs. conversion curves for the SET-LRP of DEGMA. Reaction conditions: $[DEGMA]_0 : [I]_0 : [Cu(0)]_0 : [L]_0 = 100: 1: 1: 1$, 25°C.

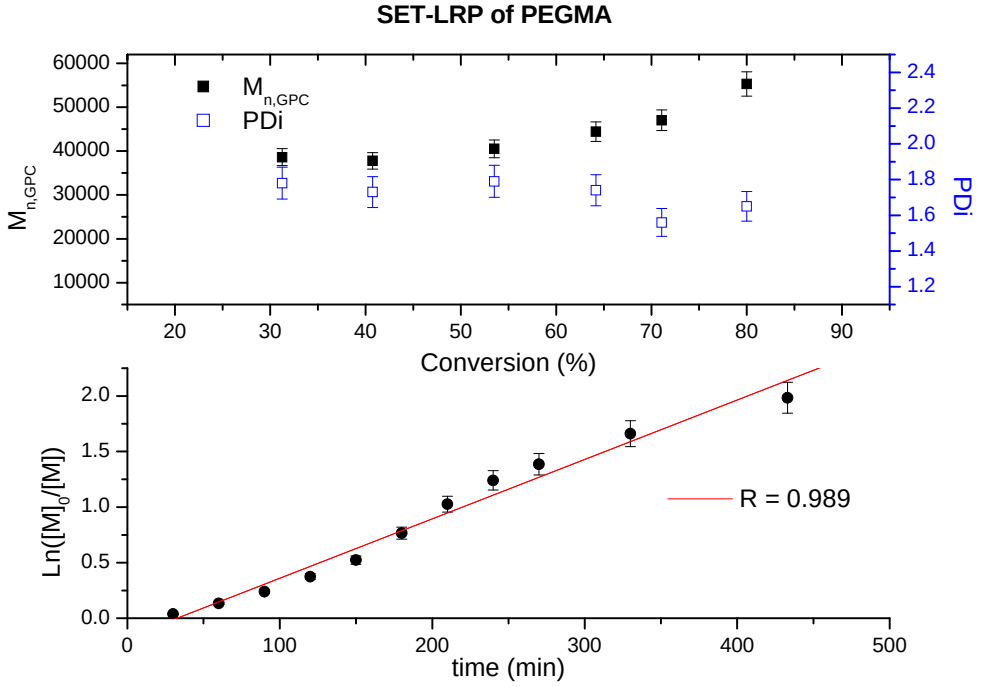

Figure 93. Semilogarithmic kinetic curves and Mn, PDi vs. conversion curves for the SET-LRP of PEGMA. Reaction conditions: $[PEGMA]_0 : [I]_0 : [Cu(0)]_0 : [L]_0 = 100: 1: 1: 2$, 25°C.

The kinetic plots of the homo-polymerisation of DEGMA and PEGMA with the pyrene initiator are shown in Figure 92 and Figure 93, respectively. Linear fit lines were drawn in both cases, although it is slightly slow at the beginning and an introduction period is observed in both cases, which may be due to the heterogenous nature of the catalyst system. At the beginning the amount of Cu (0) dissolved in the system is smaller, therefore an introduction period is observed and the PDi is also higher at the beginning. The molecular weights increase with conversion in both cases, although the PDi of the polymers is slightly high, around 1.3 for DEGMA and around 1.7 for PEGMA.

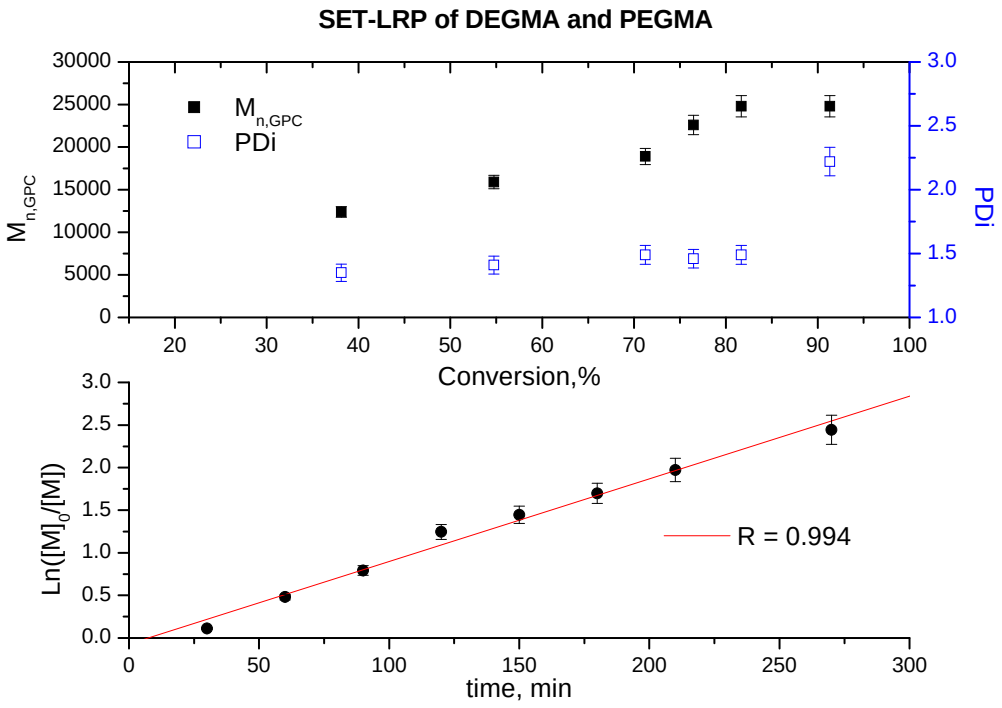

Figure 94. Semilogarithmic kinetic curves and Mn, PDi vs. conversion curves for the SET-LRP of PEGMA and DEGMA. Reaction conditions: $[PEGMA]_0 : [DEGMA]_0 : [I]_0 : [Cu(0)]_0 : [L]_0 = 10 : 90 : 1 : 1 : 2$, 25˚C.

The SET-LRP behaviour of the copolymerisation of PEGMA and DEGMA has also been investigated and shows living nature as well. The first order kinetic is linear, and as the conversion increases, the molecular weight of the copolymer increases as well, although the PDi is slightly high (~1.5), Figure 94.

A typical ^{1}H NMR of the pyrene polymer (**31**) is shown in Figure 95. The peak at ~8 ppm (peak ***a***) corresponds to the protons on the pyrene ring, the peak at 4.1 ppm (peak ***b***) is the -OCH_2 of the PEGMA and DEGMA chain, with the ratio of the integrations, $(4 \times I_{4.0}) / (2 \times I_{2.8})$, the number of the repeat unit (DP) on the main chain can be obtained, and therefore the average molecular weight can be calculated.

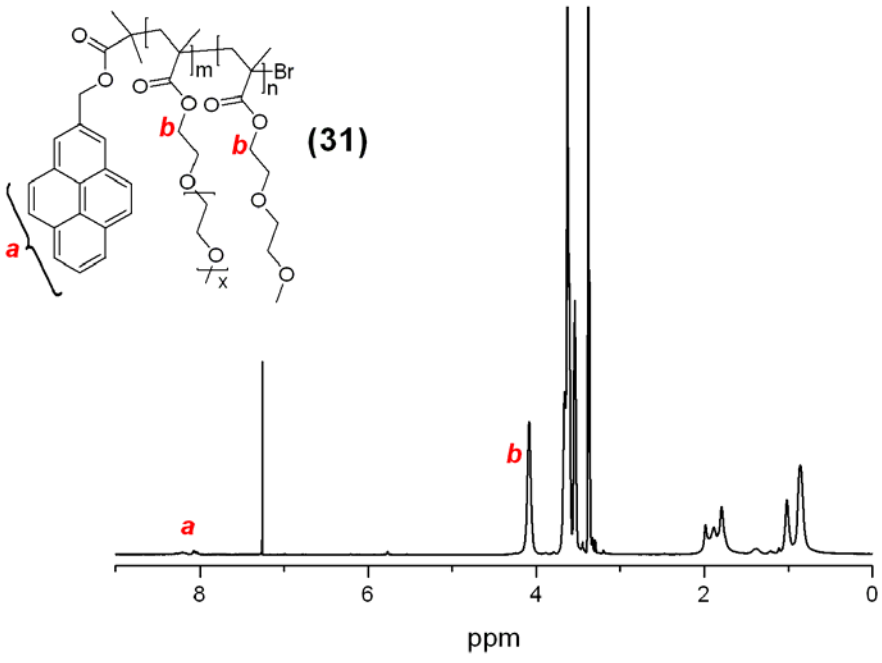

Figure 95. ^{1}H NMR spectrum of pyrene-containing PEG copolymer (Polymer 31).

4.4.2 Non-covalent modification of CNTs with pyrene-terminal polymers

All the results show that ethylene glycol methacrylate favours SET-LRP without adding polar solvents and a fast polymerisation rate is obtained at room temperature. Cloud points (LCSTs) of these polymers have been measured using Varian Cary 100 UV-Vis spectrophotometer with temperature controller. Results are summarised in Table 10. Actually, LCST with any temperature between 29°C to 91°C can be made by modifying the ratio of these two monomers. Polymer **31** was chosen to test its ability to solubilize carbon nanotubes. Non-covalent sidewall functionalization was carried out by mixing MWCNTs with polymer **31**. According to reports that the ratio of polymer to CNTs wt ($R_{initial}$) must be at least 2 for observing stable dispersions using pyrene-containing polymers[317]. A $R_{initial}$ of 5 was used here to stablize the MWCNTs in water. After a short sonication, a stable dispersion of MWCNTs is observed, Figure 96B, when this solution was heated above the LCST of polymer (60°C in this case), the solution became cloudy and carbon nanotubes begin to aggregate and start to precipitate, Figure 96C. After cooling the vial to a temperature under LCST of polymer **(31)**, the MWCNTs can be redispersed again, although agitation is required. Furthermore, the modified nanotubes were recovered by centrifuge and washed with water several times in order to eliminate the copolymer excess. The recovered polymer modified MWCNT can form stable dispersions in water at room temperature, which confirms the π-π stacking results in the strong adsorption of pyrene moiety with MWCNT. The grafting ratio (GR), defined as the mass ratio of grafted polymer to nanotubes, was estimated by TGA and found to be in the 0.35-0.45 ranges. The MWCNT-(**31)** solution was also tested using UV-Vis spectrophotometer after diluted to a concentration of 0.05 mg/mL, as seen from Figure 96A, the same pattern is observed with polymer **31** solution, except a slight

shift to the right (higher temperature). In addition, the absorbance of MWCNT-**(31)** is more than 0 even at the beginning, this is due to the existence of MWCNTs in the solution, as the absorbance of polymer **31** solution is set to zero. TEM further confirms the successful adsorption of the pyrene-functional polymers onto carbon nanotubes, as a clear polymer layer could be observed around the MWCNT, Figure 96D.

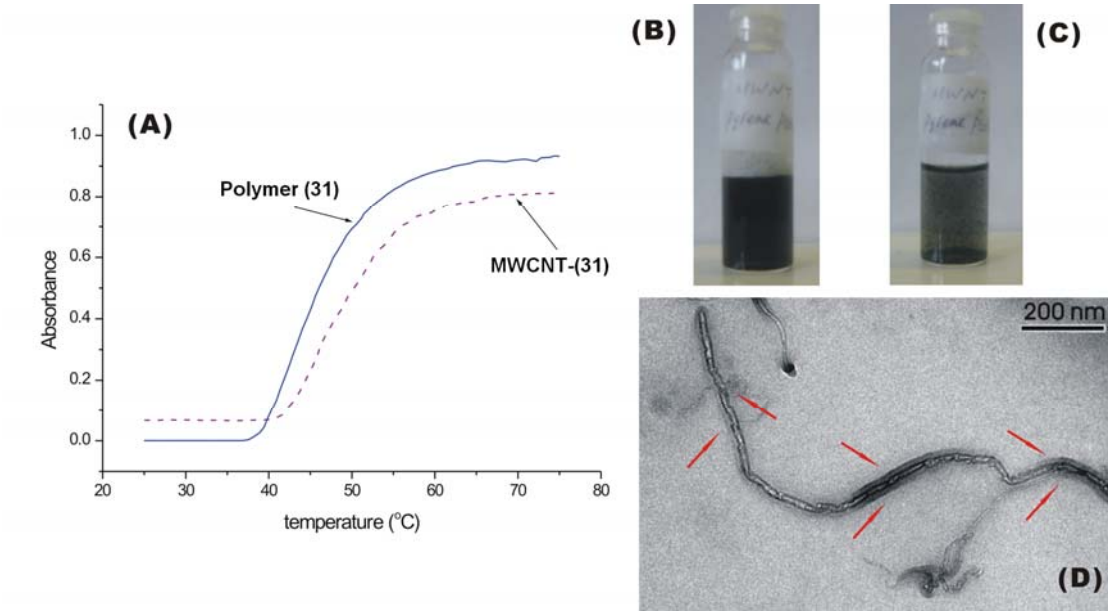

Figure 96. Plots of absorbance as a function of temperature measured for aqueous solutions (3mg/mL) (A) of polymer 31 and polymer 31 modified MWCNTs; Polymer 31 modified MWCNTs dispersed in water at ambient temperature (B) and after heated to 60°C (C); TEM of polymer 31 (D).

Control experiment has also been carried out using the procedure mentioned above. 5.0 mg of Polymer **31** (control A), a non-pyrene-containing PEGMA-DEGMA copolymer (Polymer **33**, made by ATRP using methyl 2-bromopropionate as an initiator, Mn = 21,970, PDi = 1.37) (control B) or a mixture of 1-pyrenebutyric acid and sodium hydroxide (control C) were dissolved in water, and 1.0 mg of MWCNT

were then added to the solution. After 5 minutes of sonication, both A and B have a good dispersion, while C cannot disperse MWCNT well. After overnight, control A still has a good dispersion and MWCNTs in B started to aggregate and precipitate. Figure 97 shows the result after 5 days. It shows clearly that the pyrene-terminal polymer has a good dispersion ability of MWCNT, polymer **33** has certain extend of dispersant ability for carbon nanotubes in water, but after some time, the nanotubes start to aggregate and precipitate, while for small pyrene molecules, it can not disperse carbon nanotubes in water.

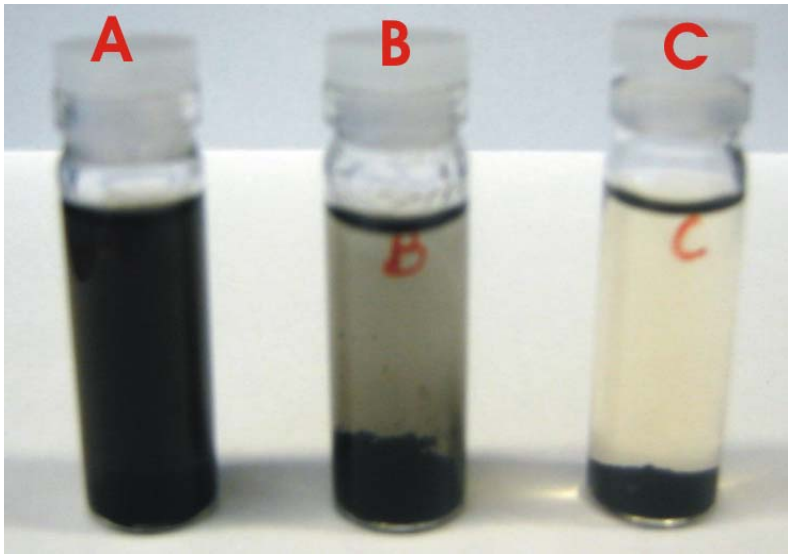

Figure 97. The control experiments of dispersing MWCNTs in aqueous solution after 5 days: A) polymer 31; B) non-pyrene polymer 33; C) 1-pyrenebutyric acid + NaOH.

The modified nanotubes were recovered by centrifuging and washing with water several times in order to eliminate the unattached polymer. The modified nanotubes were collected, dried and analysed by TGA. Trace A in Figure 98 was recorded for the control MWCNTs, which are stable until 550˚C with negligible weight loss, whereas trace B shows that polymer **31** is completely degraded at 500˚C range. The

polymer **31** modified MWCNTs show a ~40% weight loss (trace B) at the same temperature as polymer **31**. The grafting ratio (GR), defined as the mass ratio of grafted polymer to nanotubes, was then estimated to be in the 0.35-0.45 ranges.

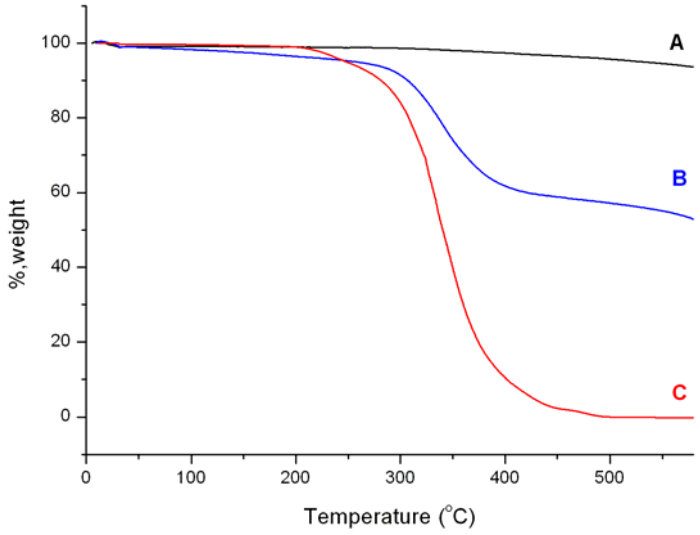

Figure 98. TGA traces for (A) MWCNT (black line); (B) Polymer 31 modified MWCNT (blue line) and (C) pure Polymer 31 (red line).

In conclusion, SET-LRPs of $PEGMA_{475}$ and DEGMA have been successfully carried out using a Cu(0)/Me_6-Tren catalyst system and a pyrene initiator at 25°C in toluene. The polymerisations show a living nature. Pyrene-terminal polymers with tuneable LCSTs can be made in this way, and applied to the synthesis of thermo-sensitive water-soluble MWCNTs.

Chapter 5 Conclusion and Outlook

The purpose of this thesis was to find models for surface modification with polymers. A comparison of existing approaches, namely the "grafting to" and "grafting from" methods, has been described. This thesis focused on discovering novel "grafting to" techniques with mild reaction conditions and high yields, or applying knowledge from other areas to improve the methods. The use of the "grafting from" method to make functional polymer brushes for different applications was also explored as an alternative to "grafting to".

Special emphasis was put on the combining of living radical polymerisation and Huisgen [2+3] cycloaddition (often termed “click” reaction) and applying it for surface modification. Both of them share a number of important features including robustness, versatility and excellent tolerance towards many functional groups. Living radical polymerisation was first used to synthesize different α-functional polymers (alkyne or azide terminal polymers) and used to modify a cellulose or organic resin surface modification through a "grafting to" approach (the "click" reaction).

The surface-initiated ATRP (a "grafting from" approach) was also used instead of "grafting to" approach using "click" chemistry in some cases to obtain thicker polymer brushes. Cellulose and organic resins were modified with initiating groups and a variety of functional polymers were then grown from the surface. For example, metronidazole containing polymers with antibiotic properties were grafted from cellulose surface, a single enantiomer moiety was immobilised by reacting with the hydroxy groups of PGMA on Aquagel resin surface with the potential as chiral stationary phases (CSP) for HPLC chromatography, a “clickable” alkyne monomer was grown from resin surface and then reacted with an azido-functional carbohydrate

through the "click" reaction to give a solid support with lectin-binding properties and opening the way for their potential application in affinity chromatography, sensors and other protein recognition/separation fields.

Carbon nanotubes (CNTs) were also chosen as a model for surface modification with polymers. The aim was increase the dispersability of the CNTs in solvents and enlarge the application areas of CNTs due to polymers' own functional properties. CNTs were first converted to a solid support ATRP initiator by an esterification reaction and styrene was grafted from CNTs through surface-initiated ATRP (a "grafting from" approach), the PSt modified CNTs were then used to form isoporous membranes. In another case, poly(amidoamine) (PAMAM) dendrons were covalently attached to MWCNTs through a "grafting to" approach. And finally, pyrene-functionalised polymers were synthesised and then used to modify CNTs by a noncovalent method and thus thermo-sensitive water-dispersible CNTs were made.

As outlined above this thesis focused on the surface modification with polymers. The combination of living radical polymerisation and Huisgen [2+3] cycloaddition was very successful and a useful tool for surface modification. Some future work may be carried out as described below. The antibiotic property and activity of the metronidazole-containing polymer needs to be investigated and different ratio between the metronidazole moiety and water-soluble copolymer can be tried. For mannose-functional beads, the purification of complex mixtures of mannose-binding biologically relevant lectins needs investigated and future research on the synthesis and use of immobilized ligands bearing a plethora of different sugar epitopes can be carried out. The chiral separation property of the modified Aquagel beads is being tested and using monomers with more hydroxyl groups like mannose or galactose will

increase the loading of single enantiomer and may increase its chiral separation property.

Chapter 6 Experimental Section

6.1 Reagents and materials

Surfactant free cotton fabric was provided by Unilever (Port Sunlight, UK). Wang and Merrifield resins were supplied by Avecia Ltd (Blackley, Manchester, UK) (loading: 1 mmol g^{-1} and 1.5 mmol g^{-1} respectively). Multiwalled carbon nanotubes (Aldrich, OD = 3-10 nm, ID = 1-3 nm, length = 0.1-10 μm, >99%), 1-Pyrenemethanol (Aldrich, 98.0%), ethylenediamine (Aldrich, 99.0%) were used as received, poly(ethylene glycol) methyl ether methacrylate (PEGMA, Aldrich, average Mn ~475) and di(ethylene glycol) methyl ether methacrylate (DEGMA, Aldrich, 95.0%) were stored at 4˚C and used as received. Copper(I) bromide (Aldrich, 98 %) was purified according to the method of Keller and Wycoff.[401] $[(PPh_3)_3CuBr]$[402], 2-bromo-2-methyl-propionic acid benzyl ester[403], 2-bromo-2-methylpropionic acid 6-hydroxyhexyl ester[404], Hostasol methacrylate (HMA)[378] and 3-Azido-propan-1-ol [405] were prepared as described earlier and stored at 0ºC. Triethylamine (Fischer, 99 %) was stored over sodium hydroxide pellets. All other reagents and solvents were obtained at the highest purity available from Aldrich Chemical Company and used without further purification unless stated.

6.2 Analysis and characterisation

All reactions were carried out using standard Schlenk techniques under an inert atmosphere of oxygen-free nitrogen, unless otherwise stated. Molar mass distributions were measured using size exclusion chromatography (SEC), on a system equipped with two PL gel 5 mm mixed C-columns (300 × 7.5 mm) and one PL gel 5 mm guard

column (50 × 7.5 mm) (Polymer Laboratories) with differential refractive index detection using THF/triethylamine (95:5) or chloroform/triethylamine (95:5) at 1.0 mL min^{-1} as the eluent. Poly(MMA) standards (200 to 1.5 × 10^6 g/mol) and poly(styrene) standards (540 to 1.64 × 10^6 g/mol)were used to calibrate the SEC. The analysed samples contained (0.2 % vol) toluene as the flow marker. The M_n reported in the M_n vs Conversion (%) plots are obtained from SEC data calibrated with PMMA standards. NMR spectra were obtained on a Bruker DPX300 and Bruker DPX400 spectrometer. All chemical shifts are reported in ppm (δ) relative to tetramethylsilane, referenced to the chemical shifts of residual solvent resonances (^1H and ^{13}C). The following abbreviations were used to explain the multiplicities: s = singlet, d = doublet, t = triplet, bs = broad singlet, m = multiplet. The conversions were calculated via ^1H NMR by following the decreasing of the integrals of the monomer vinyl signals (5.6 and 6.2 ppm), using the peak of mesitylene (6.9 ppm) as internal standard. Infrared absorption spectra were recorded on a Bruker VECTOR-22 FTIR spectrometer using a Golden Gate diamond attenuated total reflection cell. The thermal gravimetric analysis (TGA) dates were collected on a Perkin Elmer TGA 7, heating from 50˚C to 600˚C at 20˚C/min under nitrogen. The wettability testing procedure for cottons is as follows: individual yarns were taken from the fabric and cut into short segments (1 cm in length) for testing. The cotton yarn was attached to a wire and hung on the balance in a vertical orientation to determine the force during the testing. A beaker containing water was slowly levelled at a constant speed to make the yarn immersed in the water surface. FE-SEM was carried out on a Joel JSM 6100 microscope, with an accelerating voltage of 10 kV equipped with Oxford JSIS analytical system. Confocal microscopy was performed on a Zeiss LSM 510 system with the 488 nm band of an argon-ion laser used for excitation. The filters in the

experimental set-up were chosen to allow the measurement of the fluorescence at λ = 505 nm. The transmission electron microscopy (TEM) was recorded by JEOL 2000 FX TEM with accelerating voltage of 200 KV, the energy dispersive spectrum (EDS) was obtained by EDAX analytical system. Cloudy points (LCSTs) of polymers were measured using Varian Cary 100 UV-Vis spectrophotometer with temperature controller. The wavelength is set to 670 nm, heated with a rate of 20 ˚C/min. HPLC-SEC and HPLC-FL spectra were determined by a HP 1050 UV-detector and a Hitachi L7480 FL-detector. The UV absorption dates were collected from Perkin Elmer Lambda 25 UV/vis spectrometer. The Mass spectra were obtained using a Micromass Autospec apparatus. ESI-MS dates were recorded from Bruker esquire 2000. Elemental analyses were performed by the Warwick Analytical Service Ltd (UK). All reactions on polymeric beads were carried out using a FirstMate® benchtop synthesizer (Argonaut Technologies Limited) which utilises vertical agitation so as to avoid undue damage to the polymeric resins. Atomic force microscope (AFM) images were recorded on a CSM Instruments Atom Force Microscope. Imaging was performed in contact mode in air using a Pointprobe Plus probe with a nominal spring constant of ~0.15 N . m-1 and a resonance frequency of 11-12 kHz. The length of the cantilever was 452 mm and the radius was better than 7 nm. Analysis of the image was performed in CSM Instruments ImagePlus v. 3.1.10.

6.3 Synthesis of ligands: *N*-(*n*-propyl)-2-pyridylmethanimine

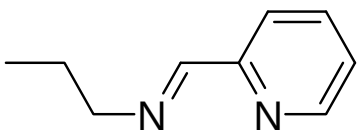

The ligands used for polymerisation were prepared as literature[406]. Pyridine-2-carboxaldehyde (40 mL, 0.42 mol) was dissolved in 50 mL of diethyl ether. The

solution was cooled in an ice-water bath and propyl amine (41 mL, 0.50 mol) was added drop wise. After complete addition of the amine, anhydrous magnesium sulphate (10.00 g) was added. The system was kept at ambient temperature with stirring and filtrated consequently to remove the solid. After removing the solvent, the product was purified by distillation under reduced pressure to give golden yellow oil.

Yield: 81.0%, Bp: 70^{o}C/0.4 Torr.

ν/cm^{-1}: 1653

δ_H (300 MHZ, $CDCl_3$)/ppm: 8.62 (m, 1H), 8.34 (s, 1H), 7.96 (m, 1H), 7.70 (m, 1H), 7.26 (m, 1H), 3.61 (t, *J* = 4.4 Hz, 2H), 1.72 (m, 2H), 0.95 (t, *J* = 4.4 Hz, 3H). δ_C (75.5 MHZ, $CDCl_3$)/ppm: 161.6, 154.6, 149.4, 136.2, 124.6, 121.1, 62.9, 23.6, 11.6.

CHN Analysis. Calculated for $C_9H_{12}N_2$: C, 72.9; H, 8.2; N, 18.9. Found: C, 72.0; H, 8.0; N, 18.4.

Mass Spectrometry *(m/z)*: 149 [M+1].

6.4 Synthesis of initiators for TMM-LRP

6.4.1 N-*Hydroxy succinimide 2-bromo-2-methyl propionate (1)*

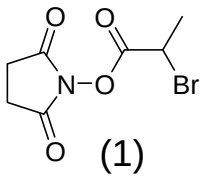

(1)

To a solution of *N*-hydroxy succinimide (17.8 g, 0.15 mol) in 150 mL of dichloromethane (DCM) was added triethylamine (28.1 mL, 0.2 mol), the solution was kept in an ice-water bath while stirring under a N_2 atmosphere for 10 minutes. Subsequently 2-bromo-2-methyl propionyl bromide (21 mL, 0.165 mol) was added dropwise over 30 minutes. The mixture was kept at ambient temperature for 45 minutes, and then decanted into 250 mL of ice-water with stirring, the organic layer

was separated and washed with saturated Na_2CO_3 solution (2 × 100 mL), H_2O (2 × 100 mL), saturated Na_2CO_3 solution (2 × 100 mL), and dried over $MgSO_4$ for 1 hour. The solid was removed by filtration, the DCM was removed by rotary-evaporator, and a yellow viscous oil was obtained. The crude product was purified by recrystallization from hot diethyl ether, and colourless crystals were obtained.

Yield: 72 %.

IR (neat) $\tilde{\nu}$ =: 1808, 1781(C_{cycl}=O), 1728, 1445, 1385, 1245 cm^{-1};

^{1}H NMR (300 MHZ, $CDCl_3$)/ppm: 1.96 (d, *J* = 6.78 Hz; 3H, CH(C*H*$_3$)Br); 2.87 (s, 4H, Hcycl), 4.61 (q, *J* = 7.03 Hz; 1H, C*H*(CH_3)Br); **^{13}C NMR** (75.5 MHZ, $CDCl_3$)/ppm: 168.69 (2C, Ccycl=O); 166.17 (1C, C=O); 34.97 (1C, *C*H(CH_3)Br); 25.74 (2C, Ccycl); 21.67 (1C, CH(*C*H$_3$)Br).

CHN Analysis. Calculated for $C_7H_8NO_4Br$: C, 33.62; H, 3.22; N, 5.60, Found; C, 33.54; H, 3.15; N, 5.39.

6.4.2 2-Bromo-2-methyl propionic acid 6-acetylsulfanyl-hexyl ester (2)

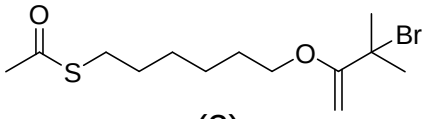

(2)

The synthesis proceeded via coupling of thioacetic acid s-(6-hydroxy-hexyl) ester and 2-bromopropionic bromide in dichloromethane.

PPh_3 (4.05g, 15.44 mmol) was dissolved in THF (25 ml) and the solution was cooled to 0 ^oC. Di-isopropyl azodicarboxylate (DIAD) (3.2 ml, 15.44 mmol) was added and the reaction mixture was stirred for 30 minutes. 2-bromo-2-methyl propionic acid 6-hydroxy-hexyl ester (3.75 g, 14.04 mmol) and thioacetic acid (1.1 ml, 15.44 mmol) in

THF (15 ml) was added dropwise over 15 minutes and the mixture was stirred for 1 hour at 0℃ and 4 hours at ambient temperature. The resulting solution was evaporated to dryness and dissolved in diethylether. The precipitated $O=PPh_3$ was filtered off, and the filtrate was evaporated to dryness. The precipitation procedure was repeated several times. And the crude product was purified by column.

IR (solid, ATR cell) ν/cm^{-1}: 1732 (C=O ester), 1694 (C=O thioester);

^{1}H NMR δ_H (300 MHz, $CDCl_3$)/ppm: 1.34-1.46 (m, 4H, CH_2); 1.53-1.73 (m, 4H, CH_2), 1.92 (s, 6H, CH_3), 2.32 (s, 3H, $SC(O)CH_3$), 2.86 (t, *J* = 7.2 Hz; 2H, CH_2S), 4.16 (t, *J* = 6.5 Hz; 2H, CH_2O); ^{13}C NMR δ_C (75.5 MHZ, $CDCl_3$)/ppm: 195.75 (1C, C=O thioester); 171.49 (1C, C=O ester); 65.90 (1C, CH_2O); 55.72 (1C, $C(CH_3)_2Br$); 30.54 (2C, CH_3), 29.14 (1C, CH_2), 28.72 (1C, CH_2), 28.06 (1C, CH_2), 27.96 (1C, CH_2), 25.12 (1C, CH_2)

Mass Spectrometry *(m/z)*: 346 [M+23]

6.4.3 2-Bromo-2-methyl-propionic acid 3-azido-propyl ester (3)

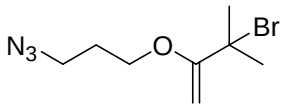

(3)

A solution of 3-azido-propan-1-ol (3.69 g, 36.5 mmol) and triethylamine (5.7 mL, 40 mmol) in Et_2O (50 mL) was cooled to 0 ^oC and 2-bromo-2-methyl propionyl bromide (5.0 mL, 40 mmol) was added slowly via syringe (over ca. 1 min). After stirring for 1 h at 0^oC and overnight at ambient temperature the resulting white suspension was filtered and the pale yellow solution washed with saturated $NaHCO_3$ aqueous solution (2 x 100 mL) and dried with $MgSO_4$. After filtration the solvent was removed under reduced pressure and the yellow oily residue was purified by flash chromatography

(CC, SiO_2, Petroleum ether / Et_2O 20:1, R_f(s) 0.15) to give **(5)** (6.4 g, 25.6 mmol, yield: 70 %) as colourless oil.

IR (neat) $\tilde{\nu}$ = : 2972, 2932, 2098, 1735, 1462, 1273, 1162, 1108 cm^{-1};

^{1}H NMR (400.03 MHz, $CDCl_3$, 298 K) δ = 1.93 (s, 6H, CH_3); 1.96 (app. quint., *J* = 6.4 Hz, 2H, $CH_2CH_2CH_2$), 3.44 (t, 2H, *J* = 6.6 Hz, CH_2N_3), 4.27 (t, *J* = 6.2 Hz, 2H, CH_2OH); **^{13}C NMR** (100.59 MHz, $CDCl_3$, 298 K) δ = 28.08 (1C, $CH_2CH_2CH_2$), 30.81 (2C, CH_3); 48.14 (1C, CH_2N_3), 55.78 (1C, $CBr(CH_3)_2$); 62.84 (1C, CH_2OH), 171.63 (1C, CO_{ester}).

Mass Spectrometry *(m/z)*: 271 [M+23]

6.4.4 2-Bromo-2-methyl-hept-6-yn-3-one (4)

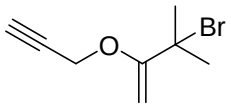

(4)

Triethylamine (10.8 g, 107 mmol) was added to a solution of prop-2-yn-1-ol (5.00 g, 89.1 mmol) in dichloromethane (100 mL) at 0^{o}C whilst stirring under a N_2 atmosphere for 10 minutes. 2-Bromo-2-methyl-propionyl bromide (11.83 mL, 83.04 mmol) was subsequently added dropwise over 30 minutes. After stirring at ambient temperature overnight the solution was filtered and the solvent removed under reduced pressure to give a slightly yellow liquid that was purified by the removal of volatiles in vacuo to give (6) as a colourless liquid (12.3 g, yield 68 %)

IR (neat) $\tilde{\nu}$ =: 3295, 1738(C_{cycl}=O), 1269, 1152, 1107 cm^{-1};

^{1}H NMR δ_H (400 MHz, $CDCl_3$)/ppm: 1.94 (s, 6H, $C(CH_3)_2Br$); 2.50 (t, *J* = 2.5 Hz; 1H, C≡CH), 4.75 (d, *J* = 2.5 Hz; 2H, CH_2); **^{13}C NMR** (100.59 MHz, $CDCl_3$) δ =

171.34 (1C, C=O); 77.19 (1C, *C*≡CH); 75.94 (1C, C≡*C*H); 55.38 (1C, *C*H(CH_3)$_2$Br); 53.89 (1C, CH_2); 31.11 (2C, CH_3).

Mass Spectrometry *(m/z)*: 204 [M+1]

6.4.5 2-Bromo-2-methyl-propionic acid pyren-1-ylmethyl ester

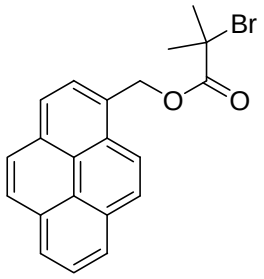

(29)

0.5 g (2.15 mmol) 1-Pyrenemethanol and 0.9 mL (6.45 mmol) triethylamine were dissolved in 30 mL dry THF in a 250 mL two-neck flask. Then 0.8 mL (6.45 mmol) 2-Bromoisobutyryl bromide dissolved in 10 mL dry THF was added drop wise to the flask under stirring at 0 ˚C. The mixture was stirred at room temperature overnight. After the mixture was filtered, the solvent was removed under vacuum. The crude product was dissolved in 100 mL CH_2Cl_2 and washed with 1.0 M HCl, saturated $NaHCO_3$ solution and distilled water respectively. The organic layer was collected and dried over anhydrous MgSO4 overnight. The final product was further purified by recrystallization in methanol.

IR (neat): $\tilde{\nu}$ = 3042, 2970, 1724, 1590, 1458, 1389, 1271, 1154, 1103, 1062, 1009 cm^{-1};

^{1}H NMR ($CDCl_3$), d (ppm): 8.27-7.99 (m, 9H, pyrenyl), 5.91 (s, 2H, CH_2), 1.84-1.81 (s, 6H, CH_3). **^{13}C NMR** (100.59 MHz, $CDCl_3$, 298 K) δ = 30.97 (2C, CH_3), 53.28 (1C, (CH_3)$_2$*C*Br); 66.65 (1C, CH_2O), 123.11-128.45 (9C, CH of pyrene); 125.09-141.09 (7C, C of pyrene), 171.83 (1C, CO_{ester}).

Mass Spectrometry *(m/z)*: 382 [M+1]

6.5 Synthesis of α-functional materials

6.5.1 Synthesis of azido-terminal materials

6.5.1.1 5-[1,3-dioxo-1H-benzo[3,4]isothiochromeno[7,8,1-def]isoquinolin-2(3H)-yl]pentyl, (Hostasol azide), (7)

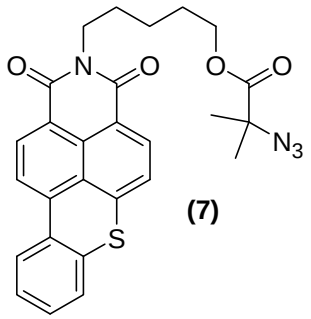

(7)

2-(8-(2-bromodimethyl)-3,6-dioxa-octyl)-thioxantheno[2,1,9-dej]isoquinoline-1,3-dione[407] (0.48 g, 0.89 mmol) and sodium azide (0.117 g, 1.78 mmol) were dissolved in a mixture of acetone (50 mL) and water (10 mL) and the resulting solution refluxed overnight at 60°C. The acetone and other volatiles were removed under reduced pressure, 50 mL of water was added and the mixture extracted with dichloromethane (3 x 50 mL). The organic layers were collected together and dried over $MgSO_4$. Removal of volatiles under reduced pressure gave the product, **(7)**, as an orange solid (0.40 g, 0.80 mmol, 90 %).

IR (neat): $\tilde{\nu}$ = 2940, 2108, 1733, 1685, 1641, 1580, 1560, 1515, 1445, 1384, 1362, 1245, 1138, 1084, 966, 838, 758, 747, 712, 641, 597, 564, 547, 535 cm^{-1};

^{1}H NMR (400.03 MHz, $CDCl_3$, 298 K), δ = 1.45 (s, 6H, CH_3); 1.52 (t, 2H, CH_2); 1.78 (m, 4H, CH_2); 4.19 (m, 4H, CH_2), 7.2-8.7 (m, 8H, CH); **^{13}C NMR** (100.59 MHz, $CDCl_3$, 298 K). δ = 23.59 (1C, CH_2), 24.58 (2C, CH_3), 27.66 (1C, CH_2), 28.38 (1C,

CH_2), 40.20 (1C, NCH_2), 63.28 ($CN_3(CH_3)_2$), 65.93 (1C, CH_2O), 118.08 (2C, C), 119.21 (1C, CH), 120.42 (1C, CH), 121.24 (1C, C), 126.15 (1C, CH), 126.51 (1C, CH), 127.69 (1C, CH), 127.99 (1C, C), 130.06 (1C, CH), 130.36 (1C, C), 130.79 (1C, CH), 131.72 (1C, C), 132.54 (1C, CH), 136.67 (1C, C), 140.54 (1C, C), 163.44 (2C, C=O), 163.88 (1C, C=O).

CHN Analysis. Calculated for $C_{27}H_{24}N_4O_4S$: C, 64.78; H, 4.83; N, 11.19; Found C, 64.10; H, 4.46; N, 10.98.

6.5.1.2 Monomethoxy-PEG$_{5000}$-N$_3$ (6)

Monomethoxy-PEG_{5000} (12.5 g, 2.50 mmol) was dissolved in toluene (100 mL) and the residual water in the polymer removed by Dean-Stark azeotropic distillation. The solution was subsequently cooled to 0^{o}C prior to the addition of triethylamine (0.35 mL, 2.5 mmol) and methanesulfonyl chloride (11.4 g, 100 mmol) was added dropwise over a 3 hours, the ice bath was then removed and the mixture allowed to stir at ambient temperature overnight. The ammonium salts were removed by filtration filtered and the solvent removed under reduced pressure, the residues were subsequently dissolved in ethyl acetate and passed through a short silica column. Finally, the polymer was precipitated into Et_2O to give the expected intermediate as white waxy solid. 2 g (0.4 mmol) of this product and sodium azide (0.26 g, 4.02 mmol) were dissolved in DMF (50 mL) and the resulting solution stirred at 60^{o}C for 24 h. The final product, **(6)**, was purified by dialysis using Watson Marlow dialysis pump and water removed by freeze-drying. Molecular weights of the PEG before and after transformation: $M_{n,PEG}$ = 12 100 g mol^{-1}, PDi = 1.02; $M_{n,(2)}$ = 11 300 g mol^{-1}, PDi = 1.02. IR of **(6)**: $\tilde{\nu}$ = 2881, 2091, 1466, 1359, 1341, 1279, 1240, 1147, 1098, 1060, 959, 842, 657, 613 cm^{-1}

6.5.1.3 Azido-terminal poly(MMA-co-HMA) (5)

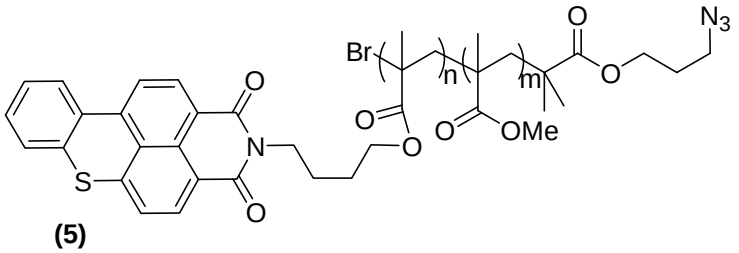

(5)

A sealed dried Schlenk flask containing initiator 2-bromo-2-methyl-propionic acid 3-azido-propyl ester (**3**) (0.584 g, 2.34 mmol), MMA (10 mL, 93.4 mmol), HMA (0.214 g, 0.467 mmol), *N*-(n-propyl)-2-pyridyl methanimine (0.797 mL, 4.67 mmol) and mesitylene (0.5 mL, internal ^{1}H NMR standard), were dissolved in 20 mL of toluene prior to degassing by four freeze-pump-thaw cycles. The solution was transferred, via cannula, to a second Schlenk tube containing CuBr (0.335 g, 2.34 mmol), previously evacuated and refilled with N_2. Polymerisation was carried out at 90 ˚C with samples being taken periodically using a degassed syringe for molecular weight (SEC) and conversion analysis (^{1}H NMR, based on the change of vinyl integrations during reaction with mesitylene being added and employed as internal standard). Once a conversion of 90 % was achieved, the polymerisation was quenched by opening to air. Copper salts were removed by passing through a short neutral alumina column, and the polymer isolated via precipitation from toluene solution to 10-fold excess of petroleum ether, as fine powders. Polymers were isolated via filtration and volatiles removed in a vacuum oven overnight at 40^{o}C. Use of a visibly fluorescent co-monomer allowed for the synthesis of fluorescently tagged polymers **(5)**, which facilitated the characterisation of the corresponding cotton-polymer/resin-polymer hybrid materials using fluorescence analytical techniques.

6.5.1.4 Synthesis of azido-terminal sugar, 3'-azidopropyl-α-D-mannopyranoside

6.5.1.4.1 2'-Bromoethyl 2,3,4,6-tetra-O-acetyl-a-D-mannopyranoside

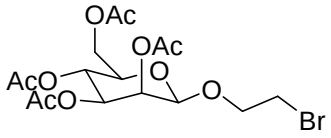

This product was prepared following the protocol described by Hayes *et al.*.[408] To a solution of 1,2,3,4,6-penta-O-acetyl-α-D-mannopyranoside (11.8 g, 30.3 mmol) and 2-bromo-1-ethanol (12.4 g, 99.5 mmol) in anhydrous dichloromethane (ca. 100 mL), boron trifluoride etherate (23.6 g, 166 mmol) was added at -20 °C, under inert atmosphere. The cold bath is then removed and after 6 hours, the solution was neutralised with a saturated solution of $NaHCO_3$ (100 mL) and subsequently washed 2 times with deionised water. The organic phase was dried over magnesium sulphate, filtered and the solvent was evaporated under vacuum. The resulting oil was purified by column chromatography on silica gel using petroleum ether : diethyl ether 1: 1 as an eluent. The product was obtained as orange oil. Yield = 48 %.

IR (neat): $\tilde{\nu}$ =2958, 1743, 1435, 1368, 1218, 1136, 1084, 1046, 979, 910 cm^{-1}.

^{1}H NMR (400.03 MHz, $CDCl_3$, 298 K) δ = 1.99 (s, 3H, CH_3); 2.04 (s, 3H, CH_3); 2.10 (s, 3H, CH_3); 2.15 (s, 3H, CH_3); 3.45(m, 2H, CH_2Br); 3.75-3.89 (m, 2H, OCH2); 3.96-4.12 (m, 3H, $CHCH_2OAc$); 4.23 (m, 1H, CH); 4.81 (d, *J* = 1.75 Hz, 1H, CH); 5.21-5.35 (m, 3H, 3×CH). **^{13}C NMR** (100.59 MHz, $CDCl_3$, 298 K) δ = 20.82 (1C, CH_3); 20.89 (1C, CH_3); 21.02 (1C, CH_3); 21.11 (1C, CH_3); 29.74 (1C, CH_2Br); 62.56 (1C, CH_2OAc); 65.98 (1C, CH); 68.56 (1C, CH); 68.63 (1C, CH); 68.68 (1C, CH_2CH_2O); 69.08 (1C, CH); 97.91 ($C_{anomeric}$); 169.88 (1C, $CH_3C(O)O$); 169.95 (1C, $CH_3C(O)O$); 169.97 (1C, $CH_3C(O)O$); 170.38 (1C, $CH_3C(O)O$).

CHN Analysis. Calculated for $C_{16}H_{23}BrO_{10}$ C, 42.21; H, 5.09; Found C, 42.16; H, 5.17..

Mass Spectrometry (+ESI-MS) *m/z*: 477 [M+Na].

6.5.1.4.2 2'-Azidoethyl 2,3,4,6-tetra-O-acetyl-a-D-mannopyranoside

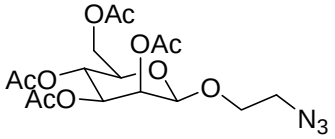

2'-Bromoethyl 2,3,4,6-tetra-O-acetyl-α-D-mannopyranoside (6.33 g, 13.9 mmol) was treated with NaN_3 (5.42 g, 83.3 mmol) in DMF (ca. 150 mL) and the reaction mixture was stirred at 60 °C for 3hours. The solvent was evaporated under vacuum and the oily residue was redisolved into 150 mL of dichloromethane. This solution was washed with deionised water (3×80 mL) and dried with magnesium sulfate. Column chromatography on silica gel using a mixture of methanol : diethyl ether 1 : 9 as eluent afforded the product as a thick orange oil which crystallised over time. Yield = 75 %.

IR (neat): $\tilde{\nu}$ =2958, 1743, 1435, 1368, 1218, 1136, 1084, 1046, 979, 910 cm^{-1}.

^{1}H NMR (400.03 MHz, $CDCl_3$, 298 K) δ = 1.93 (s, 3H, CH_3); 1.98 (s, 3H, CH_3); 2.04 (s, 3H, CH_3); 2.09 (s, 3H, CH_3); 3.45(m, 2H, CH_2N_3); 3.66-3.86 (m, 2H, CH_2CH_2O); 3.99-4.15 (m, 3H, $CHCH_2OAc$); 4.23 (1H, CH); 4.85 (d, *J* = 1.75 Hz, 1H, CH); 5.21-5.35 (m, 3H, 3×CH). **^{13}C NMR** (100.59 MHz, $CDCl_3$, 298 K) δ = 21.08 (1C, CH_3); 21.13 (1C, CH_3); 21.16 (1C, CH_3); 21.30 (1C, CH_3); 50.79 (1C, CH_2N_3); 62.89 (1C, CH_2OAc); 66.43 (1C, CH); 67.48 (1C, CH); 68.68 (1C, CH_2CH_2O); 69.28 (1C, CH); 69.08 (1C, CH); 98.18 ($C_{anomeric}$); 170.18 (1C, $CH_3C(O)O$); 170.23 (1C, $CH_3C(O)O$); 170.43 (1C, $CH_3C(O)O$); 171.04 (1C, $CH_3C(O)O$).

CHN Analysis. Calculated for $C_{16}H_{23}N_3O_{10}$ C, 46.04; H, 5.55; N 10.07; Found C, 46.23; H, 5.54; N 10.15.

Mass Spectrometry (+ESI-MS) *m/z*: 440 [M+Na].

6.5.1.4.3 2'- Azidoethyl -O-a-D-mannopyranoside

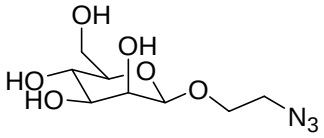

A solution of sodium methoxide (25% w/w in MeOH, 0.50 mL, 2.32 mmol) was added to a stirred solution of 2'- Azidoethyl -O-a-D-mannopyranoside (2.90 g, 6.95 mmol) in methanol (20 mL). After 30 minutes the solution was acidified with Amberlite IR-120H+ to pH 6. The ion exchange resin was removed by filtration, and the solvent evaporated under vacuum to afford the product as a white powder. Yield = 86 %.

IR (neat): $\tilde{\nu}$ =3358 (bs), 2927, 2097, 1644, 1301, 1262, 1132, 1056, 976, 913, 881, 812 cm^{-1}

^{1}H NMR (400.03 MHz, D_2O, 298 K) δ = 3.45 (m, 2H, CH_2N_3); 3.55-3.60 (m, 2H, $CH_2CH_2N_3$); 3.61-3.67 (m, 2H, CH_2OH); 3.67-3.91 (m, 4H, 4×CH); 4.92 (d , *J* = 1. 5 Hz, 1H, CH). **^{13}C NMR** (100.59 MHz, D_2O, 298 K) δ = 50.20 (1C, CH_2N_3); 60.91 (1C, CH_2OH); 66.30 (1C, CH_2CH_2O); 66.68 (1C, CH); 69.97 (1C, CH); 70.39 (1C, CH); 72.89 (1C, CH); 99.81 ($C_{anomeric}$);

CHN Analysis. Calculated for $C_8H_{15}N_3O_6$ C, 38.55; H, 6.07; N, 16.86; Found: C, 38.35; H, 6.11; N, 16.76;

Mass Spectrometry (+ESI-MS) *m/z*: 272[M+Na].

6.5.2 Synthesis of alkyne-terminal materials

6.5.2.1 Alkyne-terminal poly(PEGMA)

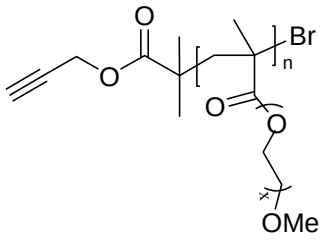

A sealed dried Schlenk flask containing initiator 2-bromo-2-methyl-hept-6-yn-3-one (**4**) (0.41 g, 2.0 mmol), PEGMA (20 mL, 20.0 mmol), *N*-(n-propyl)-2-pyridyl methanimine (0.685 mL, 4.0 mmol) and mesitylene (1.0 mL, internal ^{1}H NMR standard), were dissolved in 60 mL of toluene prior to degassing by four freeze-pump-thaw cycles. The solution was transferred, via cannula, to a second Schlenk tube containing CuBr (0.287 g, 2.0 mmol), previously evacuated and refilled with N_2. Polymerisation was carried out at 50 ˚C with samples being taken periodically using a degassed syringe for molecular weight (SEC) and conversion analysis (^{1}H NMR, based on the change of vinyl integrations during reaction with mesitylene being added and employed as internal standard). Once a conversion of 90 % was achieved, the polymerisation was quenched by opening to air. Copper salts were removed by passing through a short neutral alumina column, and the polymer isolated via precipitation from toluene solution to 10-fold excess of diether ether, as pale yellow oil. The polymer was further purified by dialysis in water (molecular weight cut-off: 6000-8000).

6.5.2.2 alkyne-terminal poly(MMA-co-HMA) (11)

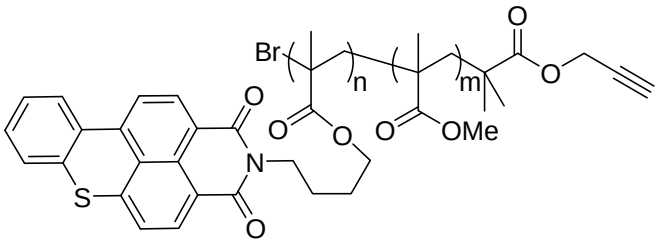

A sealed dried Schlenk flask containing initiator 2-bromo-2-methyl-hept-6-yn-3-one (**4**) (0.191 g, 0.934 mmol), MMA (10 mL, 93.4 mmol), HMA (0.0855 g, 0.187 mmol), and *N*-(n-propyl)-2-pyridyl methanimine (0.417 mL, 1.87 mmol), were dissolved in 20 mL of toluene prior to degassing by four freeze-pump-thaw cycles. The solution was transferred, via cannula, to a second Schlenk tube containing CuBr (0.134 g, 0.934 mmol), previously evacuated and refilled with N_2. Polymerisation was carried out at 90 ˚C with samples being taken periodically using a degassed syringe for molecular weight (SEC) and conversion analysis (^{1}H NMR, based on the change of vinyl integrations during reaction with mesitylene being added and employed as internal standard). Once a conversion of 90 % was achieved, the polymerisation was quenched by opening to air. Copper salts were removed by passing through a short neutral alumina column, and the polymer isolated via precipitation from toluene solution to 10-fold excess of petroleum ether, as fine powders. Polymers were isolated via filtration and volatiles removed in a vacuum oven overnight at 40^{o}C.

6.5.3 Synthesis of hydroxyl-terminal PAMAM dendron[409,410]

6.5.3.1 3-[[2-(2-Hydroxy-ethoxy)-ethyl]-(2-methoxycarbonyl-ethyl)-amino]-propionic acid methyl ester (HO-PAMAM-$(COOCH_3)_2$)

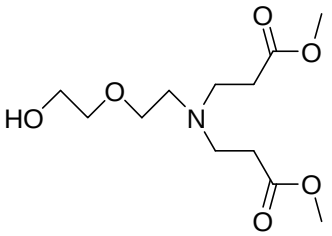

2-(2-Amino-ethoxy)-ethanol (2.10 g, 0.02 mol), MA (17.80mL, 0.20 mol) were dissolved in 30 mL of methanol, the solution was stirred at ambient temperature for 48 h. The volatile materials were removed under vacuum, and quantitative product was obtained as colourless oil.

IR (neat): $\tilde{\nu}$ = 3431, 2951, 2851, 1733, 1438, 1197, 1122.

^{1}H NMR (400.03 MHz, $CDCl_3$, 298 K)/ppm: δ = 2.46 (t, *J* = 7.0 Hz, 4H, $CH_2C{=}O$); 2.65 (t, *J* = 5.3 Hz, 2H, CH_2N); 2.83 (t, *J* = 7.0 Hz, 4H, $N(CH_2)_2$), 3.53-3.56 (m, 4H, $C\underline{H}_2OC\underline{H}_2$), 3.65 (s, 6H, CH_3), 3.68-3.69 (m, 2H, C<u>H</u>2OH). **^{13}C NMR** (100.59 MHz, $CDCl_3$, 298 K)/ppm: δ = 32.4 x 2, 50.1 x 2, 51.8 x 2, 53.8, 62.0, 69.6, 72.6, 173.1 x 2.

CHN Analysis. Calculated for $C_{12}H_{23}NO_6$: C, 52.0; H, 8.4; N, 5.0. Found: C, 51.9; H, 8.4; N, 5.0.

Mass Spectrometry (+ESI-MS) *m/z*: 278 (M+1)

6.5.3.2 *N*-(2-Amino-ethyl)-3-{[2-(2-amino-ethylcarbamoyl)-ethyl]-[2-(2-hydroxy-ethoxy)-ethyl]-amino}-propionamide.

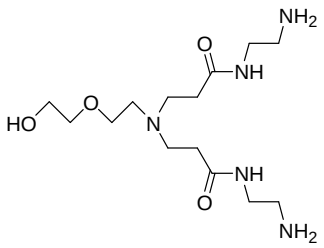

3-[[2-(2-Hydroxy-ethoxy)-ethyl]-(2-methoxycarbonyl-ethyl)-amino]-propionic acid methyl ester (2.77g, 0.01 mol), ethylene diamine (6.70 mL, 0.10 mol) were dissolved

in 20 mL of methanol, the solution was stirring at ambient temperature for 48h, the ethylene diamine was removed by azeotropic distillation using toluene/methanol mixture. The product was obtained as pale yellow oil and used directly for next step without further purification.

6.5.3.3 3-[[2-(3-{2-{2-[Bis-(2-methoxycarbonyl-ethyl)-amino]-ethylcarbamoyl}-ethyl}-2[2-(2-hydroxy-ethoxy)-ethyl]-amino)-propionylamino]-ethyl]-(2-methoxycarbonyl-ethyl)-amino]-propionic acid methyl ester (HO-PAMAM-($COOCH_3$)$_4$).

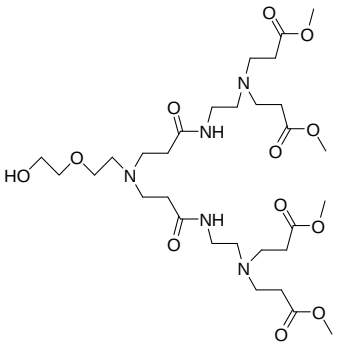

N-(2-Amino-ethyl)-3-{[2-(2-amino-ethylcarbamoyl)-ethyl]-[2-(2-hydroxy-ethoxy)-ethyl]-amino}-propionamide (1.67 g, 0.01 mol), MA (17.80 mL, 0.20 mol) were dissolved in 30 mL of methanol, the solution was stirred at ambient temperature for 48 h, the methanol and unreacted MA were distilled under vacuum, the crude was purified using silica column with ethyl acetate/methanol (7:1) as solvent, the product was obtained as a pale yellow oil. (5.33 g, 7.86 mmol, 78.6%)

IR (neat): $\tilde{\nu}$ = 3325, 2951, 2831, 1735, 1649, 1542, 2437, 1358.

^{1}H NMR (400.03 MHz, $CDCl_3$, 298 K)/ppm: δ = 2.36-2.50 (m, 12H); 2.53 (t, *J* = 6.0 Hz, 4H); 2.70-2.75 (m, 10H), 2.87 (t, *J* = 6.8 Hz, 4H), 3.28 (m, 3.25-3.29, 4H), 3.52-3.54 (m, 2H), 3.58 (t, *J* = 5.0 Hz, 2H), 3.66 (s, 12H), 3.68-3.70 (m, 2H). **^{13}C NMR**

(100.59 MHz, $CDCl_3$, 298 K, selected peaks)/ppm: δ = 32.8, 33.5, 37.3, 49.3, 50.9, 51.8, 53.1, 53.2, 61.7, 69.3, 72.9, 172.4, 173.2.

CHN Analysis. Calculated for $C_{30}H_{55}N_5O_{12}$: C, 53.16; H, 8.18; N, 10.33. Found: C, 52.97; H, 8.21; N, 10.17.

MS: 678 (M+1)

6.5.3.4 HO-PAMAM-$(COOCH_3)_8$

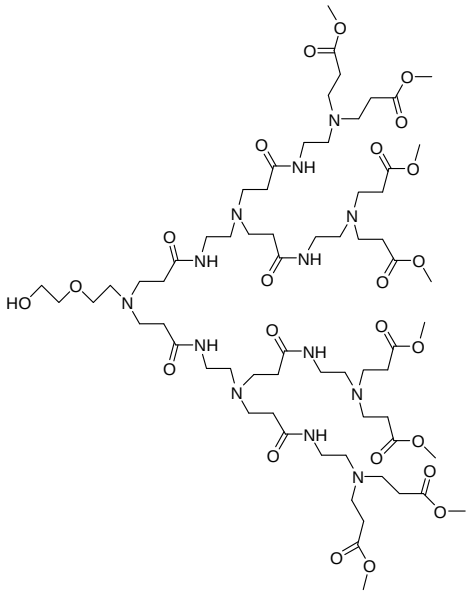

The product was obtained by silica column, ethyl acetate/methanol (2:1) as solvent, yield: 71.4%.

IR (neat): $\tilde{\nu}$ = 3291, 2951, 2828, 1731, 1643, 1538, 1436, 1358.

^{1}H NMR (400.03 MHz, $CDCl_3$, 298 K, selected peaks)/ppm: δ = 2.27-2.38 (m, 28H), 2.46-2.52 (m, 12H), 2.61-2.77 (m, 30H), 3.18-3.22 (m, 12H), 3.46-3.51 (m, 4H), 3.60 (s, 24H), 3.63-3.65 (m, 2H). **^{13}C NMR** (100.59 MHz, $CDCl_3$, 298 K, selected peaks)/ppm: δ = 32.7, 33.51, 33.9, 37.3, 37.6, 49.3, 49.9, 50.5, 51.8, 52.6, 53.0, 53.2, 61.5, 69.3, 72.8, 172.7, 172.9, 173.2.

MS: 1480 (M+2)

6.5.3.5 HO-PAMAM-$(COOCH_3)_{16}$

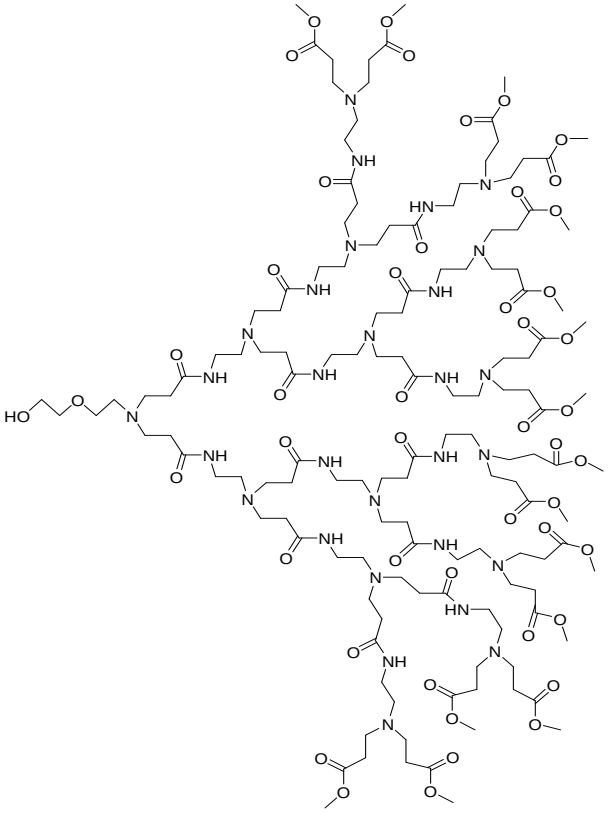

The product was purified by silica column, ethyl acetate/methanol (1:2) as solvent, yield: 68.3%.

IR (neat): $\tilde{\nu}$ = 3282, 2952, 2828, 1733, 1644, 1542, 1437, 1198.

^{1}H NMR (400.03 MHz, $CDCl_3$, 298 K, selected peaks)/ppm: δ = 2.32-2.42 (m, 60H), 2.50-2.57 (m, 28H), 2.71-2.80 (m, 62H), 3.23-3.26 (m, 28H), 3.50-3.55 (m, 4H), 3.64 (s, 48H), 3.66-3.68 (m, 2H). **^{13}C NMR** (100.59 MHz, $CDCl_3$, 298 K, selected peaks)/ppm: δ = 32.7, 33.8, 37.2, 37.5, 49.3, 49.9, 50.1, 50.5, 51.7, 52.5, 53.0, 61.4, 72.8, 172.4, 172.6, 173.1.

MS: 3083 (M+3)

6.5.4 Synthesis of pyrene-terminal polymers

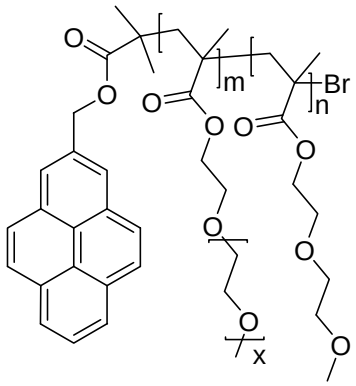

(30) **m = 0, n = 100**
(31) **m = 10, n = 90**
(32) **m = 100, n = 0**

Pyrene-terminal polymers containing different ratios of $PEGMA_{475}$ and DEGMA were synthesised using SET-LRP. A typical polymerisation procedure is: a sealed dried Schlenk flask containing initiator 2-bromo-2-methyl-propionic acid pyren-1-ylmethyl ester (0.034 g, 0.09 mmol), PEGMA (0.431 g, 0.9 mmol), DEGMA (1.53 g, 8.1 mmol), Tren-Me_6 (0.024 mL, 0.09 mmol) and mesitylene as internal ^{1}H NMR standard dissolved in 2.4 mL of toluene was degassed by four freeze-pump-thaw cycles. The solution was then transferred via cannula to another Schlenk tube containing Cu(0) (0.0058 g, 0.09 mmol) previously evacuated and filled with N_2. The polymerisation was carried out at 25 ˚C. Samples were taken periodically using a degassed syringe for molecular weight (SEC) and conversion analysis (^{1}H NMR). Once a conversion of 90 % was reached, the polymerisation was quenched by opening to air. The final mixture was diluted in toluene and passed through a short neutral alumina column, and the polymer was precipitated from toluene solution to 10-fold excess of diethyl ether as pale yellow oil. The polymer was further purified by dialysis in water (molecular weight cut-off: 6000-8000).

6.6 Cellulose surface modification

6.6.1 cotton surface modification through click chemistry

6.6.1.1 4-Chlorocarbonyl-butyric acid prop-2-ynyl ester (8)

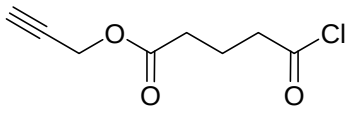

(8)

Glutaric anhydride (1.52 g, 13.3 mmol), propargyl alcohol (0.820 g, 14.6 mmol) and DMAP (0.12 g, 1.0 mmol) were dissolved in anhydrous CH_2Cl_2 (20 mL). The solution was subsequently stirred overnight at ambient temperature. The resulting orange solution was diluted to 100 mL with DCM, and washed with 20 mL of 0.5M HCl solution then with brine (10 mL). The organic layer was dried over $MgSO_4$. Following filtration the solvent was removed under reduced pressure to give an orange residue that was purified by flash chromatography and give a colourless oil (1.31 g, 7.71 mmol), **(7a)**. **(7a)** (1.00 g, 5.88 mmol), and 0.1 mL DMF were dissolved in anhydrous CH_2Cl_2 (10 mL) prior to the addition of oxalyl chloride (1 mL, 11.62 mmol) dropwise and subsequent stirring under nitrogen at ambient temperature for one hour. The product, **(8)**, was isolated under high vacuum as slightly yellow oil (1.45 g, 7.71 mmol).

IR (neat): $\tilde{\nu}$ = 3280, 1791, 1736, 1387, 1156 cm^{-1};

^{1}H NMR (300.03 MHz, $CDCl_3$, 298 K) δ = 2.03 (m, 2H, CH_2), 2.46 (m, *3*H, C≡CH + CH_2), 3.01 (t, *J* = 7.2 Hz, 2H, CH_2), 4.69 (d, *J* = 2.5 Hz, 2H, OCH_2); **^{13}C NMR** (100.59 MHz, $CDCl_3$, 298 K) δ = 19.72 (1C, CH_2), 32.90 (1C, CH_2), 32.94 (1C, CH_2), 52.07 (1C, CH_2), 75.06 (1C, CH, C≡*C*H), 77.64 (1C, C), 172.18 (1C, C), 178.96 (1C, C).

6.6.1.2 Cotton-alkyne synthesis

Cotton sheet was cut into appropriate size squares and dried for 15 minutes at 110°C under nitrogen. The cotton sheet (approximately 0.5 cm × 1 cm) was wetted with anhydrous pyridine (30 mL) and DMAP (15 mg) for 1 h prior to the addition of 4-Chlorocarbonyl-butyric acid prop-2-ynyl ester (8) (0.5 g in 10 mL anhydrous DMF solution). The reaction mixture was subsequently heated to 60 °C and kept at this temperature for 20 h. The cotton sheet was removed and rinsed thoroughly with acetone and distilled water prior to sonication in distilled water, acetone, dichloromethane and finally methanol.

6.6.1.3 Click reaction to Cotton

A sealed dry Schlenk flask containing CuBr, N-(n-propyl)-2-pyridyl methanimine and azide terminated polymers in toluene solution was degassed by four freeze-pump-thaw cycles. The alkyne functionalized cotton sheets were then added to the Schlenk under nitrogen and stirred at 70 °C overnight. Depending on the type of polymers being clicked, the cotton sheets were removed and rinsed thoroughly with dichloromethane or distilled water prior to sonication in dichloromethane/distilled water, acetone and finally methanol.

6.6.2 Synthesis of Metronidazole modified cotton

6.6.2.1 Metronidazole methylacrylate (MTD-MA)

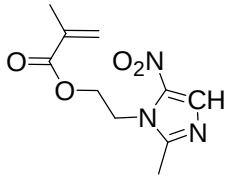

MTD-MA

Metronidazole (20g, 0.1169 mol), dichloromethane (200cm^3) and triethylamine (19.5cm^3, 0.1402 mol) were added to a 3-necked round-bottomed flask and the mixture degassed under nitrogen. The reaction was cooled to 0°C before the dropwise addition of methacryloyl chloride (10.2cm^3, 0.1402 mol). The reaction was allowed to warm to room temperature overnight. The reaction mixture was washed with saturated sodium carbonate solution followed by water and dried over magnesium sulphate before the solvent was evaporated. The resulting yellow oil was eluted through a silica frit using dichloromethane, increasing to 10% methanol. The second fraction was evaporated to yield the product as a yellow solid (21g, 75%).

^{1}H NMR ($CDCl_3$, 400MHz, 298K) δ (ppm): 8.0 (s, 1H, C*H*N), 6.1 (t, 1H, C*H* vinyl, J=1.0), 5.6 (m, 1H, C*H* vinyl, J=1.5), 4.7 (t, 2H, C*H*$_2$CN, J=5.27, 5.01), 4.5 (t, 2H, C*H*$_2$CO, J=5.27, 5.01), 2.45 (s, 3H, CH_3CN, J=), 1.9 (t, $CH_3C{=}CH_2$, J=1.27).

^{13}C NMR ($CDCl_3$, 400MHz, 298K) δ (ppm): 172.40 (1 C, *C*=O), 166.64 (1C, *C*NO_2), 150.84 (1C, CH_3*C*H=CH), 135.40 (1C, NC=*C*CH_3), 133.17 (1C, N*C*=CCH_3), 126.66 (1C, CH_3CH=*C*H), 62.62 (1C, O*C*H_2CH_2), 45.08 (1C, OCH_2*C*H_2), 18.16 (1C, *C*H_3CH=CH), 14.23 (1C, NC=C*C*H_3).

IR (neat) ν (cm^{-1}): 2966, 1711, 1626, 1532, 1464, 1445, 1378, 1260, 1157, 1103, 1011.

Mass Spectrometry: LRMS-EI calculated for $C_{10}H_{13}N_3O_4$ (M+): 239.091. Found: 239.091.

6.6.2.2 Synthesis of cotton initiator (cotton-Br)

Cotton sheet was cut into appropriate size squares and dried for 15 minutes at 110°C under nitrogen. The cotton sheet (approximately 0.5 cm × 1 cm) was wetted with anhydrous pyridine (30 mL) and DMAP (15 mg) for 1 h prior to the addition of 2-

bromoisobutyryl bromide (1.2 mL, 10 mmol). The reaction was carried out at ambient temperature for 12 h. The cotton sheets were subsequently filtered and rinsed thoroughly with dichloromethane, methanol, water, acetone, dichloromethane and dried in a vacuum oven overnight at ambient temperature.

6.6.2.3 Polymerisation from cotton-Br: Synthesis of cotton-(10).

Cu(I)Br (0.035 g, 0.24 mmol) and **Cotton-Br** were introduced in a reactor that was then deoxygenated by three vacuum/nitrogen fill cycles. A Schlenk tube was charged with monomer $PEG_{300}MA$ (4.59 g, 15.3 mmol), MN-MA (0.41g, 1.7 mmol), Bipy ligand (0.07 g, 0.45 mmol) and anisole (20 mL). The resulting solution was degassed by three freeze/pump/thaw cycles and the reactor was filled with nitrogen. The solution was then added to the reactor containing cotton and Cu(I)Br via cannula. The reactor was carried out at 25 ˚C under nitrogen and at the end of the polymerisation the mixture was open to air. The cotton were then isolated by filtration and washed sequentially with anisole, THF, diethyl ether, and finally dried under vacuum until a constant weight was obtained.

6.7 Resin surface modification

6.7.1 Wang resin surface modification through click chemistry

6.7.1.1 Synthesis of Wang resin-alkyne

All the bead-related reactions in this report have been carried out in a FirstMate® benchtop synthesizer and Wang resin (loading: 1 mmol/g, 1.0 g, 1.0 mmol) was added to a DMAP (10 mg, 0.082 mmol) solution in anhydrous pyridine (10 mL) and after 1

h 4-chlorocarbonyl-butyric acid prop-2-ynyl ester (0.50 g, 3.0 mmol) in dichloromethane (10 mL) was added. The reaction mixture was subsequently heated to 60 °C and kept at this temperature for 20 h. The resin was then filtered and rinsed sequentially with acetone, distilled water, acetone and dichloromethane. Residual traces of solvent were then removed under reduced pressure.

6.7.1.2 Click reactions to Wang resins

Reaction tubes containing $(PPh_3)_3Cu(I)Br$ and azide or alkyne terminated poly(MMA-co-HMA) in toluene solution were heated to 70 °C under nitrogen and reacted overnight in a FirstMate® benchtop synthesizer. The beads were removed by filtration and rinsed thoroughly with dichloromethane prior to sonication in dichloromethane, acetone and methanol.

6.7.2 Merrifield resin surface modification through click chemistry

6.7.2.1 Synthesis of Merrifield resin-azide

Merrifield resin(1.0 g, 1.5 mmol) was treated with NaN_3 (0.3 g, 4.5 mmol) overnight in a DMSO/H_2O (15 ml / 5ml) solution in a FirstMate® benchtop synthesizer. The resins were removed prior to filtration and rinsing thoroughly with acetone and distilled water, acetone, dichloromethane and dried under vacuum in oven.

6.7.2.2 Click reactions to Merrifield resins

Reaction tubes containing $(PPh_3)_3Cu(I)Br$ and azide or alkyne terminated poly(MMA-co-HMA) in toluene solution were heated to 70 °C under nitrogen and reacted overnight in a FirstMate® benchtop synthesizer. The beads were removed by

filtration and rinsed thoroughly with dichloromethane prior to sonication in dichloromethane, acetone and methanol.

6.7.3 Synthesis of Glycosylated Resins

6.7.3.1 Synthesis of Wang resin initiator (14)

Wang resin (loading 1 mmol/g, 2 g, 2 mmol of OH groups) was suspended in a triethylamine (2.8 mL, 20 mmol), DMAP (10 mg, 0.082 mmol) and 2-bromoisobutyryl bromide (1.2 mL, 10 mmol) solution in dichloromethane (30 mL). The reaction was carried out at ambient temperature for 12 h. The beads were subsequently filtered and rinsed thoroughly with dichloromethane, methanol, water, acetone, dichloromethane and dried in a vacuum oven overnight at ambient temperature.

6.7.3.2 Synthesis of 2-methylacrylic acid 3-trimethylsilanylprop-2-ynyl ester

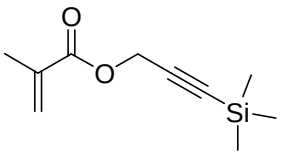

A solution of trimethylsilyl propyn-1-ol (10.0 g, 78.0 mmol) and Et_3N (14.2 mL, 101.3 mmol) in Et_2O (100 mL) was cooled to -20 °C and a solution of methacryloyl chloride (8.8 mL, 93 mmol) in Et_2O (50 mL) was added dropwise over *ca.* 1 h. The mixture was stirred at this temperature for 30 min, then at ambient temperature overnight; the ammonium salts were removed by filtration and the volatiles removed under reduced pressure. ^1H NMR analysis of the yellow oily residue did not reveal the presence of substantial amount of any impurity, but two additional faint spots were observed by TLC (petroleum ether/Et_2O 20:1) analysis, the crude product was

therefore purified by flash chromatography (CC, SiO_2, petroleum ether/Et_2O 50:1; R_f = 0.67 in petroleum ether/Et_2O 20:1). Obtained 12.4 g (63.2 mmol, 81 %)

IR (neat) ν (cm^{-1}): 2960, 1723, 1638, 1452, 1366, 1314, 1292, 1251, 1147, 1035, 971, 942, 842, 813, 761;

^{1}H NMR (400.03 MHz, $CDCl_3$, 298 K) δ = 0.16 (s, 9H, $Si(CH_3)_3$); 1.93-1.94 (m, 3H, CH_3C=CH2); 4.73 (s, 2H, OCH_2); 5.58-5.59 (m, 1H, C=C*H*H); 6.14 (m, 1H, C=CH*H*).

^{13}C NMR (100.59 MHz, $CDCl_3$, 298 K) δ = -0.2 (3C, $Si(CH_3)_3$); 18.4 (1C, CH_3C=CH_2); 53.0 (1C, OCH_2); 92.0 (1C, C≡$C$$Si(CH_3)_3$); 99.2 (1C, C≡$CSi(CH_3)_3$); 126.5 (1C, CH_3C=CH_2); 135.8 (1C, CH_3C=CH_2); 166.6 (1C, COester);

CHN Analysis: Calculated C = 61.18% H = 8.21%, Found C = 60.89% H = 8.22%;

Mass Spectrometry *(m/z)*: 219 [M+23]

6.7.3.3 Polymerisation from immobilized initiator (14): Synthesis of polymer (15)

Wang resin initiator **(14)** (0.1 g, 0.9 mmol) and Cu(I)Br (14 mg, 0.10 mmol) were introduced in a reactor that was then deoxygenated by three vacuum/nitrogen fill cycles. A Schlenk tube was charged with 2-methyl-acrylic acid 3-trimethylsilanyl-prop-2-ynyl ester monomer (1.0 g, 5.1 mmol), *N*-(ethyl)-2-pyridylmethanimine ligand (0.029 mL, 0.20 mmol) and toluene (20 mL). The resulting solution was degassed by five freeze/pump/thaw cycles and the reactor was filled with nitrogen. The brown solution was then added to the reactor containing resin and Cu(I)Br via cannula. The reactor was heated up to 70 ˚C under nitrogen and at the end of the polymerisation the mixture was allowed to cool down to ambient temperature. The beads were then isolated by filtration and washed sequentially with toluene, THF, diethyl ether, and finally dried under vacuum until a constant weight was obtained.

6.7.3.4 Preparation of resin (17)

(15) (0.2 g) was suspended in an acetic acid (1.5 mL)/THF (20 mL) mixture. Nitrogen was bubbled for approximately 10 min and the suspension was cooled to -20 °C. A 0.20 M solution of TBAF·$3H_2O$ in THF (1.5 mL) was added slowly via syringe (ca. 2-3 min). The resulting mixture was stirred at this temperature for 30 min and then warmed to ambient temperature. The reaction mixture was kept at ambient temperature overnight, the resins beads were isolated by filtration and washed sequentially with THF and diethyl ether, and then finally dried under vacuum until a constant weight was obtained, to give product Wang- **(16)** as a white powder.

(16) (0.1 g) was then added to a deoxygenated solution of $(PPh_3)_3Cu(I)Br$ (150 mg, 0.160 mmol) and α-2-azidoethyl mannopyranoside (424 mg, 1.60 mmol) in DMSO (20 mL). The mixture was heated to 60 °C under nitrogen and kept in the synthesizer for 48 h. The beads were then removed by filtration and rinsed thoroughly with DMSO, water, methanol and dichloromethane, and then dried under vacuum until a constant weight was obtained. **(17)** was isolated as an off-white solid.

6.7.3.5 Preparation of resin (13)

Similar procedures as above were used, reaction tubes containing Wang resin alkyne (0.33 g), $(PPh_3)_3Cu(I)Br$ (0.031g 0.033 mmol) and α-2-azidoethyl mannopyranoside (87 mg, 0.33 mmol) in deoxygenated DMSO solution were heated to 60 °C under nitrogen and reacted for 48 h. The beads were then removed by filtration and rinsed thoroughly with DMSO, water, methanol, dichloromethane and then dried under vacuum to a constant mass.

6.7.3.6 Lectin-interaction studies of Glycosylated Resins

(17) (100 mg) was suspended in PBS buffer (pH 7.4, 50 mM) and poured in a glass pipette equipped with a septum at the bottom end to form a sugar beads mini-column cartridge. A solution of FITC-Con A (1 mL, 1 mg/mL) in 50 mM pH 7.4 PBS buffer was run through the cartridge. The average flow rate through the cartridge was approximately 0.3 mL/min. When all the solution was eluted (the residual solution still present in the cartridge was eluted by applying a very gentle pressure of compressed air at the top of the column) 50 μL of the starting FITC–Con A solution and the sample solution eluted from the column were analysed by SEC HPLC in a system equipped with a fluorescence detector (λ_{ex} 495 nm, λ_{em} 525 nm). The cartridge was subsequently washed with further 1 mL of 50 mM PBS buffer (pH 7.4). The lectin bound to the column was finally eluted with a 4.0 M solution in 50 mM PBS buffer (pH 7.4) of α-methyl-D-mannopyranoside, a competitive monovalent ligand for Con A.

6.7.4 Aquagel resin surface modification through surface-initiated LRP.

6.7.4.1 Synthesis of Aquagel resin initiator (18)

Aquagel resin (loading 1 mmol/g, 1 g, 1 mmol of OH groups) was suspended in a 2-bromoisobutyryl bromide (1.2 mL, 10 mmol) solution in anhydrous pyridine (100 mL). The reaction was carried out at ambient temperature for 24 h. The beads were subsequently filtered and rinsed thoroughly with dichloromethane, methanol, water, acetone, dichloromethane and dried in a vacuum oven overnight at ambient temperature.

6.7.4.2 Polymerisation from Aquagel resin (18): Synthesis of (19)

Aquagel resin initiator **(18)** (1 g, 1 mmol) and Cu(I)Br (30 mg, 0.21 mmol) were introduced in a reactor that was then deoxygenated by three vacuum/nitrogen fill cycles. A Schlenk tube was charged with glycerol methacrylate (2.5 g, 15.6 mmol), Bipy ligand (65.6 mg, 0.42 mmol) and methanol (30 mL). The resulting solution was degassed by five freeze/pump/thaw cycles and the reactor was filled with nitrogen. The solution was then added to the reactor containing resin and Cu(I)Br via cannula. The reactor was heated up to 25 ˚C under nitrogen and at the end of the polymerisation, the beads were then isolated by filtration and washed sequentially with methanol, THF, diethyl ether, and finally dried under vacuum until a constant weight was obtained.

6.7.4.3 Synthesis of Aquagel resin (20)

(19) (1.0 g, ~ 5.6 mmol OH) was suspended in anhydrous pyridine (3.0 mL). enantiomer (R)-(+)-1-phenylethyl isocyanate (EtPhNCO) (0.96 g, 6.5 mmol) was added slowly via syringe. The resulting mixture was stirred and kept at ambient temperature for 24h, the resins beads were isolated by filtration and washed sequentially with water, methanol, THF and diethyl ether, and then finally dried under vacuum until a constant weight was obtained.

6.8 Carbon nanotube (CNT) surface modification

6.8.1 Polystyrene modified MWCNT

6.8.1.1 MWCNT-COOH (21)

MWCNT were converted into MWCNT-COOH by treatment with HNO_3 as previously described[334,411-413]. Briefly, 0.5 g of MWCNT was ultrasonicated in 50 mL of 70% HNO_3 aqueous solution for 30 minutes, and then the suspension was refluxed for 48 h. The MWCNT-COOH was collected by filtration, washed with water, acetone, diethyl ether, and dried in a vacuum oven overnight.

6.8.1.2 MWCNT initiator (23)

0.2 g of the MWCNT's-COOH, 50 mL of toluene, 10 mL of $SOCl_2$ were poured into a 100 mL round bottom flask, the flask was ultrasonicated for 30 mins, warmed up to 70 ^oC under N_2 and stirred at this temperature for 24 h. The excess $SOCl_2$ was then distilled off along with some toluene, until the volume was reduced to about half. The suspension was then cooled down to ambient temperature under nitrogen and a solution of 2-bromo-2-methyl-propionic acid 6-hydroxy-hexyl ester (2 g) in toluene (20 mL) was added via syringe and the resulting suspension was stirred at ambient temperature for 24 h then at 100 ^oC for further 24 h. The MWCNT initiator **(23)** was collected by filtration, washed with methanol/triethylamine (9:1), methanol, DCM, diethyl ether, and dried in vacuum oven overnight.

6.8.1.3 Polymerisation of Styrene from MWCNT surface, synthesis of (24)

The polymerisation was conducted in a flask sealed with a rubber septum under nitrogen atmosphere. The MWCNTs (33 mg) were added to a flask containing styrene (38.4 mmol, 4.0 g), Cu(I)Br (0.018 mmol, 2.5 mg), Bipy (0.036 mmol, 5.5 mg) and xylene (2 mL). Nitrogen was bubbled into the solution mixture for 30 minutes before the reaction temperature was set to 110 °C. The reaction was let to proceed at this temperature for 22 h. The amount of grafted organic species onto MWCNTs after 22

h was 98 wt.-% as determined by TGA analysis. The resulting organic-inorganic hybrid particles (CNT-g-PSt) were diluted in DCM and recovered by drop-wise precipitation in methanol and subsequent filtration.

6.8.1.4 Cleavage of polystyrene from CNT surface

A 40 mg sample of CNT-g-PSt was dissolved in 40 ml of THF in a 100 ml round flask fitted with a condenser. 10 mL of 1M (KOH/ethanol) was then added to the flask. The contents of the flask were boiled under reflux for three days. The carbon nanotubes were then filtered off and the polystyrene was analysed by SEC.

6.8.1.5 Formation of isoporous membranes

In order to obtain honeycomb membranes was the following procedure used: 40 mg of CNT-g-PSt was dissolved in $CHCl_3$. Five drops of the solution was thereafter applied to a glass substrate inside a closed chamber with a controlled humidity (RH 70 %) at ambient temperature. A water saturated airstream was let to pass above the polymer solution inside the humidity chamber and the polymer started to precipitate and an opaque film was formed within 30 seconds. The quality of the grey/black film was thereafter analysed with optical microscope, SEM and AFM.

6.8.2 Modification of MWCNT with PAMAM dendron

6.8.2.1 PAMAM Dendron-MWCNT

0.2 g of the MWCNTs-COOH, 50 mL of toluene, 10 mL of $SOCl_2$ were poured into a 100 mL round bottom flask, the system was ultrasonicated for 30 mins, warmed up to 70 ^oC under N_2 and stirred at this temperature for 24 h. The excess $SOCl_2$ was then distilled off along with some toluene, until the volume was reduced to about half. The

suspension was then cooled down to ambient temperature under nitrogen and a solution of hydroxyl-dendron (2 g) in toluene (20 mL) was added via syringe and the resulting suspension was stirred at ambient temperature for 24 h then at 100 ^{o}C for further 24 h. The PAMAM-MWCNTs was collected by filtration, washed with methanol/triethylamine (9:1), methanol, diethyl ether, and dried in vacuum oven overnight.

6.8.2.2 Silver particles deposition experiments: PAMAM-MWCNT-Ag(0)

PAMAM-MWCNT (10 mg) and 1.0 mL of 0.5 M $AgNO_3$ aqueous solution were mixed in a brown vial and the mixture was ultrasonicated for 20 mins in the dark. The solid present in suspension was isolated by centrifugation, and the isolated solid was suspended in pure water and ultrasonicated again. This procedure was repeated several times, until no visible AgCl precipitate was observed upon addition of NaCl aqueous solution. The Ag^{+}/PAMAM-MWCNT's complex was suspended again in 1.0 mL of pure water, subjected to ultrasonication, then 0.10 mL of 37% formaldehyde aqueous solution was added. The mixture was ultrasonicated for 20 mins, and then centrifuged and the solid was washed with pure water, methanol, diethyl ether, and finally dried in vacuum over overnight. The control reaction was performed following the same procedure, using MWCNT-COOH instead of PAMAM-MWCNT.

6.8.3 Thermo-responsive water-dispersible MWCNTs

6.8.3.1 Non-covalent attachment of pyrene-terminal polymer to MWCNT surface

In a typical experiment, 5.0 mg of pyrene-terminal polymer was dissolved in 5.0 mL of de-ionised water in a small vial. 1.0 mg of MWCNT was then added to the polymer solution. After sonication for 5 minutes, the solution was used for TEM analysis. The

modified nanotubes were further recovered by centrifuge and washed with water several times in order to eliminate the unattached polymer. The modified nanotubes were dispersed again in water by sonication for 5 minutes.

6.8.3.2 Thermal-responsive test

The thermal-responsive test was carried out in a clear oil bath with temperature control. The MWCNT-polymer solution was heated gradually to above the cloudy point, until the MWCNTs started to aggregate and precipitate. The vial was then taken out and immersed in a cool water bath. After the mixture was cooled down, the vial was taken out and given a gentle agitation, a re-dispersion of the MWCNTs was then observed.

Chapter 7 References

(1) Black, F. E.; Hartshorne, M.; Davies, M. C.; Roberts, C. J.; Tendler, S. J. B.; Williams, P. M.; Shakesheff, K. M.; Cannizzaro, S. M.; Kim, I.; Langer, R. *Langmuir* **1999**, *15*, 3157-3161.

(2) Lenz, P. *Adv. Mater.* **1999**, *11*, 1531-1534.

(3) Xia, Y.; Qin, D.; Yin, Y. *Curr. Opin. Colloid Interface Sci.* **2001**, *6*, 54-64.

(4) Kataoka, D. E.; Trolan, S. M. *Nature (London)* **1999**, *402*, 794-797.

(5) Kricka, L. J. *Clin. Chim. Acta* **2001**, *307*, 219-223.

(6) Krishnan, M.; Namasivayam, V.; Lin, R.; Pal, R.; Burns, M. A. *Current Opinion in Biotechnology* **2001**, *12*, 92-98.

(7) Lahiri, J.; Isaacs, L.; Grzybowski, B.; Carbeck, J. D.; Whitesides, G. M. *Langmuir* **1999**, *15*, 7186-7198.

(8) Sullivan, T. P.; Huck, W. T. S. *Eur. J. Org. Chem.* **2003**, 17-29.

(9) Niklason, L. E.; Gao, J.; Abbott, W. M.; Hirschi, K. K.; Houser, S.; Marini, R.; Langer, R. *Science***1999**, *284*, 489-493.

(10) James, C. D.; Davis, R.; Meyer, M.; Turner, A.; Turner, S.; Withers, G.; Kam, L.; Banker, G.; Craighead, H.; Isaacson, M.; Turner, J.; Shain, W. *IEEE Trans. Biomed. Eng.* **2000**, *47*, 17-21.

(11) Langer, R. *Accounts of Chemical Research* **2000**, *33*, 94-101.

(12) Santini, J. T., Jr.; Richards, A. C.; Scheidt, R.; Cima, M. J.; Langer, R. *Angew. Chem., Int. Ed. Engl.* **2000**, *39*, 2396-2407.

(13) Tidwell, C. D.; Ertel, S. I.; Ratner, B. D.; Tarasevich, B.; Atre, S.; Allara, D. L. *Langmuir* **1997**, *13*, 3404-3413.

(14) Ratner, B. D.; Johnston, A. B.; Lenk, T. J. *J. Biomed. Mater. Res.* **1987**, *21*, 59-90.

(15) Ulman, A. *Chem. Rev.* **1996**, *96*, 1533-1554.

(16) Pierson, H. O. *Handbook of Chemical Vapor Deposition - Principles, Technology and Applications.* ; 2nd ed.; William Andrew Publishing/Noyes, 1999.

(17) Farrow, R. F. C. *Molecular Beam Epitaxy: Applications to Key Materials*; Noyes Publications 1995.

(18) Finklea, H. O.; Robinson, L. R.; Blackburn, A.; Richter, B.; Allara, D.; Bright, T. *Langmuir* **1986**, *2*, 239-44.

(19) Rubinstein, I.; Sabatani, E.; Maoz, R.; Sagiv, J. *Proc. - Electrochem. Soc.* **1986**, *86-14*, 175-80.

(20) Allara, D. L.; Nuzzo, R. G. *Langmuir* **1985**, *1*, 45-52.

(21) Allara, D. L.; Nuzzo, R. G. *Langmuir* **1985**, *1*, 52-66.

(22) Ogawa, H.; Chihara, T.; Taya, K. *J. Am. Chem. Soc.* **1985**, *107*, 1365-9.

(23) Sagiv, J. *J. Am. Chem. Soc.* **1980**, *102*, 92-8.

(24) Silberzan, P.; Leger, L.; Ausserre, D.; Benattar, J. J. *Langmuir* **1991**, *7*, 1647-51.

(25) Le Grange, J. D.; Markham, J. L.; Kurkjian, C. R. *Langmuir* **1993**, *9*, 1749-53.

(26) Gun, J.; Sagiv, J. *J. Colloid Interface Sci.* **1986**, *112*, 457-72.

(27) Gun, J.; Iscovici, R.; Sagiv, J. *J. Colloid Interface Sci.* **1984**, *101*, 201-13.

(28) Tillman, N.; Ulman, A.; Schildkraut, J. S.; Penner, T. L. *J. Am. Chem. Soc.* **1988**, *110*, 6136-44.

(29) Brandriss, S.; Margel, S. *Langmuir* **1993**, *9*, 1232-40.

(30) Mathauer, K.; Frank, C. W. *Langmuir* **1993**, *9*, 3002-8.

(31) Mathauer, K.; Frank, C. W. *Langmuir* **1993**, *9*, 3446-51.

(32) Carson, G.; Granick, S. *J. Appl. Polym. Sci.* **1989**, *37*, 2767-72.

(33) Kessel, C. R.; Granick, S. *Langmuir* **1991**, *7*, 532-8.

(34) Dubois, L. H.; Nuzzo, R. G. *Annu. Rev. Phys. Chem.* **1992**, *43*, 437-63.

(35) Lee, T. R.; Laibinis, P. E.; Folkers, J. P.; Whitesides, G. M. *Pure Appl. Chem.* **1991**, *63*, 821-8.

(36) Troughton, E. B.; Bain, C. D.; Whitesides, G. M.; Nuzzo, R. G.; Allara, D. L.; Porter, M. D. *Langmuir* **1988**, *4*, 365-85.

(37) Nuzzo, R. G.; Allara, D. L. *J. Am. Chem. Soc.* **1983**, *105*, 4481-3.

(38) Sabatani, E.; Cohen-Boulakia, J.; Bruening, M.; Rubinstein, I. *Langmuir* **1993**, *9*, 2974-81.

(39) Bharathi, S.; Yegnaraman, V.; Rao, G. P. *Langmuir* **1993**, *9*, 1614-17.

(40) Laibinis, P. E.; Whitesides, G. M.; Allara, D. L.; Tao, Y. T.; Parikh, A. N.; Nuzzo, R. G. *J. Am. Chem. Soc.***1991**, *113*, 7152-67.

(41) Walczak, M. M.; Chung, C.; Stole, S. M.; Widrig, C. A.; Porter, M. D. *J. Am. Chem. Soc.* **1991**, *113*, 2370-8.

(42) Laibinis, P. E.; Whitesides, G. M. *J. Am. Chem. Soc.* **1992**, *114*, 9022-8.

(43) Shimazu, K.; Sato, Y.; Yagi, I.; Uosaki, K. *Bull. Chem. Soc. Jpn.* **1994**, *67*, 863-5.

(44) Demoz, A.; Harrison, D. J. *Langmuir* **1993**, *9*, 1046-50.

(45) Stratmann, M.; Volmer, M.; Wolpers, M. *Adv. Mater. Processes, Proc. Eur. Conf., 1st* **1990**, *2*, 989-94.

(46) Liu, Q.; Xu, Z. *Langmuir* **1995**, *11*, 4617-22.

(47) Sheen, C. W.; Shi, J. X.; Maartensson, J.; Parikh, A. N.; Allara, D. L. *J. Am. Chem. Soc.* **1992**, *114*, 1514-15.

(48) Gu, Y.; Lin, Z.; Butera, R. A.; Smentkowski, V. S.; Waldeck, D. H. *Langmuir* **1995**, *11*, 1849-51.

(49) Nagasaki, Y.; Kataoka, K. *Trends in Polymer Science (Cambridge, United Kingdom)* **1996**, *4*, 59-64.

(50) Ruhe, J.; Knoll, W. *Journal of Macromolecular Science, Polymer Reviews* **2002**, *C42*, 91-138.

(51) Zhao, B.; Brittain, W. J. *Progress in Polymer Science* **2000**, *25*, 677-710.

(52) Edmondson, S.; Osborne, V. L.; Huck, W. T. S. *Chem. Soc. Rev.* **2004**, *33*, 14-22.

(53) Tsubokawa, N.; Hosoya, M.; Yanadori, K.; Sone, Y. *Journal of Macromolecular Science, Chemistry* **1990**, *A27*, 445-57.

(54) Bridger, K.; Vincent, B. *Eur. Polym. J.* **1980**, *16*, 1017-21.

(55) Ben Ouada, H.; Hommel, H.; Legrand, A. P.; Balard, H.; Papirer, E. *J. Colloid Interface Sci.* **1988**, *122*, 441-9.

(56) Dyer, D. J. *Adv. Funct. Mater.* **2003**, *13*, 667-670.

(57) Jordan, R.; Ulman, A.; Kang, J. F.; Rafailovich, M. H.; Sokolov, J. *J. Am. Chem. Soc.* **1999**, *121*, 1016-1022.

(58) Zhao, B.; Brittain, W. J. *J. Am. Chem. Soc.* **1999**, *121*, 3557-3558.

(59) Buchmeiser, M. R.; Sinner, F.; Mupa, M.; Wurst, K. *Macromolecules* **2000**, *33*, 32-39.

(60) Ejaz, M.; Yamamoto, S.; Ohno, K.; Tsujii, Y.; Fukuda, T. *Macromolecules* **1998**, *31*, 5934-5936.

(61) Lee, S. B.; Koepsel, R. R.; Morley, S. W.; Matyjaszewski, K.; Sun, Y.; Russell, A. J. *Biomacromolecules* **2004**, *5*, 877-882.

(62) Brantley, E. L.; Holmes, T. C.; Jennings, G. K. *J. Phys. Chem. B* **2004**, *108*, 16077-16084.

(63) Li, X.; Wei, X.; Husson, S. M. *Biomacromolecules* **2004**, *5*, 869-876.

(64) Jordan, R.; Ulman, A. *J. Am. Chem. Soc.* **1998**, *120*, 243-247.

(65) Husemann, M.; Mecerreyes, D.; Hawker, C. J.; Hedrick, J. L.; Shah, R.; Abbott, N. L. *Angew. Chem., Int. Ed. Engl.***1999**, *38*, 647-649.

(66) Choi, I. S.; Langer, R. *Macromolecules* **2001**, *34*, 5361-5363.

(67) Lattuada, M.; Hatton, T. A. *Langmuir* **2007**, *23*, 2158-2168.

(68) Loennberg, H.; Zhou, Q.; Brumer, H., III; Teeri, T.; Malmstroem, E.; Hult, A. *Biomacromolecules* **2006**, *7*, 2178-2185.

(69) Chen, G.-X.; Kim, H.-S.; Park, B. H.; Yoon, J.-S. *Macromol. Chem. Phys.* **2007**, *208*, 389-398.

(70) Wieringa, R. H.; Siesling, E. A.; Geurts, P. F. M.; Werkman, P. J.; Vorenkamp, E. J.; Erb, V.; Stamm, M.; Schouten, A. J. *Langmuir* **2001**, *17*, 6477-6484.

(71) Jaworek, T.; Neher, D.; Wegner, G.; Wieringa, R. H.; Schouten, A. J. *Science* **1998**, *279*, 57-60.

(72) Qu, L.; Veca, L. M.; Lin, Y.; Kitaygorodskiy, A.; Chen, B.; McCall, A. M.; Connell, J. W.; Sun, Y.-P. *Macromolecules* **2005**, *38*, 10328-10331.

(73) Kim, N. Y.; Jeon, N. L.; Choi, I. S.; Takami, S.; Harada, Y.; Finnie, K. R.; Girolami, G. S.; Nuzzo, R. G.; Whitesides, G. M.; Laibinis, P. E. *Macromolecules* **2000**, *33*, 2793-2795.

(74) Juang, A.; Scherman, O. A.; Grubbs, R. H.; Lewis, N. S. *Langmuir* **2001**, *17*, 1321-1323.

(75) Moon, J. H.; Swager, T. M. *Macromolecules* **2002**, *35*, 6086-6089.

(76) Feng, J.; Stoddart, S. S.; Weerakoon, K. A.; Chen, W. *Langmuir* **2007**, *23*, 1004-1006.

(77) Jordan, R.; Ulman, A.; Kang, J. F.; Rafailovich, M. H.; Sokolov, J. *J. Am. Chem. Soc.* **1999**, *121*, 1016-1022.

(78) Advincula, R.; Zhou, Q.; Park, M.; Wang, S.; Mays, J.; Sakellariou, G.; Pispas, S.; Hadjichristidis, N. *Langmuir* **2002**, *18*, 8672-8684.

(79) Sakellariou, G.; Park, M.; Advincula, R.; Mays, J. W.; Hadjichristidis, N. *J. Polym. Sci., A: Polym. Chem.* **2005**, *44*, 769-782.

(80) Chen, S.; Chen, D.; Wu, G. *Macromol. Rap. Commun.* **2006**, *27*, 882-887.

(81) Zhao, B.; Brittain, W. J. *Macromolecules* **2000**, *33*, 342-348.

(82) Georges, M. K.; Veregin, R. P. N.; Kazmaier, P. M.; Hamer, G. K. *Macromolecules* **1993**, *26*, 2987-2988.

(83) Husseman, M.; Malmstro?m, E. E.; McNamara, M.; Mate, M.; Mecerreyes, D.; Benoit, D. G.; Hedrick, J. L.; Mansky, P.; Huang, E.; Russell, T. P.; Hawker, C. J. *Macromolecules* **1999**, *32*, 1424-1431.

(84) Blomberg, S.; Ostberg, S.; Harth, E.; Bosman, A. W.; Van Horn, B.; Hawker, C. J. *J. Polym. Sci., A: Polym. Chem.***2002**, *40*, 1309-1320.

(85) Li, J.; Chen, X.; Chang, Y.-C. *Langmuir* **2005**, *21*, 9562-9567.

(86) Matsuno, R.; Otsuka, H.; Takahara, A. *Soft Matter* **2006**, *2*, 415-421.

(87) Chiefari, J.; Chong, Y. K.; Ercole, F.; Krstina, J.; Jeffery, J.; Le, T. P. T.; Mayadunne, R. T. A.; Meijs, G. F.; Moad, C. L.; Moad, G.; Rizzardo, E.; Thang, S. H. *Macromolecules* **1998**, *31*, 5559-5562.

(88) Rizzardo, E.; Chiefari, J.; Chong, Y. K.; Ercole, F.; Krstina, J.; Jeffery, J.; Le, T. P. T.; Mayadunne, R. T. A.; Meijs, G. F.; Moad, C. L.; Moad, G.; Thang, S. H. *Macromol. Symp.* **1999**, *143*, 291-307.

(89) Boivin, J.; Ramos, L.; Zard, S. Z. *Tet. Lett.* **1998**, *39*, 6877-6880.

(90) Destarac, M.; Brochon, C.; Catala, J. M.; Wilczewska, A.; Zard, S. Z. *Macromol. Chem. Phys.* **2002**, *203*, 2281-2289.

(91) Baum, M.; Brittain, W. J. *Macromolecules* **2002**, *35*, 610-615.

(92) Tsujii, Y.; Ejaz, M.; Sato, K.; Goto, A.; Fukuda, T. *Macromolecules* **2001**, *34*, 8872-8878.

(93) You, Y.-Z.; Hong, C.-Y.; Pan, C.-Y. *Nanotechnology* **2006**, *17*, 2350-2354.

(94) Kamigaito, M.; Ando, T.; Sawamoto, M. *Chem. Rev.* **2001**, *101*, 3689-3745.

(95) Matyjaszewski, K.; Xia, J. *Chem. Rev.* **2001**, *101*, 2921-2990.

(96) Jakubowski, W.; Matyjaszewski, K. *Macromolecules* **2005**, *38*, 4139-4146.

(97) Min, K.; Gao, H.; Matyjaszewski, K. *J. Am. Chem. Soc.* **2005**, *127*, 3825-3830.

(98) Jakubowski, W.; Min, K.; Matyjaszewski, K. *Macromolecules* **2006**, *39*, 39-45.

(99) Jakubowski, W.; Matyjaszewski, K. *Angew. Chem., Int. Ed. Engl.* **2006**, *45*, 4482-4486.

(100) Percec, V.; Guliashvili, T.; Ladislaw, J. S.; Wistrand, A.; Stjerndahl, A.; Sienkowska, M. J.; Monteiro, M. J.; Sahoo, S. *J. Am. Chem. Soc.* **2006**, *128*, 14156-14165.

(101) Kim, J.-B.; Bruening, M. L.; Baker, G. L. *J. Am. Chem. Soc.* **2000**, *122*, 7616-7617.

(102) Liu, Y.; Klep, V.; Zdyrko, B.; Luzinov, I. *Langmuir* **2004**, *20*, 6710-6718.

(103) Angot, S.; Ayres, N.; Bon, S. A. F.; Haddleton, D. M. *Macromolecules* **2001**, *34*, 768-774.

(104) Ejaz, M.; Tsujii, Y.; Fukuda, T. *Polymer* **2001**, *42*, 6811-6815.

(105) Carlmark, A.; Malmstroem, E. *J. Am. Chem. Soc.* **2002**, *124*, 900-901.

(106) Carlmark, A.; Malmstroem, E. E. *Biomacromolecules* **2003**, *4*, 1740-1745.

(107) Matyjaszewski, K.; Miller, P. J.; Shukla, N.; Immaraporn, B.; Gelman, A.; Luokala, B. B.; Siclovan, T. M.; Kickelbick, G.; Valiant, T.; Hoffmann, H.; Pakula, T. *Macromolecules* **1999**, *32*, 8716-8724.

(108) Huang, W.; Kim, J. B.; Bruening, M. L.; Baker, G. L. *Macromolecules* **2002**, *35*, 1175-1179.

(109) Jones, D. M.; Huck, W. T. S. *Adv. Mater.* **2001**, *13*, 1256-1259.

(110) Kim, J. B.; Huang, W.; Bruening, M. L.; Baker, G. L. *Macromolecules* **2002**, *35*, 5410-5416.

(111) Huang, W.; Baker, G. L.; Bruening, M. L. *Angew. Chem., Int. Ed. Engl.* **2001**, *40*, 1510-1512.

(112) Jones, D. M.; Smith, J. R.; Huck, W. T. S.; Alexander, C. *Adv. Mater.* **2002**, *14*, 1130-1134.

(113) Osborne, V. L.; Jones, D. M.; Huck, W. T. S. *Chem. Commun.* **2002**, *8*, 1838-1839.

(114) Treat, N. D.; Ayres, N.; Boyes, S. G.; Brittain, W. J. *Macromolecules* **2006**, *39*, 26-29.

(115) Huang, X.; Wirth, M. J. *Anal. Chem.* **1997**, *69*, 4577-4580.

(116) Perruchot, C.; Khan, M. A.; Kamitsi, A.; Armes, S. P.; Von Werne, T.; Patten, T. E. *Langmuir* **2001**, *17*, 4479-4481.

(117) Chen, X.; Randall, D. P.; Perruchot, C.; Watts, J. F.; Patten, T. E.; Von Werne, T.; Armes, S. P. *J. Colloid Interface Sci.* **2003**, *257*, 56-64.

(118) Wu, T.; Efimenko, K.; Vle?ek, P.; S?ubr, V.; Genzer, J. *Macromolecules* **2003**, *36*, 2448-2453.

(119) Bontempo, D.; Tirelli, N.; Feldman, K.; Masci, G.; Crescenzi, V.; Hubbell, J. A. *Adv. Mater.* **2002**, *14*, 1239-1241+1180.

(120) Zheng, G.; Sto?ver, H. D. H. *Macromolecules* **2002**, *35*, 7612-7619.

(121) Guerrini, M. M.; Charleux, B.; Vairon, J. P. *Macromol. Rap. Commun.* **2000**, *21*, 669-674.

(122) Jayachandran, K. N.; Takacs-Cox, A.; Brooks, D. E. *Macromolecules* **2002**, *35*, 4247-4257.

(123) Teranishi, T.; Miyake, M. *Chem. Mater.* **1998**, *10*, 594-600.

(124) Teranishi, T.; Kiyokawa, I.; Miyake, M. *Adv. Mater.* **1998**, *10*, 596-599.

(125) Teranishi, T.; Hosoe, M.; Miyake, M. *Adv. Mater.* **1997**, *9*, 65-67.

(126) Lenk, T. J.; Hallmark, V. M.; Rabolt, J. F.; Ha?ussling, L.; Ringsdorf, H. *Macromolecules* **1993**, *26*, 1230-1237.

(127) El Sayed, A. M. *J. Appl. Polym. Sci.* **2002**, *86*, 1248-1252.

(128) Koutsos, V.; Van Der Vegte, E. W.; Pelletier, E.; Stamouli, A.; Hadziioannou, G. *Macromolecules* **1997**, *30*, 4719-4726.

(129) Koutsos, V.; Van Der Vegte, E. W.; Hadziioannou, G. *Macromolecules* **1999**, *32*, 1233-1236.

(130) Corbierre, M. K.; Cameron, N. S.; Sutton, M.; Mochrie, S. G. J.; Lurio, L. B.; Ru?hm, A.; Lennox, R. B. *J. Am. Chem. Soc.* **2001**, *123*, 10411-10412.

(131) Zhu, M. Q.; Wang, L. Q.; Exarhos, G. J.; Li, A. D. Q. *J. Am. Chem. Soc.* **2004**, *126*, 2656-2657.

(132) Shan, J.; Nuopponen, M.; Jiang, H.; Kauppinen, E.; Tenhu, H. *Macromolecules* **2003**, *36*, 4526-4533.

(133) Lowe, A. B.; Sumerlin, B. S.; Donovan, M. S.; McCormick, C. L. *J. Am. Chem. Soc.* **2002**, *124*, 11562-11563.

(134) Sumerlin, B. S.; Lowe, A. B.; Stroud, P. A.; Zhang, P.; Urban, M. W.; McCormick, C. L. *Langmuir* **2003**, *19*, 5559-5562.

(135) Mansfield, T. L.; Iyengar, D. R.; Beaucage, G.; McCarthy, T. J.; Stein, R. S.; Composto, R. J. *Macromolecules* **1995**, *28*, 492-499.

(136) Quirk, R. P.; Yin, J.; Fetters, L. J. *Macromolecules* **1989**, *22*, 85.

(137) Huang, H.; Penn, L. S. *Macromolecules* **2005**, *38*, 4837-4843.

(138) Hadziioannou, G.; Patel, S.; Granick, S.; Tirrell, M. *J. Am. Chem. Soc.* **1986**, *108*, 2869-2876.

(139) Watanabe, H.; Tirrell, M. *Macromolecules* **1993**, *26*, 6455-6466.

(140) Dhoot, S.; Watanabe, H.; Tirrell, M. *Colloids Surf. A* **1994**, *86*, 47-60.

(141) Patel, S. S.; Tirrell, M. *Annu. Rev. Phys. Chem.* **1989**, *40*, 597-635.

(142) Webber, R. M.; Van Der Linden, C. C.; Anderson, J. L. *Langmuir* **1996**, *12*, 1040-1046.

(143) Kumacheva, E.; Klein, J.; Pincus, P.; Fetters, L. J. *Macromolecules* **1993**, *26*, 6477-6482.

(144) Perahia, D.; Wiesler, D. G.; Satija, S. K.; Fetters, L. J.; Sinha, S. K.; Milner, S. T. *Phys. Rev. Lett.* **1994**, *72*, 100-103.

(145) Carvalho, B. L.; Tong, P.; Huang, J. S.; Witten, T. A.; Fetters, L. J. *Macromolecules* **1993**, *26*, 4632-4639.

(146) Taunton, H. J.; Toprakcioglu, C.; Fetters, L. J.; Klein, J. *Macromolecules* **1990**, *23*, 571.

(147) Dhinojwala, A.; Granick, S. *Macromolecules* **1997**, *30*, 1079.

(148) Kilbey Ii, S. M.; Watanabe, H.; Tirrell, M. *Macromolecules* **2001**, *34*, 5249.

(149) Schorr, P. A.; Kwan, T. C. B.; Kilbey Ii, S. M.; Shaqfeh, E. S. G.; Tirrell, M. *Macromolecules* **2003**, *36*, 389.

(150) Anastassopoulos, D. L.; Vradis, A. A.; Toprakcioglu, C.; Smith, G. S.; Dai, L. *Macromolecules* **1998**, *31*, 9369-9371.

(151) Karim, A.; Tsukruk, V. V.; Douglas, J. F.; Satija, S. K.; Fetters, L. J.; Reneker, D. H.; Foster, M. D. *J. Phys. II* **1995**, *5*, 1441-1456.

(152) Jones, R. A. L.; Lehnert, R. J.; Scho?nherr, H.; Vancso, J. *Polymer* **1999**, *40*, 525-530.

(153) Luzinov, I.; Julthongpiput, D.; Malz, H.; Pionteck, J.; Tsukruk, V. V. *Macromolecules* **2000**, *33*, 1043-1048.

(154) Julthongpiput, D.; LeMieux, M.; Tsukruk, V. V. *Polymer* **2003**, *44*, 4557-4562.

(155) Sirard, S. M.; Gupta, R. R.; Russell, T. P.; Watkins, J. J.; Green, P. F.; Johnston, K. P. *Macromolecules* **2003**, *36*, 3365-3373.

(156) Qin, S.; Qin, D.; Ford, W. T.; Resasco, D. E.; Herrera, J. E. *Macromolecules* **2004**, *37*, 752-757.

(157) Kolb, H. C.; Finn, M. G.; Sharpless, K. B. *Angew. Chem. Int. Ed.* **2001**, *40*, 2004-2021.

(158) Kolb, H. C.; Sharpless, K. B. *Drug Discovery Today* **2003**, *8*, 1128-1137.

(159) Huisgen, R. *Proceedings of the Robert A. Welch Foundation Conference on Chemical Research* **1961**, *4*, 61-86, discussion 87-95.

(160) Lee, L. V.; Mitchell, M. L.; Huang, S.-J.; V, F.; Sharpless, K. B.; Wong, C.-H. *J. Am. Chem. Soc.* **2003**, *125*, 9588-9589.

(161) Manetsch, R.; Krasinski, A.; Radic, Z.; Raushel, J.; Taylor, P.; Sharpless, K. B.; Kolb, H. C. *J. Am. Chem. Soc.* **2004**, *126*, 12809-12818.

(162) Wang, Q.; Chan, T. R.; Hilgraf, R.; V, F.; Sharpless, K. B.; Finn, M. G. *J. Am. Chem. Soc.* **2003**, *125*, 3192-3193.

(163) Speers, A. E.; Cravatt, B. F. *Chemistry & Biology* **2004**, *11*, 535-546.

(164) Link, A. J.; Tirrell, D. A. *J. Am. Chem. Soc.* **2003**, *125*, 11164-11165.

(165) Speers, A. E.; Adam, G. C.; Cravatt, B. F. *J. Am. Chem. Soc.* **2003**, *125*, 4686-4687.

(166) Fazio, F.; Bryan, M. C.; Blixt, O.; Paulson, J. C.; Wong, C. H. *J. Am. Chem. Soc.* **2002**, *124*, 14397-14402.

(167) Wu, P.; Feldman, A. K.; Nugent, A. K.; Hawker, C. J.; Scheel, A.; Voit, B.; Pyun, J.; Frechet, J. M. J.; Sharpless, K. B.; V, F. *Angew. Chem. - Int. Ed.* **2004**, *43*, 3928-3932.

(168) Joralemon, M. J.; Nugent, A. K.; Matson, J. B.; O'Reilly, R. K.; Hawker, C. J.; Wooley, K. L. *Polym. Mater. Sci. Eng.* **2004**, *91*, 195.

(169) Opsteen, J. A.; Van Hest, J. C. M. *Chem. Commun.* **2005**, *11*, 57-59.

(170) Helms, B.; Mynar, J. L.; Hawker, C. J.; Frechet, J. M. J. *J. Am. Chem. Soc.* **2004**, *126*, 15020-15021.

(171) Binder, W. H.; Kluger, C. *Macromolecules* **2004**, *37*, 9321-9330.

(172) O'Reilly, R. K.; Hawker, C. J.; Wooley, K. L. *Polym. Prepr. (Am. Chem. Soc., Div. Polym. Chem.)* **2004**, *45*, 780.

(173) Huisgen, R. *1,3-Dipolar Cycloaddit. Chem.* **1984**, *1*, 1-176.

(174) V, R.; Green, L. G.; V, F.; Barry Sharpless, K. *Angew. Chem., Int. Ed. Engl.* **2002**, *41*, 2596-2599.

(175) Tornoe, C. W.; Christensen, C.; Meldal, M. *J. Org. Chem.* **2002**, *67*, 3057-3064.

(176) Rostovtsev, V. V.; Green, L. G.; Fokin, V. V.; Sharpless, K. B. *Angew. Chem., Int. Ed. Engl.* **2002**, *41*, 2596-2599.

(177) Matyjaszewski, K.; Xia, J. *Chem. Rev.* **2001**, *101*, 2921-2990.

(178) Mantovani, G.; V, L.; Tao, L.; Haddleton, D. M. *Chem. Commun.* **2005**, 2089-2091.

(179) Sumerlin, B. S.; Tsarevsky, N. V.; Louche, G.; Lee, R. Y.; Matyjaszewski, K. *Macromolecules* **2005**, *38*, 7540-7545.

(180) Gao, H.; Louche, G.; Sumerlin, B. S.; Jahed, N.; Golas, P.; Matyjaszewski, K. *Macromolecules* **2005**, *38*, 8979-8982.

(181) Gao, H.; Matyjaszewski, K. *Macromolecules* **2006**, *39*, 4960-4965.

(182) Johnson, J. A.; Lewis, D. R.; Diaz, D. D.; Finn, M. G.; Koberstein, J. T.; Turro, N. J. *J. Am. Chem. Soc.* **2006**, *128*, 6564-6565.

(183) Lutz, J.-F.; Boerner, H. G.; Weichenhan, K. *Macromolecules* **2006**, *39*, 6376-6383.

(184) Klemm, D.; Schmauder, H. P.; Heinze, T. *Biopolymers* **2002**, *6*, 290-292.

(185) Kaplan, D. L. *Biopolymers from Renewable Resources* **1998**, 367.

(186) Klemm, D.; Heublein, B.; Fink, H. P.; Bohn, A. *Angew. Chem., Int. Ed. Engl.***2005**, *44*, 3358-3393.

(187) Haddleton, D. M.; Jasieczek, C. B.; Hannon, M. J.; Shooter, A. J. *Macromolecules* **1997**, *30*, 2190-2193.

(188) Chen, G.; Tao, L.; Mantovani, G.; Ladmiral, V.; Burt, D. P.; Macpherson, J. V.; Haddleton, D. M. *Soft Matter* **2007**, *3*, 732-739.

(189) Haddleton, D. M.; Rullay, A. K.; Limer, A. J.; Carrington, S.; Keely, S.; Brayden, D. *Polym. Prepr. (Am. Chem. Soc., Div. Polym. Chem.)* **2004**, *45*, 253-254.

(190) Samuelson, J. *Antimicrob. Agents Chemother.* **1999**, *43*, 1533-1541.

(191) Petrin, D.; Delgaty, K.; Bhatt, R.; Garber, G. *Clin. Microbio. Rev.* **1998**, *11*, 300-317.

(192) Zaat, J. O.; Mank, T. G.; Assendelft, W. J. *Trop. Med. Int. Health.* **1997**, *2*, 63-82.

(193) Shinn, D. L. S. *Lancet.* **1962**, 111.

(194) Yarlett, N.; Gorrell, T. E.; Marczak, R.; Muller, M. *Mol. Biochem. Parasitol.* **1985**, *14*, 29-40.

(195) Finegold, S. M. *Ann. Intern. Med.* **1980**, *93*, 585-7.

(196) Tally, F. P.; Goldin, B. R.; Sullivan, N.; Johnston, J.; Gorbach, S. L. *Antimicrob. Agents Chemother.* **1978**, *13*, 460-5.

(197) Church, D. L.; Bryant, R. D.; Sim, V.; Laishley, E. J. *Anaerobe* **1996**, *2*, 147-153.

(198) Jokipii, A. M.; Myllyla, V. V.; Hokkanen, E.; Jokipii, L. *J Antimicrob. Chemother.* **1977**, *3*, 239-45.

(199) McNulty, C. A. *Am. J. Gastroenterol.* **1987**, *82*, 245-7.

(200) Rauws, E. A.; Langenberg, W.; Houthoff, H. J.; Zanen, H. C.; Tytgat, G. N. *Gastroenterology* **1988**, *94*, 33-40.

(201) Rauws, E. A.; Tytgat, G. N. *Lancet* **1990**, *335*, 1233-5.

(202) Gorbach, S. L. *Clin. Infect. Dis.* **1994**, *18 Suppl 4*, S305-10.

(203) Goldman, P.; Koch, R. L.; Yeung, T. C.; Chrystal, E. J. T.; Beaulieu, B. B., Jr.; McLafferty, M. A.; Sudlow, G. *Biochem. Pharmacol.* **1986**, *35*, 43-51.

(204) Lutz, J. F.; Hoth, A. *Macromolecules* **2006**, *39*, 893-896.

(205) Han, S.; Hagiwara, M.; Ishizone, T. *Macromolecules* **2003**, *36*, 8312-8319.

(206) Lutz, J. F.; Akdemir, O.; Hoth, A. *J. Am. Chem. Soc.* **2006**, *128*, 13046-13047.

(207) Greenwald, R. B. *J. Cont. Rel.* **2001**, *74*, 159-171.

(208) Bhadra, D.; Bhadra, S.; Jain, P.; Jain, N. K. *Pharmazie* **2002**, *57*, 5-29.

(209) Zalipsky, S.; Gilon, C.; Zilkha, A. *Eur. Polym. J.* **1983**, *19*, 1177-83.

(210) Pasut, G.; Guiotto, A.; Veronese, F. M. *Expert Opin. Ther. Pat.* **2004**, *14*, 859-894.

(211) Yamaoka, T.; Tabata, Y.; Ikada, Y. *J. Pharm. Sci.* **1994**, *83*, 601-6.

(212) Veronese, F. M. *Biomaterials* **2001**, *22*, 405-417.

(213) Zacchigna, M.; Di Luca, G.; Cateni, F.; Maurich, V. *Eur. J. Pharm. Sci.* **2004**, *23*, 379-384.

(214) Harris, J. M.; Chess, R. B. *Nat. Rev. Drug Disc.* **2003**, *2*, 214-221.

(215) Zalipsky, S. *Bioconj. Chem.* **1995**, *6*, 150-65.

(216) Matsunaga, T.; Suzuki, T.; Tanaka, M.; Arakaki, A. *Trends Biotechnol.* **2007**, *25*, 182-188.

(217) Matsunaga, T.; Okamura, Y.; Tanaka, T. *J. Mater. Chem.* **2004**, *14*, 2099-2105.

(218) Shinkai, M. *J. Biosci. Bioeng.* **2002**, *94*, 606-613.

(219) Stamm, C.; Marty, F.; Vaterlaus, A.; Weich, V.; Egger, S.; Maier, U.; Ramsperger, U.; Fuhrmann, H.; Pescia, D. *Science* **1998**, *282*, 449-451.

(220) Bruckl, H.; Panhorst, M.; Schotter, J.; Kamp, P. B.; Becker, A. *IEE Proceeding Nanobiotech.* **2005**, *152*, 41-46.

(221) Ugelstad, J.; Berge, A.; Ellingsen, T.; Schmid, R.; Nilsen, T. N.; M?rk, P. C.; Sienstad, P.; Hornes, E.; Olsvik *Prog. Polym. Sci.* **1992**, *17*, 87-161.

(222) Zhu, D.-W. *Macromolecules* **1996**, *29*, 2813-17.

(223) Guyomard, A.; Fournier, D.; Pascual, S.; Fontaine, L.; Bardeau, J. F. *Eur. Polym. J.* **2004**, *40*, 2343.

(224) Krajnc, P.; Toplak, R. *React. Funct. Polym.* **2002**, *52*, 11.

(225) Kaldor, S. W.; Siegel, M. G.; Fritz, J. E.; Dressman, B. A.; Hahn, P. J. *Tet. Lett.* **1996**, *37*, 7193.

(226) Coppola, G. M. *Tet. Lett.* **1998**, *39*, 8233.

(227) Guino, M.; Brule, E.; De Miguel, Y. R. *J. Comb. Chem.* **2003**, *5*, 161.

(228) Peters, E. C.; Svec, F.; Frechet, J. M. J.; Viklund, C.; Irgum, K. *Macromolecules* **1999**, *32*, 6377-6379.

(229) Barrett, A. G. M.; Cramp, S. M.; Roberts, R. S.; Zecri, F. J. *Organic Letters* **1999**, *1*, 579-582.

(230) Meyer, U.; Svec, F.; Frechet, J. M. J.; Hawker, C. J.; Irgum, K. *Macromolecules* **2000**, *33*, 7769-7775.

(231) Hemstroem, P.; Szumski, M.; Irgum, K. *Anal. Chem.* **2006**, *78*, 7098-7103.

(232) Chen, G.; Tao, L.; Mantovani, G.; Geng, J.; Nystrom, D.; Haddleton, D. M. *Macromolecules* **2007**, *ASAP*.

(233) Ambrosi, M.; Cameron, N. R.; Davis, B. G. *Org. Biomol. Chem.* **2005**, *3*, 1593-1608.

(234) Wilson, D. S.; Nock, S. *Section Title: Biochemical Methods* **2002**, *6*, 81-85.

(235) Langenhan, J. M.; Thorson, J. S. In *Curr. Org. Synth.* 2005; Vol. 2, p 59-81.

(236) Wang, D.; Liu, S.; Trummer, B. J.; Deng, C.; Wang, A. *Nat Biotech* **2002**, *20*, 275-281.

(237) Fukui, S.; Feizi, T.; Galustian, C.; Lawson, A. M.; Chai, W. *Nat Biotech* **2002**, *20*, 1011-1017.

(238) Kiessling, L. L.; Cairo, C. W. *Nat Biotech* **2002**, *20*, 234-235.

(239) Park, S.; Shin, I. *Angew. Chem., Int. Ed. Engl.***2002**, *41*, 3180-3182.

(240) Schwarz, M.; Spector, L.; Gargir, A.; Shtevi, A.; Gortler, M.; Altstock, R. T.; Dukler, A. A.; Dotan, N. *Glycobiology* **2003**, *13*, 749-754.

(241) Smith, E. A.; Thomas, W. D.; Kiessling, L. L.; Corn, R. M. *J. Am. Chem. Soc.* **2003**, *125*, 6140-6148.

(242) Ejaz, M.; Ohno, K.; Tsujii, Y.; Fukuda, T. *Macromolecules* **2000**, *33*, 2870-2874.

(243) Stenzel, M. H.; Zhang, L.; Huck, W. T. S. *Macromol. Rap. Commun.* **2006**, *27*, 1121-1126.

(244) Sun, X.-L.; Faucher, K. M.; Houston, M.; Grande, D.; Chaikof, E. L. *J. Am. Chem. Soc.* **2002**, *124*, 7258-7259.

(245) Faucher, K. M.; Sun, X.-L.; Chaikof, E. L. *Langmuir* **2003**, *19*, 1664-1670.

(246) Sun, X.-L.; Cui, W.; Haller, C.; Chaikof, E. L. *ChemBioChem* **2004**, *5*, 1593-1596.

(247) Vazquez-Dorbatt, V.; Maynard, H. D. *Biomacromolecules* **2006**, *7*, 2297-2302.

(248) Spain, S. G.; Albertin, L.; Cameron, N. R. *Chem. Commun.* **2006**, 4198-4200.

(249) Housni, A.; Cai, H.; Narain, R. *Polym. Prepr. (Am. Chem. Soc., Div. Polym. Chem.)* **2007**, *48*, 888-889.

(250) Yang, Q.; Xu, Z.-K.; Hu, M.-X.; Li, J.-J.; Wu, J. *Langmuir* **2005**, *21*, 10717-10723.

(251) Yang, Q.; Tian, J.; Dai, Z.-W.; Hu, M.-X.; Xu, Z.-K. *Langmuir* **2006**, *22*, 10097-10102.

(252) Yang, Q.; Tian, J.; Hu, M.-X.; Xu, Z.-K. *Langmuir* **2007**, *23*, 6684-6690.

(253) Satish, P. R.; Surolia, A. *Methods for Affinity-Based Separations of Enzymes and Proteins* **2002**, 115-129.

(254) Ortega-Munoz, M.; Lopez-Jaramillo, J.; Hernandez-Mateo, F.; Santoyo-Gonzalez, F. *Advanced Synthesis & Catalysis* **2006**, *348*, 2410-2420.

(255) Slater, M.; Snauko, M.; Svec, F.; Frechet, J. M. J. *Anal. Chem.* **2006**, *78*, 4969-4975.

(256) Mantovani, G.; V, L.; Tao, L.; Haddleton, D. M. *Chem. Commun.* **2005**, 2089-2091.

(257) Ladmiral, V.; Mantovani, G.; Clarkson, G. J.; Cauet, S.; Irwin, J. L.; Haddleton, D. M. *J. Am. Chem. Soc.* **2006**, *128*, 4823-4830.

(258) Hodges, J. C.; Harikrishnan, L. S.; Ault-Justus, S. *J. Comb. Chem.* **2000**, *2*, 80-88.

(259) Ayres, N.; Haddleton, D. M.; Shooter, A. J.; Pears, D. A. *Macromolecules* **2002**, *35*, 3849-3855.

(260) Becker, M. L.; Liu, J.; Wooley, K. L. *Biomacromolecules* **2005**, *6*, 220-228.

(261) Fournier, D.; Pascual, S.; Montembault, V.; Haddleton, D. M.; Fontaine, L. *J. Comb. Chem.* **2006**, *8*, 522-530.

(262) Bittiger, H.; Schnebli, H. P. *Concanavalin A as a Tool* **1976**.

(263) Phondke, G. P.; Sainis, K. B.; Joshi, N. N. *J. Biosci* **1983**, *5*, 137-148.

(264) Lin, S. S.; Levitan, I. B. *Trends Neurosci.* **1991**, *14*, 273-277.

(265) Mironov, S. L. *Trends Neurosci.* **1992**, *15*, 13.

(266) Dimick, S. M.; Powell, S. C.; McMahon, S. A.; Moothoo, D. N.; Naismith, J. H.; Toone, E. J. *J. Am. Chem. Soc.* **1999**, *121*, 10286-10296.

(267) Valle-Delgado, J. J.; Molina-Bolivar, J. A.; Galisteo-Gonzalez, F.; Galvez-Ruiz, M. J.; Feiler, A.; Rutland, M. W. *J. Phys. Cond. Matter* **2004**, *16*.

(268) Ilisz, I.; Berkecz, R.; Peter, A. *J. Sep. Sci.* **2006**, *29*, 1305-1321.

(269) Lam, S.; Malikin, G. *Chirality* **1992**, *4*, 395-399.

(270) Wainer, I. W. *Trends Anal. Chem.* **1993**, *12*, 153-158.

(271) Blaschke, G.; Kraft, H. P.; Fickentscher, K.; Kohler, F. *Chromatographische Racemattrennung von Thalidomid und teratogene Wirkung der Enantiomere.* **1979**, *29*, 1640-1642.

(272) Taylor, D. R.; Maher, K. *J. Chrom Sci.* **1992**, *30*, 67.

(273) Omote, M.; Sato, K.; Ando, A.; Kumadaki, I. *Curr. Org. Synth.* **2007**, *4*, 137-150.

(274) Maruoka, K.; Ooi, T.; Kano, T. *Chem. Commun.* **2007**, 1487-1495.

(275) Blaser, H. U.; Pugin, B.; Spindler, F. *J. Mol. Catal. A: Chem.* **2005**, *231*, 1-20.

(276) Caldwell, J. *J. Chrom. A* **1996**, *719*, 3-13.

(277) Francotte, E. R. *J. Chrom. A* **2001**, *906*, 379-397.

(278) Aboul-Enein, H. Y.; Ali, I. *Chiral Separations by Liquid Chromatography and Related Technologies* **2003**.

(279) *Chiral Separation Techniques: A Practical Approach, 3rd Completely Revised and Updated Edition* **2006**.

(280) Dobashi, A.; Dobashi, Y.; Hara, S. *J. Liq. Chromatogr.* **1986**, *9*, 243-267.

(281) Dobashi, Y.; Hara, S. *Tet. Lett.* **1985**, *26*, 4217-4220.

(282) Pirkle, W. H.; House, D. W.; Finn, J. M. *J. Chrom.* **1980**, *192*, 143-158.

(283) Pirkle, W. H.; Finn, J. M.; Schreiner, J. L.; Hamper, B. C. *J. Am. Chem. Soc.* **1981**, *103*, 3964-3966.

(284) Bressolle, F.; Audran, M.; Pham, T. N.; Vallon, J. J. *J. Chrom. B* **1996**, *687*, 303-336.

(285) Okamoto, Y.; Kaida, Y. *J. Chrom. A* **1994**, *666*, 403-419.

(286) Oguni, K.; Oda, H.; Ichida, A. *J. Chrom. A* **1995**, *694*, 91-100.

(287) Yashima, E.; Okamoto, Y. *Bull. Chem. Soc. Jpn.* **1995**, *68*, 3289-3307.

(288) Okamoto, Y.; Yashima, E. *Angew. Chem., Int. Ed. Engl.***1998**, *37*, 1021-1043.

(289) Yashima, E. *J. Chrom. A* **2001**, *906*, 105-125.

(290) Ward, T. J.; Farris Iii, A. B. *J. Chrom. A* **2001**, *906*, 73-89.

(291) Choi, H. J.; Hyun, M. H. *Journal of Liquid Chromatography and Related Technologies* **2007**, *30*, 853-875.

(292) Nakano, T. *J. Chrom. A* **2001**, *906*, 205-225.

(293) Sellergren, B. *J. Chrom. A* **2001**, *906*, 227-252.

(294) Takeuchi, T.; Haginaka, J. *J. Chrom. B* **1999**, *728*, 1-20.

(295) Remcho, V. T.; Tan, Z. J. *Anal. Chem.* **1999**, *71*.

(296) Haginaka, J. *J. Chrom. A* **2001**, *906*, 253-273.

(297) Davankov, V. A.; Rogozhin, S. V. *J. Chrom. A* **1971**, *60*, 280-283.

(298) Gubitz, G.; Schmid, M. G. *Biopharm. Drug Dispos.* **2001**, *22*, 291-336.

(299) Pettersson, C.; Schill, G. *J. Chrom.* **1981**, *Vol. 204*, 179-183.

(300) Eliel, E. L.; Wilen, S. H. *Stereochemistry of Organic Compounds* **1994**.

(301) Iijima, S. *Nature* **1991**, *354*, 56-58.

(302) Bezryadin, A.; Lau, C. N.; Tinkham, M. *Nature (London)* **2000**, *404*, 971-974.

(303) Day, T. M.; Unwin, P. R.; Wilson, N. R.; Macpherson, J. V. *J. Am. Chem. Soc.* **2005**, *127*, 10639-10647.

(304) Yoon, B.; Wai, C. M. *J. Am. Chem. Soc.* **2005**, *127*, 17174-17175.

(305) Kong, J.; Chapline, M. G.; Dai, H. *Adv. Mater.* **2001**, *13*, 1384-1386.

(306) Kam, N. W. S.; Dai, H. *J. Am. Chem. Soc.* **2005**, *127*, 6021-6026.

(307) Kam, N. W. S.; Liu, Z.; Dai, H. *J. Am. Chem. Soc.* **2005**, *127*, 12492-12493.

(308) Bandow, S.; Rao, A. M.; Williams, K. A.; Thess, A.; Smalley, R. E.; Eklund, P. C. *J. Phys. Chem. B* **1997**, *101*, 8839-8842.

(309) Duesberg, G. S. *Chem. Commun.* **1998**, 435-436.

(310) O'Connell, M. J.; Boul, P.; Ericson, L. M.; Huffman, C.; Wang, Y.; Haroz, E.; Kuper, C.; Tour, J.; Ausman, K. D.; Smalley, R. E. *Chem. Phys. Lett.* **2001**, *342*, 265-271.

(311) Star, A.; Stoddart, J. F.; Steuerman, D.; Diehl, M.; Boukai, A.; Wong, E. W.; Yang, X.; Chung, S. W.; Choi, H.; Heath, J. R. *Angew. Chem., Int. Ed. Engl.***2001**, *40*, 1721-1725.

(312) Steuerman, D. W.; Star, A.; Narizzano, R.; Choi, H.; Ries, R. S.; Nicolini, C.; Stoddart, J. F.; Heath, J. R. *J. Phys. Chem. B* **2002**, *106*, 3124-3130.

(313) Star, A.; Liu, Y.; Grant, K.; Ridvan, L.; Stoddart, J. F.; Steuerman, D. W.; Diehl, M. R.; Boukai, A.; Heath, J. R. *Macromolecules* **2003**, *36*, 553-560.

(314) Tang, B. Z.; Xu, H. *Macromolecules* **1999**, *32*, 2569-2576.

(315) Chen, R. J.; Zhang, Y.; Wang, D.; Dai, H. *J. Am. Chem. Soc.* **2001**, *123*, 3838-3839.

(316) Gomez, F. J.; Chen, R. J.; Wang, D.; Waymouth, R. M.; Dai, H. *Chem. Commun.* **2003**, *9*, 190-191.

(317) Petrov, P.; Stassin, F.; Pagnoulle, C.; Jerome, R. *Chem. Commun.* **2003**, *9*, 2904-2905.

(318) Lou, X.; Daussin, R.; Cuenot, S.; Duwez, A. S.; Pagnoulle, C.; Detrembleur, C.; Bailly, C.; Jerome, R. *Chem. Mater.* **2004**, *16*, 4005-4011.

(319) Gao, H.; Kong, Y. *Annu. Rev. Mater. Res.* **2004**, *34*, 123-150.

(320) Xia, H.; Wang, Q.; Qiu, G. *Chem. Mater.* **2003**, *15*, 3879-3886.

(321) Kang, Y.; Taton, T. A. *J. Am. Chem. Soc.* **2003**, *125*, 5650-5651.

(322) Chen, J.; Hamon, M. A.; Hu, H.; Chen, Y.; Rao, A. M.; Eklund, P. C.; Haddon, R. C. *Science* **1998**, *282*, 95-98.

(323) Zhang, J.; Zou, H.; Qing, Q.; Yang, Y.; Li, Q.; Liu, Z.; Guo, X.; Du, Z. *J. Phys. Chem. B* **2003**, *107*, 3712-3718.

(324) Riggs, J. E.; Guo, Z.; Carroll, D. L.; Sun, Y.-P. *J. Am. Chem. Soc.* **2000**, *122*, 5879-5880.

(325) Hill, D. E.; Lin, Y.; Rao, A. M.; Allard, L. F.; Sun, Y.-P. *Macromolecules* **2002**, *35*, 9466-9471.

(326) Liu, Y.; Yao, Z.; Adronov, A. *Macromolecules* **2005**, *38*, 1172-1179.

(327) Qin, S.; Qin, D.; Ford, W. T.; Herrera, J. E.; Resasco, D. E.; Bachilo, S. M.; Weisman, R. B. *Macromolecules* **2004**, *37*, 3965-3967.

(328) Gao, C.; Vo, C. D.; Jin, Y. Z.; Li, W.; Armes, S. P. *Macromolecules* **2005**, *38*, 8634-8648.

(329) Czerw, R.; Guo, Z.; Ajayan, P. M.; Sun, Y.-P.; Carroll, D. L. *Nano Lett.* **2001**, *1*, 423-427.

(330) Yao, Z.; Braidy, N.; Botton, G. A.; Adronov, A. *J. Am. Chem. Soc.* **2003**, *125*, 16015-16024.

(331) Baskaran, D.; Mays, J. W.; Bratcher, M. S. *Angew. Chem., Int. Ed.* **2004**, *43*, 2138-2142.

(332) Lin, Y.; Zhou, B.; Fernando, K. A. S.; Liu, P.; Allard, L. F.; Sun, Y.-P. *Macromolecules* **2003**, *36*, 7199-7204.

(333) Cao, L.; Yang, W.; Yang, J.; Wang, C.; Fu, S. *Chem. Lett.* **2004**, *33*, 490-491.

(334) Hong, C.-Y.; You, Y.-Z.; Wu, D.; Liu, Y.; Pan, C.-Y. *Macromolecules* **2005**, *38*, 2606-2611.

(335) Sano, M.; Kamino, A.; Shinkai, S. *Angew. Chem., Int. Ed.* **2001**, *40*, 4661-4663.

(336) Balasubramanian, K.; Burghard, M. *Small* **2005**, *1*, 180-192.

(337) Lou, X.; Detrembleur, C.; Sciannamea, V.; Pagnoulle, C.; Jerome, R. *Polymer* **2004**, *45*, 6097-6102.

(338) Nishikawa, T.; Nishida, J.; Ookura, R.; Nishimura, S. I.; Wada, S.; Karino, T.; Shimomura, M. *Mater. Sci. Eng., C* **1999**, *10*, 141-146.

(339) Nishikawa, T.; Nishida, J.; Ookura, R.; Nishimura, S. I.; Wada, S.; Karino, T.; Shimomura, M. *Mater. Sci. Eng., C* **1999**, *8-9*, 495-500.

(340) Wijnhoven, J. E. G. J.; Vos, W. L. *Science* **1998**, *281*, 802-804.

(341) Widawski, G.; Rawiso, M.; Francois, B. *Nature* **1994**, *369*, 387-389.

(342) Pitois, O.; Francois, B. *Colloid Polym. Sci.* **1999**, *277*, 574-578.

(343) Pitois, O.; Francois, B. *Eur. Phys. J. B* **1999**, *8*, 225-231.

(344) Srinivasarao, M.; Collings, D.; Philips, A.; Patel, S. *Science* **2001**, *292*, 79-83.

(345) Maruyama, N.; Koito, T.; Nishida, J.; Sawadaishi, T.; Cieren, X.; Ijiro, K.; Karthaus, O.; Shimomura, M. *Thin Solid Films* **1998**, *327-329*, 854-856.

(346) Maruyama, N.; Karthaus, O.; Ijiro, K.; Shimomura, M.; Koito, T.; Nishimura, S.; Sawadaishi, T.; Nishi, N.; Tokura, S. *Supramol. Sci.* **1998**, *5*, 331-336.

(347) Stenzel-Rosenbaum, M. H.; Davis, T. P.; Fane, A. G.; Chen, V. *Angew. Chem., Int. Ed. Engl.***2001**, *40*, 3428-3432.

(348) Stenzel, M. H. *Aust. J. Chem.* **2002**, *55*, 239-243.

(349) Boker, A.; Lin, Y.; Chiapperini, K.; Horowitz, R.; Thompson, M.; Carreon, V.; Xu, T.; Abetz, C.; Skaff, H.; Dinsmore, A. D.; Emrick, T.; Russell, T. P. *Nat. Mater.* **2004**, *3*, 302-306.

(350) Bauer, F.; Sauerland, V.; Glasel, H. J.; Ernst, H.; Findeisen, M.; Hartmann, E.; Langguth, H.; Marquardt, B.; Mehnert, R. *Macromol. Mater. Eng.* **2002**, *287*, 546-552.

(351) Min Zhi, R.; Ming Qiu, Z.; Yong Xiang, Z.; Han Min, Z.; Friedrich, K. *Polymer* **2001**, *42*, 3301-3304.

(352) Liu, Y. L.; Li, S. H. *Macromol. Rapid Commun.* **2004**, *25*, 1393.

(353) Nystrom, D.; Antoni, P.; Malmstrom, E.; Johansson, M.; Whittaker, M.; Hult, A. *Macromol. Rap. Commun.* **2005**, *26*, 524-528.

(354) Vamvounis, G.; Nystrom, D.; Antoni, P.; Lindgren, M.; Holdcroft, S.; Hult, A. *Langmuir* **2006**, *22*, 3959-3961.

(355) Tao, L.; Chen, G.; Mantovani, G.; York, S.; Haddleton, D. M. *Chem. Commun.* **2006**, 4949-4951.

(356) Tomalia, D. A.; Baker, H.; Dewald, J.; Hall, M.; Kallos, G.; Martin, S.; Roeck, J.; Ryder, J.; Smith, P. *Polym. J.* **1985**, *17*, 117-32.

(357) Tomalia, D. A.; Baker, H.; Dewald, J.; Hall, M.; Kallos, G.; Martin, S.; Roeck, J.; Ryder, J.; Smith, P. *Macromolecules* **1986**, *19*, 2466-8.

(358) Bielinska, A.; Kukowska-Latallo, J. F.; Johnson, J.; Tomalia, D. A.; Baker, J. R., Jr. *Nucleic Acids Res.* **1996**, *24*, 2176-2182.

(359) Kim, T.-I.; Seo, H. J.; Choi, J. S.; Jang, H.-S.; Baek, J.; Kim, K.; Park, J.-S. *Biomacromolecules* **2004**, *5*, 2487-2492.

(360) Malik, N.; Wiwattanapatapee, R.; Klopsch, R.; Lorenz, K.; Frey, H.; Weener, J. W.; Meijer, E. W.; Paulus, W.; Duncan, R. *J. Controlled Release* **2000**, *65*, 133-148.

(361) Zhang, X.-Q.; Wang, X.-L.; Huang, S.-W.; Zhuo, R.-X.; Liu, Z.-L.; Mao, H.-Q.; Leong, K. W. *Biomacromolecules* **2005**, *6*, 341-350.

(362) Braun, C. S.; Vetro, J. A.; Tomalia, D. A.; Koe, G. S.; Koe, J. G.; Middaugh, C. R. *J. Pharm. Sci.* **2005**, *94*, 423-436.

(363) Anon *Science (Washington, DC, United States)* **2003**, *300*, 1057.

(364) Frankamp, B. L.; Boal, A. K.; Rotello, V. M. *J. Am. Chem. Soc.* **2002**, *124*, 15146-15147.

(365) Garcia-Martinez, J. C.; Crooks, R. M. *J. Am. Chem. Soc.* **2004**, *126*, 16170-16178.

(366) Garcia-Martinez, J. C.; Lezutekong, R.; Crooks, R. M. *J. Am. Chem. Soc.* **2005**, *127*, 5097-5103.

(367) Garcia-Martinez, J. C.; Scott, R. W. J.; Crooks, R. M. *J. Am. Chem. Soc.* **2003**, *125*, 11190-11191.

(368) Scott, R. W. J.; Ye, H.; Henriquez, R. R.; Crooks, R. M. *Chem. Mater.* **2003**, *15*, 3873-3878.

(369) Gu, Y.; Xie, H.; Gao, J.; Liu, D.; Williams, C. T.; Murphy, C. J.; Ploehn, H. J. *Langmuir* **2005**, *21*, 3122-3131.

(370) Lang, H.; May, R. A.; Iversen, B. L.; Chandler, B. D. *J. Am. Chem. Soc.* **2003**, *125*, 14832-14836.

(371) Singh, A.; Chandler, B. D. *Langmuir* **2005**, *21*, 10776-10782.

(372) Scott, R. W. J.; Datye, A. K.; Crooks, R. M. *J. Am. Chem. Soc.* **2003**, *125*, 3708-3709.

(373) Scott, R. W. J.; Sivadinarayana, C.; Wilson, O. M.; Yan, Z.; Goodman, D. W.; Crooks, R. M. *J. Am. Chem. Soc.* **2005**, *127*, 1380-1381.

(374) Scott, R. W. J.; Wilson, O. M.; Oh, S.-K.; Kenik, E. A.; Crooks, R. M. *J. Am. Chem. Soc.* **2004**, *126*, 15583-15591.

(375) Frankamp, B. L.; Boal, A. K.; Tuominen, M. T.; Rotello, V. M. *J. Am. Chem. Soc.* **2005**, *127*, 9731-9735.

(376) Liu, L.; Breslow, R. *J. Am. Chem. Soc.* **2003**, *125*, 12110-12111.

(377) Tomalia, D. A.; Huang, B.; Swanson, D. R.; Brothers, H. M.; Klimash, J. W. *Tetrahedron* **2003**, *59*, 3799-3813.

(378) Tronc, F.; Li, M.; Lu, J.; Winnik, M. A.; Kaul, B. L.; Graciet, J.-C. *J. Polym. Sci., A: Polym. Chem.***2003**, *41*, 766-778.

(379) Rieth, S.; Baddeley, C.; Badjic, J. D. *Soft Matter* **2007**, *3*, 137-154.

(380) Schmaljohann, D. *Adv. Drug Delivery Rev.* **2006**, *58*, 1655-1670.

(381) Prabaharan, M.; Mano, J. F. *Macromol. Biosci.* **2006**, *6*, 991-1008.

(382) Minko, S. *Polym Rev.* **2006**, *46*, 397-420.

(383) Hashidzume, A.; Tomatsu, I.; Harada, A. *Polymer* **2006**, *47*, 6011-6027.

(384) Sawamoto, M.; Aoshima, S.; Higashimura, T. *Makromolekulare Chemie, Macromolecular Symposia* **1988**, *13-14*, 513-26.

(385) Alexander, C. *Expert Opinion on Drug Delivery* **2006**, *3*, 573-581.

(386) Piskin, E. *Expert Rev. Med. Devices* **2005**, *2*, 501-509.

(387) De Las Heras Alarco?n, C.; Pennadam, S.; Alexander, C. *Chem. Soc. Rev.* **2005**, *34*, 276-285.

(388) Alexander, C.; Shakesheff, K. M. *Adv. Mater.* **2006**, *18*, 3321-3328.

(389) Kim, H.-J.; Lee, J.-H.; Lee, M. *Angew. Chem., Int. Ed. Engl.***2005**, *44*, 5811-5814.

(390) Kanazawa, H. *Anal. Bioanal. Chem.* **2004**, *378*, 46-48.

(391) Ballauff, M.; Lu, Y. *Polymer* **2007**, *48*, 1815-1823.

(392) Faivre, M.; Campillo, C.; Pepin-Donat, B.; Viallat, A. In *Progress in Colloid and Polymer Science* 2006; Vol. 133, p 41-44.

(393) Berndt, I.; Pedersen, J. S.; Lindner, P.; Richtering, W. In *Progress in Colloid and Polymer Science* 2006; Vol. 133, p 35-40.

(394) Percec, V.; Popov, A. V.; Ramirez-Castillo, E.; Monteiro, M.; Barboiu, B.; Weichold, O.; Asandei, A. D.; Mitchell, C. M. *J. Am. Chem. Soc.* **2002**, *124*, 4940-4941.

(395) Nakashima, N.; Tomonari, Y.; Murakami, H. *Chem. Lett.* **2002**, 638-639.

(396) Pompeo, F.; Resasco, D. E. *Nano Lett.* **2002**, *2*, 369-373.

(397) Georgakilas, V.; Tagmatarchis, N.; Pantarotto, D.; Bianco, A.; Briand, J. P.; Prato, M. *Chem. Commun.* **2002**, *8*, 3050-3051.

(398) Star, A.; Steuerman, D. W.; Heath, J. R.; Stoddart, J. F. *Angew. Chem., Int. Ed. Engl.***2002**, *41*, 2508-2512.

(399) Dodziuk, H.; Ejchart, A.; Anczewski, W.; Ueda, H.; Krinichnaya, E.; Dolgonos, G.; Kutner, W. *Chem. Commun.* **2003**, *9*, 986-987.

(400) Huang, W.; Taylor, S.; Fu, K.; Lin, Y.; Zhang, D.; Hanks, T. W.; Rao, A. M.; Sun, Y. P. *Nano Lett.* **2002**, *2*, 311-314.

(401) Keller, R. N.; Wycoff, H. D. **1946**, 1-4.

(402) Gujadhur, R.; Venkataraman, D.; Kintigh, J. T. *Tet. Lett.* **2001**, *42*, 4791-4793.

(403) Hovestad, N. J.; Van Koten, G.; Bon, S. A. F.; Haddleton, D. M. *Macromolecules* **2000**, *33*, 4048-4052.

(404) Ladmiral, V. *PhD thesis: Synthesis and Characterisation of Glycopolymers from Living Radical Polymerisation* **2005**, *Chapter 5*, 200.

(405) Mantovani, G.; Ladmiral, V.; Tao, L.; Haddleton, D. M. *Chem. Commun.* **2005**, 2089-2091.

(406) Haddleton, D. M.; Crossman, M. C.; Dana, B. H.; Duncalf, D. J.; Heming, A. M.; Kukulj, D.; Shooter, A. J. *Macromolecules* **1999**, *32*, 2110-2119.

(407) Haddleton, D. M.; Rullay, A. K.; Limer, A. J.; Carrington, S.; Keely, S.; Brayden, D. *Polym. Prepr. (Am. Chem. Soc., Div. Polym. Chem.)* **2004**, *45*, 253-254.

(408) Hayes, W.; Osborn, H. M. I.; Osborne, S. D.; Rastall, R. A.; Romagnoli, B. *Tetrahedron* **2003**, *59*, 7983-7996.

(409) Tomalia, D. A. *Polymer Chemistry* **2004**, 188-200.

(410) Lothian-Tomalia, M. K.; Hedstrand, D. M.; Tomalia, D. A.; Padias, A. B.; Hall, H. K., Jr. *Tetrahedron* **1997**, *53*, 15495-15513.

(411) Hong, C.-Y.; You, Y.-Z.; Pan, C.-Y. *Chem. Mater.* **2005**, *17*, 2247-2254.

(412) Kong, H.; Gao, C.; Yan, D. *Macromolecules* **2004**, *37*, 4022-4030.

(413) Kong, H.; Gao, C.; Yan, D. *J. Am. Chem. Soc.* **2004**, *126*, 412-413.